

**BENTHIC STUDY OF THE CONTINENTAL SLOPE OFF CAPE HATTERAS,
NORTH CAROLINA**

Robert J. Diaz¹, James A. Blake², and David P. Lohse¹

¹Virginia Institute of Marine Science

School of Marine Science

College of William and Mary

Gloucester Point, VA 23062

and

²Science Applications International Corporation

89 Water Street

Woods Hole, MA 02543

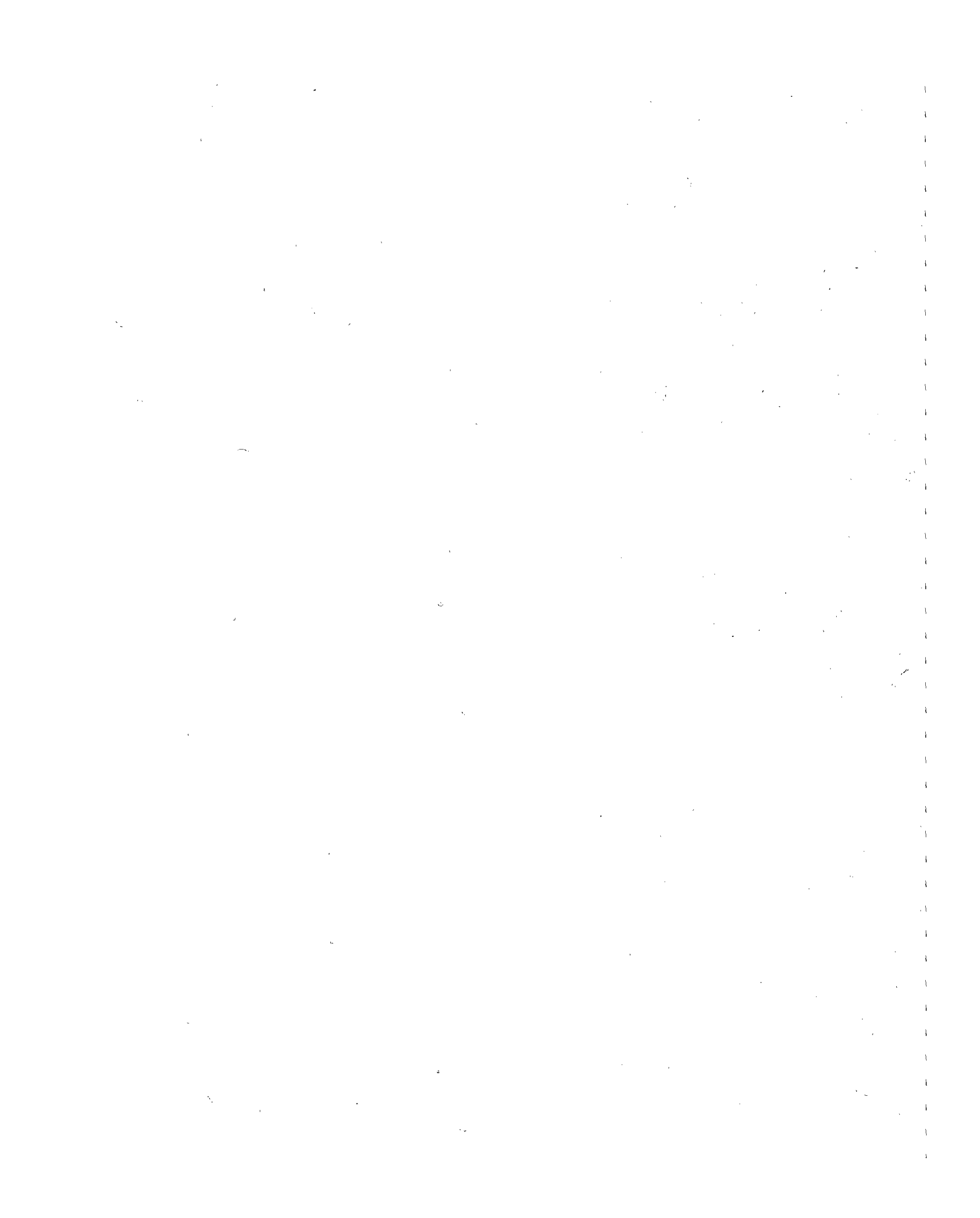
March 1993

Contract Number: 14-35-0001-30672

Prepared for: U.S. Department of the Interior

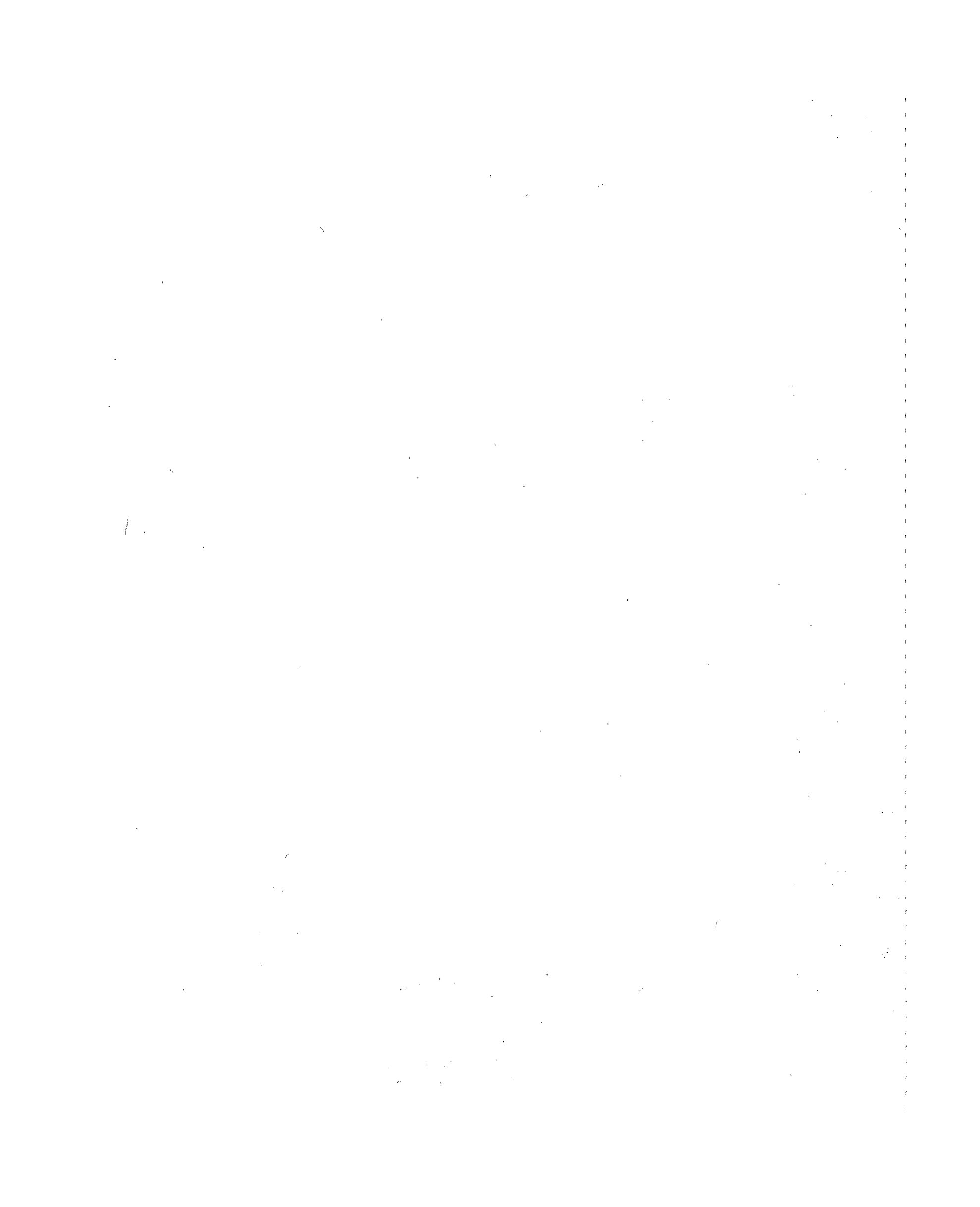
Minerals Management Service

Atlantic OCS Region



Disclaimer

"This manuscript has been reviewed by the Minerals Management Service and approved for publication. The opinions, findings, conclusions, or recommendations expressed in this report are those of the authors, and do not necessarily reflect the views or policies of the MMS. Mention of trade names or commercial products does not constitute endorsement or recommendation for use. This report has been technically reviewed according to contractual specifications; however, it is exempt from further review by the MMS Technical Communications Services Unit and the Regional Editor."



PREFACE

This study was undertaken at the request of the U.S. Minerals Management Service to determine the aerial extent of the benthic community on the continental slope off of Cape Hatteras in the vicinity of the Manteo 467 lease block. The North Carolina Environmental Sciences Review Panel raised the concern that so little information exists on this community that impacts of proposed gas exploration activities could not be defined. We conducted an intensive field survey of this region using the resources and knowledge of many scientists, technicians, and students.

We would like to thank the captain and crew of the R/V *Endeavor* for their cooperation and assistance during our two week cruise. We also thank Andy Shepard, Director of the NURC in Wilmington and chief scientist on the R/V *Seward Johnson*, for moving out of our way while we were towing the camera sled. The field work was cheerfully done by Liz Caporellie, Randy Cutter, Amanda Daly, George Hampson, Barbara Hecker, Brigitte Hilbig, Gail Plaia, Carrie Jo Thomas, Michelle Thompson, Robert Trager, Isabelle Williams, Robert Williams, David Lohse, James Blake, and myself.

We also take genuine pleasure in acknowledging the contributions of many colleagues and associates in completing this report in such a short period of time, particularly; Barbara Hecker (megafauna and her BABS approach to science), Neal Blair (pore water geochemistry), Larry Cahoon (sediment chlorophyll *a* and viable diatoms), David DeMaster (sediment accumulation rates), Rodger Harvey (sediment lipids), Movin Gibbs, Amanda Daly, Michelle Thompson and Janet Nestlerod (infaunal sample processing), Donald Rhoads (sediment fabric analysis and synthesis), Kenneth Sulak and Steven Ross (submersible videotape fish fauna review), and Andy Shepard and Cris Jensen (submersible videotape invertebrate review). We are also grateful to Robert Monroe, Professor Emeritus of Statistics, North Carolina State University, for review and advice on our field design and statistical analyses.

Special acknowledgement goes to the taxonomic experts who labored the hardest; James Blake, SAIC (polychaetes, pogonophorans); Brigitte Hilbig, SAIC (polychaetes); Isabelle Williams, SAIC (tanaidaceans, isopods, amphipods, echinoderms, miscellaneous); Paula Winchell, SAIC (nemerteans, sipunculans, miscellaneous); Amelie Scheltema, Woods Hole Oceanographic Institution (aplacophorans); Mike Rex, University of Massachusetts, Boston (gastropods); John Allen, University Marine Biological Station, Millport, Scotland (bivalves); Ron Shimek, Parametrix, Inc. (scaphopods); and Christer Erséus, Swedish Museum of Natural History, Stockholm and Robert Diaz, VIMS (oligochaetes).

We are very grateful to our Quality Review Board (QRB), which consisted of three eminent marine scientists, for their comments and direction during the study. They reviewed and commented on our field design, sample analysis protocol, and draft and final reports. Members of the QRB were; Dirk Frankenberg, Director, University of North Carolina Institute of Marine Science, Chapel Hill, NC; Fred Grassle, Director, Institute of Marine and Coastal Studies, Rutgers University, New Brunswick, NJ; Ken Tenore, Director, Chesapeake Biological Laboratory, University of Maryland, Solomons, MD.

Mac Currin and Kim Crofford of the North Carolina Office of Marine Affairs in Raleigh, NC were also very helpful in providing literature. We are also grateful for the advice and encouragement provided by John Costlow, Chair of the former ESRP and former Director of the Duke University Marine Lab. A special thanks also goes to Judy Wilson, the Contracting Officers Technical Representative, for her direction during study and for being patient.

Robert J. Diaz
Program Manager
March 1993

LIST OF CONTRIBUTORS

Dr. Neal Blair,
Department of Marine, Earth and
Atmospheric Sciences
North Carolina State University
Raleigh, NC 27695-8208

Dr. James A. Blake
Science Applications International Corporation
89 Water Street
Woods Hole, MA 02543

Dr. Larry B. Cahoon
Department of Biological Sciences
University of North Carolina at Wilmington
Wilmington, N.C. 28403

Mr. G. Randy Cutter
Virginia Institute of Marine Science
School of Marine Science
College of William and Mary
Gloucester Pt., VA 23062

Dr. David J. DeMaster
Department of Marine, Earth and
Atmospheric Sciences
North Carolina State University
Raleigh, NC 27695-8208

Dr. Robert J. Diaz
Virginia Institute of Marine Science
School of Marine Science
College of William and Mary
Gloucester Pt., VA 23062

Dr. H. Rodger Harvey
Chesapeake Biological Laboratory
University of Maryland
Center for Environmental and Estuarine Studies
Box 38, Solomons, MD 20688

Dr. Barbara Hecker
Hecker Environmental Consulting
63 School Street
Woods Hole, MA 02543

Dr. Brigitte Hilbig
Science Applications International Corporation
89 Water Street
Woods Hole, MA 02543

Dr. David Lohse
Virginia Institute of Marine Science
School of Marine Science
College of William and Mary
Gloucester Pt., VA 23062

Mr. Cris Jensen
National Undersea Research Center
University of North Carolina at Wilmington
Wilmington, NC 28403

Dr. Donald C. Rhoads
Science Applications International Corporation
89 Water Street
Woods Hole, MA 02543

Dr. Steven Ross
Marine Research Center
University of North Carolina at Wilmington
Wilmington, NC 28403

Dr. Andrew Shepard
National Undersea Research Center
University of North Carolina at Wilmington
Wilmington, NC 28403

Dr. Kenneth J. Sulak
Huntsman Marine Science Centre
St. Andrews, New Brunswick
Canada E0G 2X0

Ms. Carrie Jo Thomas
Department of Biological Sciences
University of North Carolina at Wilmington
Wilmington, N.C. 28403

Ms. Isabelle P. Williams
Science Applications International Corporation
89 Water Street
Woods Hole, MA 02543

TABLE OF CONTENTS

VOLUME I EXECUTIVE SUMMARY

VOLUME II FINAL REPORT

PREFACE	i
LIST OF CONTRIBUTORS	ii
LIST OF TABLES	vi
LIST OF FIGURES	
CHAPTER 1 - INTRODUCTION - R.J. Diaz	1
Background	1
Objectives	2
Site Description	3
Physical Habitat	3
Benthic Communities	3
Predicted Sedimentation from Drilling Activities	4
Dispersion and Deposition	5
CHAPTER 2 - SAMPLE DESIGN AND FIELD METHODS - R.J. Diaz, J.A. Blake	9
Sample Design	9
Field Methods	9
Vessel and Navigation	9
Box Core	9
Sediment Surface and Profile Imaging	11
Towed Camera Sled	11
Stations and Data Analyzed	11
CHAPTER 3 - SEDIMENT CHARACTERISTICS AND PORE WATER - D.J. DeMaster, N. Blair, R.J. Diaz	13
Introduction	13
Methods	13
Results	14
Sediment Characteristics	14
Sediment Accumulation Rates	14
Methane Concentrations	14
Discussion	19
CHAPTER 4 - SEDIMENT CHLOROPHYLL <i>a</i> , VIABLE DIATOMS, AND LIPIDS - H.R. Harvey, L.B. Cahoon, C.J. Thomas	21
Introduction	21
Methods	21
Results	22
Discussion	22

CHAPTER 5 - SEDIMENT FABRIC AND IN SITU SEDIMENTARY STRUCTURES -	
R.J. Diaz, G.R. Cutter, D.C. Rhoads	31
Introduction	31
Methods	31
Results	33
Profile Images	33
Surface Images	39
X-ray	39
Discussion	45
CHAPTER 6 - SYNTHESIS OF SEDIMENT DATA - D.C. Rhoads	47
Introduction	47
Sediment Provenances	47
Possible Transport Mechanisms	47
Sedimentation Rates	49
Post-Depositional Processes	51
CHAPTER 7 - BENTHIC INFAUNAL COMMUNITY STRUCTURE -	
J.A. Blake, B. Hilbig, I.P. Williams	53
Introduction	53
Methods	53
Results	55
Faunal Analysis	55
Dominant Species and Distributional Patterns	62
Community Pattern Analysis	67
Discussion	70
CHAPTER 8 - MEGAFAUNAL ASSEMBLAGES - B. Hecker	75
Introduction	75
Methods	75
Results	78
Sea-Floor Characteristics	78
Faunal Composition	81
Faunal Abundance and Depth Distribution	81
Transect Analysis	87
Community Analysis	104
Discussion	113
CHAPTER 9 - SYNTHESIS OF BIOLOGICAL DATA - J.A. Blake, B. Hilbig, R.J. Diaz	121
Introduction	121
Definition and Extent of Biological Communities	121
CHAPTER 10 - CONCLUSIONS - R.J. Diaz	125
Physical Habitat	125
Benthic Community Characterization and Distributional Patterns	126
OOC Model Predictions and Aerial Distribution of Benthic Community	127
LITERATURE CITED	129
INDEX	139

VOLUME III Appendices

- A Evaluation of Megabenthos from Submersible Video - A. Shepard, C. Jensen and A. Hulbert
- B Evaluation of Benthic Fish from Submersible Video - K.J. Sulak and S. Ross
- C R/V *Endeavor* cruise EN-241 Station Locations - R. Cutter
- D Macrofauna Data Collected in August/September 1992 on R/V *Endeavor* cruise EN-241. -
J. Blake, B. Hilbig
- E Megafauna Data Collected in August/September 1992 on R/V *Endeavor* cruise EN-241. -
B. Hecker

LIST OF TABLES

Table 1-1.	Current speeds and directions used in the OOC model simulations at the Manteo 467 proposed well site.	5
Table 2-1.	Summary of data collected in the vicinity of the Manteo 467 lease block on the R/V <i>Endeavor</i> cruise (EN-241) from 26 August to 6 September 1992.	12
Table 3-1.	Estimated sediment accumulation rates (cm yr^{-1}), and depth of the mixed layer (cm).	14
Table 5-1.	Data from sediment surface images presented by station.	40
Table 5-2.	Depth (cm) of sediment mixing by bioturbation as seen in the x-ray images.	46
Table 7-1.	List of species identified from sixteen samples taken off Cape Hatteras.	56
Table 7-2.	Community parameters for benthic infaunal samples from the Cape Hatteras Survey.	59
Table 7-3.	Dominant taxa and their contribution to the total fauna at stations along the 530 to 620-m isobaths.	63
Table 7-4.	Dominant taxa and their contribution to the total fauna at eight stations along the 800-m isobath.	64
Table 7-5.	Dominant taxa and their contribution to the total fauna at four stations along the 800-m isobath.	66
Table 7-6.	Dominant taxa and their contribution to the total fauna at each station along the 1,410 to 2,003-m isobaths.	68
Table 7-7.	Rank of the seven most abundant species and community statistics by cluster group.	64
Table 8-1.	Total area viewed (square meters) for 100-m depth intervals at transects surveyed with the towed camera sled.	79
Table 8-2.	List of megafaunal species enumerated from camera-sled tows off Cape Hatteras.	82
Table 8-3.	Density of dominant megafaunal species in the clusters defined by classification analysis of the 100-m depth interval data.	110
Table 8-4.	Cluster designations defined by hierarchial classification for the 100-m depth interval data on each of the transects.	111
Table 8-5.	Density of total megafauna on the middle slope at 10 locations on the eastern U.S. continental margin.	114
Table 8-6.	Estimates of the density of <i>Bathysiphon filiformis</i> (individuals m^{-2}) obtained from individual photographs taken from the towed camera sled and surface photographs at sediment profile stations.	119

Table 10-1. Summary of sedimentary characteristic within the study area. 125

Table 10-2. Summary of benthic community characteristics within the study area. 126

Table 10-3. Estimated percentage of the unusual benthic community, within the study area, covered by predicted deposition of drilling muds and cuttings. 127

Table 10-4. Estimated ratio of predicted deposition, from drilling of the proposed well in the Manteo 467 lease block, relative to monthly natural sediment accumulation rates (Predicted/Measured Accumulation). 127

LIST OF FIGURES

Figure 1-1.	Location of the Manteo lease blocks off Cape Hatteras.	2
Figure 1-2.	Predicted dispersion patterns of drilling mud and cuttings from a proposed well site located in Manteo lease block 467.	7
Figure 1-3.	Overlay of predicted dispersion and deposition patterns from the Offshore Operators' Committee model and study area.	8
Figure 2-1.	Location of sampling stations on the continental slope off Cape Hatteras.	10
Figure 3-1.	Frequency distributions of grain sizes from sediments collected off Cape Hatteras.	15
Figure 3-2.	Ternary diagram showing the classification of sediment type for each box-core station. . .	16
Figure 3-3.	Amounts of carbonate, organic carbon and nitrogen, and the ratio of C:N for sediments collected off Cape Hatteras.	17
Figure 3-4.	Depth profiles of the concentration of methane.	18
Figure 3-5.	Depth profile of the concentration of methane at Station SA10.	20
Figure 4-1.	Proportions of samples containing diatoms in each 2 cm sediment interval.	23
Figure 4-2.	Abundance of chlorophyll <i>a</i> for each transect and depth.	24
Figure 4-3.	Amount of fatty acids found for each transect and depth.	25
Figure 4-4.	Mean relative abundance of the different types of fatty acids found by a) transect and b) depth.	26
Figure 5-1.	Location of SPI camera stations.	32
Figure 5-2.	Sediment characteristics measured from profile images.	34
Figure 5-3.	Sediment profile images: clayey sediments from a) Station 26 replicate A, and b) Station SA10 replicate A.	35
Figure 5-4.	Sediment profile images: deep apparent color redox potential discontinuity (RPD) layers in images from a) Station 19 replicate B, and b) Station 21 replicate B.	36
Figure 5-5.	Sediment profile images: large void areas in images from a) Station 21 replicate A, and b) Station SA9 replicate C.	37
Figure 5-6.	Sediment profile images: presence of <i>Bathysiphon filiformis</i> in images from a) Station 4 replicate D, and b) Station 13 replicate D.	38
Figure 5-7.	Sediment profile images: subsurface fauna and burrows in images from a) Station SA9 replicate D, and b) Station 1A replicate A.	41

Figure 5-8.	Sediment surface images: different densities of <i>Bathysiphon filiformis</i> and other surface features in images from a) Station 12 replicate A, and b) Station 20 replicate A.	42
Figure 5-9.	Sediment surface images: numerous epibenthos in images from a) Station SA9 replicate A, and b) Station 10 replicate D.	43
Figure 5-10.	Sediment surface images: other fauna, and clayey clasts of sediment at the surface in images from a) Station SA9 replicate E, and b) Station SA10 replicate A.	44
Figure 6-1	Direction of bottom currents on the Atlantic continental shelf as determined from bottom drifter measurements.	48
Figure 7-1.	Location of box core stations within the study area off Cape Hatteras.	54
Figure 7-2.	Hurlbert rarefaction curves for 16 stations sampled off Cape Hatteras in 1992.	60
Figure 7-3.	Density of benthic infauna at 16 stations sampled off Cape Hatteras in 1992.	61
Figure 7-4.	Dendrograms from analysis of 1992 stations off Cape Hatteras.	69
Figure 7-5.	Results of reciprocal averaging ordination, first three axes, using the 50 most abundant species and square root transformation of densities.	71
Figure 7-6.	Density of benthic infauna from stations along the 600-m isobath.	74
Figure 8-1.	Location of camera-sled tows conducted along transects off Cape Hatteras.	76
Figure 8-2.	Topographic profiles from the camera sled tows.	80
Figure 8-3.	Photographs of common middle slope species: (a) transect B, 1,004 m, and (b) transect F, 799 m.	84
Figure 8-4.	Photographs of common middle slope species: (a) transect B, 1,728 m, and (b) transect B, 1,209 m.	85
Figure 8-5.	Density of total megafauna with depth in (a) the study area and (b) along each of the transects.	86
Figure 8-6.	Density of the wolf eelpout <i>Lycenchelys verrilli</i> with depth in (a) the study area and (b) along each of the transects.	88
Figure 8-7.	Density of the anemone <i>Actinauge verrilli</i> with depth in (a) the study area and (b) along each of the transects.	89
Figure 8-8.	Density of the witch flounder <i>Glyptocephalus cynoglossus</i> with depth in (a) the study area and (b) along each of the transects.	90
Figure 8-9.	Density of the eelpout <i>Lycodes atlanticus</i> with depth in (a) the study area and (b) along each of the transects.	91

Figure 8-10.	Density of the foraminiferan <i>Bathysiphon filiformis</i> with depth in (a) the study area and (b) along each of the transects.	92
Figure 8-11.	Photographs showing high and low densities of <i>Bathysiphon filiformis</i> : (a) Transect A, 1,560 m, and (b) Transect B, 1,138 m.	93
Figure 8-12.	Photographs from transect 1A (1,138 m) showing the variability in the density of <i>Bathysiphon filiformis</i> over small horizontal distances.	94
Figure 8-13.	Topographic profile, sea-floor characteristics, and density of total megafauna, eight common species, and <i>Bathysiphon filiformis</i> along Transect 1A.	95
Figure 8-14.	Photographs showing two instances of sea-floor disturbance observed on the northern transects: (a) Transect 1A (1,263 m), and (b) Transect 1 (756 m).	96
Figure 8-15.	Topographic profile, sea-floor characteristics, and density of total megafauna, five common species, and <i>Bathysiphon filiformis</i> along Transect 1.	98
Figure 8-16.	Topographic profile, sea-floor characteristics, and density of total megafauna, seven common species, and <i>Bathysiphon filiformis</i> along Transect A.	99
Figure 8-17.	Topographic profile, sea-floor characteristics, and density of total megafauna, six common species, and <i>Bathysiphon filiformis</i> along Transect B.	100
Figure 8-18.	Photographs of two habitats observed on Transect B: (a) 511 m, and (b) 1,736 m.	101
Figure 8-19.	Topographic profile, sea-floor characteristics, and density of total megafauna, 10 common species, and <i>Bathysiphon filiformis</i> along Transect D.	102
Figure 8-20.	Photographs of two habitats observed on Transect D: (a) 1435 m, and (b) 1729 m.	103
Figure 8-21.	Topographic profile, sea-floor characteristics, and density of total megafauna, six common species, and <i>Bathysiphon filiformis</i> along Transect E.	105
Figure 8-22.	Topographic profile, sea-floor characteristics, and density of total megafauna, 12 common species, and <i>Bathysiphon filiformis</i> along Transect F.	106
Figure 8-23.	Photographs of two habitats observed on Transect F: (a) 326 m, and (b) 1,718 m.	107
Figure 8-24.	Hierarchical classification of 100-m depth intervals from the camera-sled tows.	108
Figure 8-25.	Reciprocal averaging ordination of the camera-sled data; (a) the 100-m depth intervals, and (b) the dominant species.	112
Figure 8-26.	Density of total megafauna with depth at 10 locations on the eastern U.S. continental margin.	115
Figure 8-27.	Density of (a) the wolf eelpout <i>Lycenchelys verrilli</i> and (b) the anemone <i>Actinauge verrilli</i> with depth at 10 locations on the eastern U.S. continental margin.	116

Figure 8-28. Density of (a) the witch flounder *Glyptocephalus cynoglossus* and (b) the foraminiferan *Bathysiphon filiformis* with depth at 10 locations on the eastern U.S. continental margin. 117

CHAPTER 1. INTRODUCTION

Robert J. Diaz

Background

The need to develop reliable domestic sources of petroleum and natural gas has led to increased interest in the resources of the continental shelf and slope off the United States East Coast. The Outer Continental Shelf (OCS) Environmental Studies Program was initiated in 1973 by the U.S. Department of the Interior to evaluate the environmental consequences of exploration, development, and production of offshore energy resources. The Atlantic continental shelf, off the East Coast of the United States, has been well studied with several OCS programs that have intensively sampled physical, geological, chemical, and biological processes over broad areas of the shelf. Most of the OCS biological studies focused on energy related activities on the continental shelf (for example, Burreson and Knebel 1979, Marine Resources Research Institute 1984, Milliman and Wright 1987; see Continental Shelf Associates 1990 for the technical summaries of many OCS studies). OCS studies that extended to continental slope depths (starting at 500-600 m) and beyond were fewer (Blake et al. 1985, 1987; see Marine Geoscience Applications 1984 for other summaries). Most of these studies were part of the Atlantic Continental Slope and Rise Program (ACSAR) supported by the U.S. Department of the Interior, Minerals Management Service (MMS) from 1983 to 1987. Over the years other, non-energy-related, ecological studies of the shelf and slope have also been conducted to document benthic communities (Grassle 1967, 1987, Marine Experiment Station 1973), fisheries resources (Stehlik et al. 1991), and long-term monitoring (Northeast Monitoring Program (NEMP), Pearce et al. 1985).

A number of blocks off Cape Hatteras have been leased by Mobil Oil, which has requested permission to drill an exploratory well, at 820-m depth, in a block identified as Manteo 467 (Figure 1-1). The proposed well location is 39 miles from the coast of North Carolina. The possibility of extracting gas from the continental slope off the coast of North Carolina, particularly at slope depths, has raised a number of environmental concerns that cannot be addressed from existing data.

Because of the potential impact on the environment associated with development and production activities, the Oil Pollution Act of 1990 mandated that a panel of experts, the North Carolina Environmental Sciences Review Panel (NCSERP), be convened. Their purpose was to consider the adequacy of information available for making decisions regarding oil and gas leasing, exploration, and development off North Carolina. In their report to the Secretary of the Interior, this panel (NCSERP 1992) made several recommendations regarding information needed to understand the basic ecology of the lease areas. Among them was the recommendation that the spatial extent of an unusual benthic community found within some of the lease blocks should be determined before any exploration or development activity occurs off Cape Hatteras. If more than 5% of the unusual benthic community is covered by drill muds and cuttings, the NCSERP recommended that a study be carried out to determine the recovery rate of this community.

The benthic fish and invertebrate communities off the Cape Hatteras continental slope were found to be different from other Atlantic continental slope communities in terms of species composition, abundance, and biomass. Blake et al. (1985, 1987) were the first to find and study these unusual communities. Blake et al. (1985, 1987) surveyed 15 sites on the continental slope and rise off the North Carolina coast, and found highest abundances and biomass in the area of Manteo lease block 510, a site that is adjacent to Manteo 467. Other investigators (Schaff 1991, Ross and Sulak 1992, Sulak 1992) who concentrated their sampling in this area confirmed these results. Overall, the abundance of macrobenthic infauna was about 10 times higher, and biomass about 6 times higher, and fish abundance was about 6 times higher than at other slope areas.

The present study was developed by the Minerals Management Service to better define the nature of the continental slope benthic communities off Cape Hatteras and to delineate their areal extent. Emphasis was placed on the area around the proposed drill site in the Manteo 467 lease block (Figure-1-1):

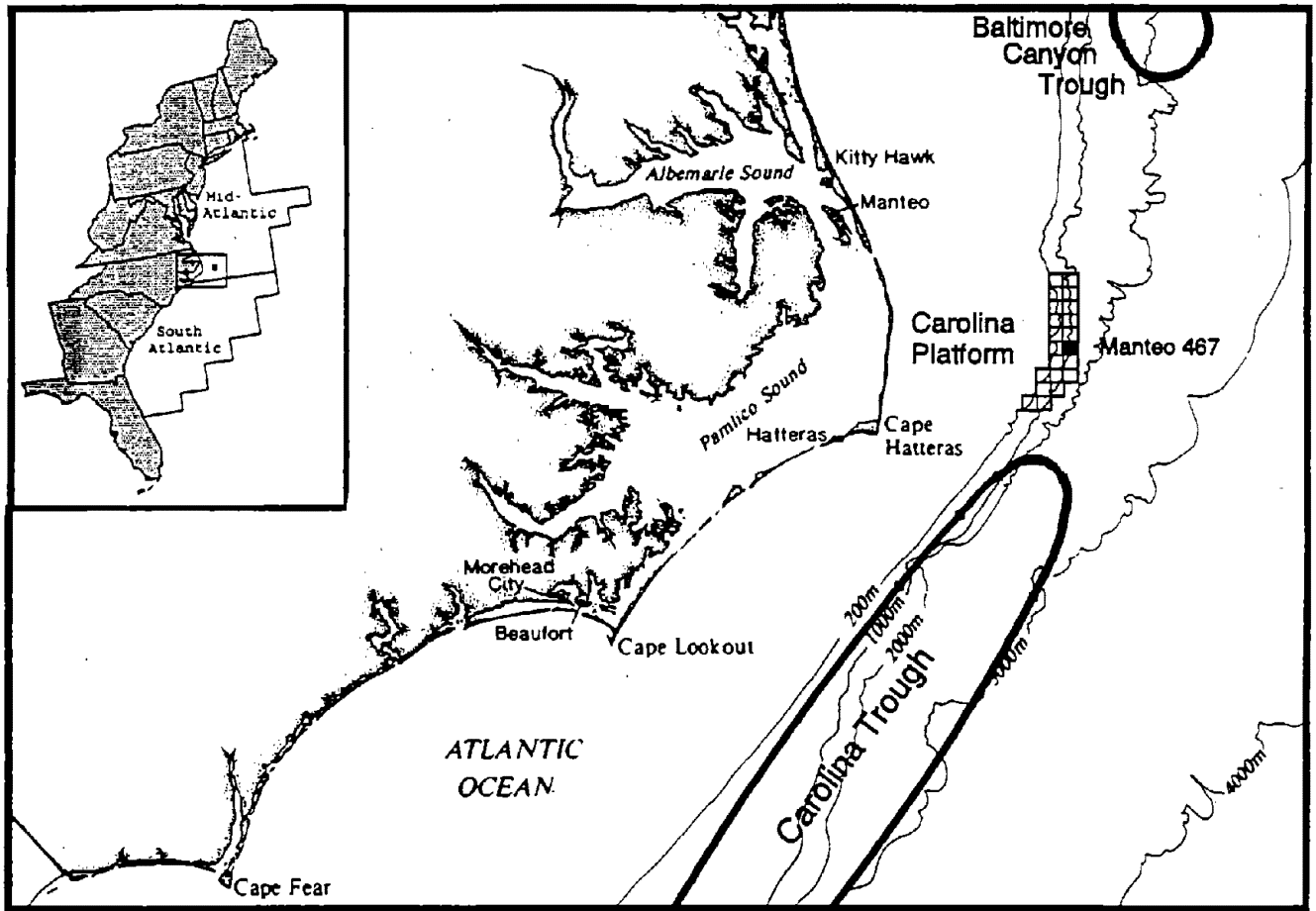


Figure 1-1. Location of the Manteo lease blocks off Cape Hatteras. Study area was centered around the Manteo 467 lease block.

Objectives

Concern was raised by the NCSRP (1992) that since not much is known about the bottom communities around the Manteo 467 lease block, exploration activities could result in significant environmental disturbance. Therefore, the principal task of this study was to survey the sea floor of the Cape Hatteras continental slope in the vicinity of the Manteo 467 site prior to initiation of exploratory drilling. The study objectives as listed in the scope of work are as follows:

1. Define the "unusual benthic community" that exists offshore North Carolina which is at its peak in the vicinity of the proposed Manteo drill site and "the Point." The working definition shall be based on species composition and relative abundance. However, the definition must also consider the impact of physical oceanographic processes, oxygen levels, and sediment types and flux.
2. Using the Offshore Operators' Committee (OOC) model (MOEPSI), estimate the area between the 300- and 1,500-m isobaths which could be covered by the deposition of muds and cuttings at the proposed drill site.
3. Survey the area of the Manteo site for the "unusual benthic community" as defined in objective No. 1. The survey must include benthic megafauna as well as the infauna.

4. Based on the results of the OOC model and the survey analyses, determine if the fraction of the "unusual benthic community" impacted by the estimated area covered by drill muds and cuttings is 5 percent or less.

The peak abundance in the vicinity of the Manteo drill site and "the Point" has not been documented or substantiated by any previous study.

Site Description

Physical Habitat

The Manteo 467 lease block is located on the continental slope off the coast of North Carolina, 72 km (45 miles) east-northeast of Cape Hatteras. The entire Manteo unit sits on top of a structural ridge called the Carolina Platform. At its northern end, where the study area is located, the Carolina Platform separates the Baltimore Canyon Trough in the north from the Carolina Trough in the south (Figure 1-1). The topography of the slope in this area is quite complex with numerous canyons, ridges, and gullies. The average slope of the bottom is about 30° to 35° with many vertical cliffs (MMS 1990). The upper slope down to approximately 650 m is steeper and topographically more complex than the middle and lower slope.

Oceanographic conditions in this region are controlled by the complex interaction of continental shelf and slope topography, and the Gulf Stream (Csanady and Hamilton 1988). Off Cape Hatteras the Gulf Stream is deflected to the east. To the north, a complex circulation pattern is developed between the Gulf Stream and coastal Labrador Sea water forming a distinct water mass known as the Slope Sea (Csanady and Hamilton 1988). This extends from Cape Hatteras to Nantucket Shoals offshore Massachusetts. Circulation within the Slope Sea is counterclockwise. The Western Boundary Undercurrent flowing from the north passes under the Gulf Stream in the area of Cape Hatteras and continues into the South Atlantic. This undercurrent passes seaward of Cape Hatteras at continental rise depths (Csanady and Hamilton 1988).

The complex hydrographic structure of the water column off Cape Hatteras results from the interactions of circulation patterns of the major currents, position of ocean fronts, Gulf Stream eddies, Gulf Stream meanders, water column stratification, and upwellings. Physical oceanographic studies (Science Applications International Corporation 1990) indicated that different water masses occupy the upper and middle slope, in the area of the Manteo lease block. Bottom currents on the rise are dominated by the Deep Western Boundary Current, while the Gulf Stream dominates surface currents. The unique nature of the bottom fauna is closely linked to the biological and physical interactions that are regulated by these currents.

Sediments at slope depths off Cape Hatteras are primarily hemipelagic calcareous sandy silts. Percentage composition of these sediments is about evenly split between sand, silt, and clay (Blake et al. 1985, 1987). At slope and rise depths there is no hard bottom; however, clay outcroppings and cliffs do appear to serve as substrate for epifauna, megabenthos, and demersal fish. The mineral quartz composes about 95% of the sand. This may indicate that this area of the continental slope is a site for local down-slope transport of sediments and other particulate materials. This terrigenous link is supported by the high levels of lead and aromatic hydrocarbons found in the sediment (Blake et al. 1985, 1987, Bothner et al. 1987). Schaff et al. (1992) also found high sediment mixing coefficients, which was attributed to bionurbation from the abundant infauna. The area also appears to have higher than average sedimentation rates for the Atlantic continental slope (Schaff et al. 1992).

Benthic Communities

Since Blake et al. (1985) first sampled the benthos of the continental slope off Cape Hatteras as part of the MMS ACSAR program, several other studies have confirmed the unusual nature of invertebrate and fish communities (Blake et al. 1987, Mobil 1990, Schaff 1991, Gooday et al. 1992, Schaff et al. 1992, Sulak 1992). Blake et al. (1985, 1987), who surveyed a broad area of the continental slope and rise off the North Carolina coast, found macroinfaunal abundances and biomass on the continental slope off Cape Hatteras, near the Manteo 467 lease block, higher than anywhere else along the entire South Atlantic continental slope and rise. They found macroinfaunal abundance to be over 46,000 individuals m⁻². A similar finding was reported by Schaff et al. (1992) who found densities over 55,000 individuals m⁻² at three nearby sites. Overall, biomass was six times higher, and biomass per individual was up to 3.4 times higher, than other slope areas at similar depths.

The species composition of the infauna off Cape Hatteras is also different from other slope habitats. Species richness and diversity are lower with a high degree of dominance by species that are cosmopolitan in distribution. The macrofauna is dominated by polychaetes and oligochaetes more typical of shallow depositional sites. Both Blake et al. (1985, 1987) and Schaff (1991) found annelid species comprised 66% to 76% of the individuals. Blake et al. (1985, 1987) found little similarity between a 600-m station off Cape Hatteras and other 600-m slope stations they sampled in the South Atlantic. They also found the fauna at a 2,000-m station off Cape Hatteras was more similar to the 600-m than to other 2,000-m stations.

A tube-building foraminiferan, *Bathysiphon filiformis*, is abundant over much of the continental slope and rise off Cape Hatteras. It can reach abundances of up to 154 individuals m⁻². Its tube is approximately 2 mm in diameter and up to 7 cm long. While it serves as an important substrate for other epifaunal species (Goody et al. 1992), it apparently has little influence on the infauna community (Schaff et al. 1992).

Trends in abundance for invertebrate megafauna on the continental slope off Cape Hatteras appear to be similar to the macroinfauna (Blake et al. 1987, Mobil 1990, Appendix A). Shepard et al. (Appendix A) analyzed video tapes of submersible dives, found the median overall relative abundance of megafauna, in the area of the proposed Mobil drill site to be about 16 to 27 individuals min⁻¹ of videotape. Sites 30 nmi north had similar relative abundances, but those 30 nmi south had relative abundances of about 2 individuals min⁻¹ videotape. Relative abundances were higher at upper slope depths (283 to 650 m) compared to middle slope depths (>650 m). The dominant sedentary megafauna are anemones of the genera *Actinauge* and *Cerianthus*, and an unidentified anemone (Mobil 1990, Appendix A). The mobile invertebrate megafauna is dominated by echinoderms. Starfish, most likely of the genus *Asterias*, are most abundant on the upper slope. In isolated areas dense aggregations of the brittlestar *Ophiura sarsi* can occur (Mobil 1990, Appendix A).

Demersal fish fauna off Cape Hatteras is distinctive in terms of composition and population density when compared to areas approximately 75 nmi north and 100 nmi south. Sulak and Ross (Appendix B), who analyzed video tapes of submersible dives, found that three species, *Lycenchelys verrilli*, *Glyptocephalus cynoglossus*, and *Myxine glutinosa*, accounted for 83% of all individuals seen. These same three species comprised 43% and 22% of the total fish fauna north and south of the Manteo 467 area, respectively. To the north the three top-ranking dominant species are *Glyptocephalus cynoglossus*, *Synaphobranchus* spp., and *Nezumia* spp. To the south the three top-ranking species are *Synaphobranchus* spp., *Myxine glutinosa*, and *Nezumia* spp. While *Nezumia* spp. was not dominant off Cape Hatteras, it was approximately equally abundant in all three areas (Sulak and Ross Appendix B).

Overall, the abundance of benthic fish off Cape Hatteras is four to seven times higher than adjacent areas north of 35° 31' latitude and south of 35° 22'. Sulak and Ross (Appendix B) found this distinctive fish fauna to be limited latitudinally to a relatively restricted portion of the continental slope. However, the exact latitudinal limits cannot be precisely defined.

Predicted Sedimentation from Drilling Activities

A byproduct of the exploratory well proposed in the Manteo 467 block will be the production of drilling muds and cuttings. In order to address objective 2 and estimate the dispersion of these byproducts at the proposed well site, in the water column and across the bottom, a mathematical model developed by the Offshore Operators' Committee (OOC) and Exxon Production Research Company was employed. The OOC model was based on the Dredged Material Model developed by the U.S. Army Corps of Engineers and U.S. Environmental Protection Agency (Brandsma et al. 1980). The OOC model predicts, as a function of water column depth, topography, and current speed and direction, the concentrations of soluble components and solids in the water column, and the initial deposition of solids on the sea floor. Output from the OOC model was then used to address objective 4.

The OOC model has been used extensively in impact assessment. The dynamic plume portion of the model has been verified in the laboratory (Brandsma and Sauer 1983). The entire model was field verified to determine how far, from a simulated well site, drilling mud would disperse in the water column and along the sea floor (O'Reilly et al. 1989). There was good agreement between the model and the field verification dataset as to the direction of dispersion and deposition of drilling muds. The OOC model predictions fell within the range of concentrations measured in the field for 75% of the water column sampling stations. Although the

amount of drilling muds initially deposited was complicated by the sedimentation of natural sediments, there was still good agreement between the OOC model and verification data (O'Reilly et al. 1989).

Dispersion and Deposition

To predict the dispersion and deposition of drilling muds and cuttings at the proposed well site in the Manteo 467 lease block, Brandsma (1990) used the OOC model. Simulations for near bottom and surface discharges were done using maximum, median, and minimum current speeds and prevailing current directions (Table 1-1). The area of sea floor represented in the final simulations for the proposed well site in the Manteo 467 lease block was a grid 61 x 129 cells. Each cell within this grid was 500' (152.4 m) on a side. The model grid represented an area approximately 9.3 x 19.7 km with the long axis of the grid aligned north-south.

Table 1-1. Current speeds and directions used in the OOC model simulations at the Manteo 467 proposed well site. Only surface (0 m) and bottom (830 m) measurements at the proposed well site are given. (a) Conditions when surface currents were maximum and minimum. (b) Conditions when bottom currents were maximum and minimum. Taken from Brandsma (1990).

Depth (m)	Maximum		Current Median		Minimum	
	Speed (kn)	Direction (°)	Speed (kn)	Direction (°)	Speed (kn)	Direction (°)
(a) Surface						
0	6.00	41	3.14	37	0.03	18
830	0.03	201	0.07	233	0.23	205
(b) Bottom						
0	3.49	36	5.74	42	2.53	47
830	0.36	197	0.10	221	0.02	351

Brandsma (1990) found that simulated discharge of 1000 barrels of drilling muds (density = 10.2 lb gal⁻¹) over 2 hrs into minimum surface currents showed no accumulation of solids on a model-simulated 300-m deep sea-floor even after 33 hrs. Based on this, Brandsma (1990) did no other simulations of mud discharges from the surface.

For the simulation of discharge from the bottom, the pattern of deposition was determined by the depth of water, rapid settling of cutting solids, and currents. For the proposed exploratory well to be drilled in the Manteo 467 lease block, Mobil (1990) estimated a total bottom discharge volume of 4000 barrels for drilling muds and cuttings. Dispersion of this volume of material was then simulated with the OOC model. The model grid captured 67 to 75% of the total solids discharged in bottom simulations. The remainder of the simulated material did not settle within the boundaries of the model (Brandsma 1990).

When currents were minimum the pattern of deposition was roughly circular around the discharge point. However, it elongated following the 197° current direction for the median and maximum currents (Figure 1-2). Minimum deposition thickness contoured on Figure 1-2 is 0.1 μm. The maximum thickness of combined drilling muds and cuttings predicted at the discharge point was 3.3 cm for minimum bottom and surface current conditions. At maximum bottom and surface currents, 1.9 cm was the predicted deposition. These maximum depositions occurred within the grid cell that contained the discharge. Overall, approximately 33 to 66% of the simulated discharged muds and cuttings were deposited in this single cell.

The area covered by >1.0 μm in the six OOC model simulations ranged from approximately 3.1 to 4.5 km² of the sea floor. The area covered by >0.1 μm, the thinnest layer predicted, ranged from 8.2 to

10.8 km² of the sea floor (Brandsma 1989). To determine the total area of the sea floor that could receive at least the minimum predicted amount of solids (0.1 μm), the predictions from all six model runs were overlaid on the study area (Figure 1-3). The OOC model, as run by Brandsma (1990), predicted approximately 12 km² of the sea floor would be effected by deposition of drilling muds from a simulated discharge of 4000 barrels of drilling muds.

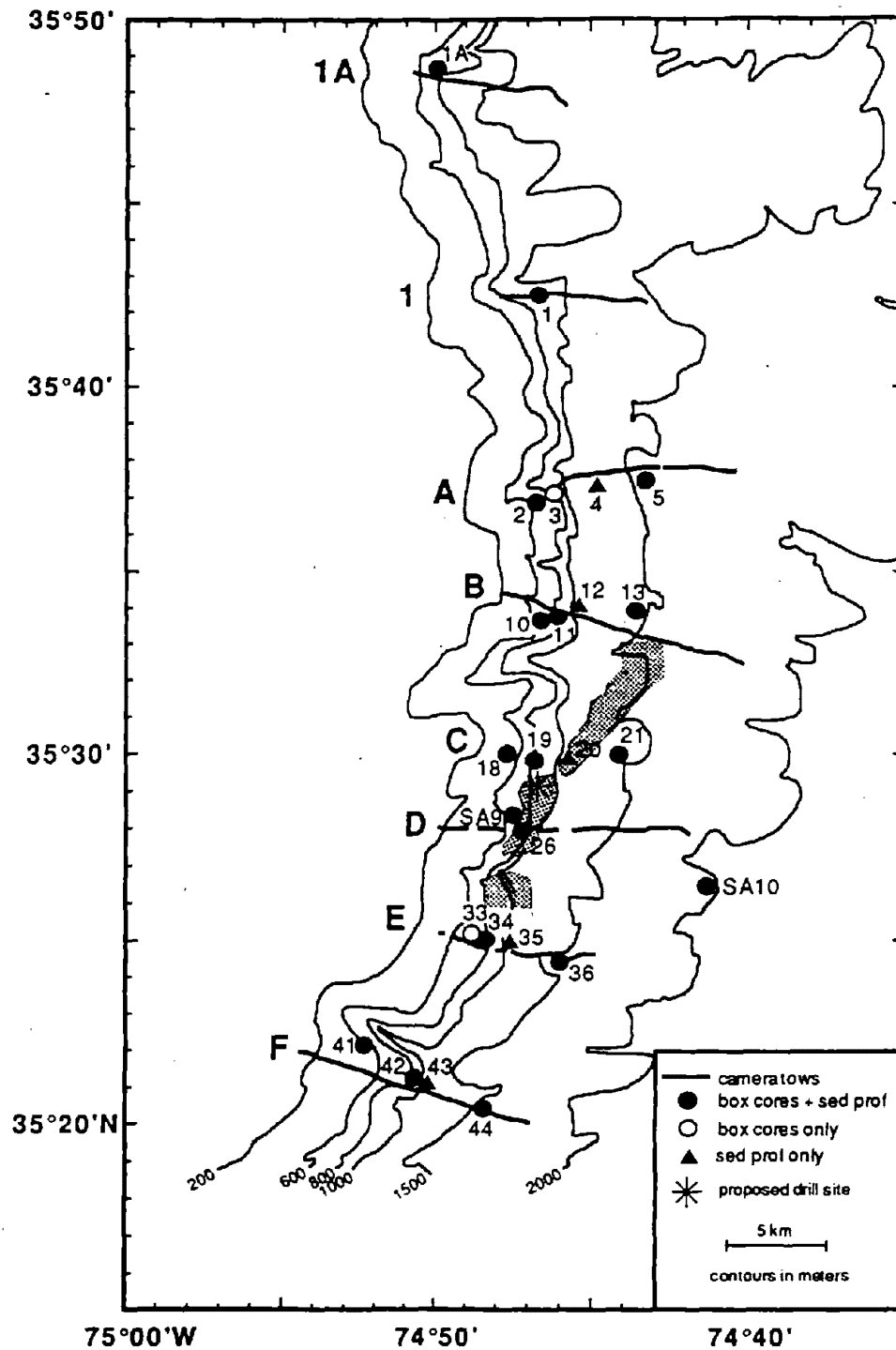


Figure 1-2. Predicted dispersion patterns of drilling mud and cuttings from a proposed well site (●) located in Manteo lease block 467. Minimum (Min), median (Mid), and maximum (Max) surface (S) and bottom (B) current conditions are presented. The thickness contoured is $0.1 \mu\text{m}$. Predictions were done with the Offshore Operators' Committee model and are taken from Brandsma (1990).

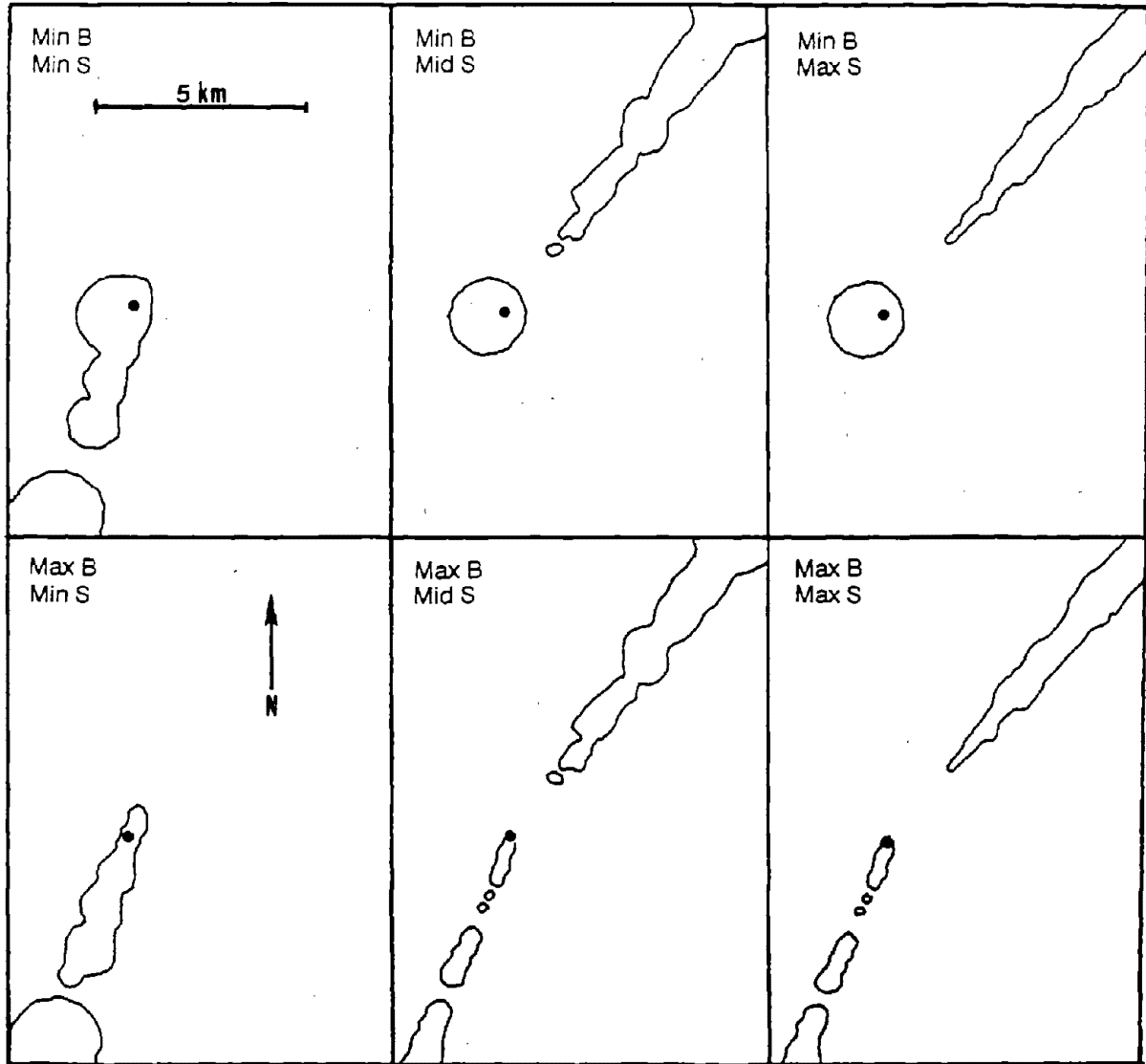


Figure 1-3. Overlay of predicted dispersion and deposition patterns (stippled area) from the Offshore Operators' Committee model (Brandsma 1990) and study area. The stippled area represents deposition of 67 to 75% of the simulated discharge of 4000 barrels of drilling muds and cuttings. The remainder of the material did not settle to the bottom within the model boundaries.

CHAPTER 2. SAMPLE DESIGN AND FIELD METHODS

Robert J. Diaz and James A. Blake

Sample Design

To address all four of our objectives the boundaries of the study area were defined based on output of the Offshore Operators' Committee (OOC) model which predicted the dispersion and accumulation of drilling muds and cuttings over the seafloor (Mobil 1990). This model predicted areas that would receive as little as 0.1 μm of deposition (see Figure 1-3). After calculating the area of the seafloor that would likely receive any deposition, the initial area to be sampled was expanded 15 km to the north and 15 km to the south of the proposed drill site (Figure 2-1). This insured that the area we sampled would be at least 20 times larger than the total area the OOC model predicted would be impacted by drilling activities and allow objective 4 to be addressed. The NCSRP (1992) recommended that if impacts from drilling activities exceeded 5% of the total area of the unusual benthic community then a benthic recovery study be initiated.

The basic field sampling consisted of six cross-shelf transects running approximately east-west. Transects were nearly perpendicular to the isobaths (Figure 2-1). Transect C was slightly north of the proposed drill site in the Manteo 467 lease block. Transect D was one previously sampled by the MMS Phase II South Atlantic studies (Blake et al. 1987). Transects B and E were about 8 km north and south of the proposed drill site, while Transects A and F were about 13 to 16 km north and south, respectively. The transects covered a distance of about 30 km (21 nmi) and spanned depths from about 200 to 1,800 m. This depth range was expected to exceed the depths occupied by the unusual benthic communities. We also sampled two historical stations (SA9 and SA10), previously occupied Blake et al. (1987), to evaluate long-term changes in the benthic community.

On each transect (A through F) stations were located at depths of 600, 800, 1,000, and 1,500 m. A single box core was collected at the 600, 800, and 1,500 m stations. Surface and sediment profile camera images were taken at the box core stations and also at the 1,000 m station. A camera sled was deployed on each transect starting at the deep (about 1,800 m) end and towed to shallow water (as shallow as 120 m).

Preliminary evaluation of surface and sediment profile camera images at sea allowed us to reevaluate the placement of stations and transects. Data from the preliminary evaluation, combined with the visual observation on the box cores, indicated that the sediments and benthic community were similar at all the transects that we had established. We added two short transects at 800 m approximately 10 and 22 km north of transect A (1 and 1A, Figure 2-1). The camera sled tow on Transect C was also relocated to these newly added transects (1 and 1A).

Field Methods

Vessel and Navigation

The R/V *Endeavor*, a University-National Oceanographic Laboratory System (UNOLS) vessel based in Rhode Island, was used to conduct the field work. The field work (cruise EN-241) was conducted from 26 August to 6 September 1992. Precise navigation was achieved with a global positioning system and calibrated LORAN-C integrated with the Science Applications International Corporation Portable Integrated Navigation Survey System. A complete listing of station coordinates is given in Appendix C.

Box Core

Samples to characterize the benthos, sediments, and chemical environment were obtained using a 0.16 m² BX-640 Ocean Instruments box core. One sample was taken at each station. Processing of the box-cores was done based on procedures developed as part of programs conducted by MMS (Blake et al. 1987) and recent studies for the U.S. Navy and the U.S. EPA off northern California (Blake et al. 1992, SAIC 1992).

The box core was partitioned into sixteen 10 x 10 cm subcores. After retrieval of the box core the entire surface of the sample was examined. Evidence of disturbance, sediment color, and any interesting or unusual biological or physical features were noted. The subcores were removed individually from the sample box for processing. From each box core nine of the subcores were combined for the macrofaunal sample.

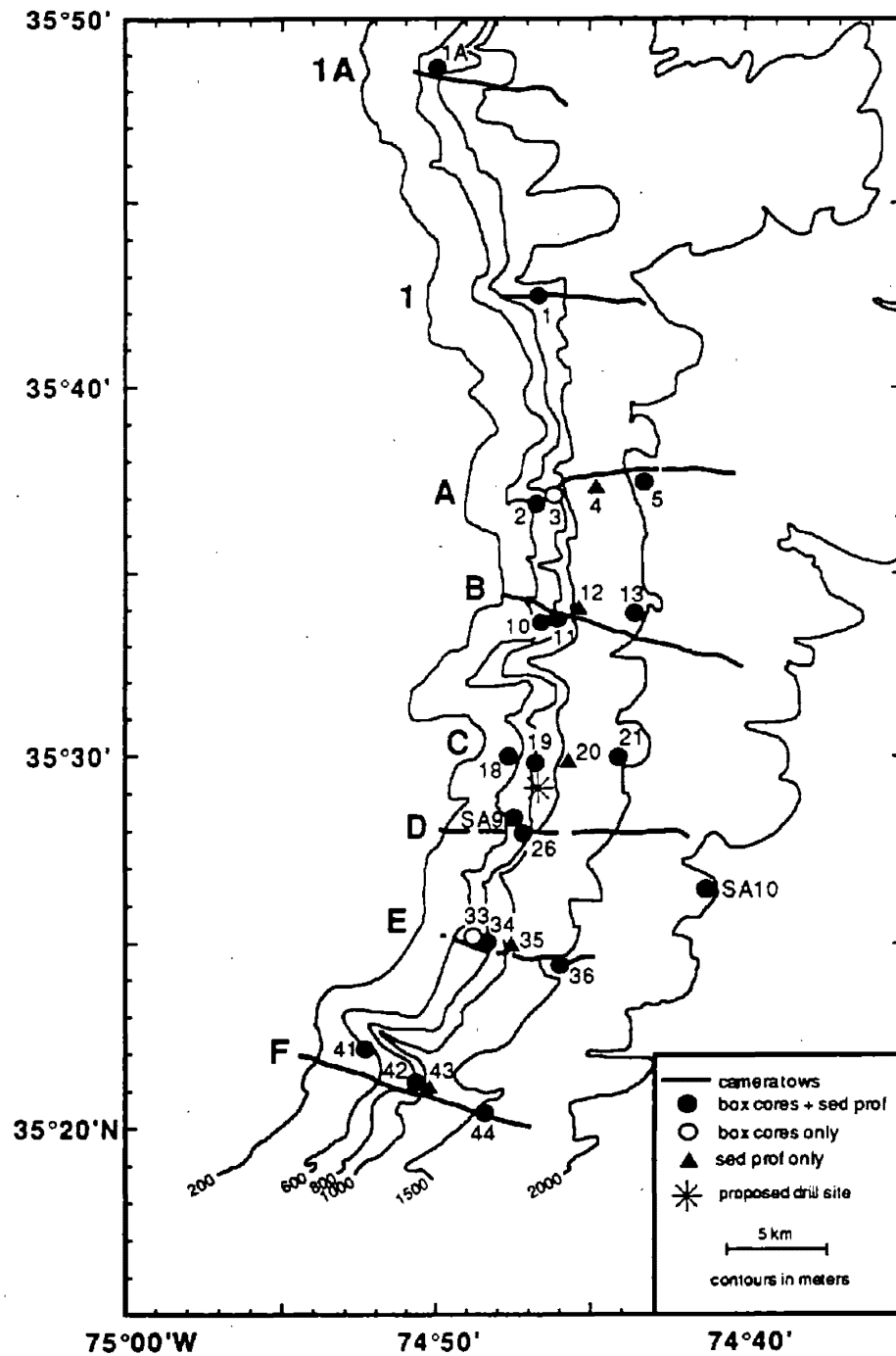


Figure 2-1. Location of sampling stations on the continental slope off Cape Hatteras.

Samples for sediment CHN, grain size, chlorophyll *a*, diatoms, lipids, methane, sulfate, dissolved inorganic carbon (CO₂), ²¹⁰Pb, and x-ray analysis were taken from the remaining seven subcores. Each box-core was processed immediately after being brought on board ship. If a subcore was considered to be disturbed, or showed evidence of leakage, it was replaced with an alternate subcore.

Sediment Surface and Profile Imaging

Standard vertical photographs were taken at a distance of approximately one meter from the bottom with a Benthos, Inc., North Falmouth, MA, Model 372 camera and double-head strobe. The camera was set to photograph an area of approximately 0.6 m². Sediment profile images were taken with a Benthos Model 3731 Sediment Profile Camera. The profile camera provided images of up to 30 cm of the upper sediment column.

Towed Camera Sled

Megafauna were photographed with the Benthic Apparatus for Biological Surveys (BABS), a towed camera sled equipped with a Benthos, Inc., Survey Model camera and single-head strobe. This type of camera system was originally developed for MMS studies on the U.S. Atlantic coast to characterize the epifauna found on the continental slope and in submarine canyons. Two sleds and associated equipment were loaned to this project by Columbia University. The sled was towed directly over the bottom. The camera was oriented facing forward at an angle of 13.5° down from the horizontal and 0.43 m above the seafloor. Illumination is provided by a 200-watt-second strobe mounted to the side and slightly above the camera. Photographs were taken at 15-second intervals. At an average speed of 1 kn, a picture is taken every 7.7 m along the track of the tow. Because of the back scatter of light from suspended particles and steep slope angles the typical usable area of the image is 2-3 m².

Stations and Data Analyzed

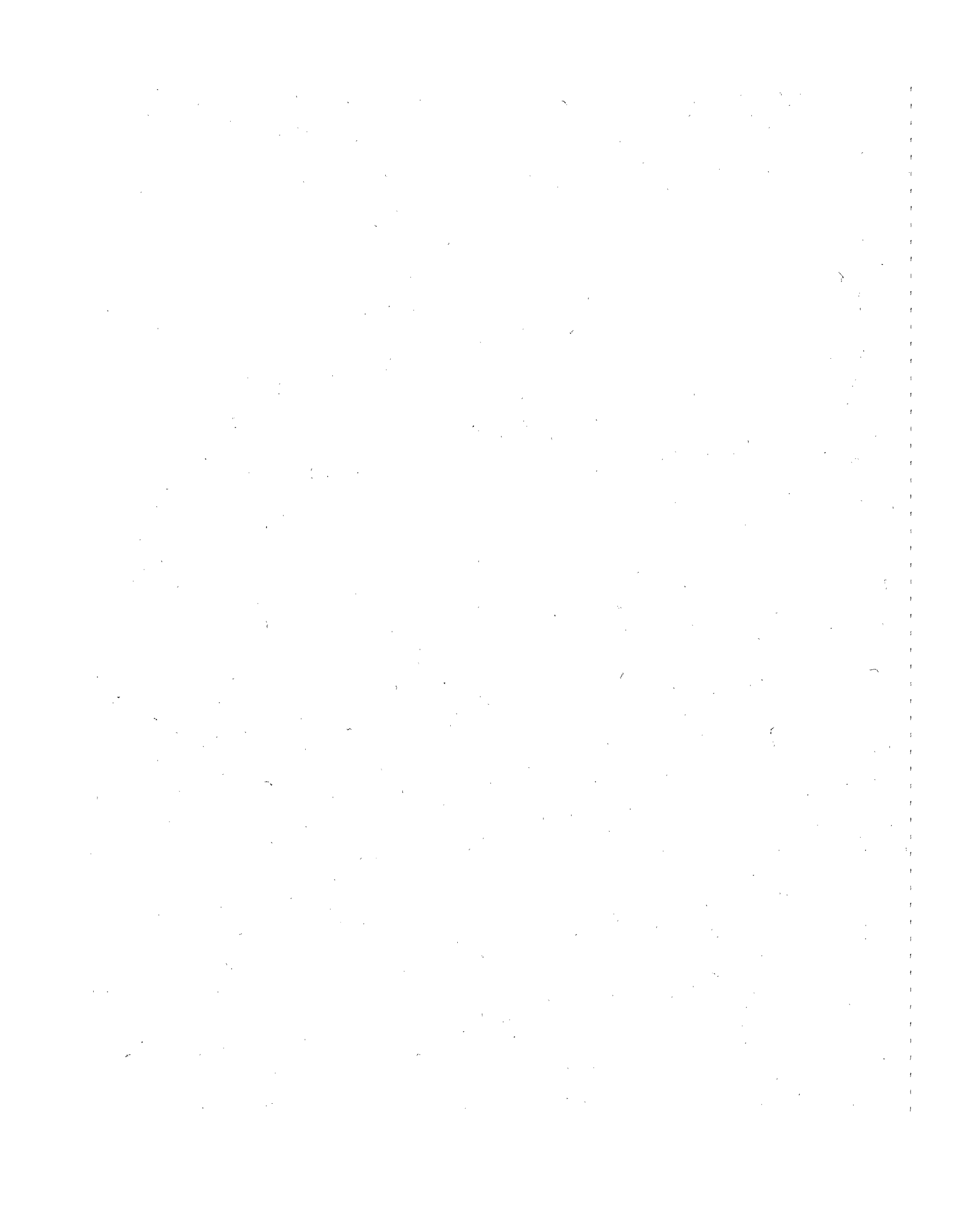
Table 2-1 summarizes the data collected at each station. Although box cores were collected at 20 stations only 16 stations were processed and analyzed for macrobenthos. The seven camera sled tows and all surface and sediment profile camera images were analyzed. All samples taken from the box core for the various sediment parameters were included.

In Chapter 1, data generated from the OOC model simulations was used to determine the area of the sea floor that would be affected by drilling of the proposed well in the Manteo 467 lease block. Chapter 3 contains data on the sediment characteristics and sedimentary processes that are crucial to understanding benthic community dynamics. Chapter 4 is a detailed evaluation of the quality and quantity of organic matter in the sediments that fuels the benthic community. Chapter 5 provides data on the relative importance of physical and biological processes in determining sediment stratigraphy and fabric. Rapid analysis of data from the sediment profile camera in the field also led us to expand the boundaries of the study area. Chapter 6 is a synthesis of sedimentological data. Chapter 7 contains data on infaunal community structure and aerial extent. Chapter 8 contains data on demersal fish, invertebrate megafauna, and physical habitat characteristics. Chapter 9 is a synthesis of biological data.

Table 2-1. Summary of data collected in the vicinity of the Manteo 467 lease block on the R/V *Endeavor* cruise (EN-241) from 26 August to 6 September 1992. The spatial arrangement of stations can be seen in Figure 2-1. Station coordinates are in Appendix C. The study objectives that each parameter addresses is also indicated. X - indicates data were included in this report. O - indicates data that were not included.

Parameter Measured	Transect Station																				Collected For Study Objective				
	1A	1	A	A	A	A	B	B	B	B	C	C	C	C	D	D	D	E	E	E		E	F	F	F
Box Core Data																									
Macrofauna	X	X	X	X		X	O	X		O	X	X		X	X	X		X	O	X		O	X	X	X
Meiofauna	O	O	O	O		O	O	O		O	O	O		O	O	O		O	O	O		O	O	O	O
Foraminifera	O	O	O	O		O	O	O		O	O	O		O	O	O		O	O	O		O	O	O	O
Grain size	X	X	X	X		X	X	X		X	X	X		X	X	X		X	X	X		X	X	X	X
Carbonate	X	X	X	X		X	X	X		X	X	X		X	X		X	X	X		X	X	X	X	
²¹⁰ Pb Profile			X	X		X				X	X			X				X				X	X		X
X-ray			X	X		X	X	X		X	X			X				X	X	X		X	X	X	X
CHN	X	X	X	X		X	X	X		X	X	X		X	X		X	X	X		X	X	X	X	
Lipids			X	X		X		X		X	X							X		X		X	X	X	
Chlorophyll <i>a</i>			X	X		X	X	X		X	X			X	X		X	X	X		X	X	X	X	
Viable Diatoms			X	X		X	X	X		X	X			X	X		X	X	X		X	X	X	X	
Methane Profile			X	X		X	X	X		X	X			X				X	X	X		X	X	X	
Sulfate Profile				O						O				O						O					
CO ₂ Profile				O						O				O						O					
Surface Images	X	X	X		X	X	X	X	X	X	X	X	X	X	X	X	X	X	X	X	X	X	X	X	
Profile Images						X	X	X		X		X	X	X	X	X					X	X	X	X	
Towed Camera Sled*	X	X	X			X								X			X				X				

* Sled was towed along indicated transects.



CHAPTER 3. SEDIMENT CHARACTERISTICS AND PORE WATER METHANE

David J. DeMaster, Neal Blair, and Robert J. Diaz

Introduction

Previous studies have shown that characteristics of the sediment, such as grain sizes and concentrations of organic compounds, can influence the composition and abundance of benthic organisms of continental shelf communities (Weston 1983, 1988, Diaz et al. 1987). Therefore, it is possible that the high density of organisms previously found on the continental slope off Cape Hatteras may have been due to some unique feature(s) of the sediment.

To address objective 1 and to determine if sediment characteristics were important in defining the areal extent of the unusual benthic community of the continental slope off Cape Hatteras, a number of sediment parameters were measured. The sediment characteristics measured included grain size distribution, concentrations of carbonate, organic carbon, and organic nitrogen, and depth profile of ^{210}Pb and pore-water methane. The depth-profile of ^{210}Pb gives information on both the rate of sediment accumulation and the sediment mixed layer depth (bioturbation). Because methane is produced during anaerobic metabolism, it provides information on the rate at which organic matter is degraded and, by inference, the rate at which metabolizable organic carbon is delivered to the sea floor. Measurements of carbonate and organic carbon and nitrogen all help to identify the sources of organic matter that support benthic populations.

Methods

From each box core station (Table 2-1) two-10 cm deep by 2.5 cm (I.D.) core samples were collected for grain size analysis, carbonate, organic carbon and nitrogen. Grain size was determined after adding sodium hexametaphosphate and sonicating to disaggregate the sediment, and the samples were sieved through a 63- μm sieve to separate the sand and mud fractions (Folk 1974). The size of the sand grains was determined using a rapid sand analyzer. The size distribution of the mud fraction was determined using an automated grain size analyzer (Sedigraph 5000) which measures grain size based on the settling rate of particles through a beam of x-rays. Calcium carbonate content was determined by adding 3 ml of 10% HCl to a known amount of dried sediment (2 to 4 g). The sediment was then rinsed free of the acid solution and dried at 60° until constant weight was achieved. The reduction in weight represented the amount of carbonate in the sediment. A Carlo Erba 1500 CNS analyzer was then used on this sample to determine the amount of organic carbon and nitrogen. The organic carbon values were subsequently adjusted to a bulk sediment basis using the percent carbonate data.

Box cores from ten stations were used to measure excess ^{210}Pb (Table 2-1). Sediment collected from five box-cores with a 5 cm (I.D.) tube was divided into 1 or 2 cm long sections. The bulk density and porosity of the sediment were measured, and then ^{210}Pb activity was determined by measuring the activity of its daughter, ^{210}Po . One ml of a calibrated ^{209}Po spike was added to 4 g of dried sediment, and then a combination of HCl, HNO_3 , HF, and HClO_4 acids was added to totally dissolve the sample. The Po isotopes were acidified in a 1.5 M HCl solution and plated onto silver disks. The activities of the Po isotopes were measured on an alpha spectrometer, and then converted to ^{210}Pb activities. A second set of ^{210}Pb measurements were made on the sediments used for x-ray images. After x-rays were taken, cores were divided into 1 or 2 cm sections, dried, and pulverized. ^{210}Pb activities were determined by direct counts of gamma-ray emissions from the radioactive decay of ^{210}Pb using a Canberra Industries, Inc. Planar Germanium detector system, and following the procedures in Cutshall et al. (1983).

For measurement of pore-water methane, 3 ml of sediment were collected using a syringe from the top 2 cm of 15 box core samples. These were placed in 40-ml bottles with 1 ml of 1 M KOH to arrest bacterial action, sealed with rubber stoppers, and stored frozen. As a control an empty bottle was sealed for each core sampled. In the laboratory the samples were thawed and then shaken immediately prior to analysis. A 5-ml aliquot of the headspace was injected into a gas chromatograph equipped with a 3 mm diameter molecular sieve (5A) column and flame ionization detector. The calibration curve was determined by three standards: 9.93, 98.6, and 1,000 ppm. The precision and accuracy of the 9.93 ppm standard were ± 0.08 and ± 0.33 ppm, while for the 98.6 ppm standard they were ± 0.18 and ± 5.88 ppm ($n=3$ for both).

Results

Sediment Characteristics

Except for two stations, very fine sand (3.5 to 4.0 ϕ) was the most abundant type of sediment (Figure 3-1). At the northernmost station (1A), the most abundant was coarse silt, while at the southernmost (44) very fine sand and clay (12.0 to 12.5 ϕ) were about equally abundant. All but five stations fell into the center of a ternary diagram (Figure 3-2), which, using the Wentworth classification scheme, places them in the silt-sand-clay category. Three of the five not in the center were deep stations (>1,400m). Mean grain size ranged from 5.3 to 8.9 ϕ and sorting from 2.3 to 5.2 ϕ .

The amounts of carbonate, organic carbon and nitrogen, and the C:N ratio are presented in Figure 3-3. There was no consistent pattern among transects or depths in the amount of calcium carbonate. Microscopic examination of the sediment revealed that much of the carbonate content was in the form of foraminiferan tests, from which over 120 species have been identified. The concentrations of organic carbon and nitrogen were about 2.5 times higher at station 1A than at the other stations. While concentrations of both compounds were below average at all three stations on transect B, there was no consistent difference in the C:N ratio among transects or depths.

Sediment Accumulation Rates

The rates of sediment accumulation and the depth of the mixed layer calculated using excess ^{210}Pb activity (total minus supported activity) are presented in Table 3-1. There was considerable variation among stations, but there were no consistent differences among transects or depths. Accumulation rates (excluding SA-10) ranged from 0.3 to 1.8 cm yr^{-1} . The excess activity of ^{210}Pb from all but one station was high (>20 dpm g^{-1}) at the sediment surface which indicates that sediment is accumulating, not eroding, on a 100-yr time scale.

Table 3-1. Estimated sediment accumulation rates (cm yr^{-1}), and depth of the sediment mixed layer (cm).

Transect	Factor	Water Depth		
		600 m	800 m	>1400 m
A	Station	2	3	5
	Rate	0.6	0.5 - 1.1	1.0 - 1.8
	Mixed	12	8	3
C	Station	18	19	21
	Rate	1.4	0.4 - 1.2	1.2
	Mixed	11	5	4
D	Station			SA10
	Rate			0.05
	Mixed			10
F	Station	41	42	44
	Rate	1.5	0.3 - 0.6	1.0
	Mixed	4	5	6

Methane Concentrations

While methane concentrations at about half of the stations were fairly constant throughout the sediment, for the other half the concentrations increased below some depth (Figure 3-4). There were fewer stations with

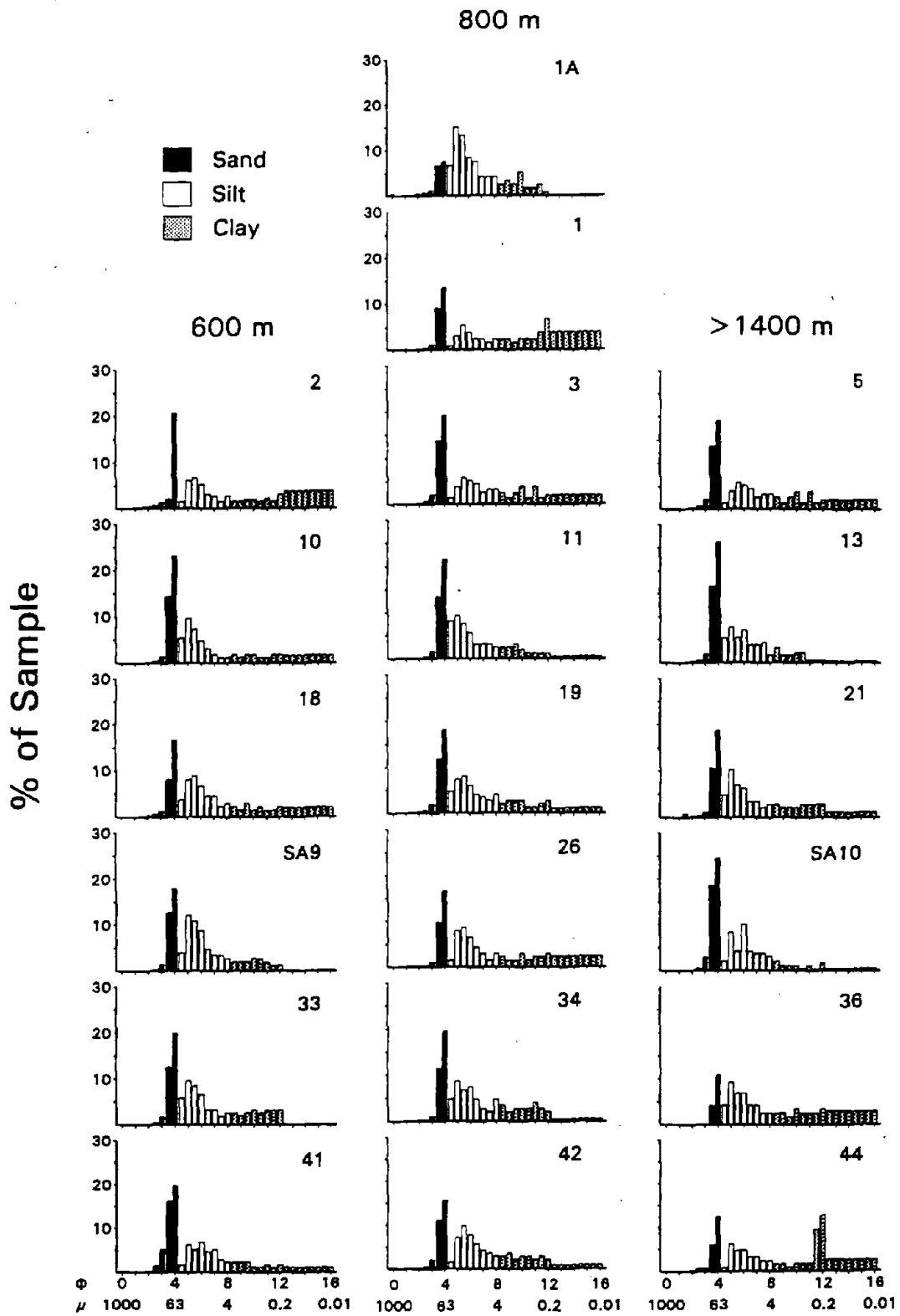


Figure 3-1. Frequency distributions of grain sizes from sediments collected off Cape Hatteras. Each interval is one-half phi. Stations arranged vertically by transect (North is top of page) and horizontally by depth. See Figure 2-1 for spatial orientation of stations.

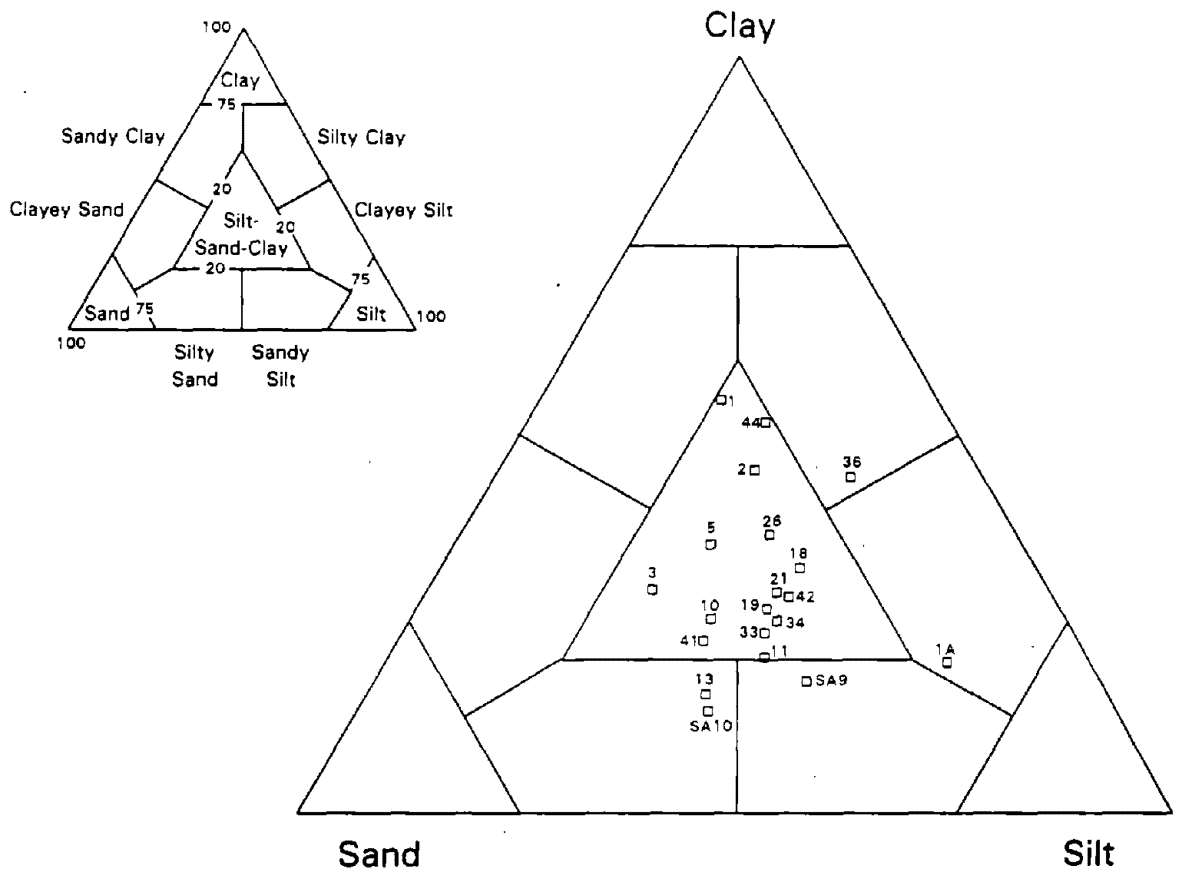


Figure 3-2. Ternary diagram showing the classification of sediment type for box-core stations.

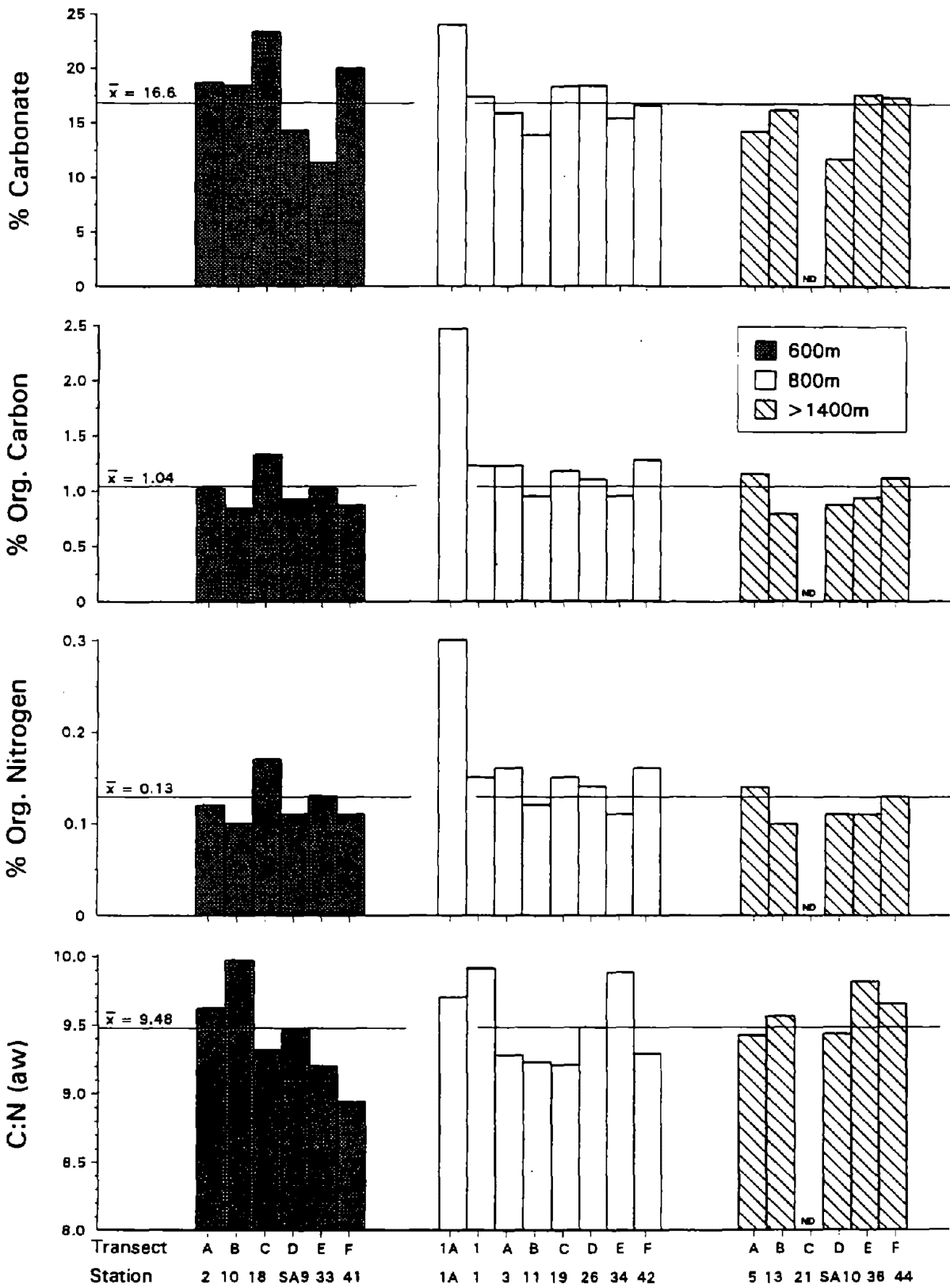


Figure 3-3. Concentration of carbonate, organic carbon and nitrogen, and C:N ratio (based on atomic weights) for sediments collected off Cape Hatteras. Lines across graphs indicate overall grand mean excluding the 800 m station on transect 1A.

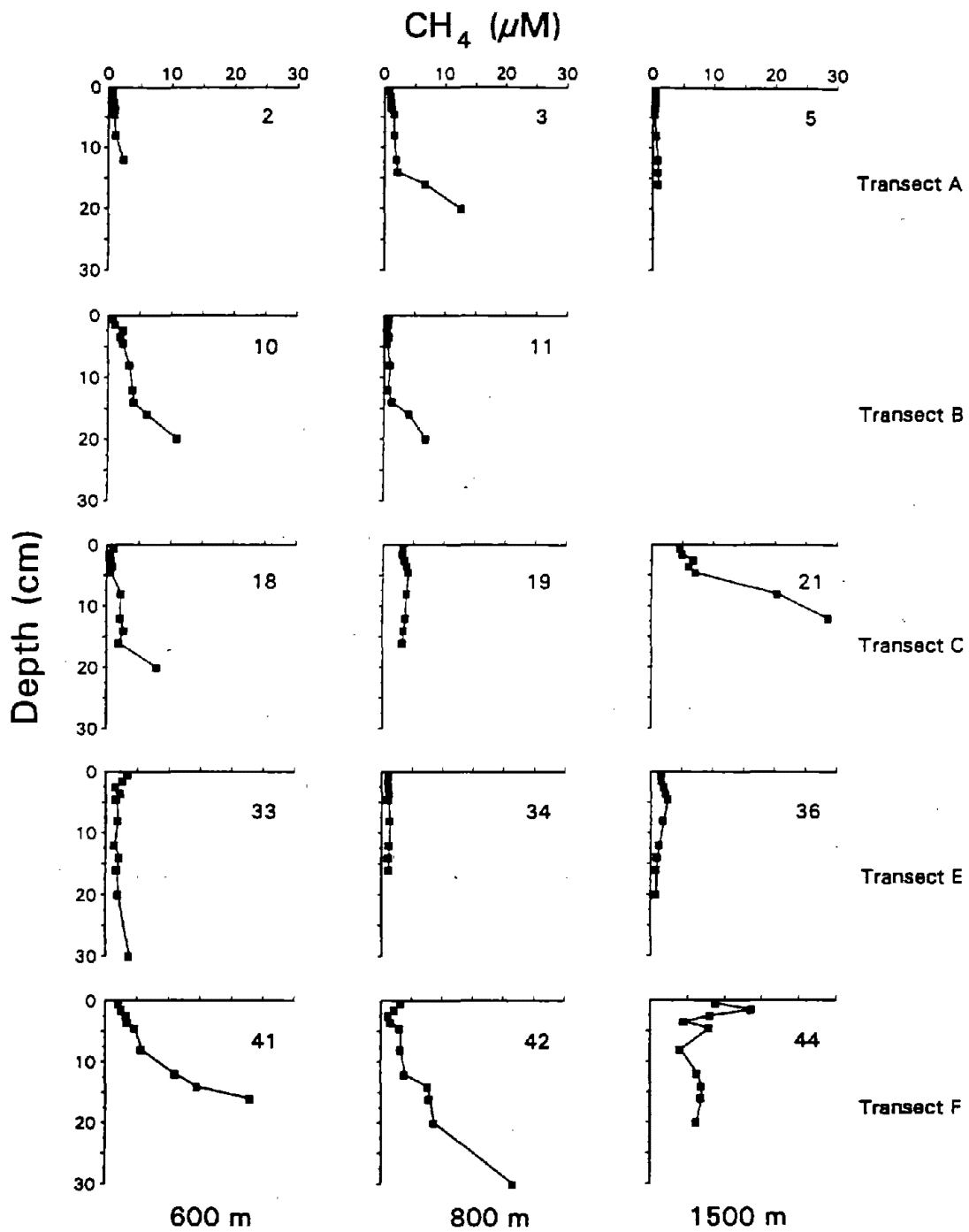


Figure 3-4. Depth profiles of methane concentration at box core stations. Stations arranged vertically by transect (North is top of page) and horizontally by depth. See Figure 2-1 for spatial orientation of stations.

constant concentrations at the shallow stations; 60% of the >1400 m stations, but only 20% of the 600-m stations, had no concentration gradients. Except for transect E, where concentrations were fairly constant for all three stations, there was no obvious pattern to the distribution among transects of these two types of depth profiles. The concentration of methane at station SA10 was inexplicably higher than any of the other stations (Figure 3-5).

Discussion

Except for the northernmost station (1A) which had higher concentrations of total organic carbon and nitrogen and a different grain size-distribution, there was no consistent difference among stations in any of the measured sediment characteristics. Therefore, there is little reason to suspect that gradients in sediment characteristics would have any systematic effect upon the benthic community over the area studied.

Preliminary measurements indicated that the rates of sediment accumulation and carbon flux on the continental slope off Cape Hatteras were unusually high (Schaff et al. 1992). Except for the deepest station (SA10), which had a sediment accumulation rate of 0.05 cm yr⁻¹, data from the current study support this with estimated rates of accumulation that ranged from 0.3 to 1.8 cm yr⁻¹. This is much higher than other areas on the continental slope where the rate of accumulation is 0.01 to 0.04 cm yr⁻¹ (Emery and Uchupi, 1972). The organic carbon content of the sediments were typical for continental slope deposits (Anderson et al. 1988) and ranged from about 1 to 2.5%. However, calcium carbonate content averaged about 17% and was much higher than other slope areas which range from 8 to 12%. Schaff et al. (1992) found the accumulation rate of organic carbon on the Cape Hatteras continental slope, their Site III within our study area, to be high >70 g Org. C m⁻² yr⁻¹. The range of organic carbon accumulation from our stations was 28 to 121 g Org. C m⁻² yr⁻¹. Calcium carbonate accumulation rates were also high at 365 to 2780 g CaCO₃ m⁻² yr⁻¹. Microscopic examination of the sediments indicated that most of the carbonate was in the form of foraminiferan tests.

Because it is produced during the anaerobic metabolism of organic matter, steep concentration gradients of methane are expected where the amount of carbon flux is high. For example, steep gradients have been found in the highly productive regions off the coast of Peru (Henrichs and Farrington 1984). In contrast, sediments with no gradient are indicative of either low carbon flux or high rates of sediment mixing. About half the stations in the current study had concentration gradients of methane. This supports the findings of Schaff et al. (1992), who found high methane concentrations at their nearby Site III, and is consistent with the high abundances of benthic organisms (Blake et al. 1985, 1987, Schaff 1991) and the high flux of carbon to the area. However, half of the stations had no evidence of gradients. Given that the rate of sediment accumulation and the abundance of benthic organisms are both high, it seems likely that this is due to intense biological reworking of the sediment rather than low carbon flux. This is supported by the fact that even at the stations with high concentrations of methane the gradients did not begin at the sediment surface. Instead they began below some depth, which for most stations was 10 cm or more, suggesting that even at these stations the upper layers of the sediment were mixed. This is supported by Schaff et al. (1992) who, at their Site III within our study area, estimated a mixing coefficient of 30 cm² yr⁻¹ in the upper 10 cm of sediment. At two other sites further south Schaff et al. (1992) estimated mixing coefficients to be 8.6 and 17 cm² yr⁻¹.

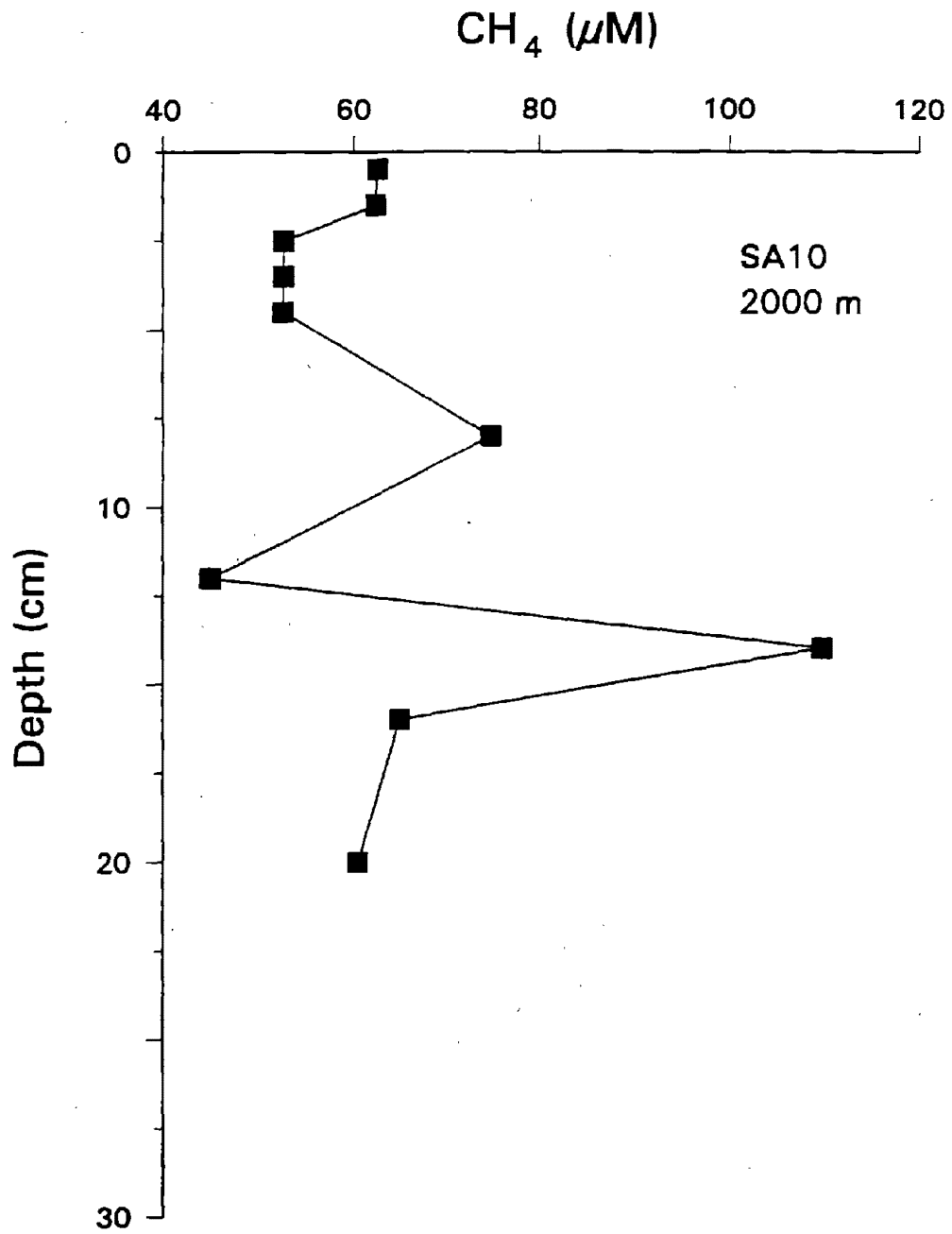


Figure 3-5. Depth profile of the concentration of methane at the 2000-m station, SA10.

CHAPTER 4. SEDIMENTARY CHLOROPHYLL A, VIABLE DIATOMS, AND LIPIDS¹

H. Rodger Harvey, Larry B. Cahoon, and Carrie J. Thomas

Introduction

Previous studies have established that benthic microalgae (mostly pennate diatoms) are important primary producers on the continental shelf (Cahoon et al. 1990, Cahoon and Cooke 1992) and shelf break and shallow slope habitats off Cape Hatteras (Cahoon and Cooke 1989, Cahoon et al. 1990, 1992, Laws and Cahoon 1992). Recent evidence also suggests that fatty acids, particularly polyunsaturated fatty acids (PUFA's), play an important role in regulating the growth and reproduction of infaunal organisms (Marsh et al. 1990). Therefore, it is possible that the high abundance of benthic organisms previously found on the continental slope off Cape Hatteras may be related to the concentrations of microalgae and organic compounds in the sediment.

To assist in the interpretation of infaunal data and address objective 1, sediments from the study area were examined for concentration of chlorophyll *a*, the presence of viable diatoms, and the concentration and composition of lipids. Differences among samples in any of these parameters could be useful in determining the aerial extent of the unusual benthic community previously described.

Methods

Samples for analysis of sediment for Chlorophyll *a* were collected from 16 box cores (Table 2-1) using a 10 cm long by 2.5 cm (I.D.) core tube. Since chlorophyll *a* degrades rapidly in dead cells, measuring its abundance gives a reasonably good estimate of the amount of living microalgae. Five replicate cores were taken from each box core and were immediately frozen. These were later extracted in 100% acetone (1:1 sediment to acetone by volume) using a modification of the technique of Whitney and Darley (1979). This technique partitions the acetone extract with hexane to remove degraded plant pigment compounds which can interfere with fluorometric and spectrophotometric analysis. This permitted the concentration of intact or viable chlorophyll *a* to be determined.

Sediment for culture of diatoms was collected from 15 box cores (Table 2-1) with a 15 cm long by 5.5 cm (I.D.) core tube. These cores were split longitudinally, and samples were collected at 2 cm intervals. These were refrigerated in darkness until cultured. For culture, a small aliquot of sediment from each sample was streaked onto a sterile nutrient agar plate using a sterilized wire loop. The plates, which consisted of 1.5% Difco Bacto-agar in sterile, filtered seawater with modified *f/2* medium (Guillard and Ryther 1962), were then incubated under a bank of 40 W cool white fluorescent lights at room temperature for several weeks and were regularly monitored for growth. Viable diatoms produced small brown colonies, which were examined with dissecting and compound microscopes.

For analysis of fatty acids all glassware used was precombusted at 450° C for 4 hours. All other components were washed first with low residue detergent (Pierce RBS-35) then by 15% HCl, and finally rinsed with dichloromethane and methanol (1:1). High purity (pesticide residue grade) solvents were used throughout. Previously frozen (-70°C) samples of unconsolidated surface material (flocs) from upper sediment surfaces were thawed under refrigeration and homogenized. Samples of weighed sediment were then transferred to 125-mm precleaned pyrex tubes with teflon lined screw caps for extraction. Subsamples were also taken for organic carbon and dry weight determination for normalization of fatty acid concentrations to floc material. Internal standards (5 α -cholestane and nonadecanoic acid) were added to samples prior to extraction. Lipids were extracted three times from each sample with sonification using dichloromethane:methanol (1:1) following the methods of Harvey et al. (1987). The lipid extract was concentrated by rotary evaporation, while the total sample was hydrolyzed with 0.2 N KOH in methanol plus 1 ml distilled water. After gently heating at 50° C for one hour, the samples were cooled, additional water was added, and the neutral fraction was removed by

¹Contribution number 086 of the Center for Marine Science Research, University of North Carolina at Wilmington.

partitioning into hexane:diethyl ether (9:1). The remaining extract was acidified to pH=2. The polar fraction, which contained all fatty acids, was dried by rotary evaporation, treated with BF₃-MeOH with fatty acid methyl esters (FAMES), and partitioned into hexane/diethyl ether (9:1). Extraction and partitioning of lipid free sediments (prepared by combustion at 450° C for 2 hr) to which a known amounts of either palmitic acid or 5 α -cholestane were added had recovery efficiencies greater than 96%.

FAMES were separated and quantified by capillary gas chromatography using a Hewlett Packard 5890A GC operated in the splitless mode with flame ionization detection. Separations were performed on a crosslinked methyl silicone column (DB-5, 30 m length, I.D. 0.32 mm, film thickness 0.25 μ m) using hydrogen as the carrier gas. A two stage temperature program was utilized; during the first stage temperatures were raised from 50° C to 120° C at a rate of 10° C min⁻¹, after which temperatures were increased to 300° C at a rate of 4° C min⁻¹. All data were collected and quantified using a dedicated data system (MAXIMA - Waters/Millipore). Peak areas were quantified by comparison with the internal standard (nonadecanoic acid), while structural identification was done using a gas chromatograph interfaced with a Hewlett Packard 5970B mass selective detector operating at 70 eV with acquisition over the range 50-450 amu. Electron impact mass spectra were obtained under the same conditions as above except that helium was used as the carrier gas and a smaller column (0.2 mm I.D.) was employed. The length of fatty acid chains and the position of double bonds were determined by comparison with both internal and external authentic standards and mass spectral interpretation. Differences among replicates only averaged \pm 12.6%, and the procedural blank contained 0.65 μ g fatty acid (equal to 2.1% of lowest sample concentration).

Results

Viable diatoms were cultured from 14 of the 15 sites sampled. While the diatoms appeared fairly uniformly distributed throughout the sedimentary column in the deep stations, they were more prevalent near the surface for the 600- and 800-m stations (Figure 4-1). They were also found deeper in the sediment at the 600 m stations. Several species, all very small forms, have been tentatively identified. These include at least one pennate species and the centric diatom *Cyclotella*. Additional taxonomic work remains to be completed.

Measurable chlorophyll *a* was found at all sites (Figure 4-2). Variability among replicates within sites was generally high (coefficient of variation ranged from 68 to 295%, mean=141%), which may have been due to dilution of the pigments by the sediments. There were no consistent patterns among depths or transects in the amount of chlorophyll *a*.

There was a large amount of variability among sites in the total amount of free and esterified fatty acids (Figure 4-3). The one station on Transect E had the highest amount, but there were no other obvious or consistent differences among transects or depths. Although a wide variety of fatty acids were present at all sites, palmitic acid (16:0) was the most abundant (Figure 4-4). Other abundant fatty acids included 16:1ⁿ⁻⁵, 18:1ⁿ⁻¹¹ and 18:0. Such distributions are typical for sediments with low labile organic content, and are similar to those observed in a number of coastal sediments (Van Vleet and Quinn 1979). There was no obvious difference in distributions among depths or transects.

Discussion

Cahoon et al. (1992) found that the concentration of chlorophyll *a* on the continental slope just below the shelf break was comparable to that in shelf sediments (Cahoon et al. 1990, Cahoon and Cooke 1992). However, they found that it declined below 100 m to levels <0.35 μ g chl *a* g⁻¹ sediment (<10 mg chl *a* m⁻²). Some of concentrations found in the current study were much higher than this, which indicates abundant *in situ* growth of and/or rapid import of microalgae.

The presence of chlorophyll *a* at each site suggests several possibilities. There could be a steady supply of chlorophyll-*a*-containing organisms to these sediments, or long lived resting cells that contain chlorophyll *a*. It is also possible that there may be chlorophyll *a* in cells which live heterotrophically in the absence of light. However, Cahoon and Cooke (1989) ruled out heterotrophic production in a study conducted *in situ* at 285 m off Onslow Bay, North Carolina. But the diatoms cultured in that study were all planktonic forms, whereas those in the present study contained at least one pennate (probably benthic) diatom which may have a better developed heterotrophic capability. Furthermore, the high content of total sedimentary organic

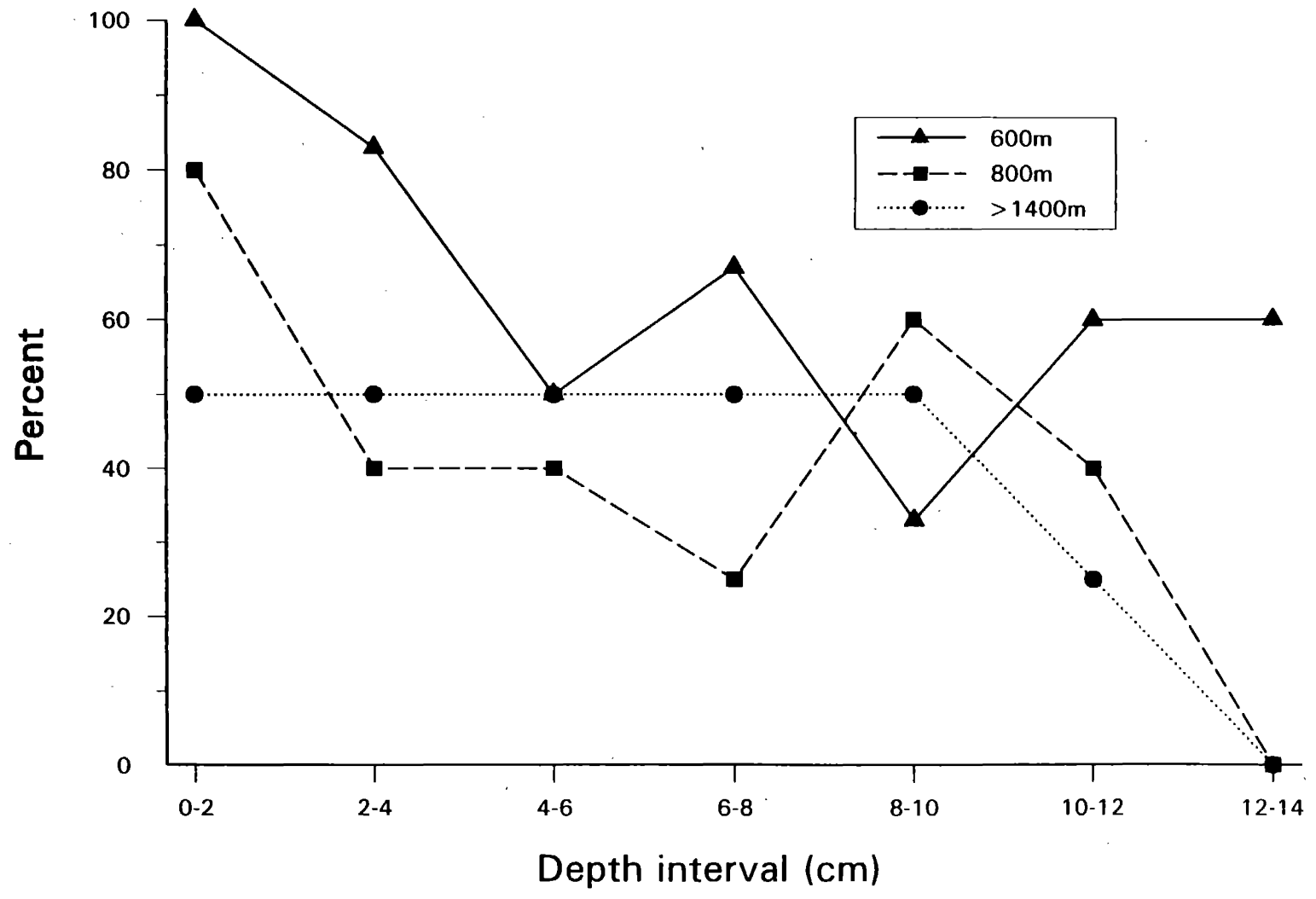


Figure 4-1. Proportions of samples containing viable diatoms in each 2 cm sediment interval.

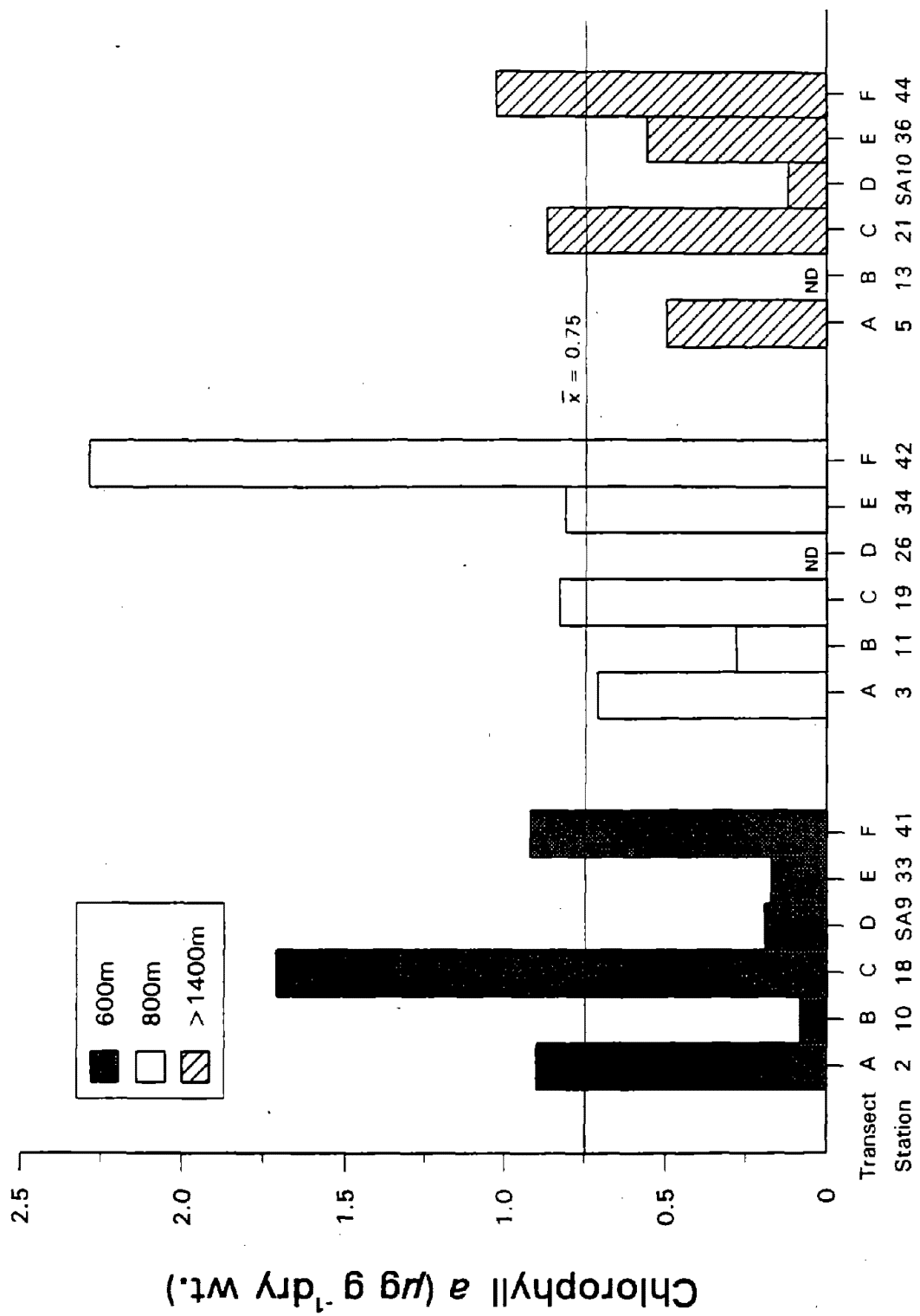


Figure 4-2. Concentration of chlorophyll *a* by each transect and depth. Line across graph represents overall grand mean. ND = no data.

Total Fatty Acids

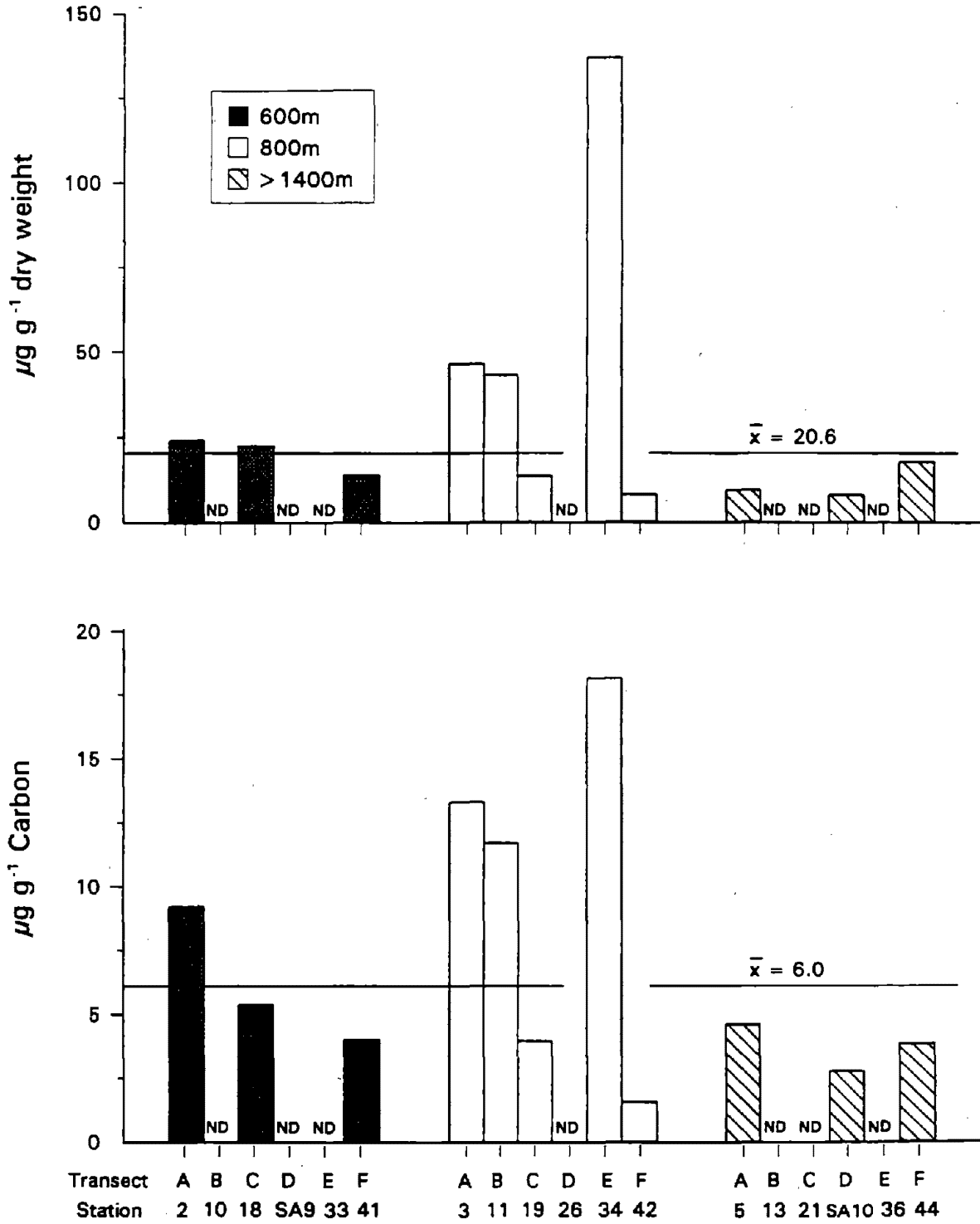


Figure 4-3. Total fatty acid concentrations at box core stations. Line across graphs represent overall grand mean excluding station on transect E. ND = do data.

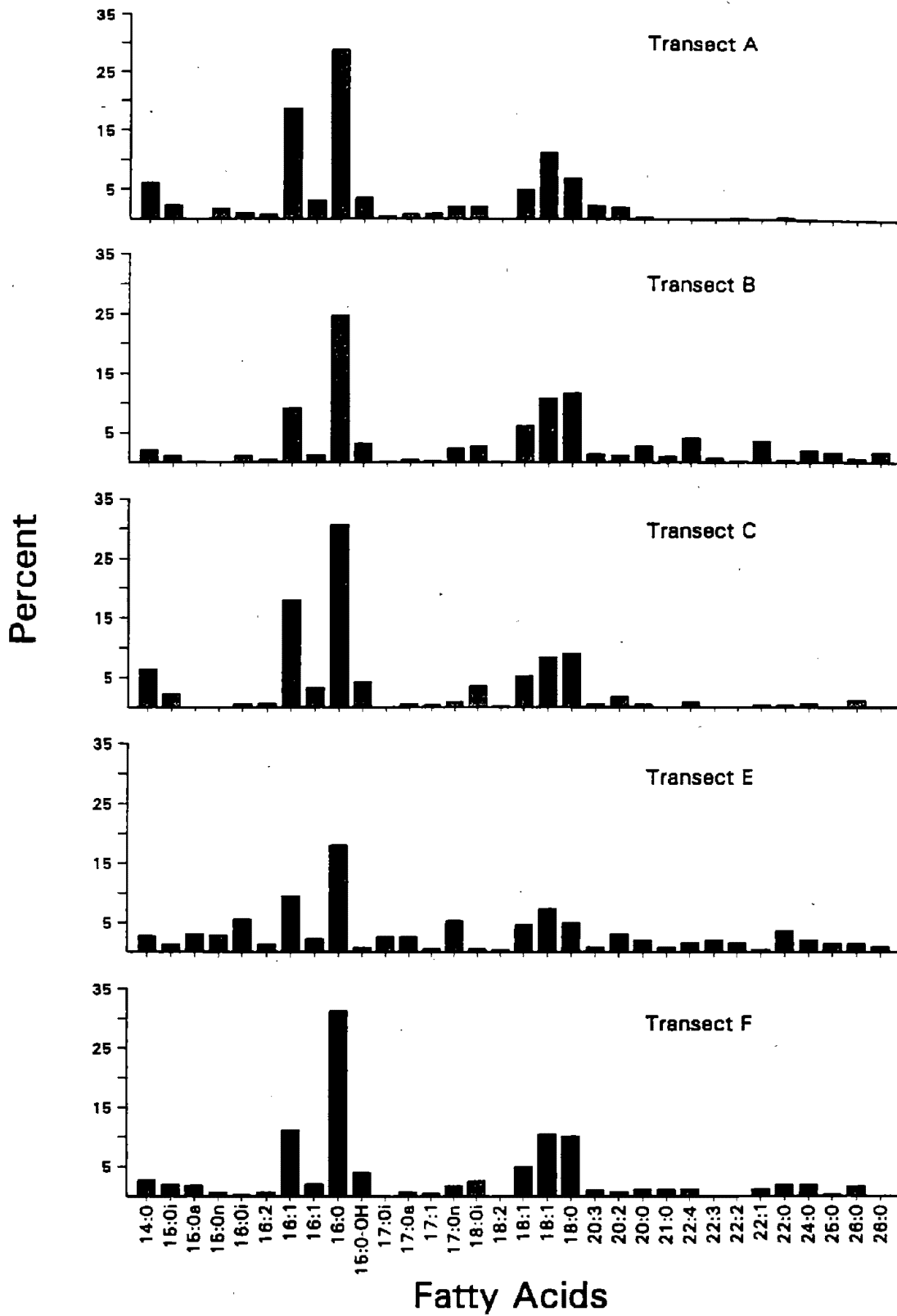


Figure 4-4a. Relative concentration of the different types of fatty acids averaged by transect.

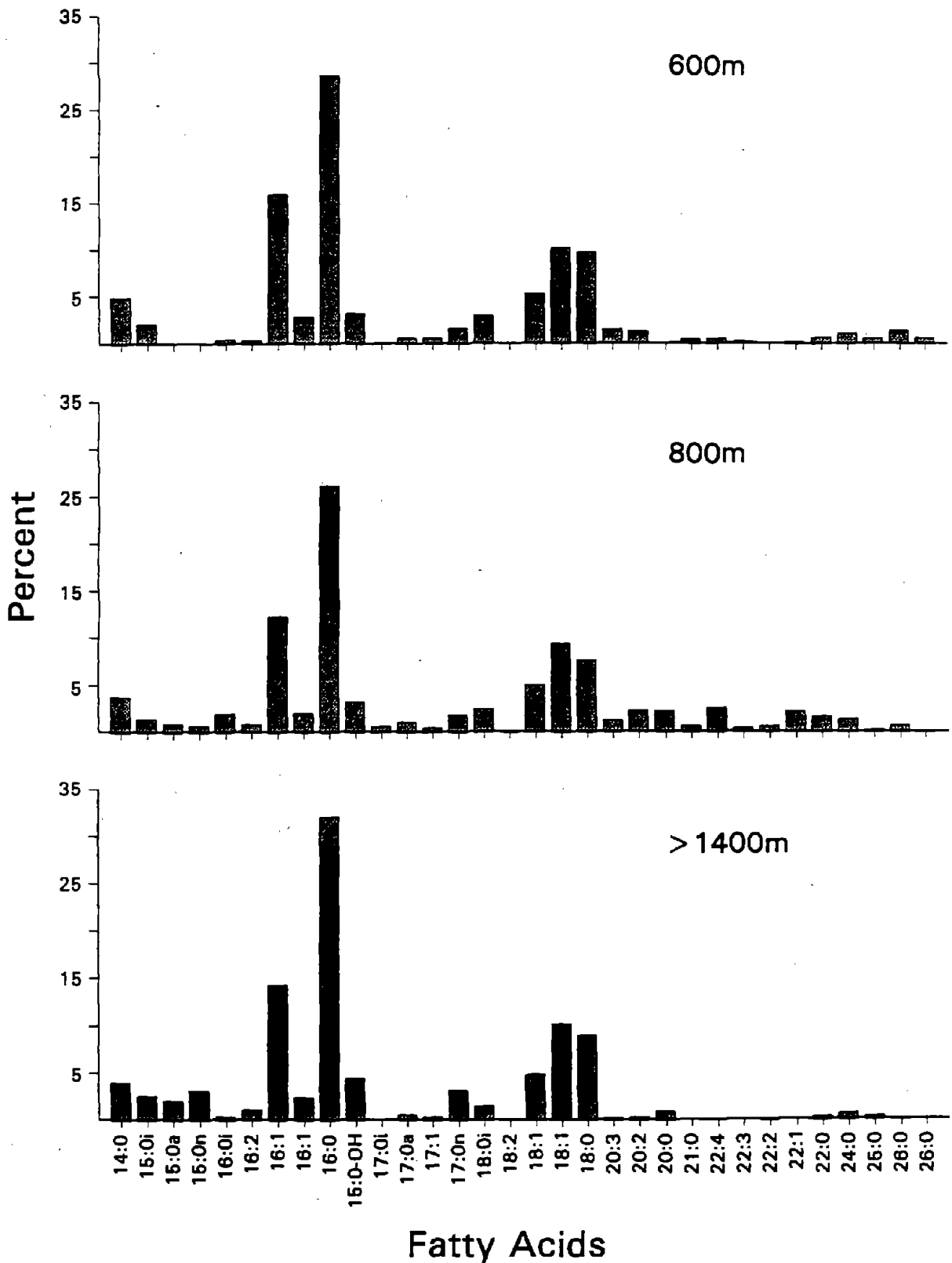


Figure 4-4b. Relative concentration of the different types of fatty acids averaged by depth.

carbon (1-2%, Chapter 3) in this area and the presence of abundant benthic infauna may also permit heterotrophic existence. Thus, heterotrophy can not be ruled out as an explanation for the presence of chlorophyll *a* at these sites.

The high variability of chlorophyll *a* concentrations within stations may result from uneven deposition of cells into biogenically formed small-scale depressions on the surface of the sediments. These aggregations may explain high local concentrations. Upward transport of fecal material, deposited in mounds, may cause local burial of plant cells, producing patches of low concentrations of viable chlorophyll. Localized heterotrophic growth of cells after deposition may also explain patchiness. This is an important issue to resolve because localized heterotrophic growth supported by imported carbon would imply a very much lower rate of carbon import in the form of microalgae than would simple uneven distribution of microalgae during downslope transport.

The presence of viable diatoms to 14 cm may be explained by the feeding activities of head-down deposit feeders, most of which are commonly encountered to depths of 14 cm or deeper. Normally these worms feed on subsurface detritus, but Dobbs and Whitlatch (1982) have shown that the maldanid *Clymenella* occasionally extends its tail end out of the top of the tube and "hoes" the surface of the sediment with its anal crown. This sediment, which contains viable diatoms, is transported down the tube to the feeding void near the anterior end of the worm. This activity is believed to represent a means of stimulating the "microbial garden" associated with head-down deposit feeders (Yingst and Rhoads 1980). If the maldanid species present off the Cape Hatteras slope environment also do this, it may explain how viable diatoms get injected deep into the sediment.

Although little information about the concentrations of fatty acids in flocculent material is available, the composition of particles collected by filtration (Mayzaud et al. 1989, Wakeham and Lee 1989, Grimalt et al. 1990, Reemstma et al. 1990) and surface sediments have been widely analyzed (e.g., Farrington et al. 1977, Van Vleet and Quinn 1979, Kennicutt and Jeffrey 1981, Venkatesan 1988). The values observed during this study are comparable to concentrations of solvent extractable fatty acids obtained from surface sediments of Narragansett Bay (35.4 $\mu\text{g g}^{-1}$ dry sediment), Rhode Island Sound (23.2 $\mu\text{g g}^{-1}$ dry sediment) and the Gulf of Maine (10.5 $\mu\text{g g}^{-1}$ dry sediment) (Van Vleet and Quinn 1979). Similar concentrations have also been observed for surface (0-1 cm) sediments in Buzzards Bay (Farrington et al. 1977). In contrast, the range of concentrations observed during the present study is less than some other coastal sediments, such as the Peru upwelling region where intense phytoplankton blooms occur in the overlying water column. In such sediments, concentrations of 765.5 $\mu\text{g g}^{-1}$ dry sediment or higher have been observed (Smith et al. 1983).

Of particular importance to benthic consumers are polyunsaturated fatty acids (PUFA's) which are thought to be important nutrients for maximal growth and reproduction (Fraser et al. 1989, Marsh et al. 1990). The principal source of these highly unsaturated acids is from phytoplankton in the overlying water column. Although the presence of polyunsaturated fatty acids in marine algae varies among taxa and growth conditions, they often comprise 30-40% of total fatty acids present (e.g., Mayzaud et al. 1976, Volkman et al. 1980, 1981, Harvey et al. 1988). The samples from the current study generally had low amounts of PUFA's (mean=5.8%, SE=1.2). This suggests that only a small fraction of the organic carbon produced photosynthetically in surface waters is available to benthic consumers in this area. The high amounts of branched and odd chain fatty acids at all the stations (mean=14.5%, SE=1.3) indicates substantial reworking either during transport through the water column or at the sediment water interface.

The composition and abundance of polyunsaturated fatty acids, which was biased towards longer chain acids, is atypical of material of algal origin. The absence of highly unsaturated C_{18} acids, such as linoleic (18:3^{9,12,15}), and the presence of only small amounts of the diunsaturated 18:2^{9,12} suggests that much of the material arriving at the surface of the sediment was well degraded. However, the presence of 22:4 and 22:3 does imply that a small fraction of algal material has been preserved during descent through the water column. While a single source of all these acids is possible (Volkman et al. 1989), it is more likely that the observed distributions in PUFA's are the result of differential preservation of algal taxa during transport through the water column either by single cells or macroaggregates (Beers et al. 1986). Such differences in preservation have also been observed in experimental systems which simulate algal decomposition during sedimentation (Harvey et al. 1991).

In addition to fatty acids of algal origin, all sites showed a significant input of bacterial acids. Iso and anteiso branched fatty acids (ca 18:0i), as well as those of odd chain length (e.g., C₁₅ and C₁₇), are rare in eukaryotic organisms, but are common in a variety of bacteria (Perry et al. 1979, Parkes and Taylor 1983). The relative abundance of these acids, which ranged from 10.6% to 23.4%, is somewhat higher than observed for other coastal sediments (Van Vleet and Quinn 1979) or sedimented particulate material (Lee and Wakeham 1989). These elevated concentrations suggest enhanced microbial activity and/or microbial input to these sediments compared to other areas. Small amounts of longer chain saturated fatty acids were also seen in many of the extracted samples (Figure 4-4). Long chain saturated fatty acids, in particular those greater than C₂₂, are generally attributed to higher plants and, thus, suggest some terrestrial input (Nichols and Johns 1985, Bianchi et al. 1989). At several sites fatty acids up to C₂₈ were observed, and long chain (>C₂₂) fatty acids were present at almost all sites.

While there was variability among sites in all the parameters examined, there were no consistent differences among depths or transects. Therefore, whatever effect these compounds have on abundances of benthic organisms should be the same throughout the study area.

THIS PAGE LEFT BLANK INTENTIONALLY

CHAPTER 5. SEDIMENT FABRIC AND *IN SITU* SEDIMENTARY STRUCTURE

Robert J. Diaz, G. Randy Cutter, and Donald C. Rhoads

Introduction

Sediment profile and bottom surface cameras have been effective in characterizing biological, chemical, and physical attributes of subsurface marine and estuarine habitats, and providing the means for quickly monitoring the spatial extent of disturbances to benthic systems (Rhoads and Germano 1986, Diaz and Schaffner 1988). Activities of biological communities and the combined characteristics of the benthic habitat are influenced by large-scale physical processes. Sedimentary fabric is the spatial arrangement of grains or grain-aggregates which produce higher order features called sedimentary structures (e.g. laminations, burrows). Both physical (e.g., current activity) and biogenic processes (e.g., bioturbation) produce sedimentary fabrics, time-integrated records of processes at a site. Therefore, the dynamics of sedimentation can often be reconstructed using fabric analysis. Biological activity may alter a habitat to the extent that physical processes can more easily disrupt surface sediments and redeposit them elsewhere. Signs of bioturbational activities include deep burrowing infaunal structures such as active voids and backfilled burrows as well as deep-lying aerobic sediments and disturbed sediment layers.

To assist in the interpretation of the biological data and address objectives 1, 3, and 4, surface and profile imaging (SPI) was used to characterize sediment surface features and attributes of the top sediment layers, and x-ray imaging was used to gain information about the sedimentary fabric. These approaches allowed a fairly rapid assessment of the overall biological and physical states of the benthos with distinguishing features on the scale of one millimeter to nearly half a meter in surface images, and less than one millimeter to about 15 cm in the profile images. Using the x-ray images and the profile camera images, the general state of mixing and bioturbation and certain chemical attributes of the sediments were assessed.

Methods

Data were collected from 23 stations in the vicinity of the Manteo 467 block with a sediment profile camera and 13 stations with a surface camera (Figure 5-1). Sediment profile images were taken with a Benthos Model 3731 Sediment Profile Camera (Benthos, Inc., North Falmouth, MA). The profile camera has a wedge-shaped prism with a plexiglass faceplate and a back mirror mounted at a 45° angle which provides images of the upper sediment column in profile. For details of sediment profile camera operation see Rhoads and Cande (1971). Standard, close-up photographs of the sediment surface were taken with a vertically-oriented Benthos Model 372 camera and double-headed strobe attached to the frame of the sediment profile camera. The surface camera was triggered about 1 m off the bottom and photographed an average area of 0.5 m², providing details of small organisms and biogenic structures. Color slide film (Fujichrome 100D Professional) was used in both surface and profile cameras. Most of the film was developed on board the vessel so that initial results could be evaluated and used in deciding the exact locations of box core stations.

Sediment profile images were analyzed visually using scaled projections and then digitally using an International Imaging Systems I²S image processor interfaced with a Prime 9955 computer. Profile images were standardized to a prism penetration depth of 15 cm, and characteristics were calculated as percent values, denoting a percent of a standard 225-cm² image. Features quantified from the profile images using the image analyzer included the depth the prism penetrated into the sediment; the surface relief of the sediment-water interface; the average depth of the apparent color redox potential discontinuity (RPD) layer; the area of aerobic sediment; and the area of sediment voids. Profile image data were analyzed using a two-way analysis of variance. Features quantified visually included the number of worm tubes at the sediment-water interface; the number of infauna; and the number of voids. See Diaz and Schaffner (1988) for more detailed descriptions of methods and measurements. The presence or absence of *Bathysiphon filiformis* foraminifera in profile images was also recorded.

Surface images were projected and analyzed visually. Image area, burrow density, and *B. filiformis* density were quantified by scaled measurements relative to the diameter of *B. filiformis*. If an image had no *B. filiformis* present, the image area was not calculated, because none of the other features provided a reliable

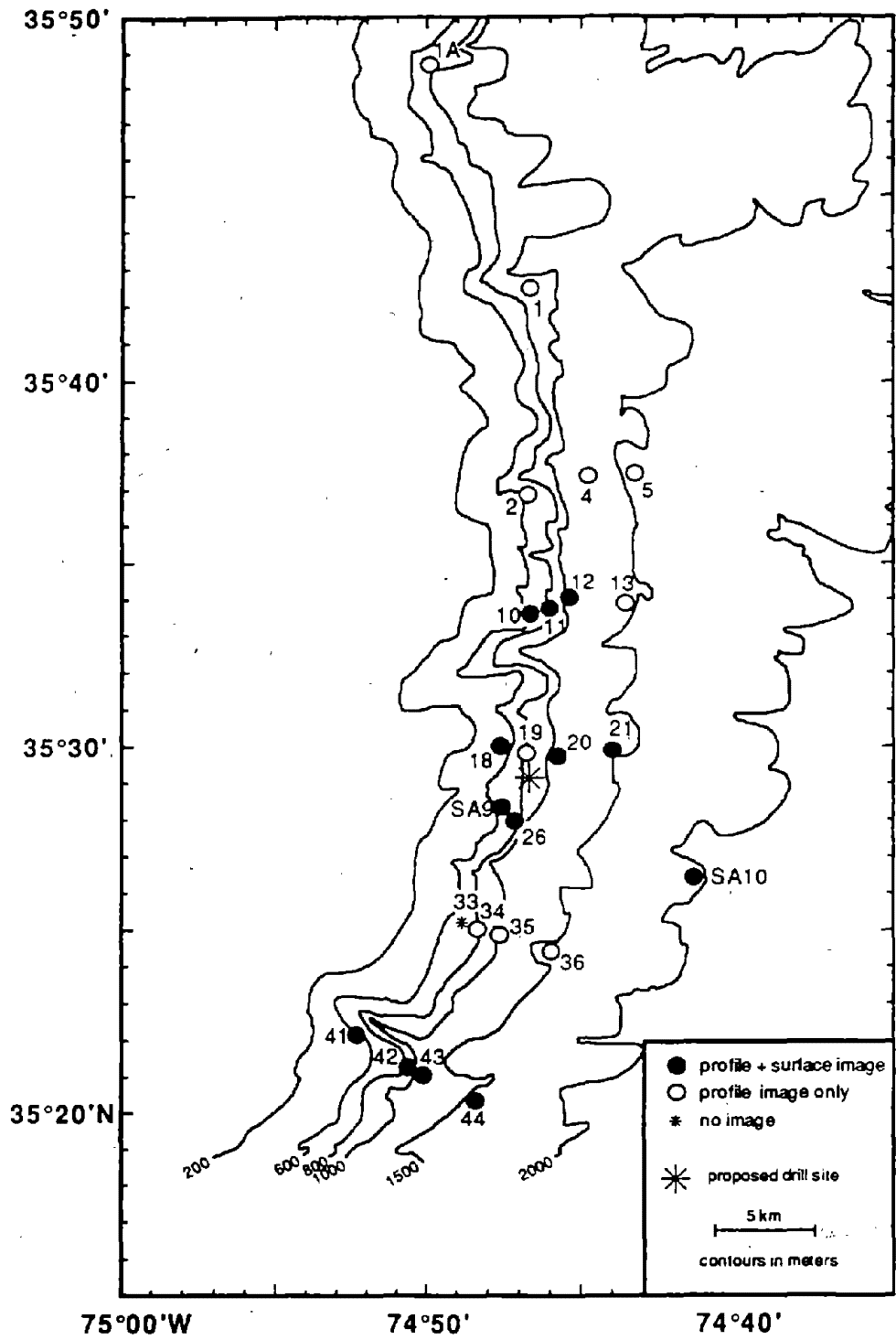


Figure 5-1 Location of SPI camera stations.

reference scale. The measured diameter of *B. filiformis* tubes preserved from the box core samples (approximately 2 mm) was used as a scaling factor to provide the actual area photographed. Presence or absence of animal tracks, clasts, tubes, tube aggregates, fish, echinoderms, anthozoans, hydroids, and other fauna in the surface images was recorded.

X-ray cores were taken with a 3-sided Plexiglas core which was pushed vertically into the sediment. The fourth side was then pushed in to obtain a tabular slice of sediment 2 cm thick by 10 cm wide. The length of the core was variable depending on the penetration of the box core. Lengths ranged from 12 to 28 cm. The methods used generally follow the x-ray techniques recommended by Bouma (1969) and are described in detail in Schaffner et al. (1987). Fabric analysis was done at 15 stations (Table 2-1). Fabric was described in terms of imaged sedimentary structures and gradients in core opaqueness or transparency (a function of x-ray exposure values, core thickness, core bulk density, texture, and mineralogy). The proportion of physical and biogenic structures were recorded for each core.

Results

Profile Images

Overall, the substrate was fairly uniform in compaction and grain size. The sediment classification data and penetration depths of the profile camera prism (Figure 5-2) show that soft silty mud was the major surface sediment type. Average prism penetration depth was 18.7 cm (SE=1.5). Most of the variability was caused by low values along transect A which resulted from weight adjustments on the prism. Uniformity of sediment compaction across the area is more clearly revealed by a two-way analysis of variance of penetration depths excluding transect A and stations 1A and 1. The results show that the variation of average prism penetration could not be attributed to water depth ($p=0.56$) or location of transect ($p=0.07$). Occurrence of clayey sediments (Figure 5-3) did not appear to follow any pattern. A high percentage of clayey sediment was seen in images from six stations covering five of the eight transects.

The microtopography of the substrates, measured as the vertical relief at the sediment-water interface (surface relief), had a mean of 1.3 cm (SE=0.11). Surface relief was occasionally augmented by bioturbation of the sediments or by biogenic structures such as mounds or burrows. Higher relief (>3 cm) reflected the physical processes of erosion controlling the larger scale geomorphic convolutions dominating the bottom (Figure 5-2). The variation of the microtopographic relief could not be attributed to water depth ($p=0.85$) or location of transect ($p=0.89$).

The apparent color redox potential discontinuity (RPD) depth had a mean of 5.3 cm (SE=0.27). No clear spatial patterns were evident for RPD depth. Three images had anomalously high RPD depths; 19B (11.3 cm), 21B (11.2 cm), and 41A (11.4 cm) (Figure 5-4). The variation of the RPD depth could not be attributed to water depth ($p=0.74$) nor location of transect ($p=0.16$). Percent aerobic area (% aerobic) indicates the portion of the sediment that is considered oxidized or aerobic, having a high reflectance that is associated with the presence of ferric hydroxide coatings on particles and low concentrations of pore-water sulfides (Rhoads and Germano 1986). The amount of aerobic sediment has been found to be correlated with the depth of infaunal bioturbation (Rhoads and Germano 1986). Mean aerobic area was 34.5% (SE=1.8) of a standardized 15 cm penetration depth image. Two replicates at station 41 were 61.5% and 76.0% aerobic (Figure 5-2). The variation in the area of aerobic sediment could not be attributed to water depth ($p=0.65$) or location of transect ($p=0.35$).

Void area, expressed as a percent of a standardized 15 cm image, ranged from 0% to 6.9%, with a mean of 0.9% (SE=0.3%). The majority of the voids were small and often inhabited by individual worms (Figure 5-5b). However, the range was skewed by a few profile images which captured large, active feeding voids at stations 21A, 21B, and 42A (Figure 5-5a). No spatial pattern was obvious for the occurrence of active feeding voids. Variation of void area percentages could not be attributed to water depth ($p=0.53$) or location of transect ($p=0.67$).

Small biogenic structures and disturbances were present in most of the images, as revealed by qualitative descriptions of sediment-water interface features. Clasts of sediment, which most likely originated in slope erosion, were seen in images from most of the stations at 1,500 m and 2,000 m, and at a few others of various depths (Figure 5-4). *B. filiformis* tubes (Figure 5-6) were present in profile images from five stations, but no geographical pattern was evident. When *B. filiformis* were present in the profile images, they were also seen in the surface images. Polychaete tubes at the sediment surface were uncommon, with images having 0 to 4 tubes; the only

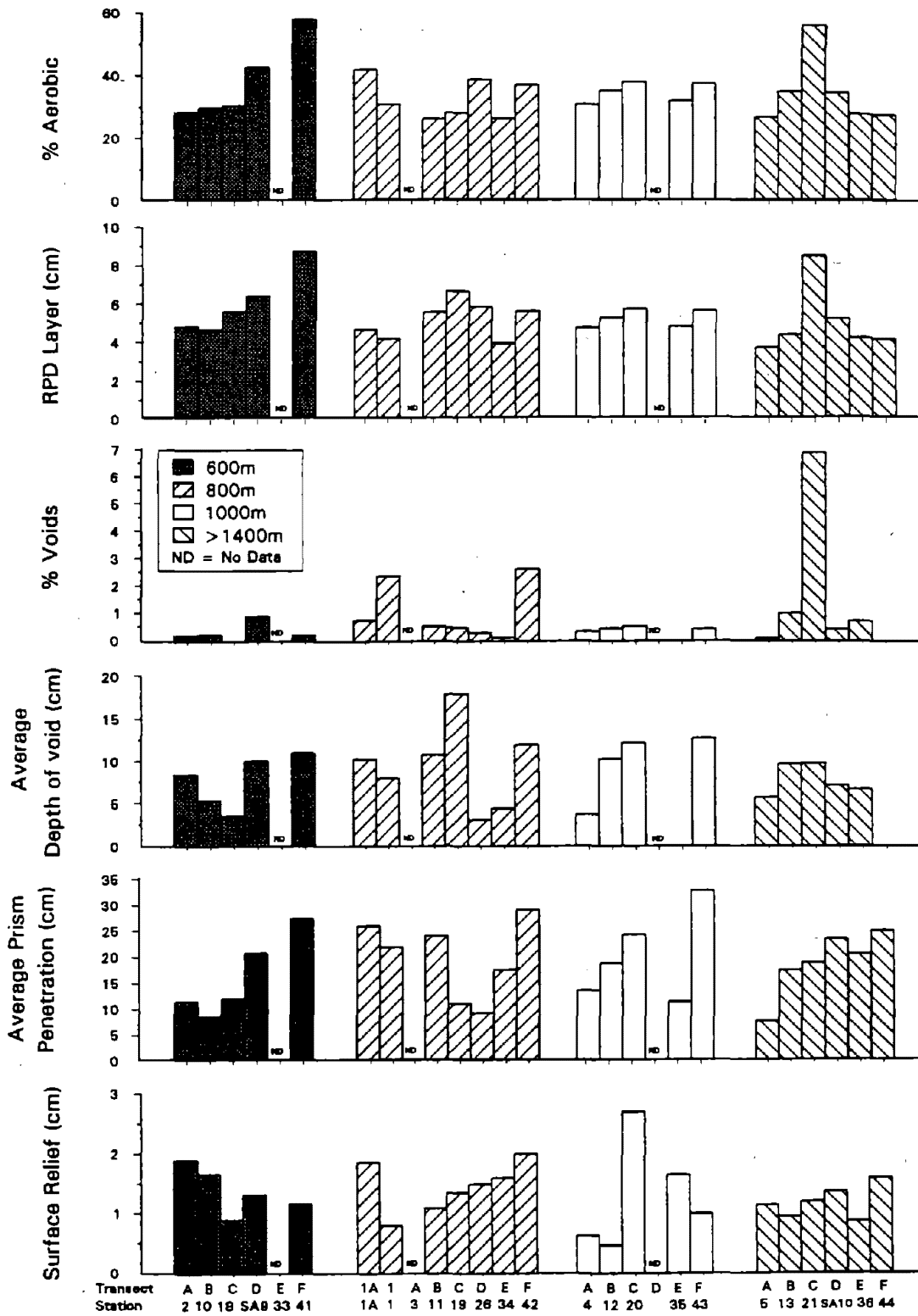
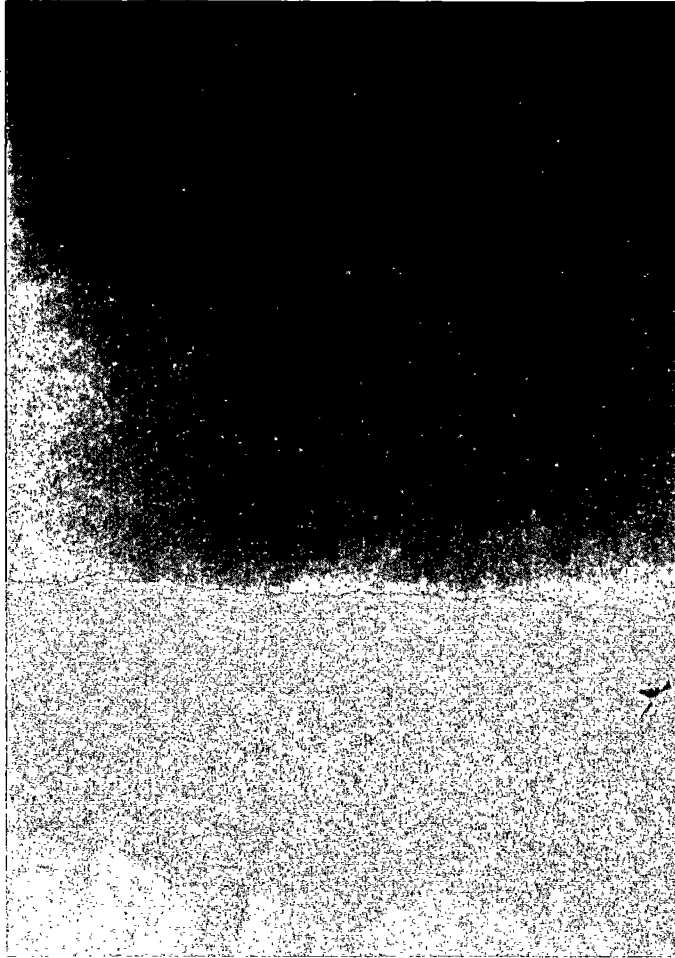


Figure 5-2. Sediment characteristics measured from profile images.

a)



b)

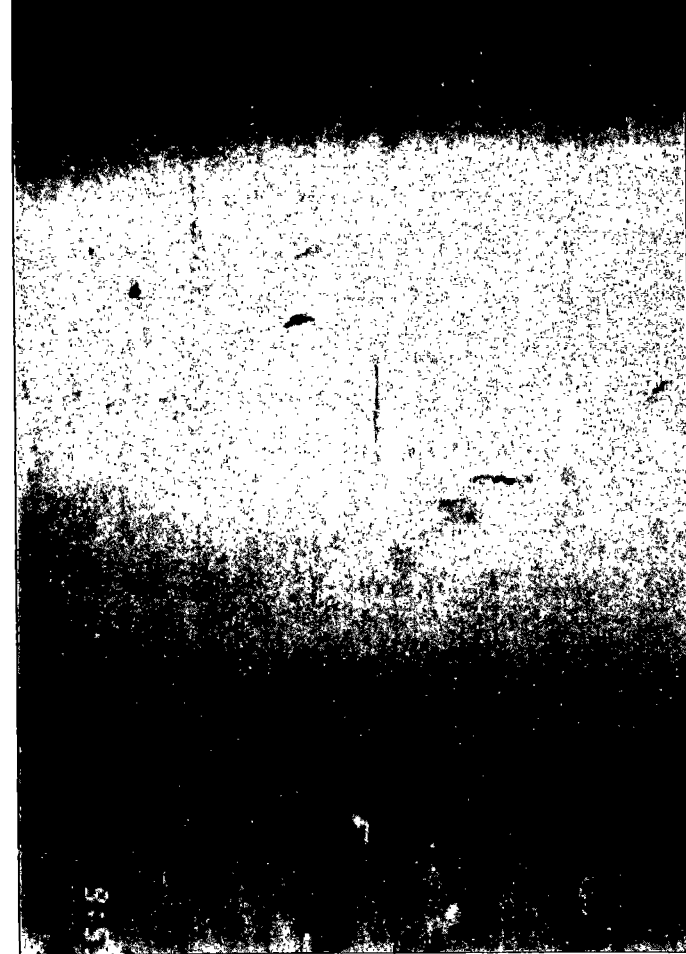
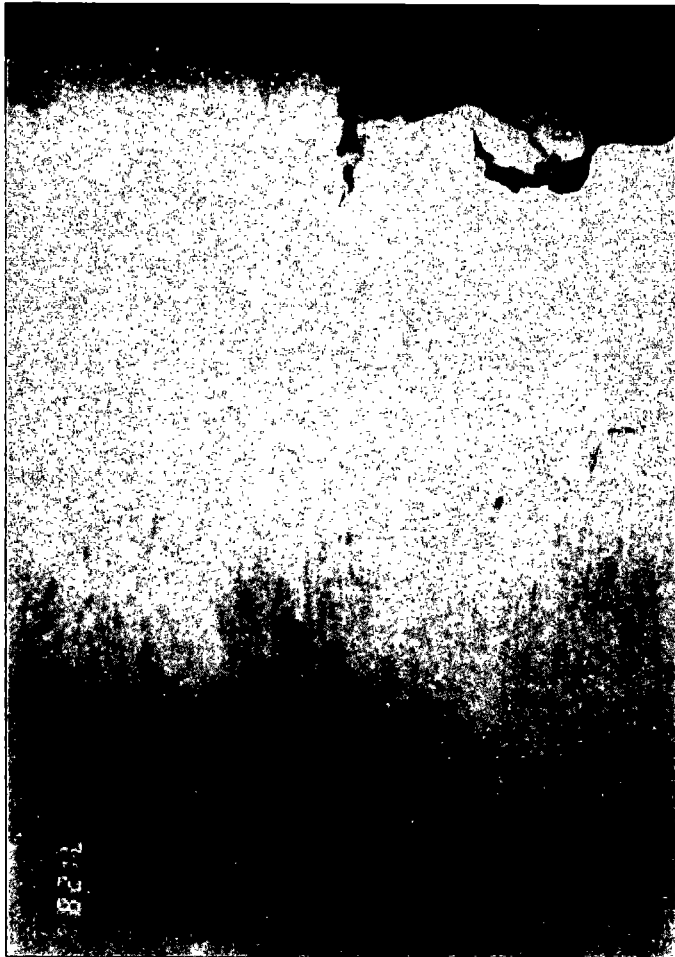


Figure 5-3. Sediment profile images: clayey sediments from a) Station 26 replicate A, with a clearly defined clay layer (lighter-colored sediment) beginning at 6 to 8 cm below the surface; and b) Station SA10 replicate A, with light-colored spots of clay in the lower portions of the image. Scale = 0.65 × actual size.



a)



b)

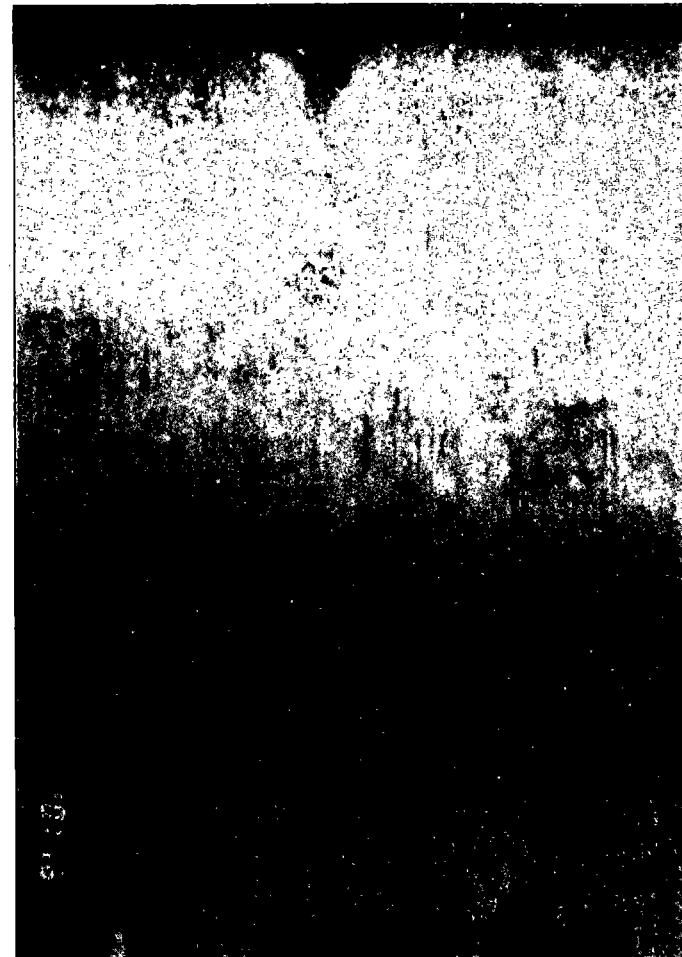


Figure 5-4. Sediment profile images: deep apparent color redox potential discontinuity (RPD) layers in images from a) Station 19 replicate B, which shows an abrupt change from aerobic to anaerobic sediments by the distinct difference in sediment color close to 11 cm below the surface, also present are several worms; and b) Station 21 replicate B, with anaerobic sediments beginning near a depth of 11 cm and changing to intensely reduced sediments near 20 cm (dark spots near bottom). Also present are active feeding voids in the aerobic area, and a large burrow opening to the surface near the center of the image. Scale = 0.65 \times .



a)



b)

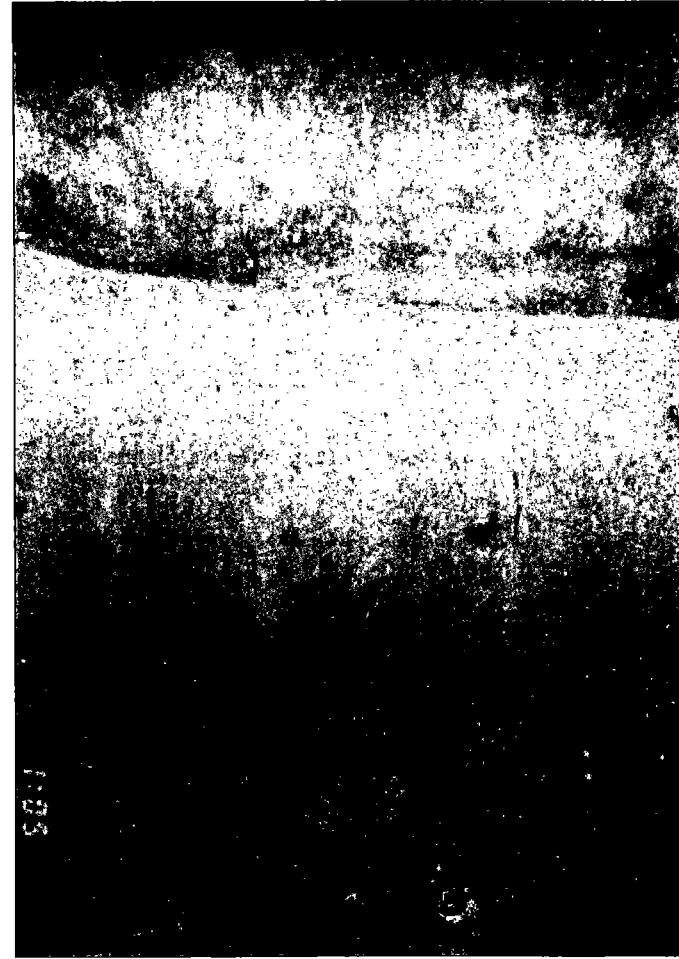
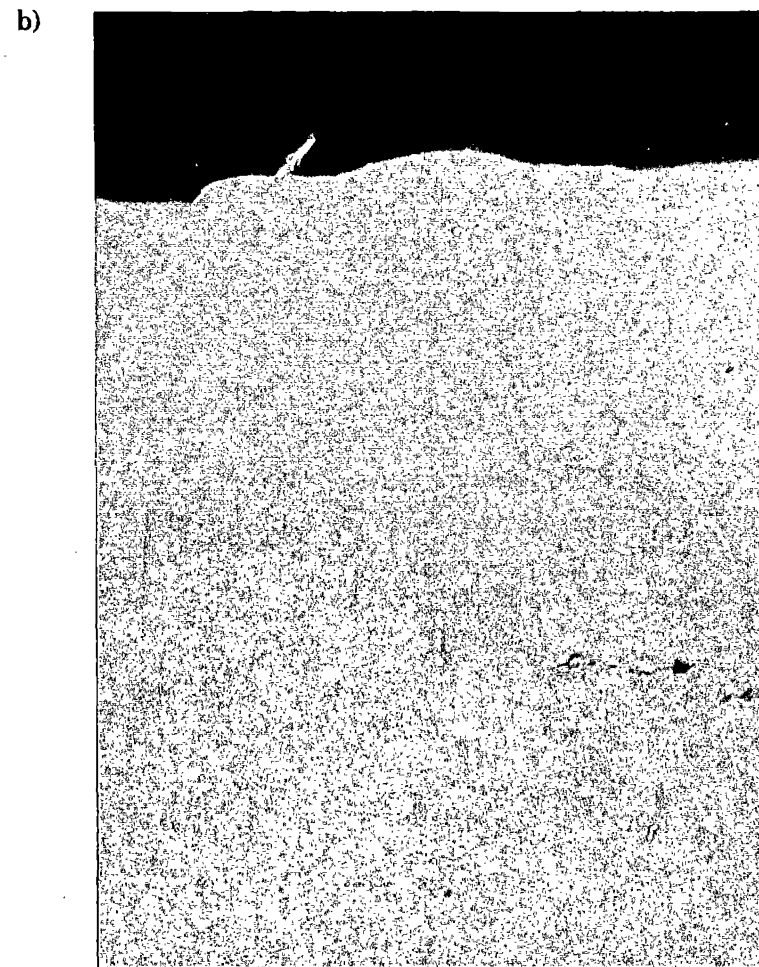
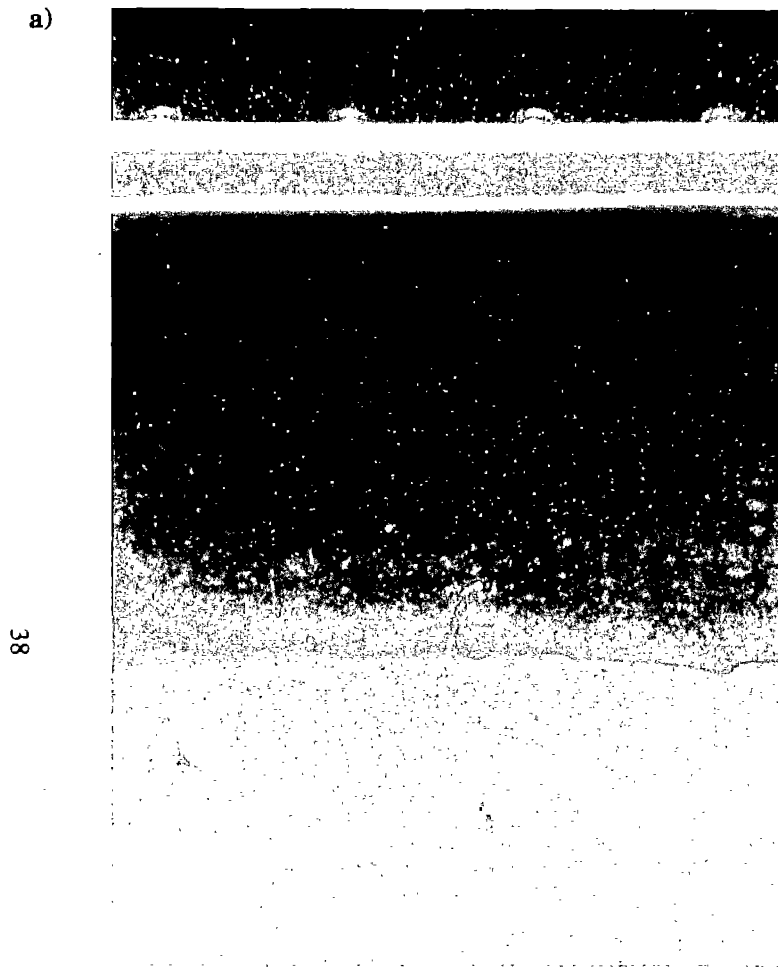


Figure 5-5. Sediment profile images: large void areas in images from a) Station 21 replicate A, which had a large void seen in the lower left of the image, and clayey clasts can be seen at the surface; and b) Station SA9 replicate C, which had seven active feeding voids, most of which occurred below the RPD layer, worms are present in both images. Scale = 0.65 \times .





38

Figure 5-6. Sediment profile images: presence of *Bathysiphon filiformis* in images from a) Station 4 replicate D, with one *B. filiformis* present at the sediment surface, and two tubes present about 3 cm below the surface; and b) Station 13 replicate D, with two *B. filiformis* at the surface, as well as large feeding voids, an oxic burrow (circular void surrounded by orangish sediment), and several worms, all present below the RPD layer. Scale=0.65x.

Reproduced from
best available copy.



exception was a possible aggregation of small tubes and sediment in one image from Station 21 (Figure 5-3). The images generally revealed an abundance of deeper burrowing infauna. Active subsurface burrows, and burrows that had been recently backfilled after the organisms responsible for their formation had vacated, ranged in density from 0 to 8 per profile image (Figure 5-7), but did not appear to follow any pattern by transect or depth.

Surface Images

Sediment surface image data covered a smaller geographic range than the profile data because of equipment problems. Sediment surface images were acquired from approximately 4 nmi north and 7 nmi south of the proposed drill site and from depths of 575 to 2,003 m (Figure 5-1). Surface images provided sufficient resolution to quantify densities of small, abundant features such as burrows and tubes of the foraminiferan *B. filiformis*. For large motile organisms, infrequent features, and features difficult to quantify (animal tracks), data were qualified according to presence or absence of the feature in surface images (Table 5-1). Actual image areas (areas photographed) ranged from 0.04 m² to 1.1 m², and had a mean of 0.5 m² (Table 5-1).

Bathysiphon filiformis tube densities ranged from 0 to 225 m⁻² and revealed a very patchy distribution (Figures 5-8 and 5-9). Burrow densities were calculated from counts of a 100-cm² portion of an image, using the scaling factor derived from the measurement of a *B. filiformis* tube. This density was then converted to square meter. Burrow density ranged from 200 to 3,700 m². Some of the densities from images that were over 1 m² in actual area photographed may be artificially low because of lower image resolution, resulting from the distance above the sediment surface at which the images were taken (e.g., Stations 26, 43, 44; Table 5-1).

Animal tracks were found in almost all the surface images, indicating a high degree of megafaunal activity (Table 5-1 and Figure 5-8). Clayey clasts were not common, appearing in images from only five stations, and in all the replicate images from only one station: SA10, the 2,000-m station (Table 5-1 and Figure 5-10). Individual tubes appeared in images from various stations, without pattern. Aggregations of tubes and associated sediment structure were more rare, appearing in images from only two stations, 10 and 26 (Figure 5-9). Fish were found in surface images from five stations. At least two species were observed; these were most likely a species of witch flounder, *Glyptocephalus cynoglossus*, and a species of eelpout, *Lycenchelys verrilli* (Figure 5-10).

Echinoderms appeared in only one image, from Station 10. Anthozoans *Actinauge verrilli* and *Cerianthus* sp., and three unidentified anthozoans appeared in images from only two stations, 44 and SA9 (Figure 5-10). Hydroids appeared in images only from station 26. Five unidentified megafauna taxa appeared in images from nine stations; most of these were animals partially buried in the sediment, many of which were probably gastropods (Table 5-1).

X-Ray Images

On Transect A, the core from Station 2 was relatively opaque to x-rays. The fabric was entirely composed of bioturbated sediment. Dark swirls at a depth of 5 to 7 cm appear to be produced by irregular urchins. The rest of the burrows are indistinct mottles produced by errant infauna. Some faint laminations in the upper 1 cm are probably an artifact of sloshing of the surface as the box core was recovered. The fabric of the core from Station 3 consisted entirely of bioturbated sediment in the form of indistinct mottles produced by errant infauna. This core was more x-ray opaque than the core from Station 2. The Station 5 core was comparable in opaqueness to Station 2 and was 100% bioturbated, consisting of indistinct mottles produced by errant infauna. The lower half of the x-ray contains relic tubes with an apparent wall thickness of about 1 mm. These were produced by sedentary infauna. Faint laminations at the surface could be sampling artifacts.

On Transect B, the core from Station 10 consisted of indistinct mottles. The upper centimeter of the core shows a surface layer of higher water content sediment related to sloshing of the core during recovery. The fabric was 100% burrow mottled by errant infauna. The Station 11 core was much more x-ray transparent than the one from Station 10. There was a gradient in density in this 20.8-cm-long core; approximately the upper 8-cm interval was more x-ray opaque than the bottom half. This gradient was the reverse of that produced by the process of compaction. All of the fabric was biogenic, consisting of indistinct burrow mottling. No qualitative difference in biogenic structures was observed down the axis of the core. On Transect C the fabric of the Station 18 core was entirely burrow mottled by errant infauna. The deep penetration of the corer (relative to the deeper stations) suggests that the bulk density of the core is lower than the deeper cores, and this difference may explain why x-rays

Table 5-1. Data from sediment surface images presented by station. Areas and densities measurements are means, and presence or absence data are from combined replicate images for a station. *Bathysiphon filiformis* = *B. fili.*

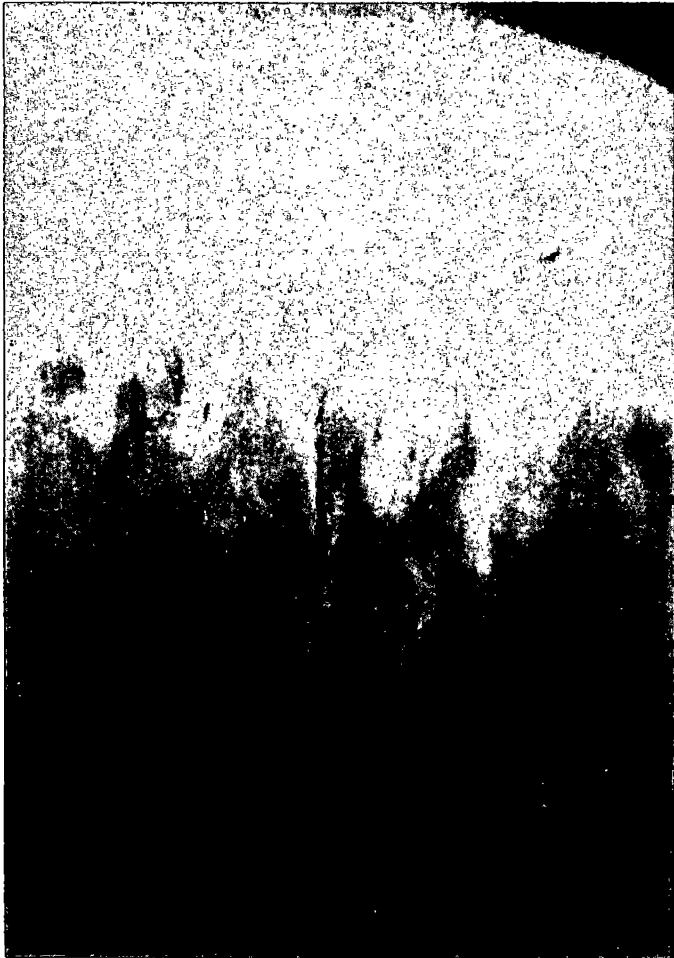
Station	Image Area	<i>B. fili.</i> Density (m ⁻²)	Burrow Density (m ⁻²)	Tracks	Clasts	Tubes	Tube Aggregates	Fish	Echinoderms	Anthozoans	Hydroids	Gastropods	Unidentified Fauna
10	0.3	7	0	+	0	+	+	+	+	0	0	0	+
11	0.6	1	1500	+	+	+	0	+	0	0	0	0	0
12	0.3	160	2900	+	0	+	0	0	0	0	0	0	+
18	.	0	.	+	+	+	+	0	0	0	0	0	+
19	.	0
20	0.6	22	1100	+	0	+	0	0	0	0	0	0	0
21
26	0.8	110	450	+	+	+	+	0	0	0	+	+	0
41	.	0	.	+	0	0	0	+	0	0	0	0	0
42	0.4	45	750	+	0	0	0	0	0	0	0	0	+
43	1.0	15	300	+	0	0	0	0	0	0	0	+	0
44	0.8	6	700	+	+	+	0	0	0	+	0	0	+
SA9	0.2	170	700	+	0	+	0	+	0	+	0	0	+
SA10	0.3	36	950	+	+	+	0	0	0	0	0	0	+

+ = feature present

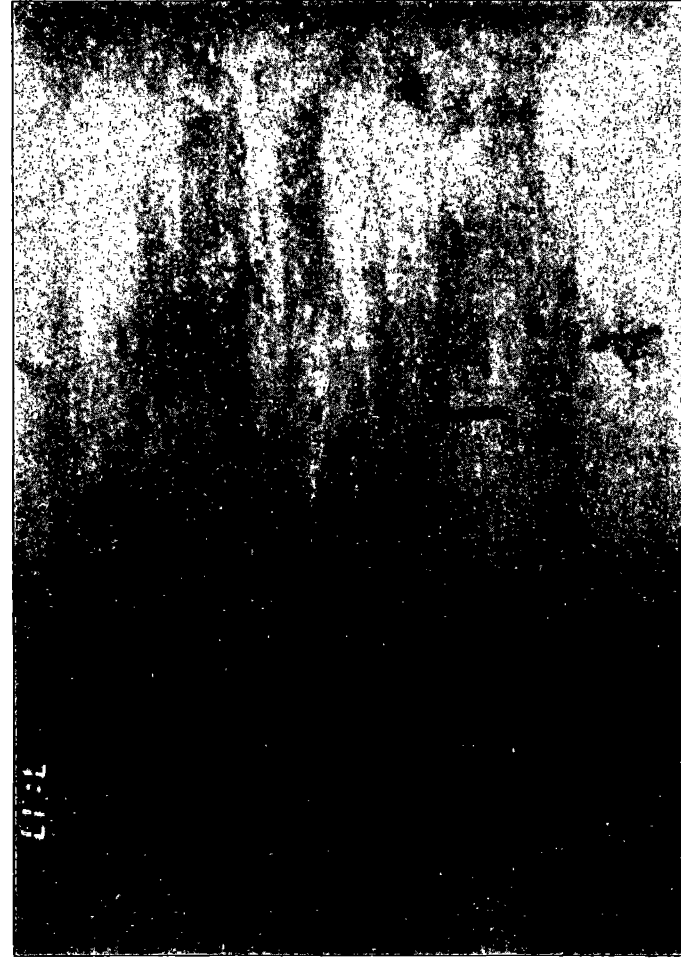
0 = feature absent

. = no data

a)



b)



41

Figure 5-7. Sediment profile images: subsurface fauna and burrows in images from a) Station SA9 replicate D, where a worm (Maldanidae) can be seen in a burrow from 10 cm to >23 cm below the surface; and b) Station 1A replicate A, with the bodies from 3 worms seen in the center of the image, and a portion of another worm apparent in the void in the far-right of the image, as well as a backfilled burrow present in the upper left (lighter-colored band of sediment extending nearly half-way down from top of image). Scale = 0.65x.

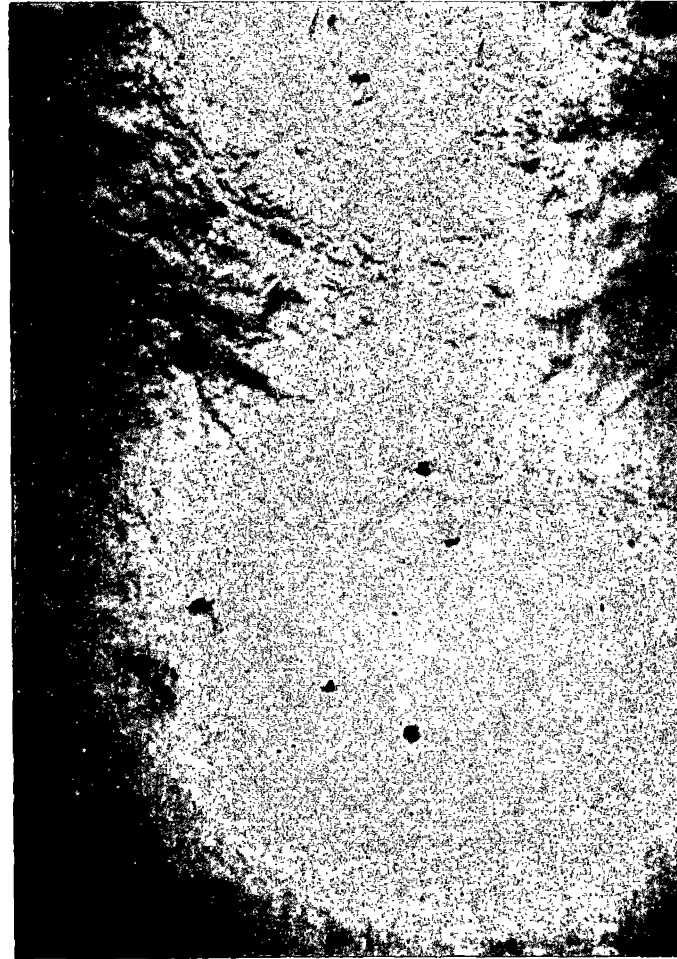
Reproduced from
best available copy.



a)



b)



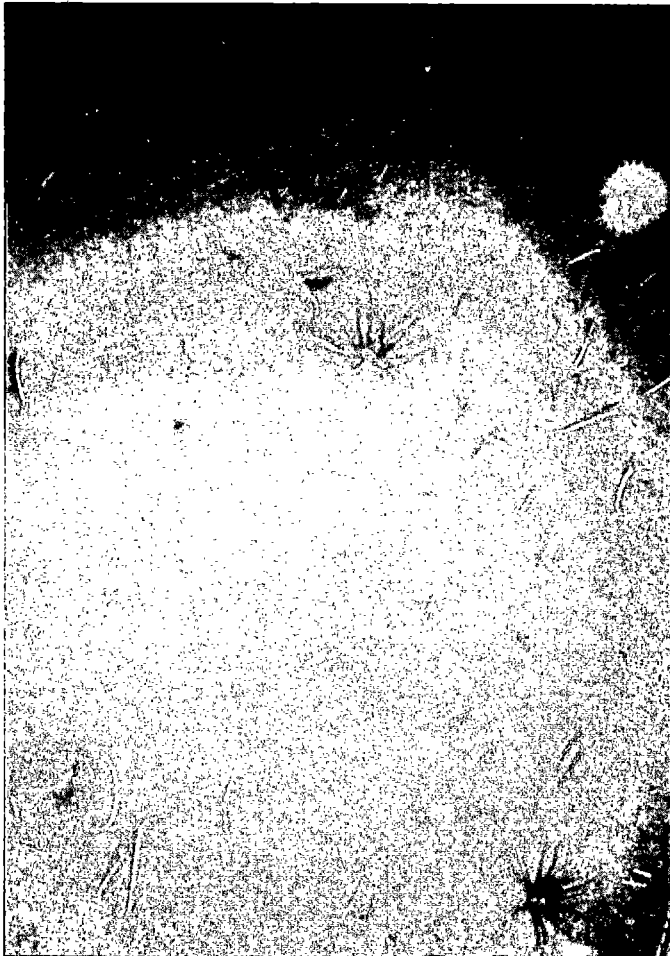
42

Figure 5-8. Sediment surface images: different densities of *Bathysiphon filiformis* and other surface features in images from a) Station 12 replicate A (actual area = 0.3 m²; scale = 0.2 × actual size), with high densities of *B. filiformis* and burrow openings; and b) Station 20 replicate A (actual area = 0.3 m²; scale = 0.2 ×), with *B. filiformis* were sparse, but large and small burrow openings were abundant, and distinct animal tracks were present.

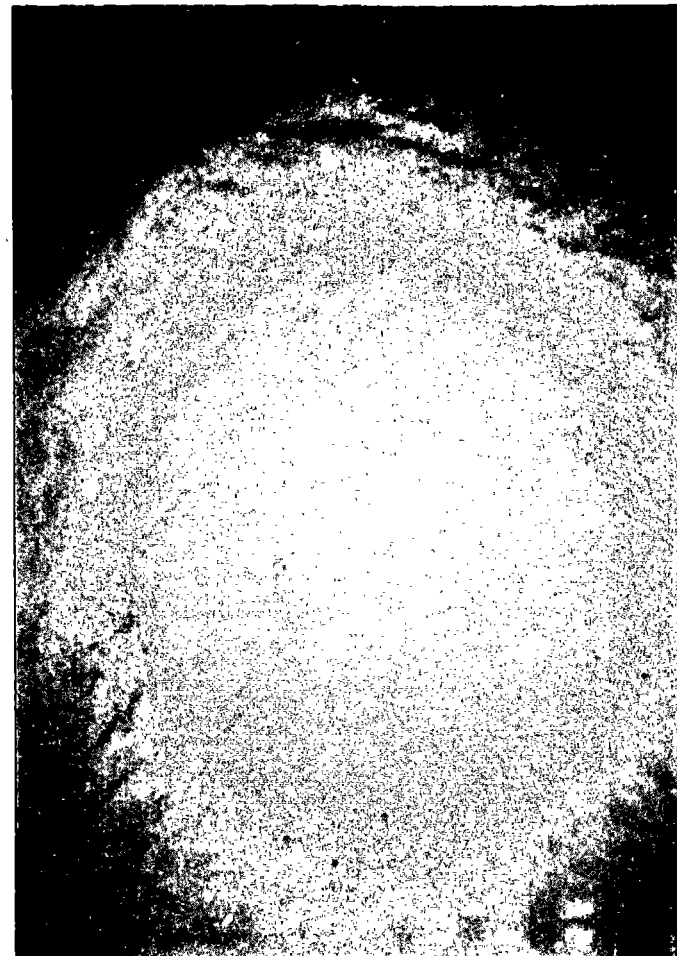
Reproduced from
best available copy.



a)



b)

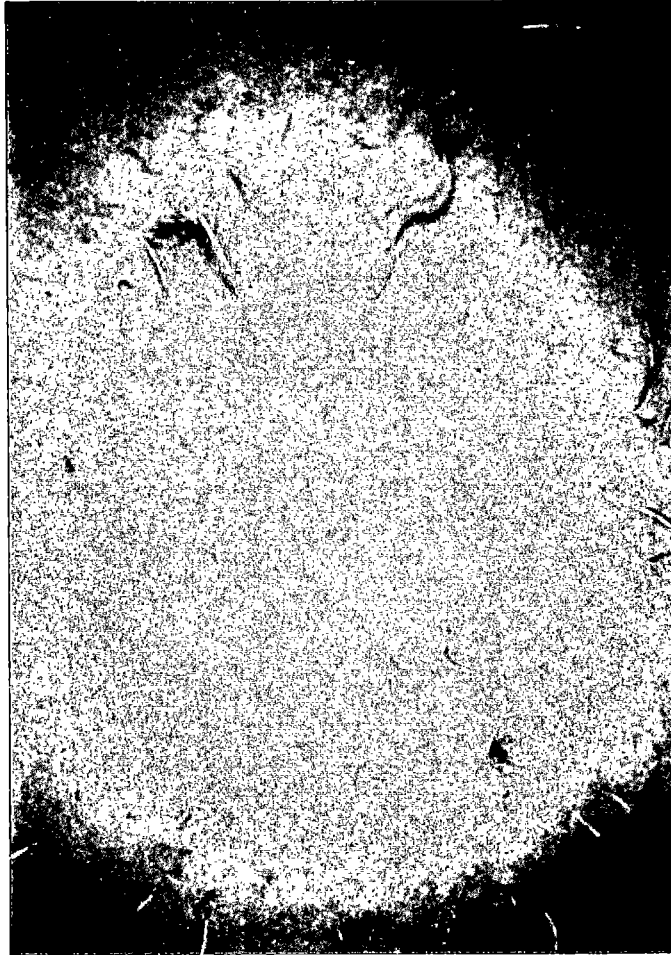


43

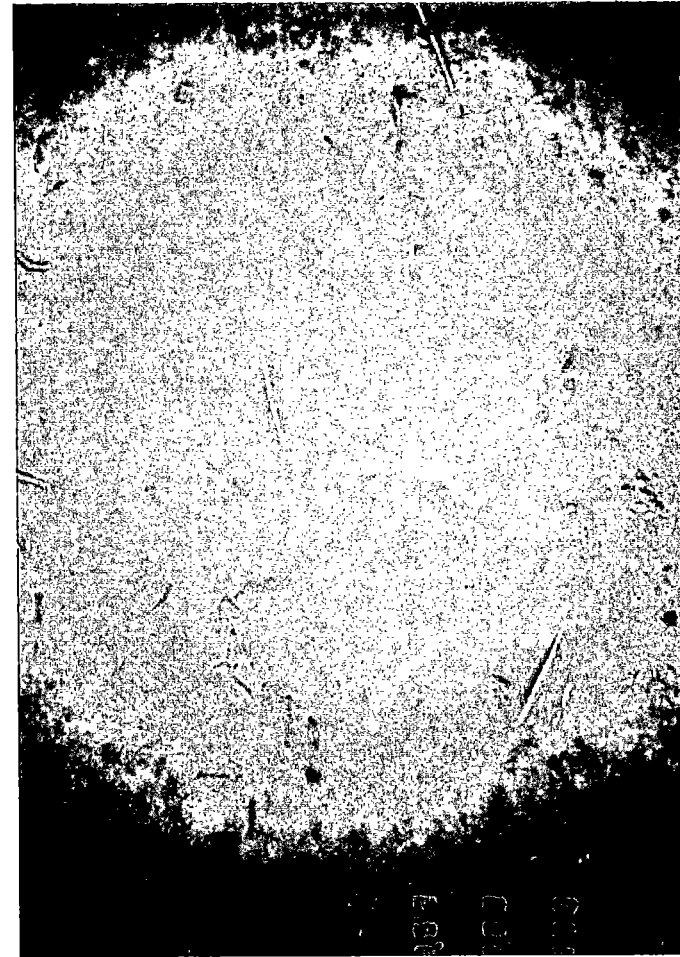
Figure 5-9. Sediment surface images: numerous epibenthos in images from a) Station SA9 replicate A (actual area = 0.3 m²; scale = 0.2×), with high densities of *Bathysiphon filiformis*, two Cerianthid anemones, and another anemone, *Actinauge verilli* (whitish animal) present; and b) Station 10 replicate D (actual area and scale unknown), with a witch flounder (*Glyptocephalus* sp.), an echinoderm, parts of other fauna buried in the sediments, and numerous animal tracks.



a)



b)



44

Figure 5-10. Sediment surface images: other fauna, and clayey clasts of sediment at the surface in images from a) Station SA9 replicate E (actual area = 0.18 m²; scale = 0.25×), with an eelpout, *Lycenchelys sp.*, and a part of another large animal present, as well as numerous *Bathysiphon filiformis* and burrows present; and b) Station SA10 replicate A (actual area = 0.18 m²; scale = 0.25×), with clayey clasts scattered over the surface, and *B. filiformis* and burrows also present.



penetrated this core better than the deeper two cores. The relatively x-ray opaque core from Station 19 had a fabric consisting of indistinct burrow mottling (errant infauna) and fragments of relic constructed tubes (sedentary infauna) below the surface. In this respect, this station resembled Station 5 (1,500 m) along transect A. Approximately the upper 6 cm was more x-ray transparent than the bottom of the core, particularly the upper 3 cm. This gradient may indicate that the depth of active burrowing (and fabric dilation) could be limited to this 6-cm interval. The upper 2 cm of the core from Station 21 was more x-ray transparent than the lower 9 cm, suggesting that the mean burrowing depth is shallow. Very faint vertical columns of more opaque sediment transect the core to a depth of about 9 cm.

On Transect D, the core from Station SA-10 was the most interesting in terms of diversity of fabrics. The upper 12.4 to 15 cm of this core consisted of imperfect laminations and the lower 8.5 to 6.0 cm consisted of a denser shell-rich interval. The contact between these two segments was relatively sharp. The upper segment consists of as many as eight or as few as four indistinct layers. These layers are recognized by the fact that they are more x-ray opaque than adjacent sediment. The layers are "bent" or partially erased by post-depositional burrowing. These layers probably represent small-scale turbidities. The lower segment shows no laminations and contains several shell fragments. A complete gastropod shell can be seen in an apex-down orientation. This orientation is typical for gastropods in quasi-fluid sediment (original water content $>> 50\%$) and is a sinking orientation. The sinking orientation represents geotechnical properties in the past because this interval of the core now contains only about 36% water and thus consists of a stiff plastic material. This lower unit probably represents a slower sedimentation interval followed by higher sedimentation rate (turbidite) intervals in the upper segment. The boundary between these two intervals of the core may represent a significant temporal hiatus (unconformity).

On Transect E, Station 33 had a relatively x-ray opaque core. The fabric was entirely biogenic and dominated by errant burrows. Some large (up to 2 cm in diameter) burrows cut across the core; one extending from the upper left to the lower right in the top half of the core and one or two extending from the lower left to the upper right in the bottom of the core. These could be produced by irregular urchins or burrowing crustaceans. Station 34 was similar to Station 33 in density and fabric except that the large burrows were not observed. The Station 36 core was less x-ray opaque than the shallower stations on this transect (33 and 34). The sediment was entirely burrow mottled. One constructed tube fragment was observed at a depth of 18 cm.

On transect F, the relatively x-ray opaque core from Station 41 contained a mottled fabric and some tubes of sedentary infauna. A scaphopod was observed in a sinking position (apex down) 6.5 to 8 cm below the surface. In the core from Station 42, the upper 10 cm appeared lighter than the bottom of the core, suggesting that 10 cm represented the maximum burrowing depth. Constructed tubes and tube fragments were observed both at depth and near the surface (malanids or *B. filiformis*). Some dark horizontal horizons in the lower half of the core may represent depositional layering or the boundaries of rather large relic burrows. The core from Station 44 had a fabric composed of indistinct burrow mottles produced by errant infauna. No constructed tubes were observed.

Discussion

Sediment profile images were dominated by deep burrowing infauna and other features that are often associated with an equilibrium system as described by Rhoads and Germano (1986). The entire survey area exhibited a deep layer of aerobic sediment, as seen from the 5.3 cm mean depth of the apparent color redox potential discontinuity (RPD) layer. The RPD layer usually appeared as a highly convoluted layer in the profile images. This most likely resulted from activities of infaunal burrowers which transport aerobic sediments into the reduced zone and provide pathways by which reduced sediments are flushed with oxygenated water.

Fine grained sediments such as those seen in the profile images have often been found to contain high levels of organic matter and to support high numbers of deposit feeding macroinvertebrates (Weston 1988). The sediment profile images from this study indicate high levels of macroinvertebrate infaunal activity seen. Greenish hues in hemipelagic deposits are characteristic of high productivity waters (Lyle 1983), and these were found in many of the profile images to depths corresponding to the deep bioturbation characteristic of the area. The sediment profile images captured numerous subsurface feeding voids, and some of the worms in the process of making deep burrows, many of which extended below the average RPD layer depth (Figure 5-2).

The area off Cape Hatteras marks the southern end of the range of *Bathysiphon filiformis*, the large agglutinated surface-feeding foraminiferan, which is generally associated with areas of high organic input (Gooday et al. 1992). High densities of *B. filiformis* were found in some of the sediment surface images from this study,

though overall a patchy and highly variable distribution was seen. Their distribution as well as surface features such as tracks, burrows, and megafauna in sediment surface images confirm the high levels of bottom faunal activity supported by the surface sediments in this area.

The x-ray images confirm that all the sediment fabrics were biogenic, except at Station SA10. This means the sedimentation rate and formation of physical sedimentary layers is slower than the rate of destruction of these laminations by bioturbational mixing. Considering that the sedimentation rates measured for this area were very high except at SA10 (Table 3-1), the bioturbational mixing was substantial (Table 5-2). High levels of activity of the benthos may be contingent to processes in the overlying water column such as current transport of organics and erosional forces. Bioturbation by the benthos, evidenced by profile images and x-ray images, contributes to the dynamic forces affecting the surface sediments by decreasing compaction of sediment layers, dilating sediment fabrics and producing lower bulk density, increasing water content, and introducing large water-filled burrows and voids. Hecker (1982, 1990b) has shown that bioturbation may be an important mechanism for destabilizing slope sediments. Dilated sediment fabrics, with less cohesion, become more susceptible to remobilization by internal waves and seismic activity. The biological activity which enriches the surface sediments also adds to the changeable character of the sediments in the area.

Table 5-2. Depth (cm) of sediment mixing by bioturbation as seen in the x-ray images.

Transect	Station	Depth of Bioturbation (cm)
A	2	11
A	3	10-12
A	5	6-8
B	10	15
B	11	15
C	18	20
C	19	6-18
C	21	5-17
D	SA10	7-10
E	33	20
E	34	12
E	36	8
F	41	10-14
F	42	10-12
F	44	??

CHAPTER 6. SYNTHESIS OF SEDIMENT DATA

Donald C. Rhoads

Introduction

This chapter is a synthesis of the sediment-related data we collected to address objective 1 (Chapters 3,4,5). It also attempts to place the study site in context with the broader U.S. Atlantic continental shelf and slope, utilizing references from other studies where appropriate.

The study area was located within transition area in terms of topography, hydrography, and types and sources of sediment. Cape Hatteras is where the Gulf Stream and Western Boundary Undercurrent (WBUC) cross. The Gulf Stream diverges north and eastward away from the shelf and slope into the North Atlantic. This is the northernmost point where Gulf Stream meanders can impinge on the shelf and upper slope, thereby affecting sediment transport. In turn, the WBUC moves from north to south and makes initial contact with the continental rise at Cape Hatteras at depths below 2,000 m. The continental shelf is constricted by the Cape to its narrowest width (30 km) in this same region, which may explain the unusually high sedimentation rates measured in the study area (see below). The narrow shelf also forms a natural north-south dividing line between two major sedimentary provenances.

Sedimentary Provenances

North of Cape Hatteras, shelf sediments are dominated by mechanically weathered arkosic (feldspar-rich) sands with clay fractions dominated by illite and chlorite. The northern area contains glacially reworked and transported sediments. Carbonate contents are less than 5%, reflecting both relatively low productivity of planktic foraminifera and dilution of biogenic carbonate by terrigenous sedimentation. Below the mud line (300 m), slope sediments are sandy silt-clays (Tucholke 1987).

South of Cape Hatteras, sediment mineralogy reflects soils exposed to extensive chemical weathering. Feldspars tend to be a minor component because they are chemically weathered to clays (kaolinite and montmorillonite). The sand fraction, therefore, consists of more chemically resistant minerals like quartz. The carbonate fraction increases south of Cape Hatteras under the influence of warmer tropical waters which stimulate planktic foraminiferal production. Shelf sediments south of Hatteras reflect the influence of deltaic deposits that once covered the shelf. These relic fluvial sands are now being reworked by waves and currents. The slope environment is dominated by silt-clay sediment (Tucholke 1987).

The study area is located slightly north of Cape Hatteras on the northern end of the Carolina Platform, a structural ridge that separates the Baltimore canyon from the Carolina trough; therefore the site shares some attributes of both the northern and southern sedimentary provenances. Carbonate contents of the study area ranged from 8 to 12% and are transitional between the carbonate-poor shelf north of Cape Hatteras (ca. 5%) and the high carbonate regime (locally 50%) to the south. The slope environment contains appreciable sand (15 to 47%) derived from the shelf north of Hatteras. Sediments in the study area are poorly sorted sandy silt-clays. The sand is derived from reworked fluvial/glacial sediments located on the shelf, and some sand may be locally derived from submarine erosion of exposed tertiary outcrops on the slope (Tucholke 1987). The grain-size frequency distributions do not provide much information about source areas. There is as much variability in percent sand content along the 600, 800, and 1,500-m isobaths as there is across isobaths.

Possible Transport Mechanisms

A line of divergence in bottom transport is located 1/2 to 3/4 of the distance from the beach to the 100-m isobath on the Atlantic continental shelf (Figure 6-1) (Bumpus 1973). Shoreward of the Bumpus line, the net drift of bottom water is toward the coast; seaward of this line, the net drift is toward the southwest (seaward) toward the slope at velocities of 5 to 10 cm s⁻¹. These velocities are sufficient to transport low-density and fine-grained seston southward along the entire outer shelf.

Surface waters outwelling from Chesapeake Bay, Delaware Bay, and even as far north as the New York Bight are associated with plankton and seston that move across the shelf. As this production dies and settles to the bottom, some of it will settle seaward of the Bumpus line and be swept southward toward the

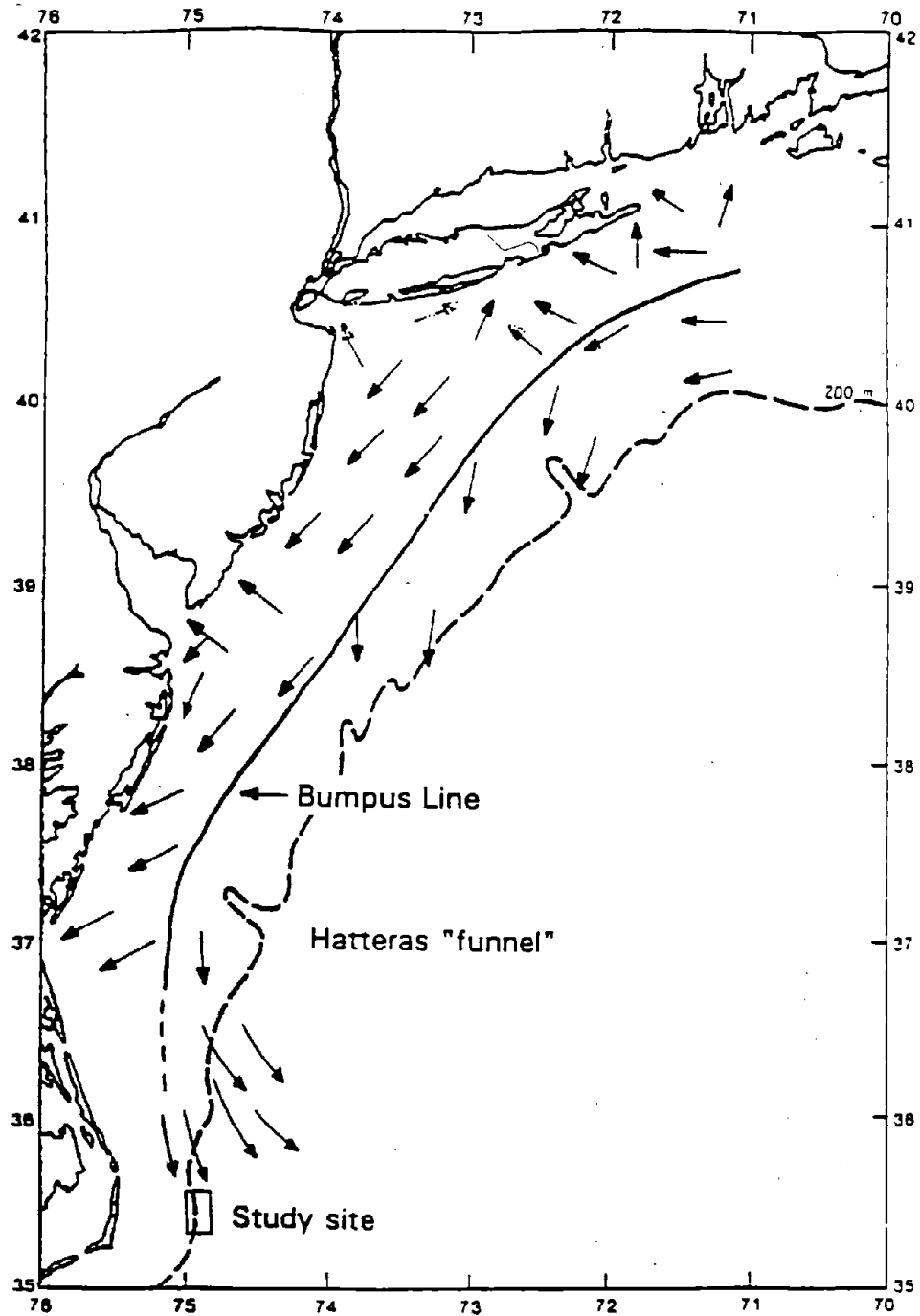


Figure 6-1

Direction of bottom currents on the Atlantic continental shelf as determined from bottom drifter measurements. Currents west of the "Bumpus" line move suspended sediments shoreward toward the mouths of estuaries. Currents east of the line move toward the south at all seasons at $5-10 \text{ cm s}^{-1}$ (modified from Williams and Godshall 1977). Note that just north of Cape Hatteras, the "Bumpus" line is directed toward the Manteo study area. In this region this may serve to "funnel" and focus outer shelf sediment onto the slope.

shelf-slope break (Figure 6-1). For example, Chesapeake Bay may itself export fine-grained sediment and planktic detritus directly to the study area as surface currents out of the Chesapeake flow toward the southwest at all seasons at a mean velocity of ca. 5 cm s^{-1} (Williams and Godshall 1977). Plankton blooms associated with outwelled Chesapeake water extend, in some cases, all the way to the shelf edge (Wiebe et al. 1987). Because the shelf narrows to only 30 km in width between Chesapeake Bay and Cape Hatteras, the Bumpus line intersects the shelf-slope; this may serve to "steer" and funnel fine-grained and organic-rich seston onto the slope in the study area. This phenomenon is called topographic blocking (Blanton 1991). Once fine-grained suspended sediment enters the slope, much of it is entrained in turbid suspensions that move down canyons and gullies. As these turbid suspensions intersect density layering (isopycnals) in the water column, the suspensions can be lifted onto these density discontinuities and be transported further south along the slope. This may be one mechanism for forming deposits between canyons. These focusing phenomena may explain the anomalously high sediment accumulation rates measured at the study area (see below).

Mechanisms for moving sands from the shelf to the slope require more kinetic energy than that provided by the relatively weak 10 cm s^{-1} mean bottom flow velocities recorded on the shelf edge east of the Bumpus line. Higher kinetic energies are available from storms passing over the shelf (Rodolfo et al. 1971), internal waves moving over the shelf-slope break (Csanady et al. 1988, Flagg 1988, Churchill et al. 1992), and incursions of Gulf Stream meanders and eddies (Blanton 1991).

South of Cape Hatteras (off Onslow Bay), the Gulf Stream can directly affect bottom sediment transport on the shelf and upper slope. A Gulf Stream meander that was observed in this area affected the bottom to 700 m, and a current meter moored at 575 m recorded velocities up to 40 cm s^{-1} near the bottom (Levine and Bergen 1983). North of Cape Hatteras, the Gulf Stream is deflected into the Atlantic, and so the meanders themselves do not intersect the slope or shelf. However, anticyclonic eddies 100 to 200 km in diameter, detached from the western edge of the diverging Gulf Stream, move along the shelf-slope break going from north to south at a velocity of 5 to 10 cm s^{-1} . Near-surface velocities within the eddies can attain 80 cm s^{-1} and decrease with depth ($2\text{-}5 \text{ cm s}^{-1}$ at 1,000 m) (Williams and Godshall 1977). The upper parts of these eddies that are in contact with the bottom near the outer shelf and upper slope have the ability to move sands over the slope edge. As eddies move toward Cape Hatteras, they are forced toward the shelf edge (the Hatteras funnel, Figure 6-1) where they may be reattached to the Gulf Stream. Once these sediments move down slope they may be entrained and moved south along convergence zones on the slope or south along contours at greater depths by the Western Boundary Current (lower slope and rise).

In addition to promoting sediment transport, subsurface intrusions of Gulf Stream water onto the shelf are known to promote local upwelling and enhanced primary productivity (Blanton 1991). Walsh et al. (1985) estimated that about 50% of the shelf primary productivity is swept off the shelf and deposited, as organic detritus, on the Mid-Atlantic Bight slope.

Sedimentation Rates

Sedimentation rates, as determined from ^{210}Pb profiles below the bioturbation depth of ca. 10 cm, indicate an accumulation rate of 0.3 to 1.8 cm yr^{-1} , excluding the 0.05 cm yr^{-1} estimated from the 2,000-m Station SA-10 which was likely recently disturbed. The minimum accumulation rate based on the age of sediment organic carbon, at a site within our study area, was at least 0.5 cm yr^{-1} (DeMaster unpublished data). Holocene sedimentation rates on the slope off the Atlantic coast range from 0.01 to 0.04 cm yr^{-1} (Emery and Uchupi 1972). Rates measured in this study are 25 to 100 times higher than these rates. Sedimentation rates of approximately 1 cm yr^{-1} reported for the Cape Hatteras continental slope stations are comparable to, or higher than, estuarine rates. For example, the long-term sediment accumulation rate of mud in Long Island Sound is only 0.09 cm yr^{-1} (Kim and Bokuniewicz 1991). Emery and Uchupi (1972) measured sedimentation rates of $40 \text{ cm 1,000 yr}^{-1}$ (0.04 cm yr^{-1}) on the slope due east of Cape Hatteras. The Emery and Uchupi (1972) rates, and those measured in this study, may not be strictly comparable because ^{210}Pb data represent short-term rates measured from the upper 15 to 30 cm interval of sediments, whereas the Emery and Uchupi (1972) data are from longer core lengths. It is well known that short-term rates may be poorly correlated with long-term rates. For example, the ^{210}Pb rates in Long Island Sound are greater by a factor of 2 than rates estimated from accumulated sediment thickness as measured over the past 8,000 years (Turekian et al. 1980).

An area on the slope with high rates of sediment input would be expected to experience local oversteepening and periodic slope failure. Evidence for this is present on all of the towed camera transects (Chapter 8). Many steeply sloping Tertiary outcrops are observed with an apparently thin cover of soft sediment. Some of these surfaces show evidence of recent soft sediment failure in the form of slump scars and erosional "rivulets." These steep slopes may represent source areas for turbidites. Depositional sites for turbidites, debris flows, and massive slump blocks can be recognized in bottom photographs by undulating topography (on horizontal scales $> > 1$ m), cohesive mud clasts projecting above an otherwise planar depositional surface of fine sediment, and the presence of relatively featureless sediment surfaces that have not had a chance to be disturbed by bioturbation and surface tracking. X-ray fabric analysis of the upper 12 to 15 cm of a core from Station SA-10 shows vertical compositional layering typical of recent turbidite sedimentation (Chapter 5). This same station has large-scale surface features typical of debris flow deposits.

The rate of sediment accumulation over the entire study site is highly variable. The towed camera sled shows a wide diversity of bottom types including barren outcrops (no sedimentation), sediment-draped outcrops (subcrops), relic overconsolidated bottoms, and erosional surfaces. The selection of box core station locations was biased toward those bottom types with a net accumulation of sediment. High sedimentation rates may account for high standing stocks of benthic invertebrates at the study area and may explain why many of the dominant species are those also found in productive continental shelf environments. An inventory of about 1 to 2% organic carbon is present in the sediments from the study site and is typical for muddy inner shelf sediments. Sedimentation of organic matter provides the fuel to sustain these high populations. Densities of benthic invertebrates recorded in this report (Chapter 7) are comparable to those described from the productive fishing grounds of Georges Bank (Neff et al. 1989).

The carbon flux rate for an 850-m station near the study area was estimated to be > 70 g C m² yr⁻¹ (Schaff et al. 1992). In this study, we have estimated an average annual accumulation rate of organic carbon of 67 g C m², with a range of 28 to 121 g C m² (Chapter 3). This flux is about 35 to 85% lower than planktic carbon sedimentation rates estimated for productive estuaries; for example, 200 g C m² yr⁻¹ for Long Island Sound and 240 g C m² yr⁻¹ for Narragansett Bay (Welsh et al. 1982). Boynton et al. (1982) compiled estimates of annual phytoplankton productivity for 45 estuarine systems and the mean value was 190 g C m² yr⁻¹. For the sedimentation rate of organic carbon to average 67 g C m² yr⁻¹ at the study site, the production driving this carbon source must be much larger because the percentage of primary production reaching the seafloor at 1000 m is typically less than 10% (Valiela 1984). Most of the organic carbon reaching the study area is refractory. High molecular weight fatty acids, which contribute up to 9% of the total long chain fatty acids ($> C_{22}$) are typical of higher plants and terrigenous inputs.

The concentration of chlorophyll-*a* in the sediments at the study site appears to be higher than average for slope sediments that do not underlay upwelling regions (Chapter 4). The values are intermediate between those recorded for sediments underlying intensive upwelling regions (5.5 to 17 μ g g⁻¹ dry wt. from 2,400-3,000 m on the slope off the Farallones, central California slope (Blake et al. 1992) and estuarine values. For example, the inventory of chlorophyll-*a* along the Manteo transects is comparable to summer chlorophyll-*a* values in Long Island Sound (Sun et al. 1991). Because the decomposition rates of phaeopigments are high, the flux of plant cells to the bottom must be very high to support the observed inventory. Chlorophyll-*a* concentrations within the upper 5 cm of the sediment column are highly variable. This is attributed to patchiness induced by the local concentration of diatom-rich floccular material in small-scale surface depressions and local variations in decomposition rates. In addition, variability down the axes of cores can be related to differences in injection rates of viable diatoms into the sediment column by feeding and burrowing activities of infaunal benthos (Dobbs and Whitlach 1982). The inventory of fatty acids in slope sediments off Cape Hatteras ranges from 8 to 137 μ g g⁻¹ dry wt. The mean value of 27 μ g g⁻¹ dry wt. falls within the range reported for estuarine sediments (10-35 μ g g⁻¹ dry wt.) but is less than concentrations found in sediments underlying more intensive and persistent upwelling zones (765 μ g g⁻¹ dry wt.) (Chapter 4).

Post-Depositional Processes

The X-ray fabric analysis of sediments, *in situ* sediment-profile images, and bottom surface photographs all showed evidence of intensive bioturbation and surface tracking. No primary structures were preserved in core profiles except at Station SA-10, which showed X-ray fabrics suggestive of recent turbidite sedimentation in the upper 12 to 15 cm. Sediment profile imaging showed bioturbated fabrics, produced by deep-burrowing deposit feeders, with an abundance of feeding voids within the sediment column. Almost every surface photograph showed evidence of extensive surface tracking by fish and megafauna. Surface mounds produced by head-down deposit feeders were also present in these photographs. A bioadvection coefficient (D_b) estimated for a site within the study area was $30 \text{ cm}^2 \text{ yr}^{-1}$ (Schaff et al. 1992), which is comparable to D_b values for Long Island Sound (Matisoff 1982). This high rate may explain why populations of viable diatoms are found at depths within the upper sediment column. Head-down feeders are capable of rapidly injecting surface floc material to depth in the sediment to stimulate bacterial activity (Dobbs and Whitlatch 1982). Also, the many burrow openings may act as passive traps which quickly remove diatoms from the surface.

Densely spaced fecal mounds were observed in many of the towed camera sled photographs (Chapter 8). The D_b values for fecal mounds may be particularly high relative to the adjacent bottom. The discharge of fecal and excavated material onto the surface can represent a significant physical disturbance factor on the seafloor and is known to produce both geochemical and biological patchiness (Rhoads and Young 1971, Aller 1982, Carney 1989, and Kukert and Smith 1992). It is likely that some of the large-scale patchiness of *Bathysiphon* is related to the burial of the tubes by surface mounds produced by head-down deposit feeders (a form of trophic group amensalism, Rhoads and Young 1970). Bioturbation also affects the shape of pore water profiles of sulphate, dissolved inorganic carbon, and methane. The depth of particle and pore water exchange, estimated from X-ray fabrics, pore-water profiles, sediment water profiles, depth distribution of feeding voids, and ^{210}Pb profiles, ranged from 8 to 20 cm. The population means from these five data sources fell between 11 and 14 cm. Again, the depth of biogenic sediment mixing is comparable to estuarine sediments.

THIS PAGE LEFT BLANK INTENTIONALLY



CHAPTER 7. BENTHIC INFAUNAL COMMUNITY STRUCTURE

James A. Blake, Brigitte Hilbig, and Isabelle P. Williams

Introduction

The continental slope off Cape Hatteras has been identified as having unusually dense assemblages of infaunal and epifaunal organisms (Blake et al. 1987, Schaff et al. 1992, Blake and Grassle unpublished). The most important studies previously conducted off Cape Hatteras were part of the Atlantic Continental Slope and Rise Program (ACSAR) supported by the MMS from 1983 to 1987. The ACSAR program was the first comprehensive effort to characterize and understand the benthic communities on the continental slope of the Western North Atlantic. Two stations off Cape Hatteras were monitored as part of the ACSAR program. Station SA-9, located at a depth of 600 m in Manteo Prospect Lease Block 510, was approximately five miles from the proposed Mobil drilling site in Block 467. Station SA-10 was located at a depth of 2000 m downslope from Station SA-9. Both of these stations were found to have unusually high infaunal densities and were dominated by infaunal invertebrates that were more typical of shallower, continental shelf depths. For example, Station SA-9 had average densities of 46,255 individuals m⁻² over three sampling periods (nine samples total) and was dominated by three polychaetes (*Cossura longocirrata*, *Scalibregma inflatum*, and *Aricidea quadrilobata*), and two oligochaetes (*Limnodriloides medioporus* and *Tubificoides intermedius*). All of these species are more typical of shallower depths. In addition to high infaunal densities, the box cores contained numerous white hardened tube-like structures that were subsequently determined to represent a tube-dwelling foraminiferan, *Bathysiphon filiformis* (Gooday et al. 1992).

This study was conducted to determine the areal extent and composition of the benthic faunal community and to address objectives 1, 3, and 4. The presence and distribution of the dominant polychaetes and oligochaetes were used to characterize the infauna.

Methods

The sampling procedures and the locations of box core stations are presented in detail in Chapter 2 and Appendix C of this report. A total of 20 box cores were taken along approximately 53 km in a north-south direction along the slope (Figure 7-1). Sixteen of these samples were fully processed for benthic infauna (Table 2-1). The biological fraction of each box core included a total surface area of 0.09 m². The top 10 cm of sediment was sieved through a 300- μ m sieve. Because larger, deep-burrowing organisms were frequently present in the samples, all of the remaining mud in the subcores was retained and sieved through a 1.0-mm sieve. This material was subsequently combined with the 10-cm sample. This procedure ensured that none of the deep-burrowing organisms were lost to the analysis. Immediately after sieving, the samples were labeled and preserved in 10% buffered formalin. The samples were resieved and transferred to 80% ethanol no more than 48 h after collection. Samples were initially sorted to major taxonomic category and subsequently identified to species. Prior to sorting, samples were stained in Rose Bengal to facilitate removal of small organisms from the sediment. The samples were then examined under a dissecting microscope and each organism, or fragment thereof, was removed. Species were identified by senior taxonomists familiar with deep-sea benthic infauna.

The final database included counts of organisms for which the identification was uncertain (juveniles, anterior fragments, etc.); these were used for density and dominance or percent contribution tabulations, but were not included in calculations of similarity or diversity indices. Small juvenile polychaetes that appeared to represent post-larval forms were excluded entirely because it could not be ascertained what these organisms were benthic species.

In order to assess patterns in the infaunal data, similarity or cluster analysis was performed using four different strategies: NESS (Normalized Expected Species Shared, Grassle and Smith 1976) and Bray-Curtis (Boesch 1977) each with group average sorting and flexible sorting ($\beta = -0.25$). For Bray-Curtis, the data were square root transformed prior to analysis to reduce the influence of high densities of dominant species. For NESS, the number of individuals (m) was set at 200. The same strategies were used for a database that was reduced to the 50 most abundant species. This latter database was then used for ordination analysis using

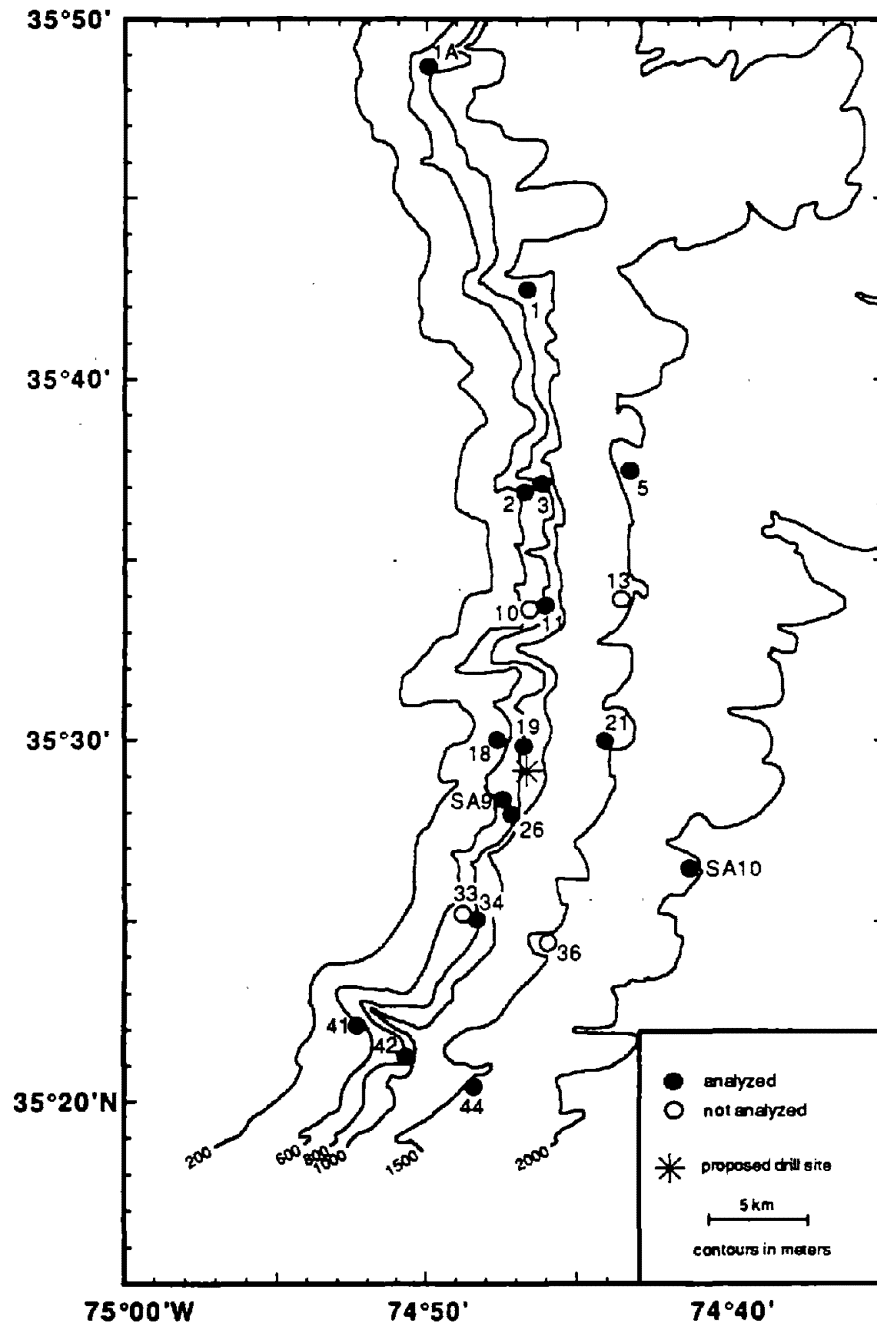


Figure 7-1. Location of box core stations within the study area off Cape Hatteras showing. Closed circles represent stations where samples were processed for benthic infauna; open circles represent stations where samples were not processed; and asterisk denotes location of the proposed Mobil drill site.

reciprocal averaging or correspondence analysis. Results of the ordination were then carefully compared to the results of the cluster analyses to assess comparability in patterns between the two methods. Benthic community parameters, including Shannon-Wiener diversity (H') and its associated evenness value (J'), were calculated along with the rarefaction method (Sanders 1968) as modified by Hurlbert (1971). The Shannon-Wiener index was calculated using the base \log_e . For the rarefaction analyses, the number of individuals was set at defined points ranging between 50 and 4000.

Results

Faunal Analysis

A total of 280 species belonging to 12 phyla were identified (Table 7-1) from the 16 box core samples. As is typical for soft-bottom infaunal communities, nearly half of all species were polychaetes (127 species, 45% of total fauna). Well-represented polychaete families included the Spionidae (10 species), Paraonidae (9 species), Cirratulidae (9 species), Phyllodocidae (8 species) and Terebellidae (7 species). The molluscs were the second most important group with 57 species (20% of total fauna). The Bivalvia were the largest group of molluscs (27 species). The crustaceans were represented by 48 species (17% of total fauna), with amphipods, isopods, and tanaidaceans contributing 18, 13, and 12 species respectively. Echinoderms contributed 18 species (6% of total fauna). Many of the echinoderms were represented only by juveniles; although these were classified as distinct species, it was often not possible to assign names to them. Several smaller phyla such as sipunculans, echiurans, priapulids, and nemerteans accounted for the remaining 30 species (11% of total fauna).

The majority of specimens removed from the box cores were small organisms, which supports previous observations that deep-sea benthic organisms have a smaller average body size than organisms from shallow-water environments (Jumars and Gallagher 1982). It is noteworthy, therefore, that the sediments on the slope off Cape Hatteras also contain large, deep-burrowing infaunal organisms of a form that is more typical of nearshore environments. The largest organisms seen in the box cores were maldanid polychaetes of the genera *Praxillella* and *Chirimia*, the very abundant scalibregmatid polychaete *Scalibregma inflatum*, and large holothurians of the genus *Molpadia*. Large, deep-burrowing sipunculans have been previously observed in box cores from Station SA-9 (Blake et al. 1987). Numerous specimens of a large agglutinated foraminiferan identified as *Bathysiphon filiformis* were also observed protruding from the sediment in the box core samples.

Benthic community parameters, including species richness (numbers of species), species diversity, and faunal density, are shown in Table 7-2. Rarefaction curves have been plotted for all stations to depict diversity patterns among stations (Figure 7-2). Species richness and diversity values are low for a continental slope environment. Species richness was highest at the two northernmost stations (1A and 1, both 800 m) and the three deepest stations (5, 44, and SA10). The lowest species richness was found at Stations 21, 2, and 3. Diversity, expressed as Hurlbert's rarefaction and Shannon-Wiener index H' , was highest at the stations with the highest species richness. The number of species per 750 individuals at these stations ranged from 67.9 (Station SA10) to 80.0 (Station 1), and H' ranged from 4.62 to 4.92. Diversity was lowest at Stations 18 (530 m), 26, 3 (800 m), and 2 (600 m) when measured with Hurlbert's rarefaction method; the number of species per 750 individuals ranged from 24.6 to 26.9. The Shannon-Wiener indices agree well with Hurlbert's rarefaction except that the lowest H' was calculated for Station 41. There are no clear depth or latitudinal trends apparent in the diversity and species richness data.

Total infaunal densities ranged from 8,533 to 89,556 individuals m^{-2} in the 16 samples (Table 7-2). The total densities from each sample as well as those of selected dominant taxa are shown in Figure 7-3. These data indicate that relatively few taxa contributed to the high total densities. The highest densities (89,556 individuals m^{-2}) were found at Station 18, the shallowest location (530 m). Total infaunal densities at three stations along the 600-m isobath (590-620 m) and nine stations along the 800-m isobath (775-815 m) were

Table 7-1. List of species identified from sixteen samples taken off Cape Hatteras.

CNIDARIA	<i>Ophryotrocha pachysoma</i> Hilbig & Blake 1991
Hydrozoa	<i>Parougia caeca</i> (Webster & Benedict 1884)
Hydrozoa sp. 1, 2, 3, 4, 5	Eunicidae
Anthozoa	<i>Marphysa</i> sp. A
Anemone sp. 1, 2	Fauveliopsidae
PLATYHELMINTHES	<i>Fauveliopsis glabra</i> (Hartman 1960)
Turbellaria sp. 1, 2, 3	<i>Fauveliopsis olgae</i> Hartmann-Schröder 1983
NEMERTEA	Flabelligeridae
Nemertea sp. A, B, C, D, E	<i>Diplocirrus hirsutus</i> (Hansen 1879)
PRIAPULIDA	Flabelligeridae sp. 1, 3
<i>Priapulus caudatus</i> Lamarck, 1816	Glyceridae
ANNELIDA	<i>Glycera lapidum</i> complex Quatrefages 1865
Polychaeta	Goniadidae
Aberrantidae	<i>Goniada maculata</i> Oersted 1845
<i>Aberranta enigmatica</i> Hartman 1965	Hesionidae
Acrocirridae	Hesionidae sp. 3
<i>Flabelligella cirrata</i> Hartman & Fauchald 1971	<i>Nereimyra punctata</i> (Müller 1788)
<i>Flabelligella</i> sp. 3	<i>Microphthalmus</i> sp. 2
Ampharetidae	Lacydoniidae
Ampharetidae sp. 8	<i>Lacydonia cirrata</i> (Hartman & Fauchald 1971)
<i>Anobothrus gracilis</i> (Malmgren 1866)	Lumbrineridae
<i>Ectysippe</i> sp. 1	<i>Abyssoninoe abyssorum</i> Orensanz 1990
<i>Melinna cristata</i> (Sars 1851)	<i>Eranno peterseni</i> Frame 1992
<i>Mugga wahrbergi</i> Eliason 1955	<i>Lumbrineris latreilli</i> (Audouin & Milne-Edwards 1833)
<i>Sosanopsis wireni</i> Hessle 1917	<i>Ninoe nigripes</i> Verrill 1873
Amphinomidae	<i>Paraninoe</i> nr. <i>brevipes</i> (McIntosh 1903)
<i>Paramphinome jeffreysi</i> (McIntosh 1868)	<i>Scoletoma fragilis</i> (Müller 1776)
Aphroditidae	Maldanidae
<i>Aphrodita</i> sp.	<i>Chirimia biceps</i> (Sars 1861)
Apostobranchidae	<i>Clymenura</i> sp. 1
<i>Apostobranchus tullbergi</i> (Théel 1879)	<i>Notoproctus</i> nr. <i>oculus</i> Arwidsson 1907
Capitellidae	<i>Praxillella gracilis</i> (Sars 1861)
<i>Barantolla</i> sp. 1, 3	<i>Praxillella praetermissa</i> (Malmgren 1866)
<i>Capitella capitata</i> complex Fabricius 1780	<i>Praxillella</i> sp. 1
<i>Heteromastus</i> sp.	Nephtyidae
<i>Notomastus latericeus</i> Sars 1851	<i>Nephtys paradoxa</i> Malm 1874
<i>Notomastus tenuis</i> Moore 1909	Nereididae
Chrysopetalidae	<i>Ceratocephale</i> nr. <i>abyssorum</i> (Hartman & Fauchald 1971)
<i>Dysponetus</i> cf. <i>gracilis</i> Hartman 1965	<i>Ceratocephale loveni</i> (Malmgren 1867)
<i>Dysponetus</i> sp. 8	<i>Nereis zonata</i> Malmgren 1867
Cirratulidae	Onuphidae
<i>Aphelochaeta marioni</i> (Saint-Joseph 1894)	<i>Onuphis rullieriana</i> (Amoureux 1977)
<i>Aphelochaeta monilaris</i> (Hartman 1960)	Opheliidae
<i>Aphelochaeta</i> sp. 6	<i>Ophelina aulogastrilla</i> (Hartman & Fauchald 1971)
<i>Chaetozone gayheadia</i> Hartman 1965	<i>Ophelina cylindricaudata</i> (Hansen 1878)
<i>Chaetozone</i> nr. <i>setosa</i> Malmgren 1867	Orbiniidae
<i>Chaetozone</i> sp. 11	<i>Leitoscoloplos</i> nr. <i>acutus</i> (Verrill 1873)
<i>Monticellina baptistae</i> Blake 1991	Oweniidae
<i>Tharyx acutus</i> Webster & Benedict 1887	<i>Galathowenia</i> sp. 1
<i>Tharyx kirkegaardi</i> Blake 1991	<i>Myriochele</i> nr. <i>heeri</i> Malmgren 1867
Cossuridae	Paraonidae
<i>Cossura brunnea</i> Fauchald 1972	<i>Aricidea catherinae</i> Laubier 1967
<i>Cossura longocirrata</i> Webster & Benedict 1887	<i>Aricidea quadrilobata</i> Webster & Benedict 1887
<i>Cossura pygodactylata</i> Jones 1956	<i>Aricidea</i> sp. 2, 3, 4, 6
<i>Cossurella</i> sp. 1	<i>Levinsenia</i> sp. 1
Dorvilleidae	<i>Paradoneis brevicirrata</i> (Strelzov 1973)
<i>Exallopus blakei</i> Hilbig 1991	<i>Paradoneis tyra</i> (Southern 1914)
<i>Ophryotrocha bifida</i> Hilbig & Blake 1991	
<i>Ophryotrocha maciolekae</i> Hilbig & Blake 1991	
<i>Ophryotrocha labidion</i> Hilbig & Blake 1991	

Table 7-1 (Continued)

Pholoidae	<i>Pholoe anoculata</i> Hartman 1965	ECHIURA	Echiura sp. 8, 9
Phyllococidae	<i>Eteone</i> sp. 1	SIPUNCULA	<i>Nephasoma capilleforme</i> (Murina 1973)
	<i>Eulalia</i> sp. 1		<i>Nephasoma diaphanes</i> (Gerould 1913)
	<i>Eumida</i> sp. 2		<i>Phascolion lutense</i> Selinka 1885
	<i>Mystides borealis</i> Théel 1879		<i>Phascolion strombus</i> (Montagu 1804)
	<i>Mystides caeca</i> Langerhans 1879	POGONOPHORA	<i>Siboglinum</i> sp. 16
	<i>Mystides rarica</i> (Uschakov 1958)	MOLLUSCA	Gastropoda
	<i>Paranaitis wahlbergi</i> (Malmgren 1865)		Cylichnidae
	<i>Protomystides anoculata</i> (Hartman & Fauchald 1971)		<i>Cylichna alba</i> (Brown 1827)
Pilargidae	<i>Ancistrosyllis groenlandica</i> McIntosh 1879		Haminoecidae
	<i>Sigambra tentaculata</i> (Treadwell 1941)		<i>Haminoea</i> sp.
	<i>Sigambra</i> sp. 1		Naticidae
Polynoidae	<i>Antinoana fusca</i> Hartman & Fauchald 1971		<i>Natica</i> sp. 1
	<i>Antinoella sarsi</i> (Malmgren 1865)		Retusidae
Sabellidae	<i>Euchone bansei</i> Ruff & Brown 1889		<i>Retusa obtusa</i> (Montagu 1807)
	<i>Euchone incolor</i> Hartman 1965		Rissoidae
	<i>Jasmineira cf. bermudensis</i> Hartman 1965		<i>Frigidoalvania brychia</i> (Verrill 1884)
Scalibregmatidae	<i>Pseudoscalibregma parvum</i> (Hansen 1878)		<i>Onoba pelagica</i> (Stimson 1851)
	<i>Scalibregma inflatum</i> Rathke 1843		<i>Pusillina harpa</i> (Verrill 1880)
Sphaerodoridae	<i>Sphaerodoropsis</i> sp. 1		Trochidae
Spionidae	<i>Aurospio dibranchiata</i> Maciolek 1981		Trochidae sp. 1
	<i>Laonice</i> sp.		Family unassigned
	<i>Prionospio aluta</i> Maciolek 1985		Opisthobranchia sp. 1
	<i>Prionospio fauchaldi</i> Maciolek 1985		Turridae
	<i>Prionospio</i> sp. 1, 8, 17		<i>Oenopota ovalis</i> (Friele 1877)
	<i>Spiophanes kroeyeri</i> Grube 1860		<i>Oenopota scalaris</i> Möller 1842
	<i>Spiophanes</i> sp. 3, 5		<i>Taraxis moerchi</i> (Malm 1861)
Syllidae	<i>Braniella pupa</i> Hartman 1965	Bivalvia	Cuspidariidae
	<i>Exogone</i> sp. 4		<i>Cuspidaria parva</i> Verrill & Bush 1898
	<i>Parapionosyllis</i> sp. 1		<i>Cuspidaria subtorta</i> (Sars 1878)
	<i>Sphaerosyllis</i> sp. 1		<i>Halonympha atlanta</i> Allen & Morgan 1981
	<i>Syllis</i> sp. 1		Kelliellidae
Terebellidae	<i>Amaeana trilobata</i> (Sars 1863)		<i>Kelliella laevis</i> Verrill 1885
	<i>Anacama globosa</i> Hartman & Fauchald 1971		<i>Kelliella nitida</i> Verrill 1885
	? <i>Scionides</i> sp.		Malletidae
	<i>Pista cf. estevanica</i> (Berkeley & Berkeley 1942)		<i>Neilonella subovata</i> (Verrill & Bush 1897)
	<i>Polycirrus</i> sp. 3		<i>Neilonella</i> sp. A
	<i>Streblosoma</i> sp. 1		Montacutidae
	Terebellidae sp. 10		<i>Montacuta tumidula</i> Dall 1899
Trichobranchidae	<i>Terebellides</i> sp. 1, 4, 5, 6		Nuculanidae
	Trichobranchidae sp. 5		<i>Ledella sandersi</i> Filatova & Shileyko 1984
	<i>Trichobranchus cf. roseus</i> (Malm 1864)		<i>Nuculana bushiana</i> (Verrill 1884)
Oligochaeta			<i>Nuculoma granulosa</i> (Verrill 1884)
Tubificidae	<i>Limnodriloides medioporus</i> Cook 1969		<i>Nuculoma similis</i> Allen 1992
	<i>Tubificoides intermedius</i> (Cook 1969)		<i>Yoldiella frigida</i> (Torell 1859)
	<i>Tubificoides</i> sp. A, B		<i>Yoldiella obesa obesa</i> Stimpson
			Nuculidae
			<i>Deminucula atacellana</i> (Schenck 1939)
			Semelidae
			<i>Semele</i> sp. 1
			Solemycidae
			<i>Solemya</i> sp. 1
			Spinulidae
			<i>Spinula</i> sp.

Table 7-1 (Continued)

Thyasiridae	
<i>Thyasira brevis</i> (Verrill & Bush 1898)	
<i>Thyasira equalis</i> (Verrill & Bush 1898)	
<i>Thyasira insignis</i> (Verrill & Bush 1898)	
<i>Thyasira obsoleta</i> (Verrill & Bush 1898)	
<i>Thyasira pygmaea</i> (Verrill & Bush 1898)	
<i>Thyasira subovata subovata</i> (Jeffreys 1881)	
Verticordidae	
<i>Polycardia densicostata</i> Locard 1898	
<i>Polycardia laevis</i> Allen & Turner 1974	
<i>Verticordia</i> sp. A	
Scaphopoda	
<i>Antalis occidentale</i> Linné 1758	
<i>Cadulus (Gadila) rushii</i> Pilsbry & Sharp 1898	
Dentalida sp.	
Gadilida sp.	
cf. <i>Pulsellum</i> sp.	
Aplacophora	
Chaetodermatidae	
<i>Chaetoderma</i> sp. 1	
<i>Falcidens caudatus</i> (Heath 1918)	
<i>Falcidens</i> sp. 1	
<i>Lepidoderma acutargatus</i> Salvini-Plaven 1992	
Dondersiidae	
Dondersiidae sp. 1, 2	
Lepidomeniidae	
<i>Wirenia</i> sp. 1, 2	
Pararrhopalidae	
Pararrhopalidae sp. 1	
Prochaetodermatidae	
<i>Prochaetoderma yongei</i> Scheltema 1985	
Family unassigned	
Pholidoskepia sp. 1, 2, 3	
ARTHROPODA	
Cumacea	
Bodotriidae	
<i>Cyclaspis</i> sp. 1, 2	
Leuconidae	
<i>Eudorella</i> cf. <i>pusilla</i> Sars 1871	
Diasylidae	
<i>Makrokylindrus</i> sp. 5	
Nannastracidae	
<i>Campylaspis</i> sp. 8	
Isopoda	
Eurycopidae	
<i>Betamorpha fusiformis</i> (Barnard 1920)	
<i>Disconectes</i> sp. 1	
Eurycopidae sp. 1	
<i>Munnopsurus</i> sp. 1	
Gnathiidae	
<i>Gnathia</i> sp. 1	
Haploniscidae	
<i>Haploniscus</i> sp. 3	
Ilyarachnidae	
<i>Ilyarachna longicornis</i> (G.O. Sars 1864)	
Macrostylidae	
<i>Macrostylis</i> sp. 2	
Munnidae	
<i>Pleurogonum rubicundrum</i> Sars 1863	
<i>Pleurogonum</i> nr. <i>spinosisimum</i> (Sars 1865)	
	Nannoniscidae
	<i>Austroniscus</i> sp. 1
	<i>Nannoniscus</i> sp. 3
	<i>Regebellator</i> sp. 1
	Tanaidacea
	Anarthruridae
	<i>Akanthophoreus</i> sp. 4
	<i>Akanthophoreus</i> sp. 5
	<i>Leptognathia breviremus</i> (Lilljeborg 1864)
	<i>Leptognathia</i> sp. 31
	<i>Leptognathiella spinicauda</i> Bird&Holdich 1985
	<i>Paranarthrura</i> cf. <i>insignis</i> Hansen 1913
	<i>Scoloura</i> sp. 1
	Leptocheiliidae
	<i>Pseudoleptocheilia filum</i> Stimpson 1853
	Pseudotanaididae
	<i>Pseudotanais</i> nr. <i>forcipatus</i> Vanhöffen 1907
	Typhlotanaididae
	<i>Peraeospinosus</i> nr. <i>spinicaudata</i> Hansen 1913
	<i>Peraeospinosus</i> sp. 1
	Amphipoda
	Aoridae
	<i>Neohela</i> sp. 1
	Caprellidae
	<i>Caprella equilibria</i> Sars 1818
	Caprellidae n.gen. n.sp. 1
	Isaeidae
	Isaeidae sp. 1, 2
	<i>Photis</i> sp. 1
	Lysianassidae
	Lysianassidae sp. 22, 23
	Oedicerotidae
	<i>Bathymedon</i> sp. 8
	<i>Monoculodes</i> sp. 3, 5, 6
	Oedicerotidae sp. 9
	Phoxocephalidae
	<i>Harpinia clavicola</i> Wating 1981
	<i>Harpinia propinqua</i> G.O. Sars 1891
	<i>Harpinia</i> sp. 8
	Stenothoidae
	<i>Metopella angusta</i> Shoemaker 1949
	Stenothoidae sp. 3
	Mysidacea
	<i>Pseudomma</i> sp. 1
	ECHINODERMATA
	Echinoidea
	Echinoidea sp.
	Ophiuroidea
	Ophiuroidea juv. sp. 1, 2, 3, 4, 5, 6, 7
	Holothuroidea
	Apoda sp. 1
	Elasipoda sp. 1
	<i>Myriothrochus</i> sp. 1
	Holothurian, spiny, white
	Holothurian, spiny, not white
	<i>Molpadia</i> nr. <i>amorpha</i> H.L. Clark 1930
	<i>Molpadia?</i> sp. 2
	Synaptidae sp.
	HEMICHORDATA
	Enteropneusta sp. 1, 6

Table 7-2. Community parameters for benthic infaunal samples from the Cape Hatteras Survey.

Stat.	Depth	Num. Spp.	Num. Ind. (m ²)	Spp./100 Ind.	Spp./250 Ind.	Spp./500 Ind.	Spp./750 Ind.	Spp./1000 Ind.	Spp./1500 Ind.	Spp./2000 Ind.	Spp./2500 Ind.	Spp./3000 Ind.	Spp./4000 Ind.	H'	J'
1	804	114	29,144	34.2	52.7	69.7	80.8	88.9	100.8	109.4	*	*	*	4.92	0.72
1A	800	74	17,288	25.0	39.6	53.4	62.0	68.1	*	*	*	*	*	3.76	0.61
2	600	39	22,788	10.4	15.0	22.4	26.9	30.4	35.3	38.8	*	*	*	2.14	0.40
3	812	41	35,178	11.4	16.7	22.3	26.1	29.0	33.2	36.2	38.6	40.5	*	2.56	0.48
5	1501	85	17,733	28.9	45.5	60.3	69.1	75.3	84.4	*	*	*	*	4.39	0.68
11	815	54	50,300	12.3	18.6	24.9	29.0	32.3	37.2	41.0	44.3	47.2	52.1	2.68	0.47
18	530	56	89,556	11.4	16.3	21.2	24.6	27.3	31.3	34.6	37.4	39.9	44.3	2.13	0.37
19	812	62	34,844	19.2	27.8	35.7	40.9	44.8	50.6	55.1	58.9	*	*	3.46	0.58
21	1410	36	10,456	11.8	19.6	27.7	33.1	*	*	*	*	*	*	2.31	0.45
26	800	52	50,167	10.3	15.3	21.0	25.1	28.4	33.5	37.6	41.2	44.3	49.7	2.22	0.39
34	775	65	24,122	19.7	31.1	41.5	48.2	53.1	60.2	64.9	*	*	*	3.10	0.52
41	590	53	39,856	11.6	18.4	25.5	30.4	34.3	40.1	44.4	47.8	50.6	*	1.98	0.34
42	785	64	15,522	21.2	32.5	43.5	51.4	57.6	*	*	*	*	*	3.58	0.60
44	1535	88	11,467	32.4	50.4	67.2	78.6	87.6	*	*	*	*	*	4.34	0.67
SA-9	620	62	38,611	13.9	22.1	30.9	36.9	41.5	48.4	53.5	57.7	61.3	*	2.64	0.44
SA-10	2003	68	8,467	27.1	43.1	58.1	67.9	*	*	*	*	*	*	4.26	0.70

* Denotes samples that were too small to calculate this value.

59

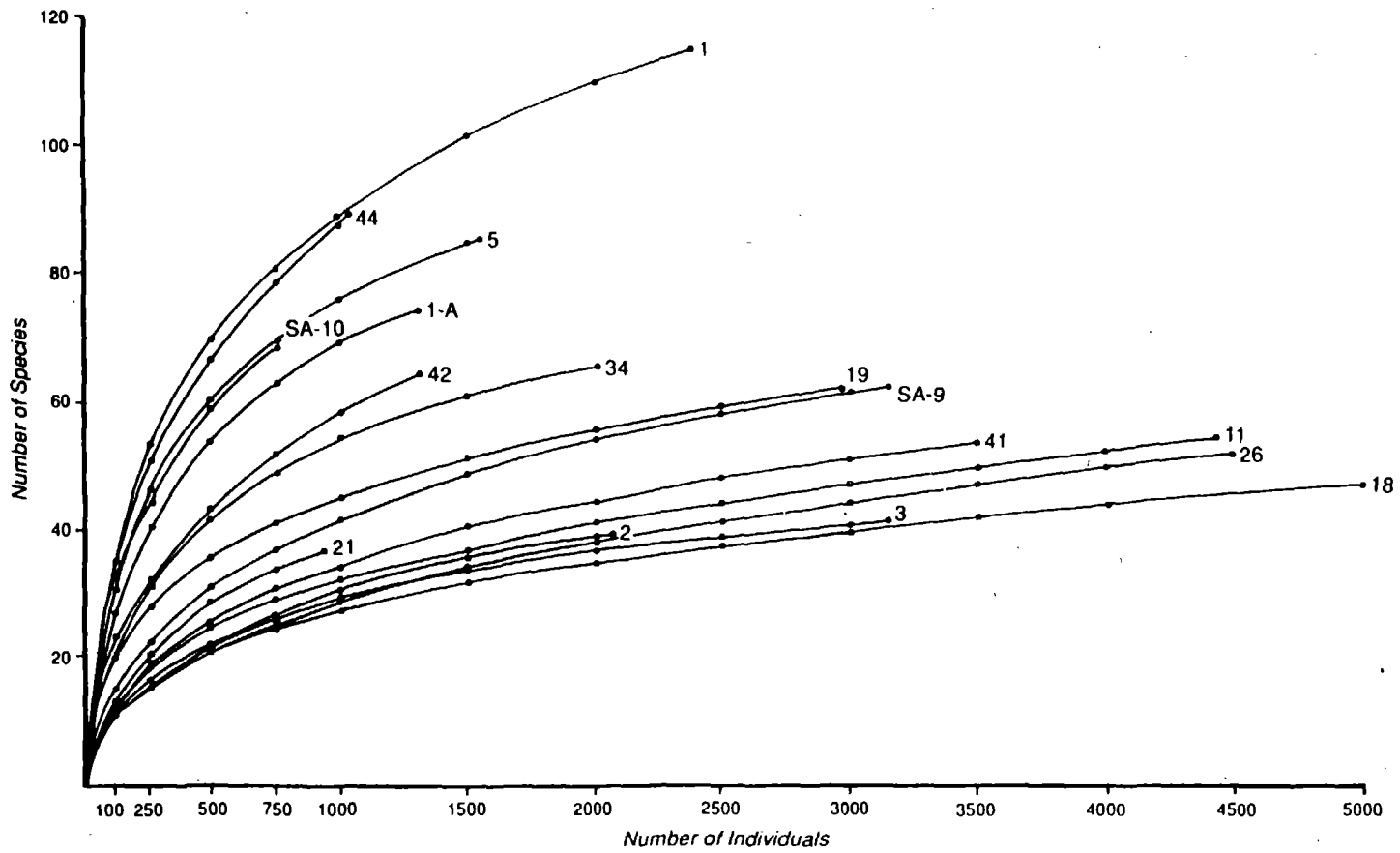


Figure 7-2. Hurlbert rarefaction curves for 16 stations sampled off Cape Hatteras in 1992.

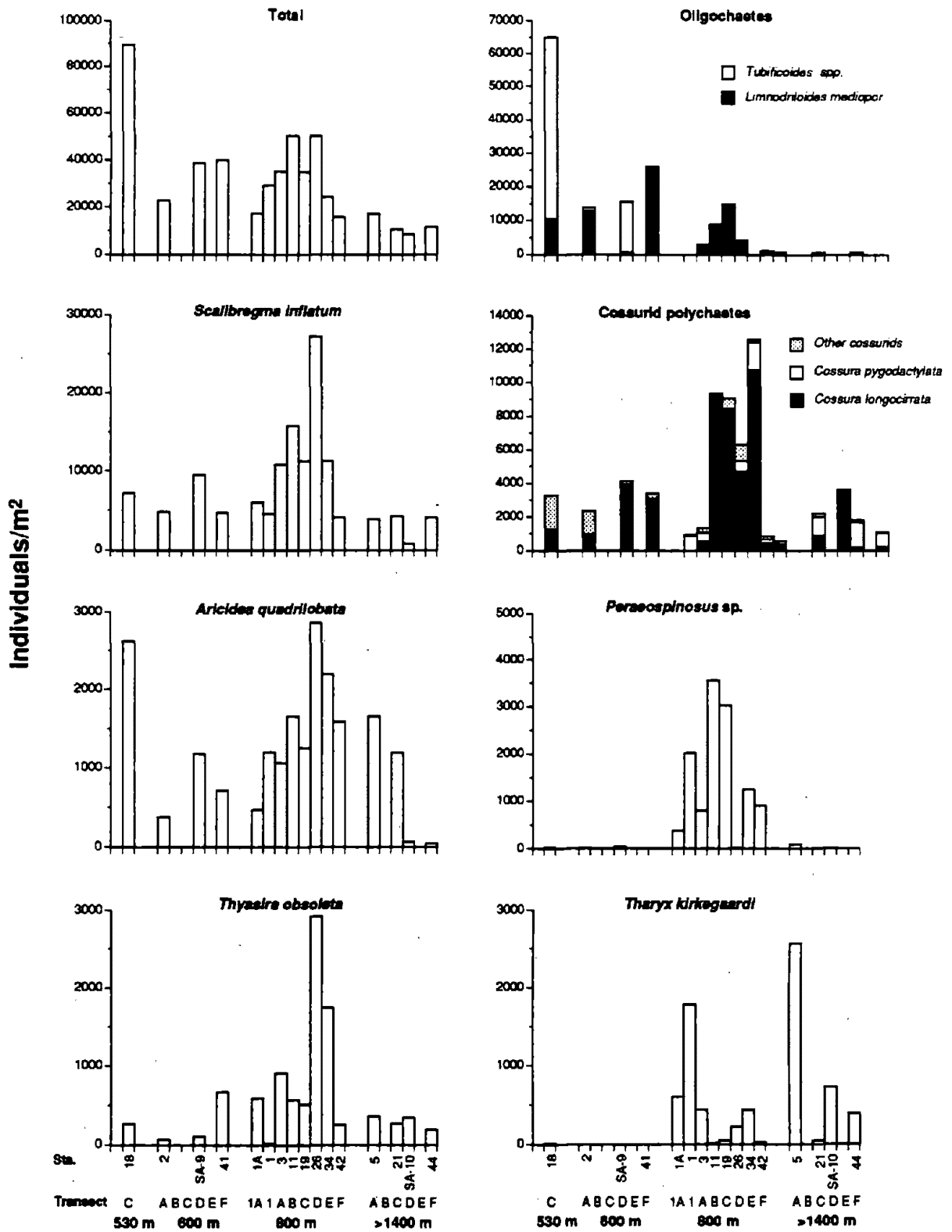


Figure 7-3. Density of benthic infauna at 16 stations sampled off Cape Hatteras in 1992. Bar graphs are for total fauna and selected species or groups of species. Stations are grouped by transect and depth intervals.

variable, ranging from 15,522 to 50,300 individuals m^{-2} . Average densities were nearly identical among the 600-m ($\bar{x}=33,752$, $SE=5,500$ individuals m^{-2}) and 800-m ($\bar{x}=32,070$, $SE=4,705$ individuals m^{-2}) stations. Stations in the 1,400- to 1,500-m depth ranges were lower, ranging from 10,522 to 17,033 individuals m^{-2} ($\bar{x}=13,219$, $SE=2,279$), and Station SA-10 at a depth of 2003 m had the lowest density at 8,522 individuals m^{-2} .

Densities of most dominant species were patchy. For example, the densities of the oligochaetes *Limnodriloides medioporus* and *Tubificoides* spp. are shown in Figure 7-3. High densities of *L. medioporus* were apparent at Stations 18 and SA-9, but were very rare elsewhere, whereas *Tubificoides* spp. were abundant at seven stations. The single most abundant polychaete was *Scalibregma inflatum*. This species had a high density of 27,222 individuals m^{-2} at Station 26. Overall, *S. inflatum* may be the least patchily distributed of the dominant taxa and was well most abundant along the 800-m isobath, but was well represented at all stations except SA-10. *Cossura longocirrata* was by far the most abundant of the cossurid polychaetes. This species was most abundant along the 800-m isobath, but was important at most other stations as well. *Cossura pygodactylata*, the second most important cossurid, was largely restricted to depths greater than the 800-m isobath. Two less common cossurid species, *Cossurella* sp. 1 and *C. brunnea*, were patchily distributed. *Aricidea quadrilobata* was the most abundant paraonid polychaete found in the study area and occurred in moderate densities at all stations except for the two deepest stations. The small cirratulid polychaete, *Tharyx kirkegaardi*, was patchily distributed throughout the study area and occurred in high density at all depths below about 775 m, including Station SA-10, the deepest station sampled. Other common species having patchy densities included the bivalve *Thyasira obsoleta* and the tanaidacean *Peraeospinosus* sp. 1. The latter species was largely restricted to the stations along the 800-m isobath.

Dominant Species and Distributional Patterns

The overall most important species, contributing 26% of the infauna of all 16 stations combined, was *Scalibregma inflatum*. This species accounted for 12 to 55% of the identified fauna at 13 of the 16 stations analyzed. *S. inflatum* appeared among the 10 most abundant species at all stations and occurred in relatively low numbers only at Stations 18 and 41 (dominated by oligochaetes) and the 2,000-m Station SA-10. Two oligochaetes, *Limnodriloides medioporus* and *Tubificoides intermedius*, were the second and third most important species, contributing 14 to 17% of the fauna of all 16 stations combined. *Limnodriloides medioporus* contributed at least 10% of the identified fauna at six stations and was the sole dominant at Station 41 (67%), whereas *Tubificoides intermedius* occurred in comparable numbers at only two stations (18 and SA-9), contributing 63% of the identified fauna at Station 18. The polychaete *Cossura longocirrata* was the fourth most important species, contributing 10% to the identified fauna of all stations combined and between 11 and 35% to the fauna of six stations, usually ranking second after *Scalibregma inflatum* (Tables 7-3 to 7-5).

When the individual stations are analyzed, a clear depth zonation appears with respect to the distribution of top ranking species. At the four upper slope stations located at depths of 530 to 620 m, the oligochaetes *Limnodriloides medioporus* (Stations 2, 41) and *Tubificoides intermedius* (Stations 18, SA-9) were the highest ranked species, while *S. inflatum* ranked either second or third. At all stations between 800 and 1500 m, *Scalibregma inflatum* was the top ranking species. *Cossura pygodactylata* was the highest ranked species at the deepest Station SA-10. The 10 most abundant taxa represent from 64 to 97% of the total fauna, and at eight of the stations these represent more than 93% (Tables 7-3 to 7-5). Such heavy contribution by just a few species, ranging across most of the depth range from 530 to 1,500 m, is atypical for deep-sea environments, but is typical for the benthic assemblages off Cape Hatteras.

Three groups of stations can be distinguished that differ slightly in the importance of individual species to total density. Stations 1A, 18, 34, 41, and 44 are clearly dominated by a single species (*S. inflatum* or one of the two dominant oligochaete species) that alone contributes between 37 and 67% of all individuals. A second group of stations (1, 2, 5, 26, and SA-10) is characterized by the dominance of two species. Except for SA-10, these dominant species are *S. inflatum* and either *Limnodriloides medioporus*, *Tharyx kirkegaardi*, or

Table 7-3. Dominant taxa and their contribution to the total fauna at stations along the 530 to 620-m isobaths. Density is individuals m⁻².

Station 2 (600 m)			Station 18 (530 m)		
Species	Percent	Density	Species	Percent	Density
<i>Limnodriloides medioporus</i>	56.31	12833	<i>Tubificoides intermedius</i>	60.81	54456
<i>Scalibregma inflatum</i>	21.21	4833	<i>Limnodriloides medioporus</i>	11.79	10556
<i>Cossurella</i> sp. 1	5.95	1356	<i>Scalibregma inflatum</i>	8.08	7233
<i>Tubificoides intermedius</i>	4.88	1111	<i>Leitoscoloplos</i> nr. <i>acutus</i>	3.86	3456
<i>Cossura longocirrata</i>	3.85	878	<i>Aricidea quadrilobata</i>	2.93	2622
<i>Aricidea quadrilobata</i>	1.66	378	<i>Cossura brunnea</i>	2.27	2033
<i>Priapulid</i> <i>caudatus</i>	0.98	222	Lumbrineridae spp.	1.55	1389
Lumbrineridae spp.	0.49	111	<i>Cossura longocirrata</i>	1.43	1278
<i>Terebellides</i> sp. 4	0.39	89	<i>Megayoldia thraciaeformis</i>	0.97	867
<i>Cossura pygodactylata</i>	0.39	89	<i>Pleurogonium rubicundrum</i>	0.82	733
<i>Thyasira obsoleta</i>	0.29	67	<i>Ophelina aulogastrella</i>	0.69	622
Cumulative Total	96.40	21967		95.19	85245
Total Density		22788			89556

Station SA-9 (620 m)			Station 41 (590 m)		
Species	Percent	Density	Species	Percent	Density
<i>Tubificoides intermedius</i>	38.49	14867	<i>Limnodriloides medioporus</i>	65.32	26033
<i>Scalibregma inflatum</i>	24.63	9511	<i>Scalibregma inflatum</i>	11.82	4711
<i>Cossura longocirrata</i>	10.04	3878	<i>Cossura longocirrata</i>	7.86	3133
<i>Terebellides</i> spp.	8.57	3311	<i>Ophelina aulogastrella</i>	2.23	889
<i>Aricidea quadrilobata</i>	3.05	1178	<i>Aricidea quadrilobata</i>	1.78	711
<i>Pleurogonium rubicundrum</i>	2.42	933	<i>Thyasira obsoleta</i>	1.67	667
<i>Limnodriloides medioporus</i>	1.93	744	Lumbrineridae spp.	1.37	544
<i>Chaetozone</i> sp. 11	1.50	578	<i>Cossura brunnea</i>	0.67	267
Lumbrineridae spp.	1.01	389	<i>Parougia caeca</i>	0.61	244
<i>Ophryotrocha maciolekae</i>	0.66	256	Sipuncula spp.	0.61	244
<i>Terebellides</i> sp. 6	0.49	189	<i>Gadilida</i> sp.	0.53	211
Hydrozoa sp. 1	0.49	189	<i>Pleurogonium rubicundrum</i>	0.50	200
Cumulative Total	93.27	36023		94.98	37854
Total Density		38622			39856

Table 7-4. Dominant taxa and their contribution to the total fauna at eight stations along the 800-m isobath. Density is individuals m⁻².

Station 1A (800 m)			Station 1 (804 m)		
Species	Percent	Density	Species	Percent	Density
<i>Scalibregma inflatum</i>	34.96	6044	<i>Scalibregma inflatum</i>	15.59	4544
<i>Ophryotrocha labidion</i>	6.81	1178	<i>Limnodriloides medioporus</i>	9.68	2822
Priapulida spp.	6.75	1167	<i>Peraeospinosus</i> sp. 1	6.94	2022
<i>Cossura pygodactylata</i>	5.21	900	<i>Tharyx kirkegaardi</i>	6.10	1778
<i>Ceratocephale</i> nr. <i>abyssorum</i>	4.63	800	<i>Aricidea quadrilobata</i>	4.12	1200
<i>Tharyx kirkegaardi</i>	3.47	600	<i>Leptognathia breviremus</i>	4.00	1167
<i>Thyasira obsoleta</i>	3.41	589	<i>Leptognathiella spinicauda</i>	4.00	1167
<i>Onoba pelagica</i>	3.34	578	Lumbrineridae spp.	3.47	1011
<i>Terebellides</i> spp.	3.21	556	<i>Exogone</i> sp. 4	3.28	956
Lumbrineridae spp.	3.15	544	<i>Nephasoma diaphanes</i>	1.98	578
<i>Aricidea quadrilobata</i>	2.70	467	<i>Ceratocephale</i> nr. <i>abyssorum</i>	1.91	556
<i>Peraeospinosus</i> sp. 1	2.19	378			
<i>Paramphinome jeffreysi</i>	2.19	378			
Cumulative Total	82.02	14178		61.08	17800
Total Density		17288			29144
Station 3 (812 m)			Station 11 (815 m)		
Species	Percent	Density	Species	Percent	Density
<i>Scalibregma inflatum</i>	30.76	10822	<i>Scalibregma inflatum</i>	31.52	15856
<i>Cossura longocirrata</i>	26.53	9333	<i>Limnodriloides medioporus</i>	29.31	14744
<i>Limnodriloides medioporus</i>	25.71	9044	<i>Cossura longocirrata</i>	16.59	8344
<i>Aricidea quadrilobata</i>	3.03	1067	<i>Peraeospinosus</i> sp. 1	7.07	3556
<i>Thyasira obsoleta</i>	2.56	900	<i>Aricidea quadrilobata</i>	3.29	1656
<i>Peraeospinosus</i> sp. 1	2.27	800	<i>Pleurogonium rubicundrum</i>	1.55	778
<i>Pleurogonium rubicundrum</i>	2.21	778	Nemertea spp.	1.33	667
<i>Tharyx kirkegaardi</i>	1.26	444	<i>Cossura brunnea</i>	1.21	611
<i>Ceratocephale</i> nr. <i>abyssorum</i>	0.57	200	<i>Thyasira obsoleta</i>	1.13	567
<i>Terebellides</i> spp.	0.51	178	<i>Praxillella</i> sp. 1	0.60	300
Nemertea spp.	0.44	156	<i>Parougia caeca</i>	0.57	289
<i>Chaetozone</i> sp. 11	0.38	133			
Cumulative Total	96.24	33856		94.17	47367
Total Density		35178			50300

Table 7-4. Continued.

Station 19 (812 m)			Station 26 (800 m)		
Species	Percent	Density	Species	Percent	Density
<i>Scalibregma inflatum</i>	32.43	11300	<i>Scalibregma inflatum</i>	54.26	27222
<i>Cossura longocirrata</i>	13.58	4733	<i>Cossura longocirrata</i>	21.40	10733
<i>Limnodriloides medioporus</i>	12.28	4278	<i>Thyasira obsoleta</i>	5.83	2922
<i>Peraeospinosus</i> sp. 1	8.71	3033	<i>Aricidea quadrilobata</i>	5.69	2856
<i>Aricidea quadrilobata</i>	3.60	1256	Hydrozoa sp. 1	4.03	2022
<i>Pleurogonium</i> nr. <i>spinosissimum</i>	3.13	1089	<i>Cossura pygodactylata</i>	3.39	1700
<i>Cossura brunnea</i>	2.84	988	<i>Capitella capitata</i> complex	0.53	267
<i>Harpinia propinqua</i>	2.39	833	<i>Chaetozona</i> sp. 11	0.51	256
Nemertea spp.	2.17	756	<i>Tharyx kirkegaardi</i>	0.44	222
<i>Cossura pygodactylata</i>	1.75	611	<i>Cossura brunnea</i>	0.33	167
<i>Levinsenia</i> sp. 1	1.50	522			
Cumulative Total	84.38	29400		96.41	48367
Total Density		34844			50167
Station 34 (775 m)			Station 42 (785 m)		
Species	Percent	Density	Species	Percent	Density
<i>Scalibregma inflatum</i>	46.75	11278	<i>Scalibregma inflatum</i>	26.13	4056
<i>Aricidea quadrilobata</i>	9.07	2189	<i>Pseudotanais</i> nr. <i>forcipatus</i>	23.55	3656
<i>Thyasira obsoleta</i>	7.23	1744	<i>Aricidea quadrilobata</i>	10.24	1589
<i>Peraeospinosus</i> sp. 1	5.20	1256	<i>Peraeospinosus</i> sp. 1	5.87	911
<i>Limnodriloides medioporus</i>	4.84	1167	<i>Limnodriloides medioporus</i>	4.80	744
<i>Terebellides</i> spp.	3.22	778	<i>Terebellides</i> spp.	3.51	544
<i>Cossura longocirrata</i>	2.12	511	<i>Harpinia propinqua</i>	2.86	444
<i>Tharyx kirkegaardi</i>	1.84	444	<i>Cossura longocirrata</i>	2.43	378
Nemertea spp.	1.75	422	<i>Thyasira obsoleta</i>	1.65	256
Lumbrineridae spp.	1.43	344	<i>Pleurogonium rubicundrum</i>	1.43	222
<i>Harpinia propinqua</i>	1.20	289	<i>Leptognathia breviremus</i>	1.22	189
<i>Renusa obtusa</i>	1.15	278	<i>Levinsenia</i> sp. 1	1.22	189
Nemertea sp. C	0.97	233			
Cumulative Total	86.78	20933		84.90	13178
Total Density		24122			15522

Table 7-5. Dominant taxa and their contribution to the total fauna at each station along the 1,410 to 2,003-m isobaths. Density is individuals m⁻².

Station 21 (1410 m)			Station 5 (1500 m)		
Species	Percent	Density	Species	Percent	Density
<i>Scalibregma inflatum</i>	40.81	4267	<i>Scalibregma inflatum</i>	21.74	3856
<i>Cossura longocirrata</i>	34.75	3633	<i>Tharyx kirkegaardi</i>	14.47	2567
<i>Aricidea quadrilobata</i>	11.37	1189	<i>Aricidea quadrilobata</i>	9.34	1656
<i>Thyasira obsoleta</i>	2.55	267	<i>Cossura pygodactylata</i>	6.08	1078
<i>Capitella capitata</i> complex	1.49	156	<i>Cossura longocirrata</i>	5.08	900
<i>Caprella equilibria</i>	0.74	78	<i>Falcidens caudatus</i>	3.95	700
<i>Ophelina cylindricaudata</i>	0.74	78	<i>Thyasira equalis</i>	3.45	611
Lumbrineridae spp.	0.74	78	<i>Myriotrochus</i> sp. 1	3.26	578
<i>Paramphinome jeffreysi</i>	0.64	67	<i>Tubificoides</i> sp. A	2.88	511
<i>Myriotrochus</i> sp. 1	0.53	56	<i>Macrostylis</i> sp. 2	2.19	389
<i>Ceratocephale</i> nr. <i>abyssorum</i>	0.53	56			
<i>Nemertea</i> sp. D	0.53	56			
Cumulative Total	95.43	9978		72.43	12844
Total Density		10456			17733

Station 44 (1535 m)			Station SA-10 (2003 m)		
Species	Percent	Density	Species	Percent	Density
<i>Scalibregma inflatum</i>	35.76	4100	<i>Cossura pygodactylata</i>	17.59	1489
<i>Cossura pygodactylata</i>	6.98	800	Terebellidae sp. 10	17.06	1444
<i>Barantolla</i> sp. 3	4.07	467	<i>Tubificoides</i> sp. A	9.32	789
<i>Harpinia propinqua</i>	3.78	433	<i>Scalibregma inflatum</i>	9.19	778
<i>Tharyx kirkegaardi</i>	3.39	389	<i>Tharyx kirkegaardi</i>	8.53	722
<i>Paradoneis tyra</i>	3.00	344	<i>Thyasira obsoleta</i>	4.07	344
<i>Scoloura</i> sp. 1	2.81	322	<i>Pseudoscalibregma parvum</i>	3.67	311
<i>Paramphinome jeffreysi</i>	2.23	256	<i>Thyasira subovata subovata</i>	3.02	256
<i>Ceratocephale</i> nr. <i>abyssorum</i>	2.13	244	<i>Cossura longocirrata</i>	2.10	178
<i>Ceratocephale loveni</i>	1.94	222	<i>Amatea trilobata</i>	1.97	167
Cumulative Total	66.09	7578		76.51	6478
Total Density		11467			8467

one of the cossurid polychaetes. The 2,000-m Station SA-10 is dominated by a different cossurid and a terebellid polychaete. The remaining six stations (3, 11, 19, 21, 42, and SA-9) are dominated by three species, mostly *S. inflatum*, one of the two oligochaete species, and *C. longocirrata*. Stations 42 and SA-9 differ somewhat from the other four stations in this group because of *Aricidea quadrilobata* occupying rank 3 at both stations and *Pseudotanais* nr. *forcipatus* ranking second at Station 42.

In addition to the contribution made by the dominant polychaetes and oligochaetes just described, several less abundant taxa appear at various stations. For example, the polychaete *Ophryotrocha labidion* and numerous juvenile priapulids are present at Station 1A; the polychaete *Exogone* sp. 4, the sipunculan *Nephasoma diaphanes*, and the tanaidaceans *Leptognatha breviremus* and *Leptognathiella spinicauda* at Station 1; the aplacophoran *Falcidens caudatus*, the holothurian *Myriotrochus* sp. 1, the oligochaete *Tubificoides* sp. A, and the isopod *Macrostylis* sp. 2 at Station 5; the polychaete *Praxillella* sp. 1 at Station 11; two crustaceans, the amphipod *Harpinia propinqua*, and the isopod *Pleurogonium* nr. *spiniosissimum* at Station 19; the polychaete *Leitoscoloplos* nr. *acutus* and the bivalve *Megayoldia thraciaeformis* at Station 18; the polychaete *Capitella capitata* complex, a species sometimes considered as an opportunist in stressed nearshore environments, and the amphipod *Caprella equilibria*, both at Station 21; Nemertea sp. C at Station 34; the polychaetes *Barantolla* sp. 3 and *Paradoneis lyra* and the tanaidacean *Scoloura* sp. 1 at Station 44; the polychaete *Pseudoscalibregma parvum*, a deep-sea species, ranked seventh at Station SA-10. All of these species exhibit a very patchy distribution (Appendix D) and are either rare or completely absent at most stations.

Two polychaetes, *Ceratocephale* nr. *abyssorum* and *Ancistrosyllis* nr. *groenlandica*, never occurred among the top 10 species, but were found at all but one station. Other widespread species with consistently low abundances include the gastropods *Cylichna alba* and *Retusa obtusa*, the polychaetes *Paramphinome jeffreysi*, *Praxillella gracilis*, and *Ophelina aulogastrilla*, and the nemerteans *Nemertea* sp. A and *Nemertea* sp. B.

Community Pattern Analysis

Two classification techniques were employed to examine infaunal community structure (Figure 7-4): the Bray-Curtis index which is heavily influenced by dominant species (Boesch 1977), and the Normalized Estimated Species Similarity (NESS) index which takes rarer species into account (Grassle and Smith 1976). The data used for the Bray-Curtis analysis was square root transformed prior to analysis, and NESS was run at an *m* of 200 individuals. Clustering of both indices resulted in the formation of four groups of stations, with the cluster structure largely determined by depth. The first cluster consisted of the four shallow stations (530-620 m), the fourth cluster consisted of the three deep stations (> 1500 m), and the second and third clusters consisted of the 800 m stations and the 1,410 m station from Transect C. The major difference between the two indices is that two stations, 19 and 34, from the second cluster of the Bray-Curtis classification (Figure 7-4A) were in the third cluster of the NESS classification (Figure 7-4B). This shift is explained in terms of dominant and rare species because Bray-Curtis is biased toward dominant species and NESS is biased toward rare species when *m* is high. Dominant species at these two stations were similar to those at the stations in cluster 2, whereas the rarer species were more similar to those in the stations in cluster 3. Both classifications indicate that a faunal break occurs between the 800 m stations at the center and the extremes of the survey area. Classification analyses using only the 50 numerically dominant species resulted in a similar pattern, indicating that the community structure was largely determined by dominant species.

The polychaete *Scalibregma inflatum* ranked as one of the top four dominants at all of the stations. This polychaete was the most abundant species at all of the stations in cluster groups 2 and 3, and at two of the stations in cluster group 4, and was the second most abundant species at three of the stations in cluster group 1 (Table 7-6). Oligochaetes dominated the fauna at the shallow stations (cluster 1), with *Tubificoides intermedius* being the top ranked species at Stations 18 and 9 and *Limnodriloides medioporus* being the top ranked species at Stations 41 and 2. Infaunal densities were quite high at these stations, and diversity was relatively low. The polychaete *Cossura longocirrata* was the second or third most abundant species at the four stations in cluster 2 (3, 11, 26, 21). *L. medioporus* was among the top three species at two of these stations. The stations in cluster 2 were also characterized by variable infaunal densities and relatively low diversity. With the exception of *S. inflatum*, no single species ranked among the top five dominants at all of the stations in cluster 3 (42, 1A, 1).

Table 7-6. Rank of the seven most abundant species and community statistics by cluster group. Rare means species was not in top ten for the group.

Cluster Stations	1 2, 18, 41, SA9	2 3, 11, 21, 26	2 or 3 19, 34	3 1, 1A, 42	4 5, 44, SA10
<i>Scalibregma inflatum</i>	2 - 3	1	1	1	1 in 2 sta.
<i>Tubificoides intermedius</i>	1 in 2 sta.	absent	rare	rare	rare
<i>Limnodriloides medioporus</i>	1 in 2 sta.	2 - rare	3 - 5	2 in 1 sta.	rare
<i>Cossura longocirrata</i>	3 - 7	2 - 3	2 - 6	6 or rare	5 or rare
<i>Peraeospinosus</i> sp. 1	rare	4 or rare	4	3 - 8	rare
<i>Cossura pygodactylata</i>	rare	6 or rare	rare	3 or rare	1 - 4
<i>Tharyx kirkegaardi</i>	rare	rare	rare	4 or rare	2 - 5
Number of Species	39 - 62	41 - 54	62 - 65	64 - 114	68 - 88
Individuals m ² x 1000	23 - 90	10 - 50	24 - 35	16 - 29	8 - 18
Species per 750 Individuals	25 - 37	25 - 33	30 - 41	51 - 81	68 - 79

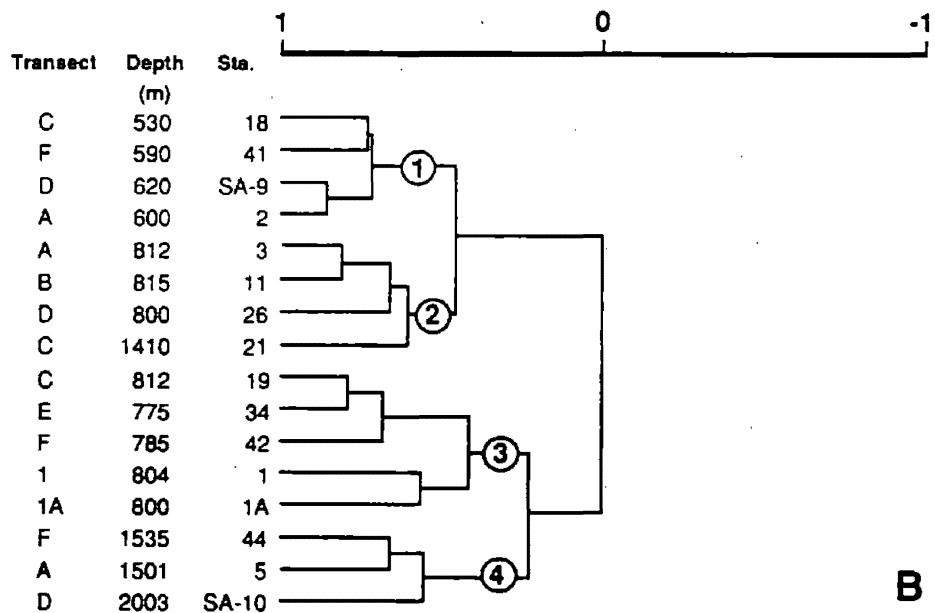
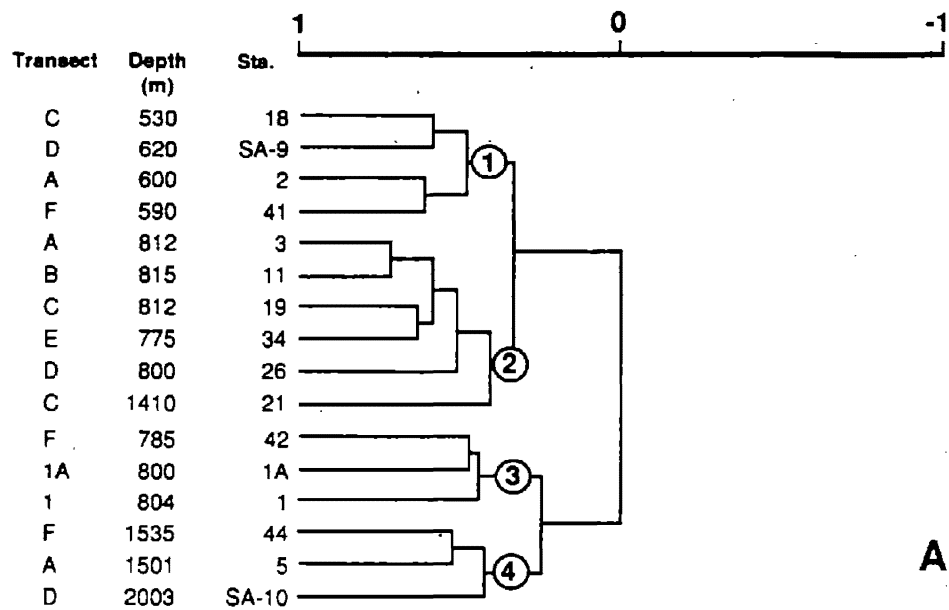


Figure 7-4. Dendrograms from analysis of 1992 stations off Cape Hatteras. A, Bray-Curtis, all species, with flexible sorting and square root transformation. B, NESS, all species at 200 individuals and flexible sorting.

Species richness was high at the stations in cluster 3, and faunal density was moderately low. Several species, particularly the tanaidacean *Peraeospinosus* sp. 1, appear to be responsible for the shift of Stations 19 and 34 from cluster 2 to cluster 3. In addition to *S. inflatum*, the deeper stations (cluster 4) were dominated by *Cossura pygodactylata* and *Tharyx kirkegaardi*. Diversity at these three stations was also high and the density was low.

The results of ordination analysis of the top 50 species at the 16 stations showed that the species most responsible for the separation of samples from the center of the ordination space usually occupy the extremes of the axes (Figure 7-5). The close grouping of the samples within the ordination space indicates that the 800 m stations are relatively homogeneous and suggests that there are no latitudinal differences in community structure within the survey area. The first axis represents the depth gradient, with the shallower stations (cluster 1) having low values and the deeper stations (cluster 4) having high values. The second axis further separates the deep stations, and the third axis further separates the 800-m stations. The two stations that shift between clusters 2 and 3 (19 and 34) have values that are intermediate to those of the stations in the two clusters. In contrast to classification, the ordination analysis indicates that the most pronounced faunal breaks occur between 530 and 590 m (Stations 18 and SA-9) and between 1,535 and 2,000 m (Stations 44 and SA-10).

Discussion

The benthic infauna on the continental slope off Cape Hatteras was discussed as part of a larger summary of the Carolina slope by Blake et al. (1987) and Blake and Grassle (unpublished). These authors indicated that more than 1,200 species of benthic invertebrates occurred in the sediments off the Carolinas in depths from approximately 600 to 3,500 m. The infauna from these deep-sea sediments is considered to be among the most diverse ever collected and serves to support recent estimates that the deep-sea benthos represents a vast reservoir of the earth's biodiversity (Grassle and Maciolek 1992). One of the conclusions arising from the studies of Blake et al. (1987) was that the continental slope off Cape Hatteras differed from other locations off the Carolinas in having faunal assemblages that were characterized by low species richness, low species diversity, and high infaunal density. The densities in fact were so high that they represented a situation more typical of shallow continental shelf locations such as the mud patch near Georges Bank (Neff et al. 1989).

As is typical of locations where infaunal density is high, a few species tend to predominate. At Stations SA-9 and SA-10 Blake et al. (1987) found that a consistent suite of species dominated over time. At 600-m Station SA-9, five annelid species and unidentified oligochaete juveniles represented 66.9% of the total number of individuals present. The dominant annelids at this station were *Cossura longocirrata*, *Scalibregma inflatum*, *Limnodriloides medioporus*, *Tubificoides intermedius*, and *Aricidea quadrilobata*. At the 2,000-m Station SA-10, two polychaete species, *Cossura longocirrata* and *Tharyx kirkegaardi*, and an amphipod, *Harpinia clivicola*, composed 43.2% of the fauna. The densities of some of these species were remarkably high for continental slope locations. Mean densities of *Cossura longocirrata* were 11,704 individuals m⁻² at Station SA-9, whereas *Scalibregma inflatum* was represented by 8,229 individuals m⁻². Although *C. longocirrata* reaches similar densities on the continental shelf (Maciolek-Blake et al. 1985), *S. inflatum* had never been observed previously in such high densities in any habitat. The 1992 data both support and modify the earlier conclusions regarding the benthic communities off Cape Hatteras. Infaunal densities in 1992, as in 1984-1985, were very high, and diversity and species richness were lower than expected for continental slope environments. The same species that were dominant at Station SA-9 in 1984-1985 were again present in the 600 to 800-m stations in the 1992 samples from a broader geographic area. Unlike the earlier studies, however, the most consistently abundant and dominant infaunal species was *S. inflatum*. The only important competitors to the dominance of *S. inflatum* were the oligochaetes *Limnodriloides medioporus* and *Tubificoides intermedius*, which were the highest ranked and most abundant species at the upper slope stations (530-620 m) where *S. inflatum* ranked second or third. *Scalibregma inflatum* was the overall dominant species at all nine of the middle slope stations (800-1,450 m). Densities of the dominant species were remarkably high for a continental slope environment. At Station 18, *T. intermedius* densities exceeded 54,000 individuals m⁻²; at Station 26, *S. inflatum* densities were 27,222 individuals m⁻². *Cossura longocirrata*, the dominant polychaete at Station SA-9 in 1984-1985, proved to have a patchy distribution in 1992, as did *Tharyx kirkegaardi*, another dominant species.

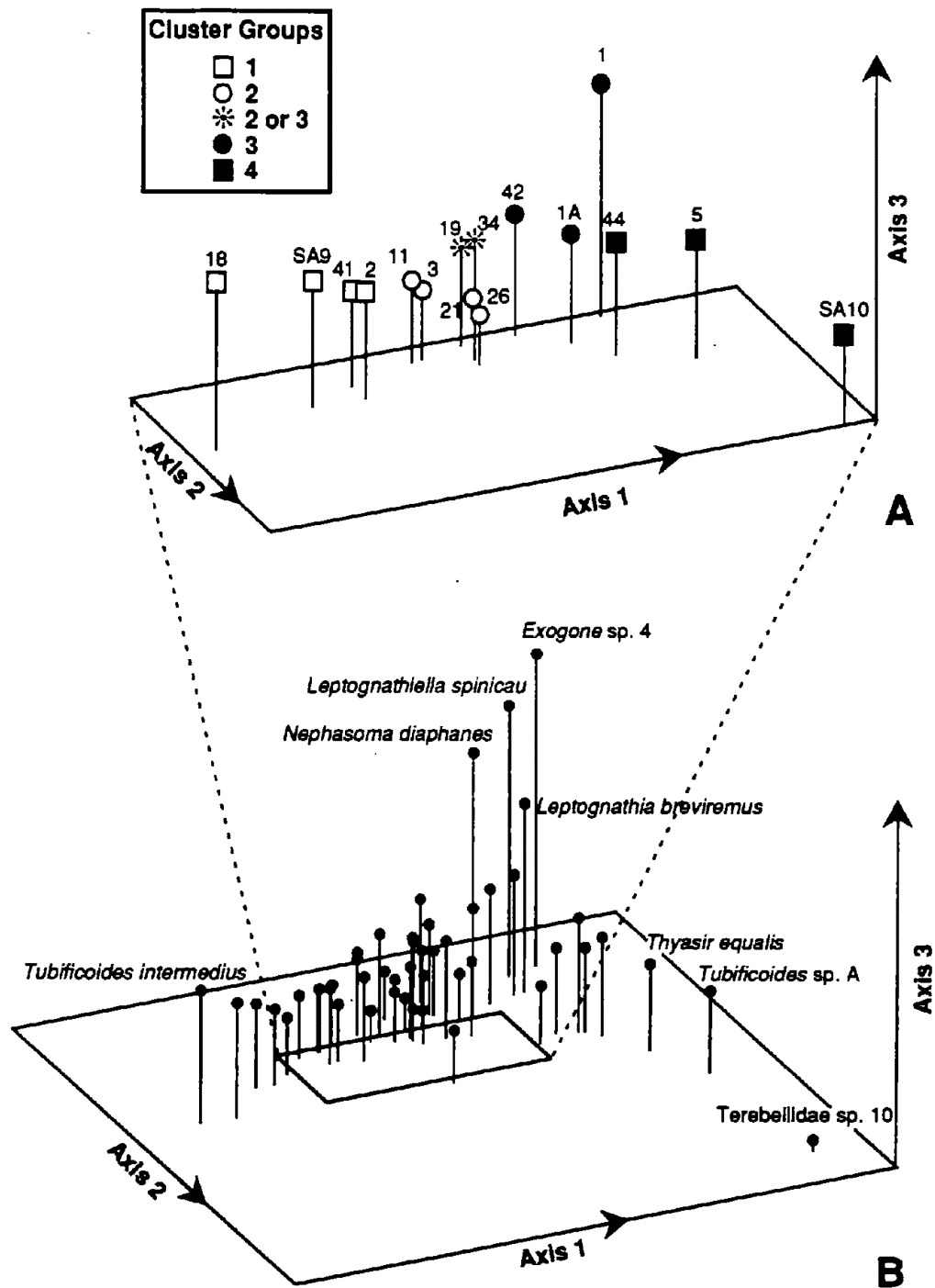


Figure 7-5. Results of reciprocal averaging ordination, first three axes, using the 50 most abundant species and square root transformation of densities. A, Ordination of stations. B, Ordination of species. Cluster group symbols refer to the station groups identified in Fig. 7-4A.

Thus, the dominance of *C. longocirrata* observed at Station SA-9 during 1984-1985 was not persistent. The species ranked third in the new sample taken from SA-9.

The results of the present study differ somewhat from that of Blake et al. (1987) in that Station SA-9 was largely dominated by *Cossura longocirrata* in 1984 and 1985. *Scalibregma inflatum* was dominant in the July 1984 samples, but *C. longocirrata* was the most abundant infaunal species in May 1985 and September 1985. These results suggest that the patterns of dominance among the very dense polychaetes and oligochaetes that characterize the sediments off Cape Hatteras may shift seasonally or year-to-year, possibly in response to variation in organic flux. Thus, the three replicates collected at Station SA-9 in September 1985, fully overlap the ranges of densities in the samples collected in August/September 1992. These results emphasize the caution that is needed in drawing conclusions from non-replicated data.

The best indicator species of the Cape Hatteras continental slope infauna is then *Scalibregma inflatum*, a moderately large, subsurface, deposit-feeding polychaete that obviously plays an important role in reworking sediments throughout the sediment column. During the box core processing, the species was observed to occur in the sediments from near the surface to depths of 15 cm or more. *Scalibregma inflatum* was either the first, second, or third ranked species at all stations between 530 and 1,410 m and was the only species to consistently exhibit such a dominance pattern.

The results of the cluster analysis support the observations that the benthic assemblages first observed at Station SA-9 in 1984-1985 are widely distributed on the continental slope off Cape Hatteras. The patterns observed in the distribution of the dominant oligochaetes in the upper slope and *Scalibregma inflatum* in the middle slope are also apparent in the cluster and ordination analysis. The four upper slope stations form a group that is distinct from the middle and lower slope stations. Similarly, Stations 5, 44, and SA-10, the deepest stations (1,500-2,000 m), form a group. The 800-m stations and Station 21 divide into two groups. One joins with the shallow stations and the other with the deep stations. Two stations, 19 and 34, switch between these 800 m groups according to whether the clustering strategy emphasizes rare or dominant species.

Thus, the *Scalibregma*-dominated infaunal communities off Cape Hatteras may be roughly divided into four assemblages: (1) an upper slope oligochaete/*Scalibregma*-dominated assemblage in depths of 530-620 m; (2) a middle slope *Scalibregma*-dominated assemblage in depths from 775 to 1,410 m; (3) a lower slope *Scalibregma/Tharyx/Aricidea/Cossura* assemblage at about 1,500 m; and (4) a lower slope *Cossura/Terebellid/oligochaete/Scalibregmatid/Tharyx*-dominated assemblage at 2,000 m.

The high density of infauna observed in 1984-1985 and again in 1992 in the continental slope sediments off Cape Hatteras has not been recorded elsewhere in the Western North Atlantic. The comprehensive census of continental slope benthos conducted as part of the ACSAR program included more than 550 box cores collected from slope depths of 550-3,000 m from the U.S./Canadian boundary to off South Carolina (Blake et al. 1985, 1987, Maciolek et al. 1987a,b). No other location on the U.S. Atlantic continental slope and rise had benthic communities with the same faunal assemblages, high densities, and low species diversities that were found in the Cape Hatteras sediments. Generally, densities tended to decrease with increasing depth in the 1992 samples, whereas species richness tended to increase with increasing depth; however, a clearly depth-related trend was obscured by the very high variability of both densities and species richness among the 800-m stations.

The high sedimentation rates for the slope off Cape Hatteras may account for dense faunal assemblages resident in the area. It is now believed that primary production on the shelf is enhanced by intrusion of Gulf Stream water (Blanton 1991). Walsh et al. (1985) estimate that about half of the total production deposited on the slope in the Mid-Atlantic Bight, is derived from the shelf. Carbon flux estimates within the study area are high and range from 28 to 121 g C m⁻² yr⁻¹. High inventories of organic carbon (1-2%) in the sediments provide the fuel to sustain the high infaunal populations.

The only other continental slope locality known to us where high inventories of organic matter, dense populations of benthic infaunal invertebrates, and active bioturbation by large subsurface deposit feeders co-exist is off San Francisco near the Farallon Islands (Blake et al. 1992, SAIC 1992). In contrast to the Cape Hatteras site, where carbon flux is largely derived from continental shelf material that is swept out over the slope, the northern California slope lies under an active upwelling zone and the sediments receive high annual inputs of phytoplankton that settles to the bottom. The chlorophyll *a* and phaeopigment concentrations that have been measured from these sediments are among the highest ever recorded in deep-sea sediments (Blake et al. 1992).

The benthic communities in northern California have very high infaunal densities in the middle slope (1,300-2,000 m), whereas off Cape Hatteras the densities are higher between 530 and 800 m. Upper slope sediments in the depth range of 600-800 m off California lie in an oxygen minimum zone and densities of infauna are sometimes reduced in the dysaerobic environment. The middle slope stations off northern California tend to have more species per sample and higher species diversity than off Cape Hatteras. In fact, the species richness and diversity values are sometimes as high as those found off Cape Lookout or Cape Fear (Blake et al. 1985, 1987).

The overall community structure off the Farallones is that of a typical deep-sea assemblage with the top ranking species contributing only a few percent (usually less than 10%) of the total fauna and the 10 most abundant species constituting about 40 to 70% of the total fauna. In contrast, the 10 most abundant species in benthic communities off Cape Hatteras may contribute from 64 to 97% of the total fauna (Tables 7-3 to 7-5).

The density of infauna does not appear to have changed from 1984-1985 to 1992. This is best illustrated in data from the 600-m isobath (Figure 7-6). By removing the shallow Station 18 at 530 m, and plotting Stations 2, 41, and SA9, the 600-m isobath is seen to have similar range in densities. The range of replicates in the historical data from Station SA-9 encompassed the range of the samples collected in 1992.

The dominant infaunal organisms on the slope off Cape Hatteras are a curious mixture of annelid worms known to be dominants on the continental shelf (*Aricidea quadrilobata*, *Cossura longocirrata*), components of continental slope assemblages (*Tharyx kirkegaardii*), and continental shelf species that have not previously been considered as dominant taxa (*Scalibregma inflatum*, *Limnodriloides medioporus*, and *Tubificoides intermedius*). Despite suggestions to the contrary (Schaff et al. 1992), none of the dominant polychaete species that occur in the Cape Hatteras sediments have been previously considered to be opportunists in the more classic sense of Pearson and Rosenberg (1978). The high input of carbon from the nearby continental shelf to an upper and middle slope environment appears to provide these species with a combination of factors conducive to the establishment of dense populations.

The presence of large, deep-burrowing maldanid polychaetes (*Praxillella* spp. and *Chirimia biceps*) and the very numerous scalibregmatid *Scalibregma inflatum* in all of the box cores suggests a transport mechanism for the movement of organic material from the surface to deeper sediment layers. Related species of *Praxillella* are known to be head-down feeders that are able to move surface flocculent material through their tubes to depth (Mangum 1964, Kudenov 1977, 1978). Viable diatom cultures (Chapter 4) were positive from 14 cm deep within the sediment. Surface photographs indicate that numerous openings of burrows were present (Chapter 5). Burrow densities of 1,000 or more per square meter were found at Stations SA-9, SA-10, 11, 42, and 44. The presence of so many burrows is further evidence that surface material can be actively transported deep into the sediments by deposit feeders.

Local episodes of rapid sedimentation or turbidity flow may also play a role in the ecology of benthic communities on the slope off Cape Hatteras. During the one year of monitoring at Stations SA-9 and SA-10 (1984-1985) off Cape Hatteras, the two sites retained a consistent community structure (Blake et al. 1987, Blake and Grassle unpublished). In the present study, six species among the dominants at SA-10 were not present in the earlier study. Although a single sample is insufficient to derive any definitive conclusions, these faunal changes draw further attention to a two-layered sedimentary structure seen in the x-ray from Station SA-10 which had turbidites in the upper 12-14 cm (Chapter 5). This result suggests that a rapid sedimentation event or flow had taken place at the station. Changes in the faunal composition further suggest that it might have taken place subsequent to November 1985 when the last ACSAR samples were collected.

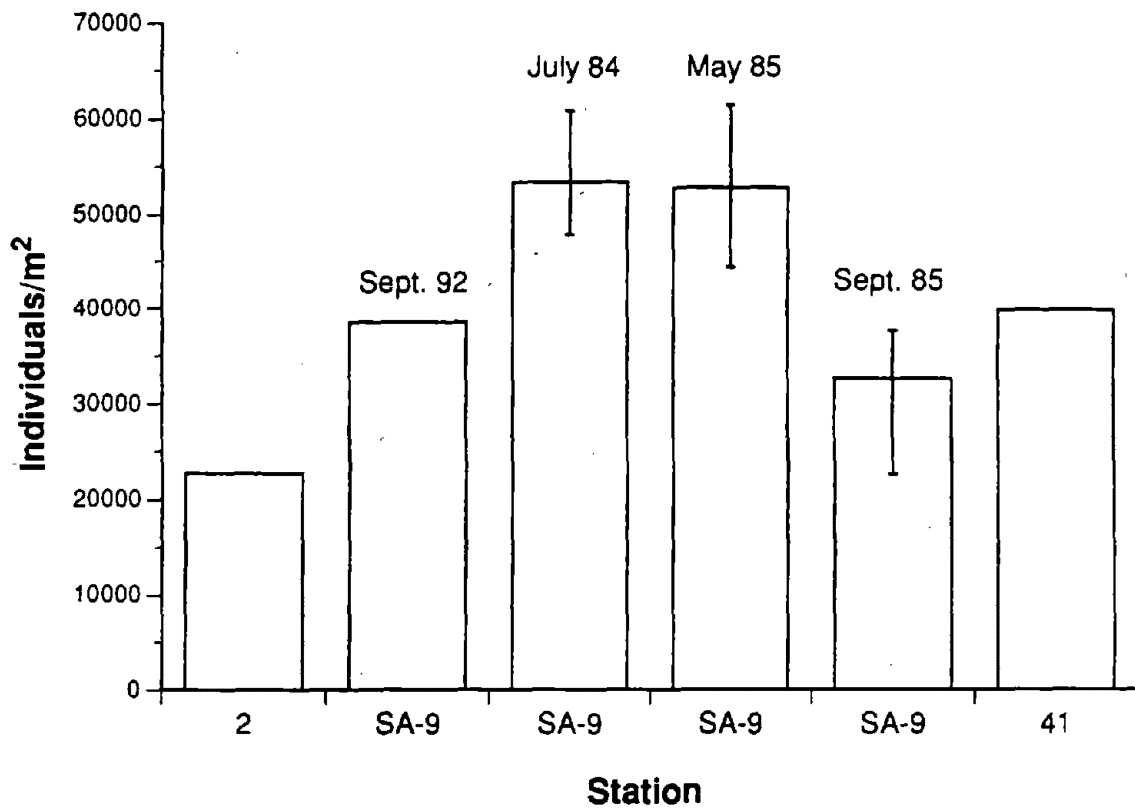


Figure 7-6. Density of benthic infauna from stations along the 600-m isobath. Historical SA-9 samples are the mean and range of three replicates.

CHAPTER 8. MEGAFUNAL ASSEMBLAGES

Barbara Hecker

Introduction

The continental slope off Cape Hatteras has been recognized as an area that supports unusually high densities of several megafaunal species and infaunal (Blake et al. 1987, Mobil 1990, Gooday et al. 1992). One of the first studies to identify the unusual nature of these communities was conducted in the middle 1980s as part of the ACSAR program sponsored by the MMS. The goal of this program was to characterize benthic communities on the continental slope of the Western North Atlantic extending from Georges Bank to Georgia. As part of this effort, in 1985 three camera-sled tows were conducted in the vicinity of the Manteo Prospect lease blocks (Blake et al. 1987). One of these tows passed within a half mile of the recently proposed Mobil drilling site in Block 467.

Densities of megafauna on the middle slope off Cape Hatteras were found to be slightly elevated in relation to most other U.S. Atlantic slope areas. Additionally, the faunal composition of these assemblages was anomalous. One of the most striking aspects of the megafaunal assemblages in this region was the high densities of two demersal fish, the wolf eelpout (*Lycenchelys verrilli*) and the witch flounder (*Glyptocephalus cynoglossus*), and an anemone (*Actinauge verrilli*). These three taxa are usually a minor component of upper and middle slope megafaunal assemblages in other regions, but they dominated the megafauna on the slope off Cape Hatteras. The other striking aspect of the epifauna in this region was the exceptionally high densities of small white tubes, subsequently identified as the tube-dwelling foraminiferan *Bathysiphon filiformis* (Gooday et al. 1992), observed on the middle and lower slope.

The data presented address objectives 1 and 3; i.e. to define and characterize the megafaunal component of these unusual assemblages and to ascertain their areal extent. These data are based on analysis of sea floor characteristics and megafaunal species seen on slides taken during seven camera-sled tows. This photographic approach has been used successfully in a number of studies of megafaunal assemblages along the eastern U.S. continental margin (Hecker et al. 1980, 1983, Blake et al. 1985, 1987, Maciolek et al. 1987a, 1987b, Hecker 1990a). Photographic methods for studying megafaunal populations have several advantages over conventional survey techniques. Deep-sea megafauna is generally too sparsely distributed to be adequately sampled by bottom grabs or box cores. Trawls cover larger areas, but give questionable quantitative results and cannot safely be used in areas of high relief such as are found on the slope off Cape Hatteras. Comparisons of density estimates obtained from trawls and still photographs show that trawl samples tend to underestimate abundances by up to an order of magnitude (Haedrich et al. 1975). Additionally, trawls frequently miss or severely undersample taxa, such as sea pens and burrowing anemones, that are attached to the seafloor (Hecker 1990a). Photographs also provide ancillary environmental information on habitat and sea-floor characteristics, but do not provide specimens for taxonomic identification. Of the various visual techniques, video tends to underestimate megafaunal abundances (Barham et al. 1967), and direct visual observation tends to overestimate abundances (Grassle et al. 1975) in comparison to still photography. As a survey tool, towed-camera systems have the added advantage of being able to cover much larger distances than either submersibles or deep-sea remotely operated vehicles.

Methods

Details of the sampling design can be found in Chapter 2. Basically, seven cross-isobath tows were conducted within an area extending approximately 30 miles north-south (Figure 8-1). Four of the transects were north of the proposed drilling site (Transects 1A, 1, A, B), and the remaining three were south of the site (Transects D, E, F). Transect D also coincided with the location of tows conducted in 1985.

Photographs were taken with the Benthic Apparatus for Biological Surveys (BABS), a towed camera sled. The sled was designed to ride on the sea floor, with a forward-pointing camera mounted at an angle of 13.5° down from horizontal positioned 0.43 m above the skids. When photographing a level surface, this configuration results in a maximum picture of approximately 5 m² of the sea floor. However, in this survey the steep topography and high concentration of suspended material substantially reduced visibility such that usually

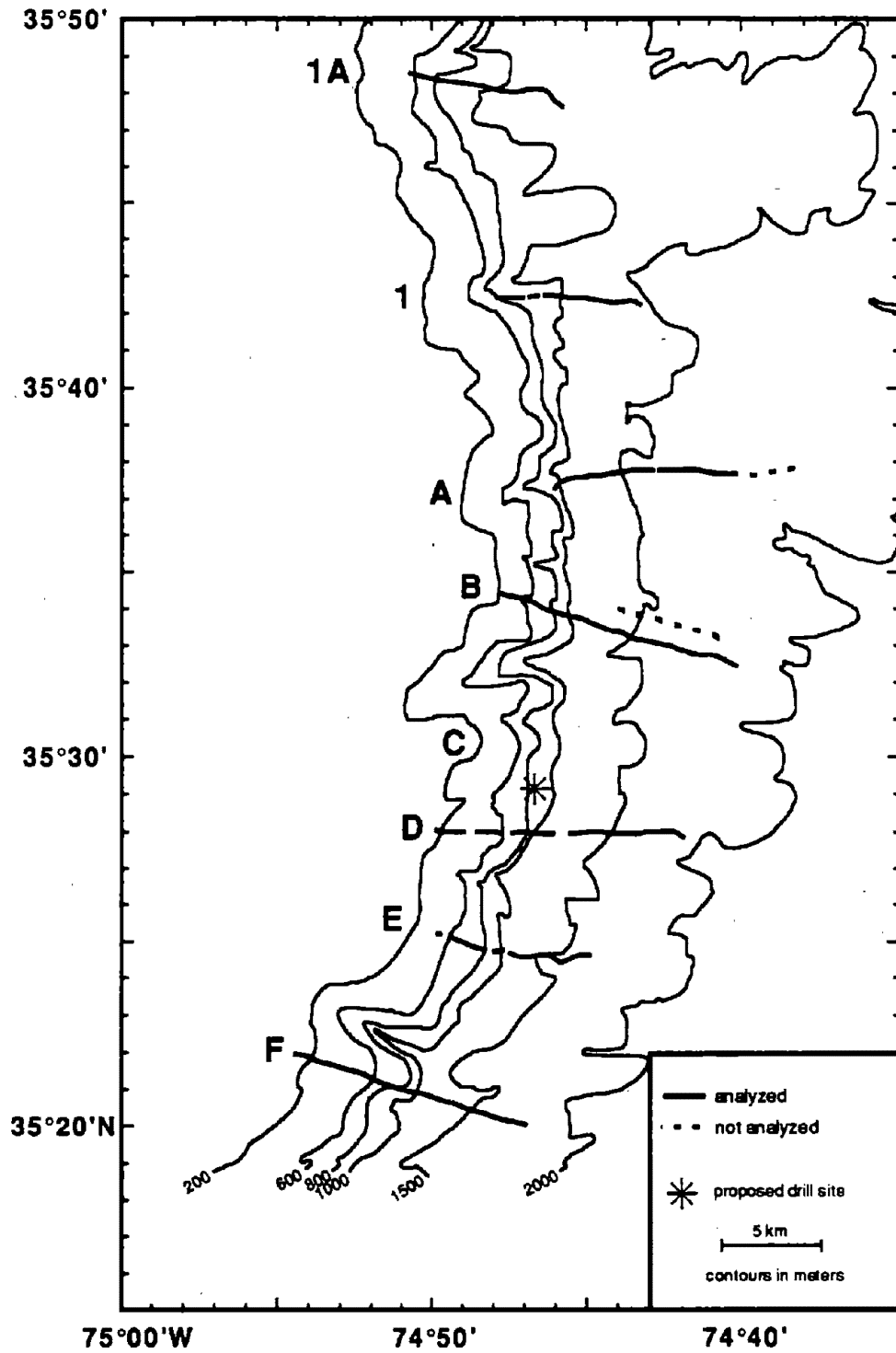


Figure 8-1. Location of camera-sled tows conducted along transects off Cape Hatteras. Breaks in the lines indicate gaps in coverage.

an area of only 3 m² was clear enough for quantitative measurement of most of the megafaunal taxa encountered. Exposures were made at automatic 15-s intervals throughout each tow. At an average towing speed of 1 km, a picture was taken at approximately 8-m intervals along the transect. The film consisted of 100- or 200-ft reels of Ektachrome slide film. Run number, time, and depth were automatically recorded on each frame.

Illumination was provided by a 200-watt strobe mounted to the side and slightly above the camera. The combination of low viewing angle and side illumination provided clear close-up photographs of most of the organisms. The resulting side views greatly aided in the identification of species, such as fish and sea pens. Close proximity to the sea floor allowed enumeration of smaller taxa, and side illumination provided shadows for discerning substrate-colored or translucent taxa. The major disadvantage of the low viewing angle was the large variation in the area photographed (square meters) when the camera sled traversed steep slopes and uneven bottom topography. In these cases, the area viewed was estimated using the position of the horizon on the photograph, the illumination of the frame, and the size of organisms and microtopography.

Each slide was analyzed for area viewed (square meters), surficial geology, microtopography, other sea-floor characteristics (i.e., disturbance, feeding depressions, tube mats), faunal associations (species in physical contact with each other), and species occurrence and abundance. Species identification from photographs is tentative. Although it was virtually impossible to identify to species every organism observed on the slides, the majority of the organisms observed were assigned to a species category. Species names were assigned to most of the abundant taxa based on "voucher" specimens collected during previous studies. Some lumping was unavoidable because differences between congeners frequently cannot be discerned in photographs.

All recognizable taxa were counted, but some, like plankton, were omitted from analyses. Organisms that could not be identified to phylum were included only in counts of total megafaunal density. General taxonomic categories (i.e., anemone, sponge, fish, sea pen) were retained for abundance estimates, but were excluded from community analysis. With the exception of *Hyalinoecia artifex*, worm tubes were counted but not included in any analyses because it was impossible to determine if they were inhabited.

Abundances of the white tubes of *Bathysiphon filiformis* were assessed in several ways. At low densities (<50 per frame) they were counted, at moderate densities (<100 per frame) they were counted in groups of roughly 10 individuals, and at high densities (>100 per frame) they were counted in groups of roughly 50 individuals. The tubes were frequently so dense (>200 per frame) that accurate counts could not be efficiently obtained. In these cases conservative estimates were made. As a result, the number of *B. filiformis* tubes per square meter is probably underestimated in regions of high density. *B. filiformis* was omitted from the analyses of megafaunal distributions for two reasons. First, protozoans are traditionally not viewed as components of the megafauna and their inclusion would preclude comparisons with data that have previously been collected. Second, the densities of *B. filiformis* were so high in relation to the megafauna that they would obscure other trends. The density and depth distribution of *B. filiformis* was analyzed for the entire study area and along individual transects.

If uncertainties about an identification arose during initial viewing, notes were made for subsequent review. The film was then totally reviewed again to check for consistency in identifications, counts, estimates of *B. filiformis* tubes, and area viewed (square meters). The notes taken during initial viewing were also checked against the film and updated.

To elucidate patterns of density with depth, the slides were grouped into 100-m depth intervals for each tow. Summaries were then generated for each depth interval, and densities were standardized to number of individuals per square meter. For overall patterns of density with depth within the survey area, depth intervals from individual tows were treated as replicates for that depth interval. Depth intervals with very sporadic coverage (<8 m²) were dropped from subsequent analyses. For comparisons with other locations along the eastern U.S. continental margin, depth sorting was conducted on the entire data set.

To investigate finer scale changes, slides from each tow were divided into roughly equal sample intervals of 20 consecutive frames. If breaks in the coverage (the camera was off bottom) exceeded 3 minutes, resulted in a depth gap of greater than 20 m, or looked like the habitat had changed, the intervals on either side of the break were divided into roughly equal intervals of 15-25 consecutive frames until the next break. Extensive areas of hard substrate were also divided into separate intervals because they represent a distinctively different habitat.

Summaries were then generated for each interval, and densities were standardized to number of individuals per square meter.

Community analysis included two multivariate pattern recognition techniques, classification and ordination. Classification and ordination were conducted on the 100-m depth intervals from each tow. Only taxa that had abundances of 10 or more individuals in the entire data set were included. Classification analysis was done using the percent similarity coefficient (Whittaker and Fairbanks 1958) and unweighted pair-group clustering (Sokal and Sneath 1963). Reciprocal averaging ordination (Hill 1973, 1974) was also used, to further define and confirm the patterns generated by the cluster analysis. Reciprocal averaging ordination is particularly useful where species turnover along a gradient is high, such as along a long transect (Warwick and Gage 1975) or over a large depth range (Wenner and Boesch 1979).

Results

A total of 4,665 pictures covering 10,918 m² of the sea floor over a depth range of 157 to 1924 m were analyzed. The total area viewed within a depth interval varied considerably, ranging from a low of 1 m² between 1,300 and 1,399 m along Transect D to a high of 436 m² between 1,700 and 1,799 m also along Transect D (Table 8-1). The area covered within a depth interval depended mainly on topographic relief, with steep regions having the least coverage and flat regions having the most. Photographic coverage was hampered in steep regions by the camera sled either flying off the bottom, resulting in no coverage, or nosing into the slope, resulting in a smaller area viewed for each frame.

Sea-Floor Characteristics

A complex gully and ridge system was characteristic of the middle and upper slope near the proposed drill site. This complexity is reflected in the topographic profiles of the transects (Figure 8-2). This system was much less pronounced toward the northern end of the survey area. The slope in the northern region also exhibited far fewer outcrops. Percent coverage (number of pictures on bottom/total number of possible pictures), which is a rough measure of topographic complexity, varied considerably among transects, ranging from a high of 88% on Transect 1 to a low of 53% on Transect D. Outcrops on the middle slope generally appeared fresh, with no attached organisms, little evidence of weathering, and fresh piles of talus at their base. In contrast, many of the outcrops on the upper slope were colonized by organisms and/or showed extensive weathering.

The sea floor throughout the survey area appeared to be structured by a combination of physical (usually on horizontal scales of <1 m) and biological processes (usually on horizontal scales of >1 m). Steep slopes frequently showed evidence of soft-sediment failure in the form of slump scars and erosional "rivulets." Flatter regions of the slope frequently had undulating topography (hummocky on horizontal scales >1 m). These regions frequently appeared to be depositional sites for turbidites, debris flows, and slump blocks. A particularly spectacular example of this was seen on the floor of a gully in the deeper part of Transect 1A. The sea floor in this area was very irregular and was characterized by numerous sediment ridges, sediment-draped boulders, and gouges. The photographs also suggest that bottom current intensities are not uniform within the survey area. Some regions showed indications of strong bottom currents in the form of either a smoothed sediment surface, asymmetric mound morphology, ripples, and/or bent over fauna; whereas other regions showed indications of weak bottom currents in the form of a fine flocculent surface layer or small-scale microtopography. The photographs also showed very high concentrations of suspended particles, indicating strong bottom currents. Suspended particle concentrations were highest on the middle slope, where they frequently obscured part of each photograph.

Most of the photographs also showed evidence of extensive biological reworking of sea-floor sediments in the form of mounds, excavations, pits, fecal material, and trails. Mounds, mostly caused by infaunal deposit feeders, were particularly prevalent on the lower slope and on some regions of the middle slope. Excavations, mostly caused by fish and crustaceans, were most prevalent on relatively flat regions of the upper and middle slope. Pits (usually 1-3 cm in diameter), which appear to be feeding depressions of deeper infaunal deposit feeders, were seen throughout the survey area. In several areas, these feeding depressions were so dense that they were the dominant feature on the sea floor. These areas were usually quite localized, but in several

Table 8-1. Total area viewed (square meters) for 100-m depth intervals at transects surveyed with the towed camera sled.

Depth Interval (m)	Transect						Total	
	1A	1	A	B	D	E		F
100-199				15	8*		122	145
200-299				34	4*		508	546
300-399				16	3*		239	258
400-499				18	6*	6*	108	138
500-599	15			20	25	1*	58	119
600-699	94	13		71	9	7*	29	223
700-799	27	65		97	35	15	20	259
800-899	60	106	3*	45	52	27	35	328
900-999	110	67	15	101	28	49	28	398
1000-1099	380	211	63	88	69	29	10	850
1100-1199	647	152	146	103	46		21	1115
1200-1299	209	26	148	155	4*	115	19	676
1300-1399		319	189	385	1*	56	93	1043
1400-1499		295	46	167	98	112	167	885
1500-1599			381	231	43	86	45	786
1600-1699			120	145	128	188	276	857
1700-1799			312	536	436	154	100	1538
1800-1899			421	52	114		104	691
1900-1999					63			63
Total	1542	1254	1844	2279	1172	845	1982	10918

* Coverage too low and patchy to be included in the data analysis.

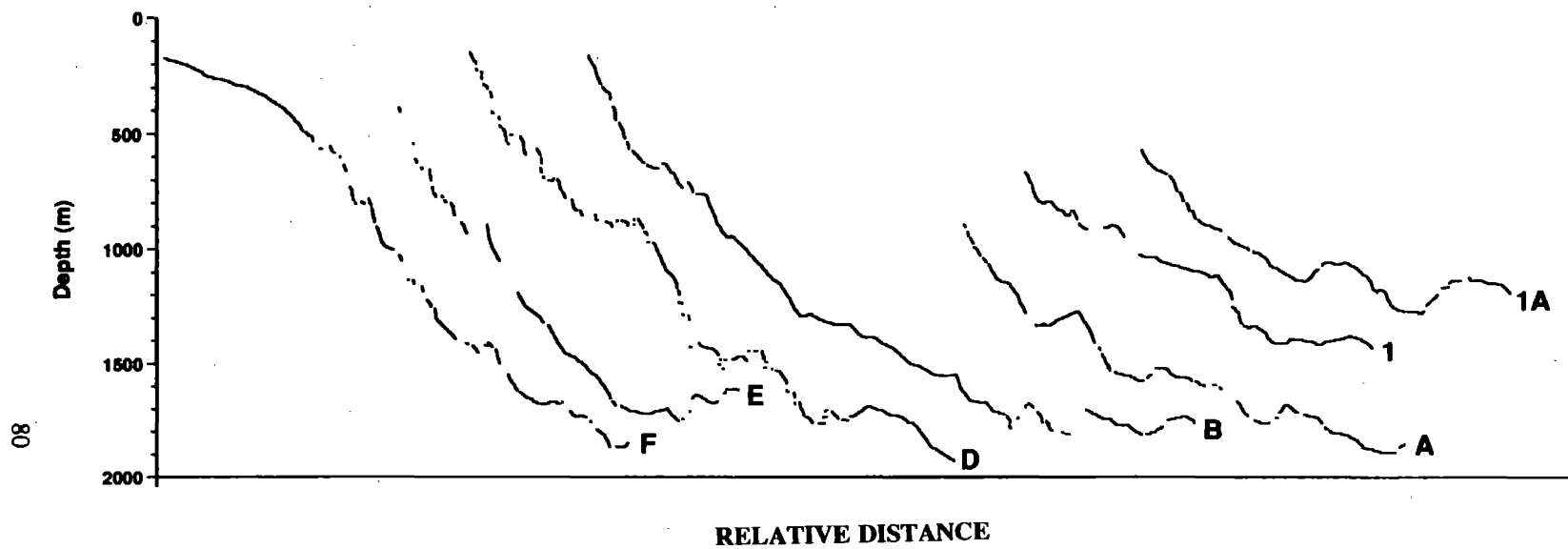


Figure 8-2. Topographic profiles from the camera sled tows. The profiles are based on depth from the transducer on the camera sled. Gaps in the line indicate that the camera sled was off the sea floor. Profiles are arranged from north to south. No attempt is made to represent spatial relationships between transects. Distance has not been corrected for variation in ship speed and is therefore approximate.

instances they extended for horizontal distances in excess of 100 m. Numerous biogenic tracks and trails were seen throughout the survey area. The most obvious examples of biogenic traces were observed on the middle slope, where the trails of either sea urchins (pock marks), witch flounder (paired scalloped lines), or quill worms (sinuous surface lines) frequently covered the entire sea floor.

Faunal Composition

A total of 20,722 megafaunal organisms were found along the seven transects analyzed (Table 8-2). Since not all depths were covered at each of the transects, and areal coverage varied among depths, care should be taken in drawing conclusions from this list. Of the total organisms counted, 7,065 were echinoderms (34%), 4,991 were coelenterates (24%), and 4,293 were fish (21%). Differences in faunal composition among the tows mainly reflected variations in the depths covered at each transect. Areal coverage on Transects A, D, E, and F was strongly biased toward the flat lower slope, accounting for the high proportion of echinoderms found on these transects. In contrast, most of the areal coverage obtained on Transects 1A and A was on the middle slope, accounting for the high proportion of fish seen along these transects. Differential coverage does not explain the high proportion of coelenterates found in Transect A or the high proportion of fish found on Transect B. More sea pens were found on the lower slope on Transect A than on any of the other transects. Relatively few organisms were encountered on the lower slope of Transect B when compared to the other transects.

The most abundant megafaunal species encountered in this survey was an echinoderm, the ophiuroid *Ophiomusium lymani* (4,981 individuals). This species was a common inhabitant of the lower slope. Another common inhabitant of the lower slope was the sea pen, *Kophobelemnon stelliferum*. This sea pen was the third most abundant species (1,499 individuals). The quill worm *Hyalinoecia artifex* was the second most abundant organism (3,020 individuals). This polychaete was found in exceptionally high densities on the upper portion of the middle slope on Transects 1A and A. The fourth most abundant organism observed was the anemone *Actinauge verrilli* (1,096 individuals), which was a common inhabitant on the upper portion of the middle slope (Figure 8-3a).

Fish frequently dominated the fauna inhabiting the middle slope. The four most abundant fish were all widely distributed in the area surveyed. Two eelpouts, *Lycenchelys verrilli* (993 individuals) and *Lycodes atlanticus* (847 individuals), were the most abundant fish encountered (Figures 8-3b and 8-4a, respectively). *Synaphobranchus* spp., which represents two species, *S. kaupi* and *S. affinis*, were the third most abundant fish encountered during the survey (708 individuals). The witch flounder, *Glyptocephalus cynoglossus* (570 individuals), was the fourth most abundant fish encountered during the survey (Figure 8-4b).

The foraminiferan *Bathysiphon filiformis* far outnumbered the megafauna observed. This protozoan was found in very high concentrations on each of the transects.

Faunal Abundance and Depth Distributions

Total megafaunal density was bimodal with peak densities of 9.5 ± 4.7 individuals m^{-2} on the upper portion of the middle slope and 3.6 ± 1.2 individuals m^{-2} on the lower slope (Figure 8-5a). Densities were uniformly low across the remainder of the middle slope. The pattern of density with depth varied among the transects (Figure 8-5b). This variability was most pronounced between 500 and 800 m, ranging from a high of 23.4 individuals m^{-2} on Transect 1 to a low of 0.8 individuals m^{-2} on Transect D. The exceptionally high densities found in the shallower portion of both northern transects (1A and 1) mainly reflected high abundances of *Hyalinoecia artifex*; this species was not found in high numbers on the other two transects (B and F) that had adequate coverage in the depth range of 500 to 800 m. A combination of sampling artifact and/or habitat differences may explain the low densities found on Transects D and E. The low densities on these two transects may reflect the patchy coverage obtained in this depth range. However, these transects also had abundant outcrops that were rarely colonized. Faunal densities were uniformly low between 900 and 1,600 m on all seven transects. Megafaunal densities were moderate to high between 1,600 and 1,900 m on four of the Transects (A, D, E, F) and low on Transect B. These densities are mainly a reflection of moderate to high abundances of *Ophiomusium lymani* on the lower slope. The very low densities on Transect B do not appear to be a sampling artifact since photographic coverage was high and all three of the depth intervals (1600, 1700,

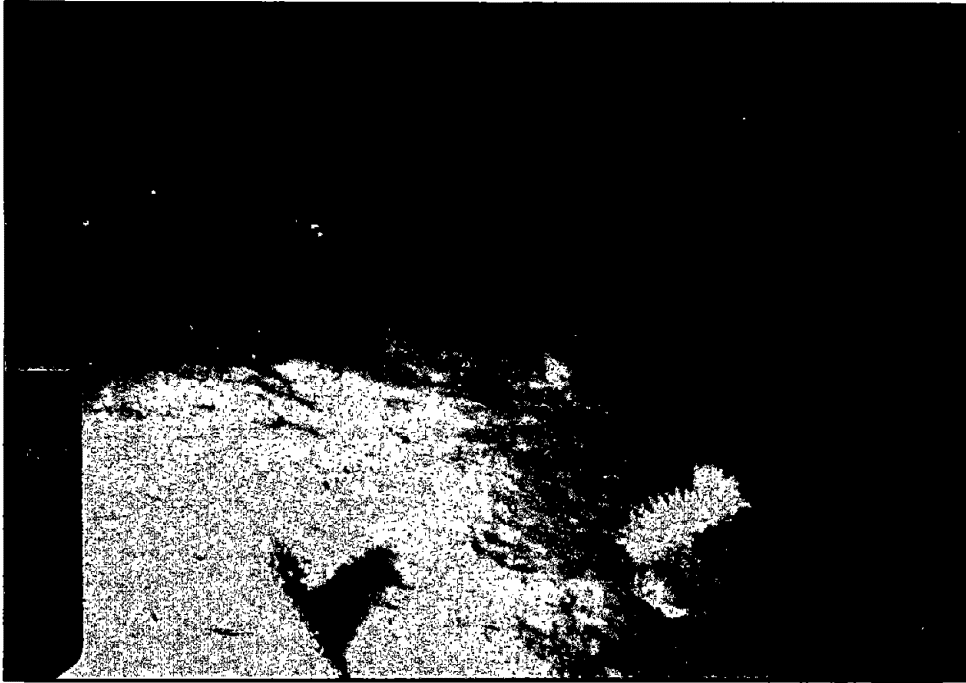
Table 8-2. List of megafaunal species enumerated from camera-sled tows off Cape Hatteras.

Taxon	Transect							All
	1A	1	A	B	D	E	F	
Fish								
Unidentified fish	51	77	71	89	27	22	63	400
<i>Lycenchelys verrilli</i>	146	95	83	434	105	72	58	993
<i>Lycodes atlanticus</i>	25	163	253	253	43	99	11	847
<i>Lycenchelys paxilla</i>	21	2	70	16	8	-	7	124
<i>Glyptocephalus cynoglossus</i>	173	190	67	94	21	13	12	570
<i>Synaphobranchus</i> spp.	206	150	181	89	28	27	27	708
<i>Simenchelys parasiticus</i>	9	6	-	3	3	2	1	24
<i>Venefica</i> sp.	-	-	9	-	6	9	5	29
<i>Myxine glutinosa</i>	6	4	1	32	7	5	50	105
<i>Ophichthus cruentifer</i>	-	-	-	-	-	-	7	7
Unidentified macrurid	-	-	-	1	1	-	1	3
<i>Nezumia</i> spp.	17	23	12	23	13	2	17	107
<i>Coryphaenoides carapinus</i>	-	-	11	4	5	3	1	24
<i>Coelorhynchus carminatus</i>	-	-	-	-	-	-	4	4
<i>Dicrolene intransigra</i>	12	26	31	9	16	31	5	130
<i>Antimora rostrata</i>	-	-	2	-	1	-	1	4
<i>Halosauropsis machrochir</i>	-	-	1	1	2	2	-	6
<i>Aldrovandia</i> spp.	1	3	13	1	6	13	3	40
<i>Chimera</i> sp.	-	-	-	1	1	-	-	2
<i>Bathysaurus ferox</i>	-	-	-	-	-	-	1	1
<i>Polycanthonotus challengeri</i>	-	-	-	1	-	-	1	2
<i>Benthosaur</i> sp.	-	-	-	-	-	1	1	2
<i>Alepocephalus agassizii</i>	-	-	1	-	1	1	1	4
<i>Alepocephalus</i> sp. 2	-	-	-	-	-	-	1	1
Unidentified morid	-	1	-	1	-	-	15	17
<i>Phycis chesteri</i>	2	7	-	1	-	-	2	12
<i>Urophycis reggia</i>	-	-	-	-	-	-	4	4
<i>Merluccius albidus</i>	-	-	-	-	-	-	29	29
<i>Scyliorhinus retifer</i>	-	-	-	-	-	-	1	1
<i>Peristedion miniatum</i>	-	-	-	-	-	-	3	3
Unidentified batfish	2	-	-	-	-	-	1	3
<i>Helicolenus dactylopterus</i>	-	-	-	-	-	-	13	13
<i>Chlorophthalmus agassizii</i>	-	-	-	-	-	-	71	71
Cottunculid sp.	-	-	-	2	-	-	-	2
<i>Raja</i> sp.	-	-	-	-	-	-	1	1
Coelenterates								
Unidentified alcyonarian	1	-	-	-	-	-	-	1
<i>Anthomastus grandifloris</i>	-	-	-	-	-	2	-	2
General sea pen	8	-	18	1	5	48	9	89
<i>Kophobelemnon stelliferum</i>	2	-	1000	3	107	175	212	1499
<i>Distichoptilum gracile</i>	4	-	705	-	20	71	185	985
Fine-white sea whip	-	-	157	-	24	89	77	347
White/purple sea pen	49	-	-	-	-	-	-	49
<i>Pennatula grandis</i>	2	1	15	-	2	66	24	110
<i>Umbellula</i> sp.	-	-	-	-	2	2	2	6
<i>Anthoptilum grandiflorum</i>	-	-	2	-	-	1	2	5
<i>Flabellum alabastrum</i>	58	-	-	-	-	-	-	58
Unidentified anemone	18	-	3	6	7	-	46	80
<i>Actinauge verrilli</i>	159	502	123	171	75	3	63	1096
<i>Cerianthid</i> spp.	-	187	2	13	14	-	137	353
<i>Cerianthus borealis</i>	7	-	-	15	1	1	108	132
<i>Bolocera tudiae</i>	-	1	-	2	-	-	70	73
<i>Halcurias pilatus</i>	-	-	-	-	-	-	33	33
<i>Chondrophelia coronata</i>	-	-	5	1	7	2	5	20
Sparse-tentacled anemone	-	4	-	30	-	-	19	53
Anthozoan on <i>Parapagurus</i>	-	2	-	-	-	2	1	5

Table 8-2. (continued).

Taxon	Transect							All
	1A	1	A	B	D	E	F	
Echinoderms								
Unidentified ophiurid	-	-	2	-	-	-	1	3
<i>Ophiomusium tymani</i>	-	-	950	28	1009	595	2399	4981
<i>Asteronyx loveni</i>	-	-	109	-	4	23	26	162
<i>Amphilimna olivacia</i>	-	-	-	117	-	11	104	232
<i>Ophiura sarsi</i>	74	-	-	-	-	-	3	77
<i>Ophiocantha bidentata</i>	-	-	13	-	-	2	13	28
Echinoid								
<i>Phormosoma placenta</i>	55	4	28	1	3	13	39	143
<i>Hygrosoma petersi</i>	-	3	8	-	3	2	7	23
<i>Echinus affinis</i>	-	-	-	-	-	-	1	1
<i>Echinus alexandri</i>	-	-	1	-	-	-	-	1
Unidentified asteroid	-	5	2	2	1	5	-	15
<i>Astropectin americanus</i>	-	-	-	5	12	-	451	468
<i>Plutonaster agassizii</i>	5	9	80	29	4	6	2	135
<i>Dytaster grandis</i>	-	-	10	-	-	-	1	11
Brisingid	-	-	-	-	1	-	-	1
Holothurian								
<i>Peniagone</i> sp.	-	-	-	-	669	2	-	671
<i>Paelopatides gigantia</i>	-	-	85	-	6	-	12	103
<i>Mesothuria lactea</i>	-	-	3	-	-	-	5	8
Purple burrowing holothurian	-	-	-	-	2	-	-	2
Crustaceans								
Unidentified crustacean	2	5	-	3	1	-	8	19
Translucent crustacean	-	-	-	-	-	-	186	186
<i>Cancer</i> spp.	-	-	-	14	-	-	82	96
<i>Geryon quinquedens</i>	2	3	-	-	-	-	1	6
<i>Bathynectes longispina</i>	-	-	-	-	-	-	14	14
<i>Munida valida</i>	-	-	-	-	-	-	23	23
<i>Munida iris?</i>	-	-	-	-	-	-	21	21
<i>Parapagurus alaminos</i>	-	2	-	-	-	2	1	5
<i>Colosendies colossea</i>	-	-	11	3	3	2	2	21
Red/white spider crab	-	-	-	-	-	-	1	1
Unidentified shrimp	13	51	29	40	12	72	24	241
Irridescent shrimp	-	-	-	-	-	-	7	7
Isopod parasite on <i>Nezumia</i>	-	2	-	3	2	-	-	7
Miscellaneous								
<i>Hyalinoecia artifex</i>	1883	1058	-	-	-	-	79	3020
Polychaete	-	-	-	41	-	9	-	50
Unidentified sponge	2	-	-	7	3	21	24	57
<i>Euplecteta</i> sp.	-	-	1	-	-	-	-	1
Octopus	3	7	1	1	-	1	2	15
Gastropod	16	73	60	123	15	19	29	335
Echiurid	-	-	2	1	-	-	2	5
Brachiopod	-	-	-	61	10	15	-	86
Unidentified organism	15	29	19	35	11	9	34	152
Coelenterates	308	695	2030	242	264	460	992	4991
Echinoderms	134	21	1291	182	1714	659	3064	7065
Fish	671	747	806	1055	294	302	418	4293
Total megafauna	3049	2695	4250	1811	2329	1573	5015	20722
Foraminiferan								
<i>Bathysiphon filiformis</i>	41700	54200	40200	66400	23050	33500	19350	278400

(a)



(b)

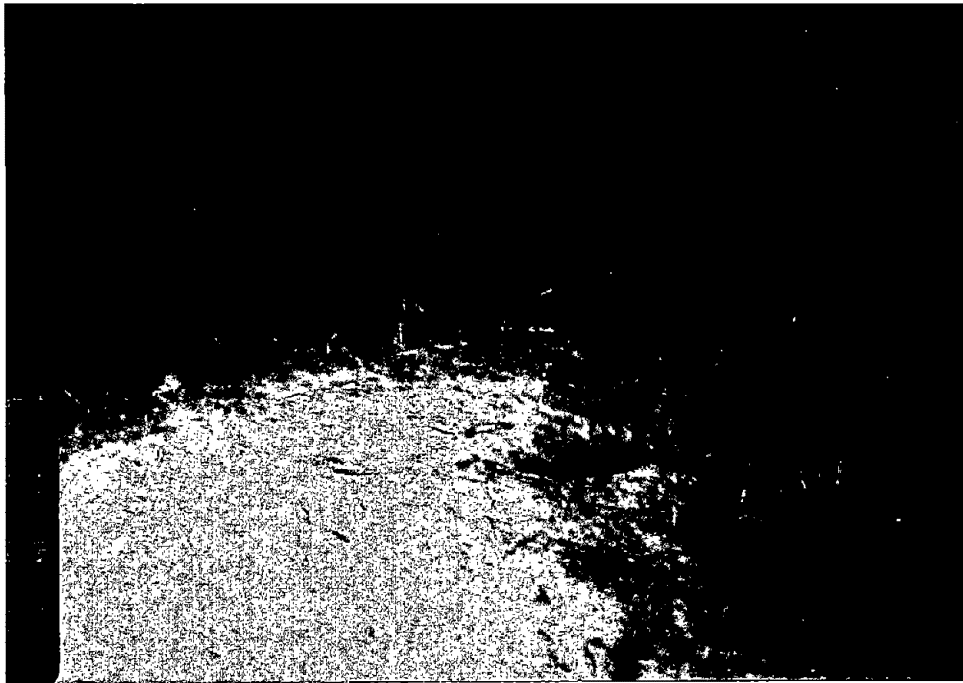
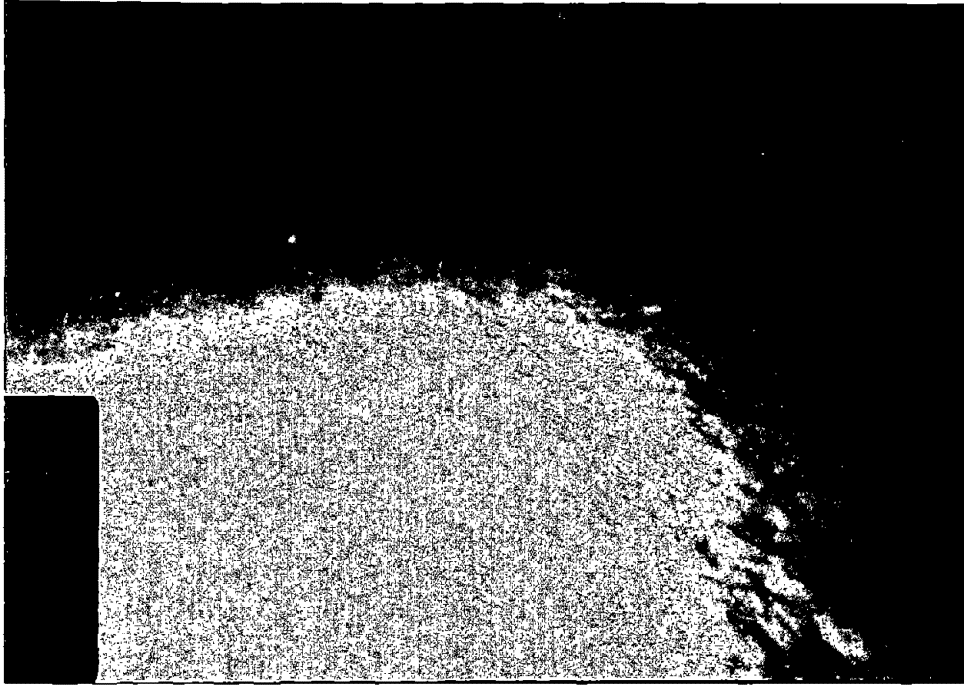


Figure 8-3.

Photographs of common middle slope species: (a) several *Actinauge verrilli*, a gastropod with its trail leading to the anemone on the right, and a *Nezumia* spp. (Transect B, 1004 m); and (b) seven *Lycenchelys verrilli*, a gastropod, a few *Bathysiphon filiformis*, and numerous tracks on the sediment surface (Transect F, 799 m).



(a)



(b)



Figure 8-4.

Photographs of common middle slope species: (a) a large male *Lycodes atlanticus* and numerous feeding depressions (transect B, 1728 m); and (b) *Glyptocephalus cynoglossus* moving off the sea floor, a *Lycenchelys verrilli*, and few *Bathysiphon filiformis* (transect B, 1209 m).



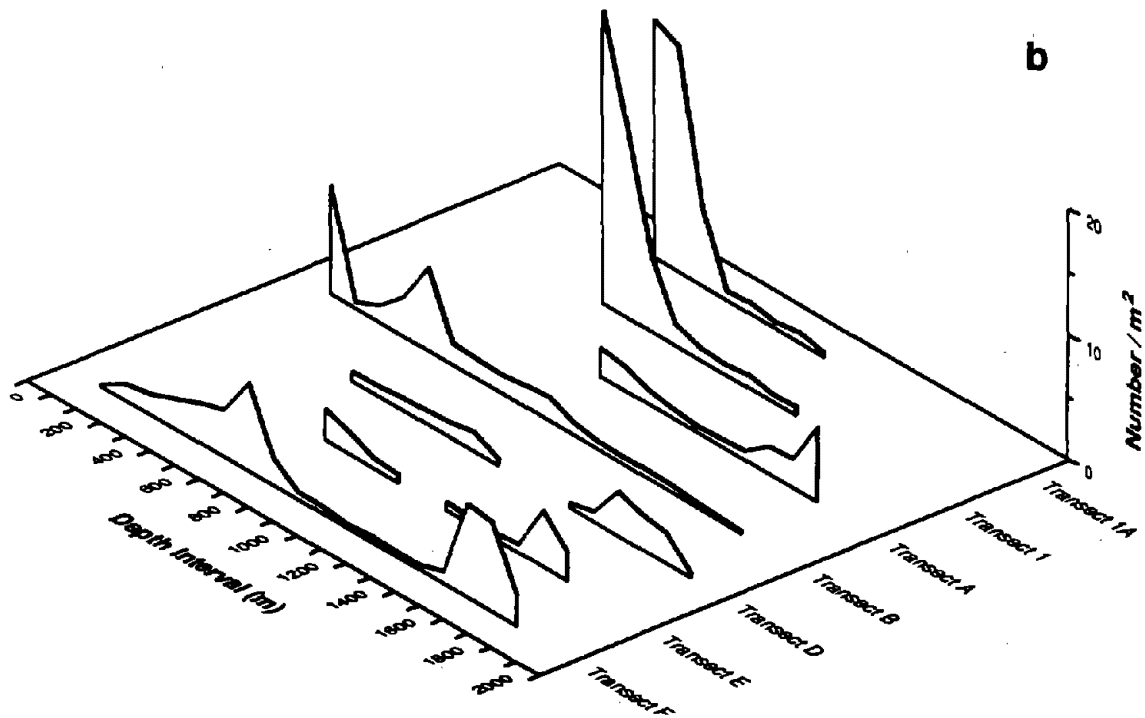
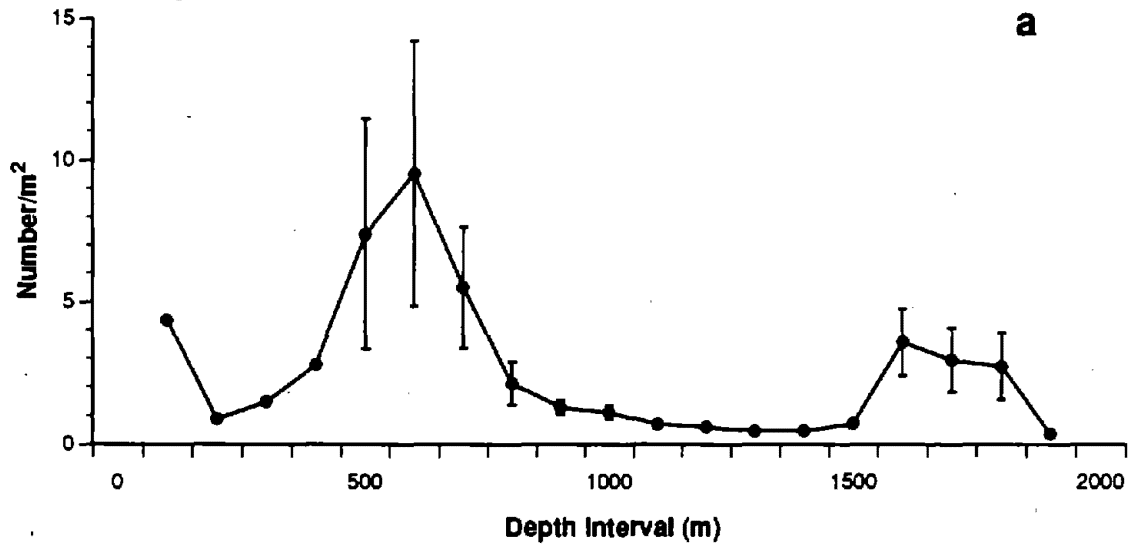


Figure 8-5. Density of total megafauna with depth in (a) the study area and (b) along each of the transects. The number of samples used for each depth interval for the entire study area (a) can be seen on Table 8-1, error bars are one standard error.

1800 m) had uniformly low densities.

Two species, *Lycenchelys verrilli* (Figure 8-6) and *Actinauge verrilli* (Figure 8-7), were frequently dominant components of the megafauna inhabiting the upper portion of the middle slope (500 to 1100 m). *Lycenchelys verrilli* was found over a depth range of 400 to 1,300 m and was most abundant between 400 and 900 m (Figure 8-6a). This eelpout was consistently more abundant on Transect B (Figure 8-6b). *Actinauge verrilli* was found over a similar depth range and was most abundant between 600 and 800 m (Figure 8-7a). The high variability in the density of *A. verrilli* was largely a reflection of its high abundance (4.3 and 4.4 individuals m⁻²) in the two shallower depth intervals of Transect 1 (Figure 8-7b). These exceptionally high densities appeared related to the numerous *Hyalinoecia artifex* found in this area, since many juveniles of *A. verrilli* were seen attached to the tubes of these polychaetes. *Glyptocephalus cynoglossus* was found over a depth range of 400 to 1,500 m and its density was relatively uniform over most of this depth range (Figure 8-8a). This flounder was consistently more abundant on Transect 1 than on any of the other transects (Figure 8-8b). *Lycodes atlanticus* was usually found below 1,000 m and was frequently the dominant inhabitant of the lower portion of the middle slope (1,100 to 1,600 m). This eelpout was found in peak densities of 0.3 ± 0.1 individuals m⁻² between 1,400 and 1,500 m (Figure 8-9a). This species was consistently less abundant on Transect F (Figure 8-9b).

Bathysiphon filiformis was usually restricted to depths below 700 m and was present in highest densities between 1,200 and 1,500 m (Figure 8-10a). The depth distribution of *B. filiformis* was bimodal, with decreased abundances between 1,100 and 1,200 m and between 1,600 and 1,900 m. Relatively low densities of *B. filiformis* were found between 1,100 and 1,200 m on most of the transects. The pattern of density with depth varied considerably among and within transects (Figure 8-10b). Because all of the slides taken in a given depth interval were pooled within transects, the depth distribution graphs show general trends. Local densities based on individual photographs ranged from 0 to 175 individuals m⁻². Some of the variability in the distribution of *B. filiformis* may be attributed to habitat differences both among and within transects. This foraminiferan was most abundant in relatively flat areas where the sea floor was not heavily disturbed by the activity of other organisms (Figure 8-11a). However, in many instances, possible explanations for exceptionally low abundances were not obvious. An example of this can be seen in Figure 8-11b where a flat slope was inhabited by very few *B. filiformis*. Similar variations in the abundance of this foraminiferan were frequently seen over horizontal scales of only several meters. An example of this can be seen in two adjacent photographs from Transect 1A. The first photograph shows moderately high abundances of *B. filiformis* (Figure 8-12a), and the second photograph taken 8 m further along the transect shows very low abundances (Figure 8-12b).

Transect Analysis

Continuous plots of depth and faunal density were used to examine finer scale changes in faunal composition along a transect. In addition to highlighting the habitat preferences of some species, these plots provide insight into mechanisms that may control faunal distributions. The depth profiles and *Bathysiphon filiformis* densities were based on individual photographs, and the megafaunal densities were based on groups of consecutive photographs (15 to 25 frames). The megafaunal densities are arranged in columns that depict faunal densities on the sea floor below them.

The slope along the northernmost transect (1A) was relatively flat and exhibited few outcrops (Figure 8-13). The seafloor in a gully near the deeper end of the transect was very disturbed and appeared to be the remains of a debris flow (Figure 8-14a). The ridge seaward of this gully was totally pock-marked by sea urchins. Very high densities of *Hyalinoecia artifex* were found at the shallower end of the transect. A dense bed of *Ophiura sarsi* was encountered only at the shallower end of this region. Other species seen within this area included *Actinauge verrilli* and *Lycenchelys verrilli*. Densities of both species were lower on the steep areas down-slope of this region and slightly higher on flat areas. Faunal abundances further down-slope were uniformly low, and no single species dominated the fauna. Higher faunal densities were found on the ridge at the deeper end of this transect. Fauna inhabiting this region included the echinoid *Phormosoma placenta*, the scleractinian *Flabellum alabastrum*, and an unidentified sea pen (with a white axis and purple polyps). The coral and sea pen were not seen at any of the other transects. *B. filiformis* was most abundant on the flatter middle portion of this transect. This foraminiferan was very sparse at the shallower end of the transect, in the

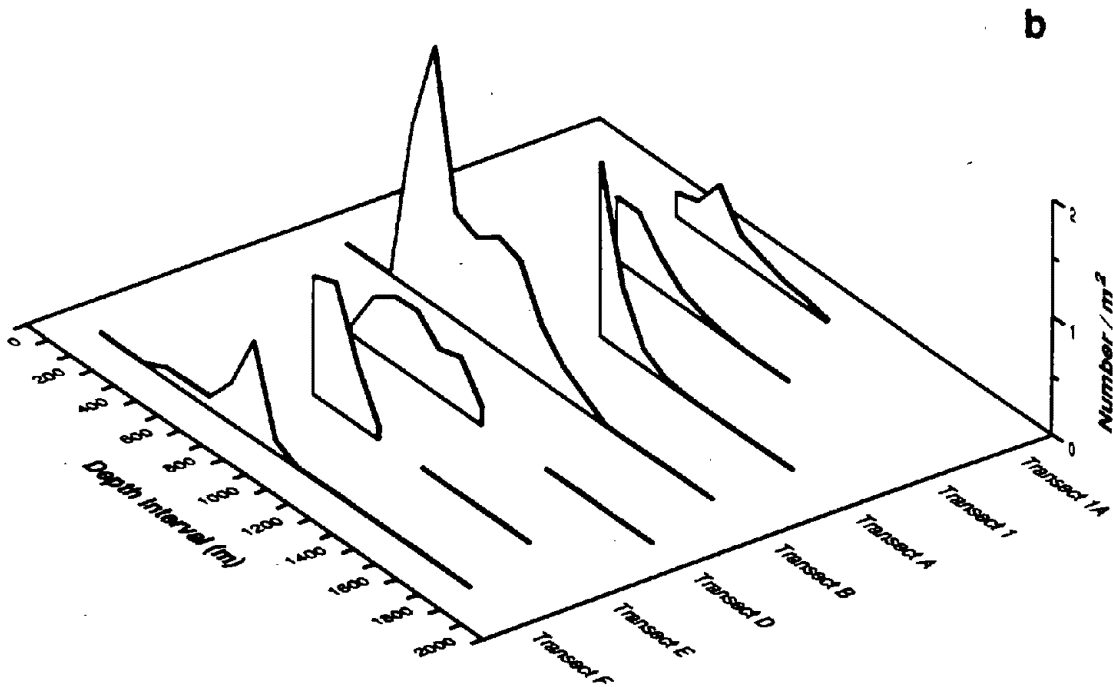
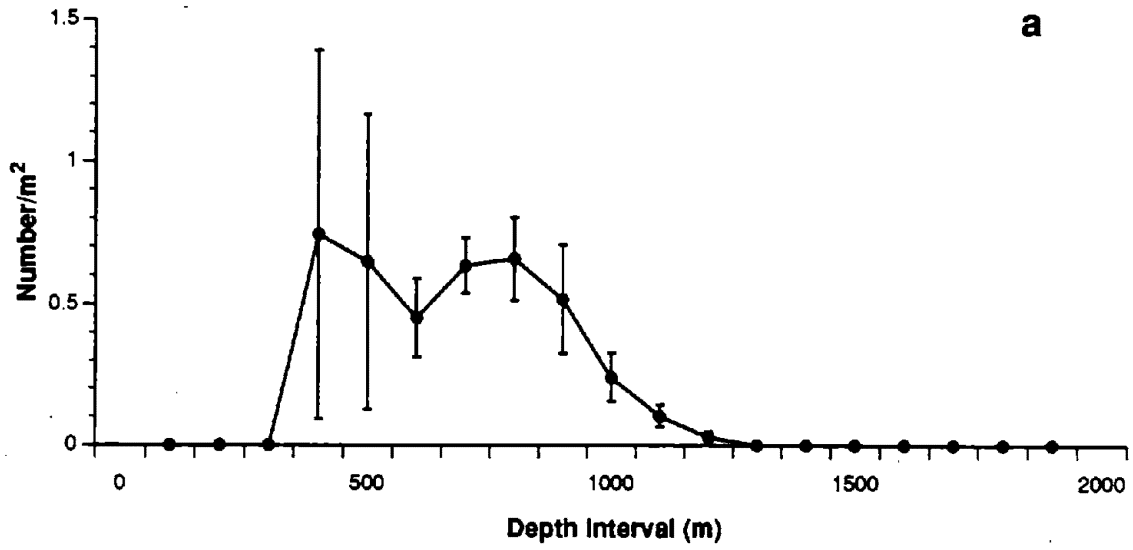


Figure 8-6. Density of the wolf eelpout *Lycenchelys verrilli* with depth in (a) the study area and (b) along each of the transects. The number of samples used for each depth interval for the entire study area (a) can be seen on Table 8-1, error bars are one standard error.

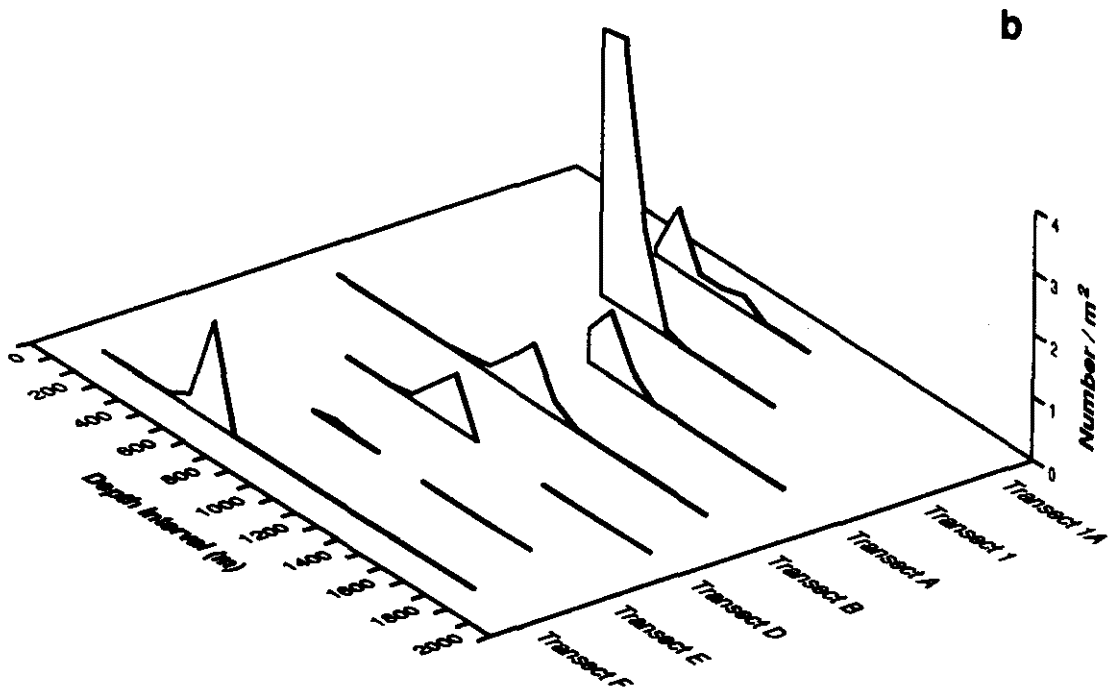
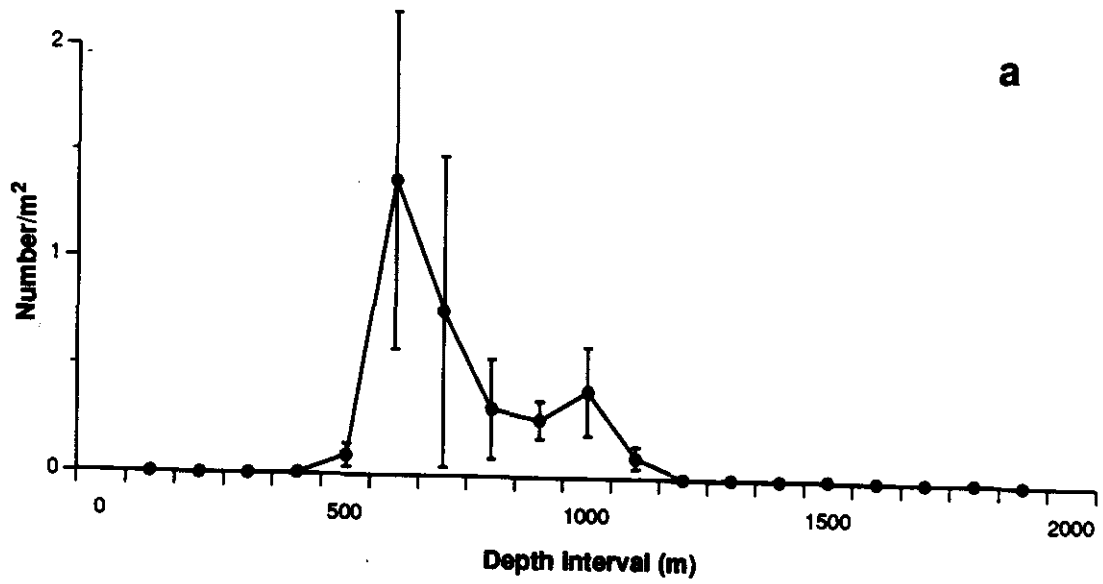


Figure 8-7. Density of the anemone *Actinauge verrilli* with depth in (a) the study area and (b) along each of the transects. The number of samples used for each depth interval for the entire study area (a) can be seen on Table 8-1, error bars are one standard error.

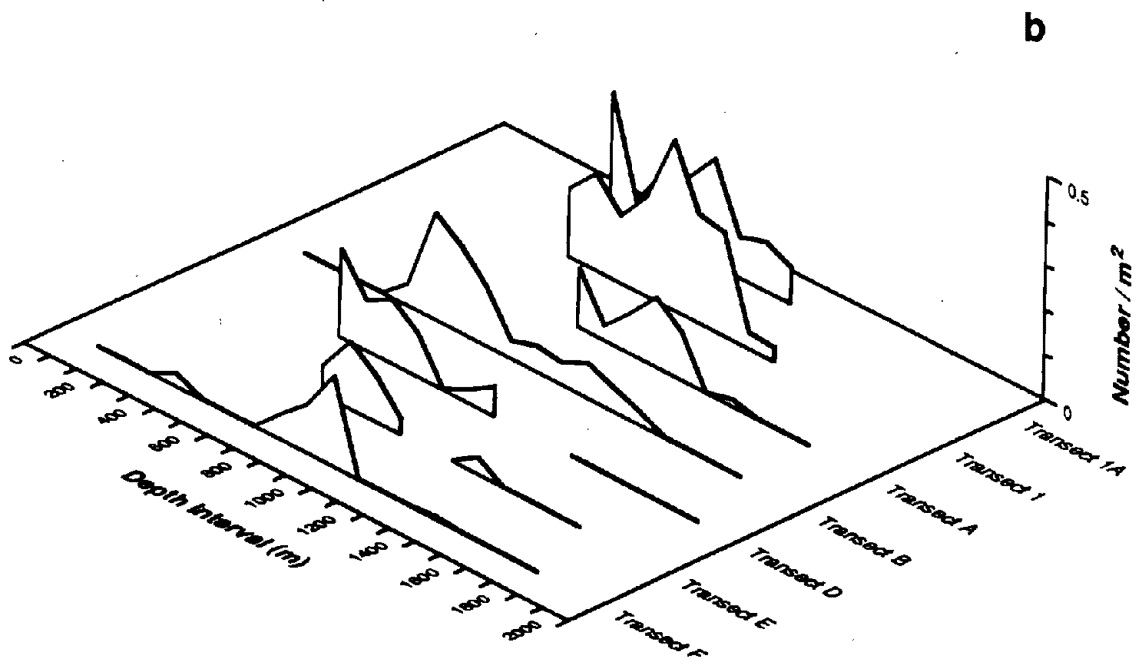
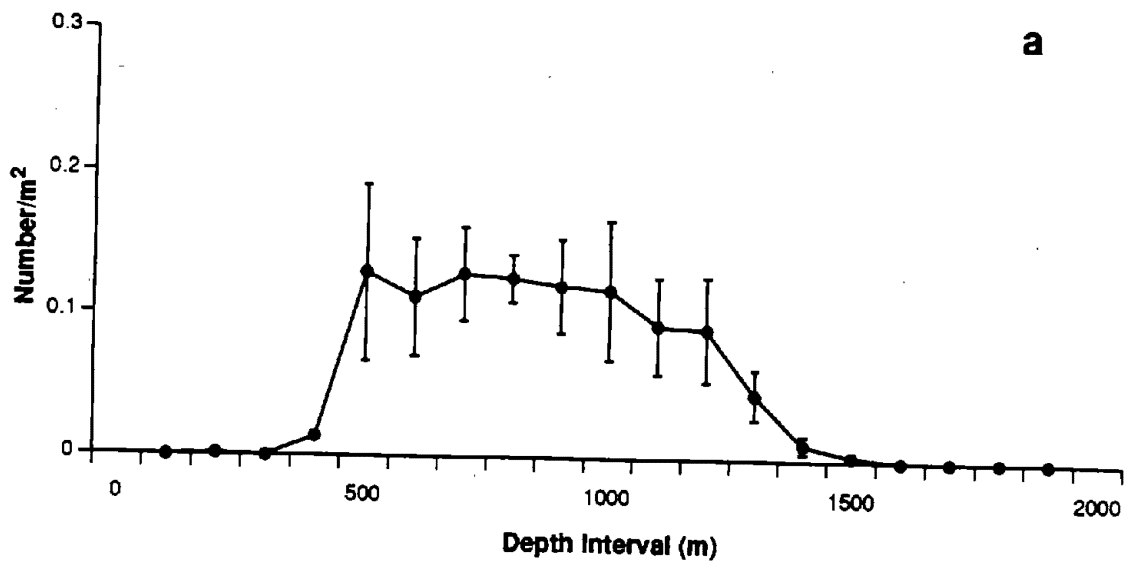


Figure 8-8. Density of the witch flounder *Glyptocephalus cynoglossus* with depth in (a) the study area and (b) along each of the transects. The number of samples used for each depth interval for the entire study area (a) can be seen on Table 8-1, error bars are one standard error.

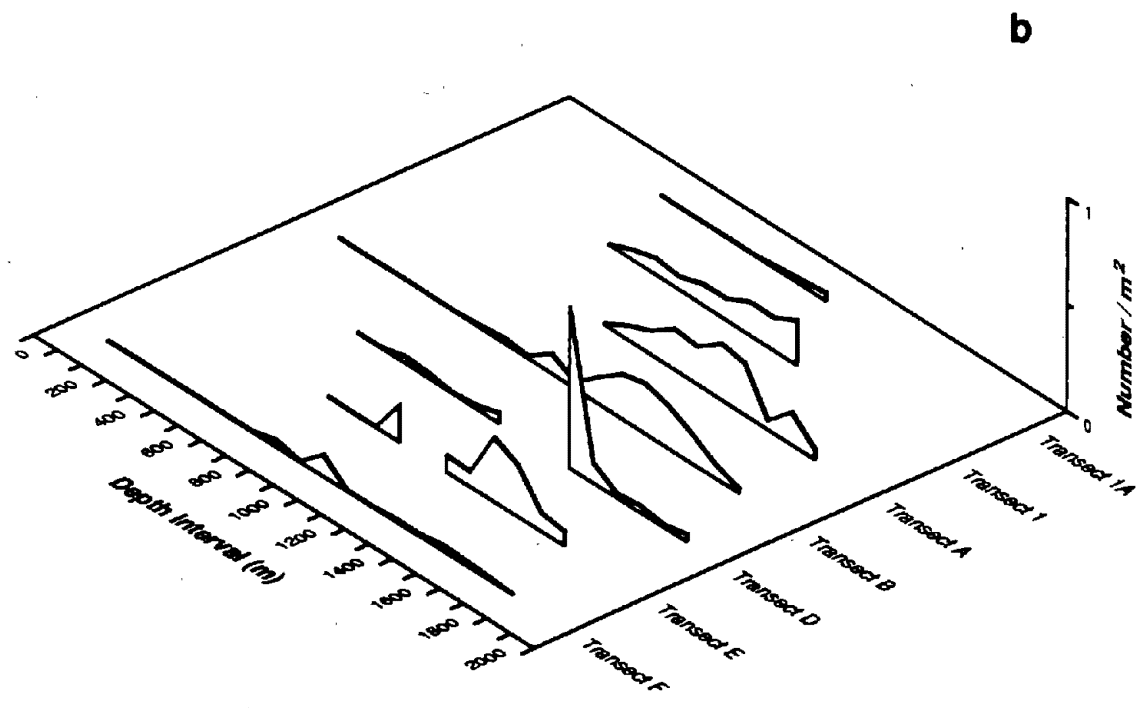
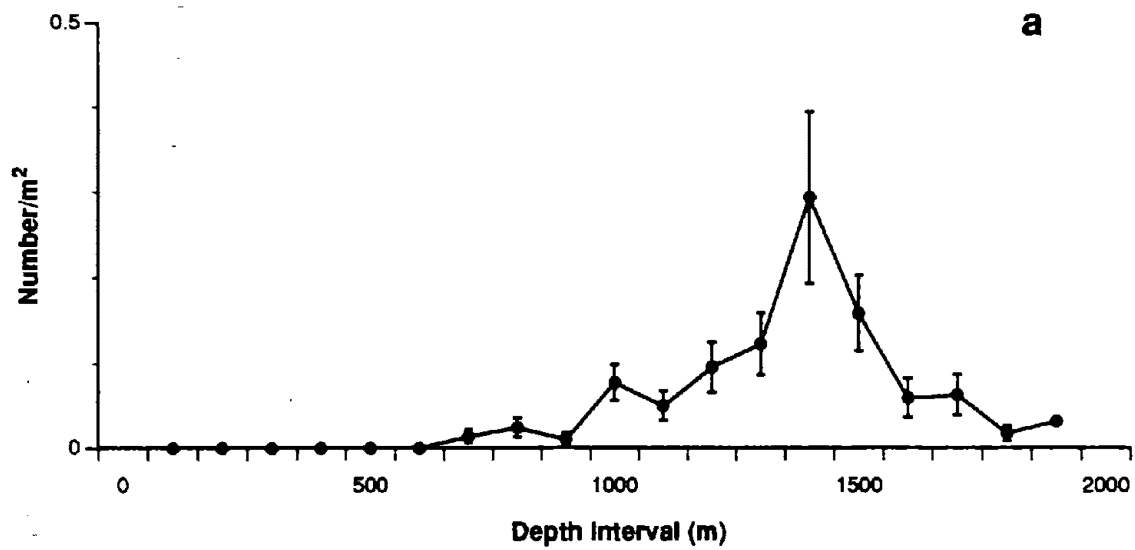


Figure 8-9. Density of the eelpout *Lycodes atlanticus* with depth in (a) the study area and (b) along each of the transects. The number of samples used for each depth interval for the entire study area (a) can be seen on Table 8-1, error bars are standard error.

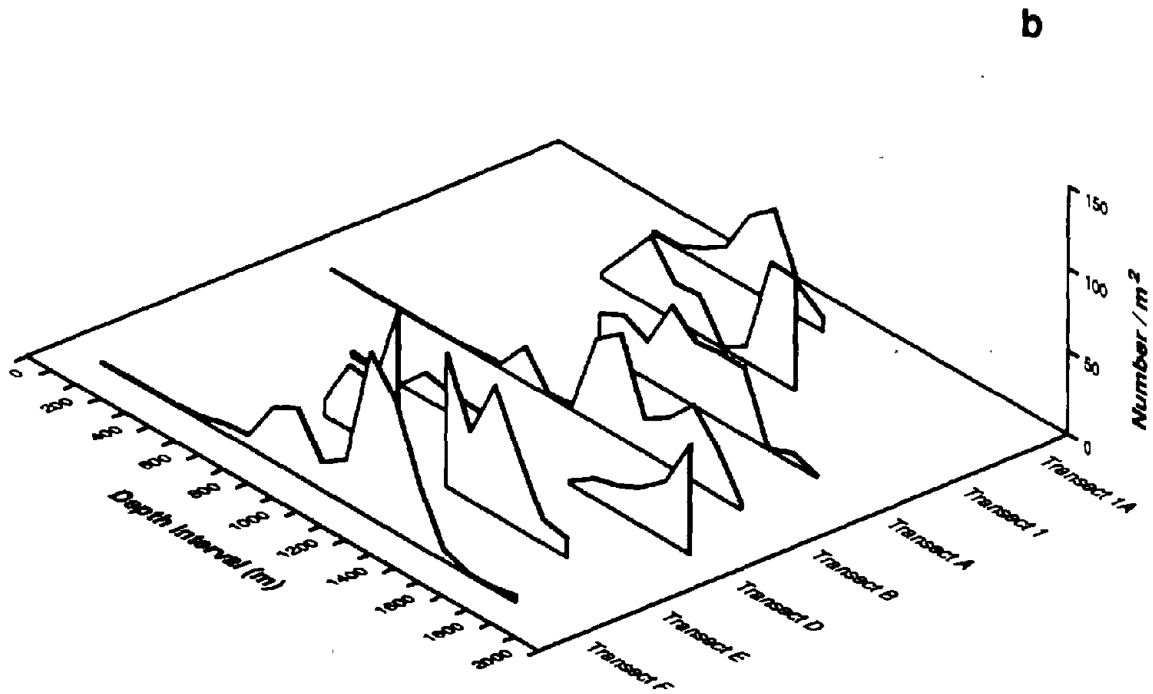
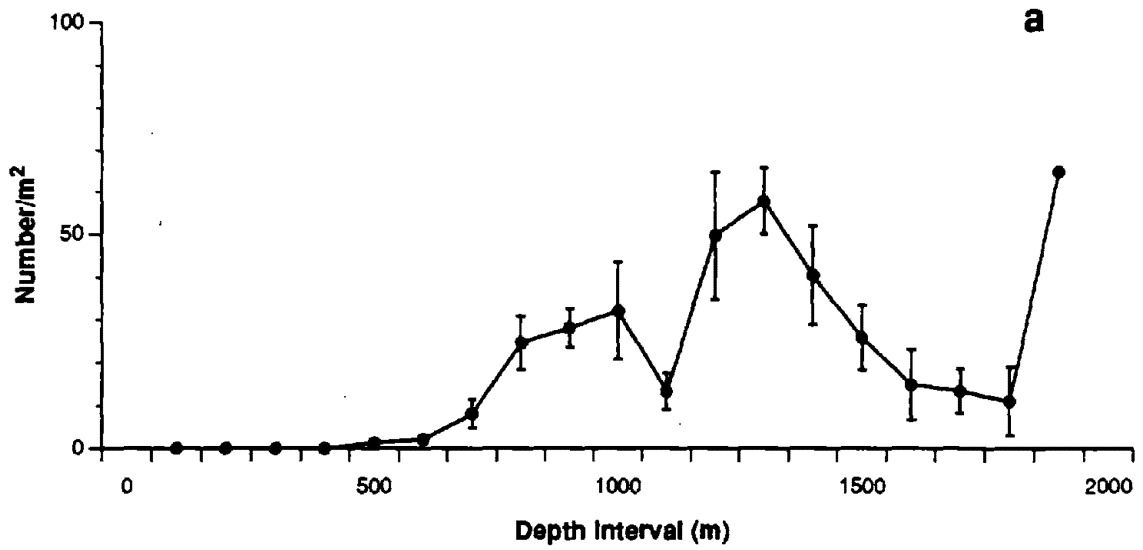
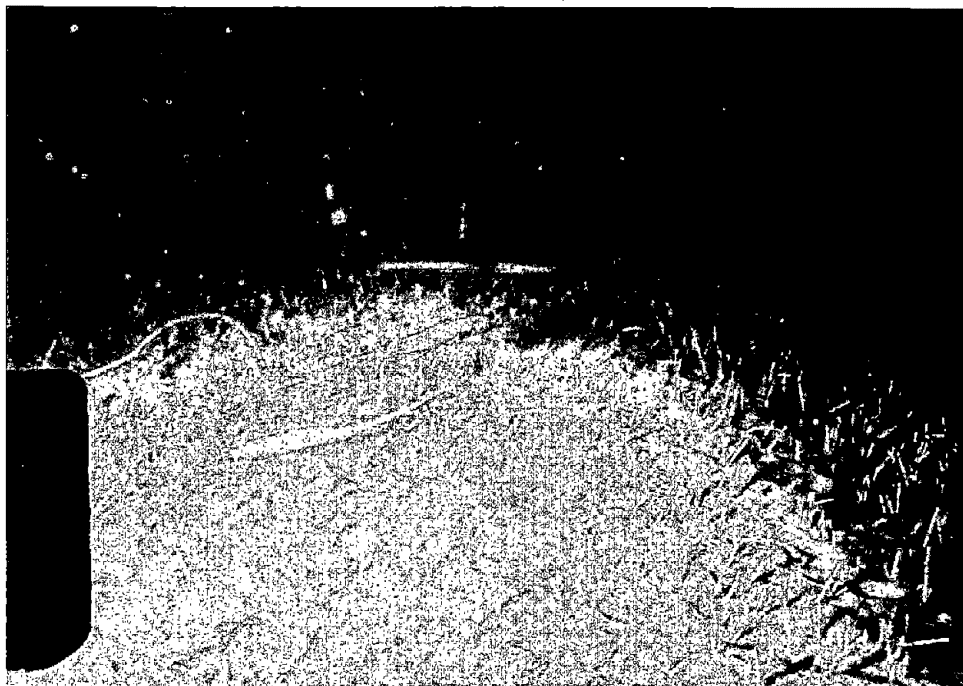


Figure 8-10. Density of the foraminiferan *Bathysiphon filiformis* with depth in (a) the study area and (b) along each of the transects. The number of samples used for each depth interval for the entire study area (a) can be seen on Table 1, and the error bars show standard errors.

(a)



(b)

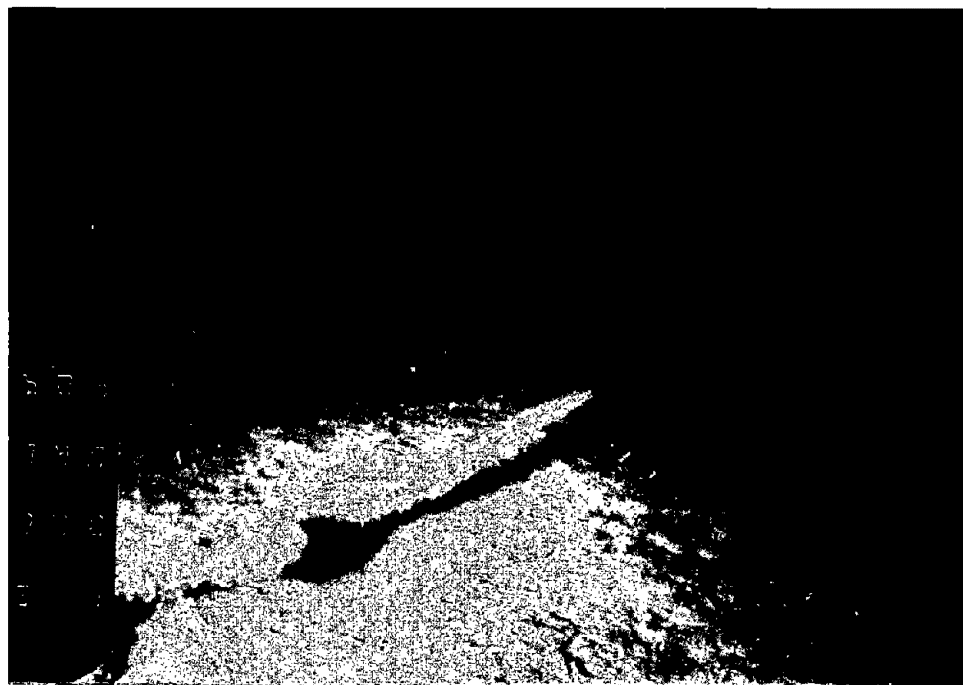
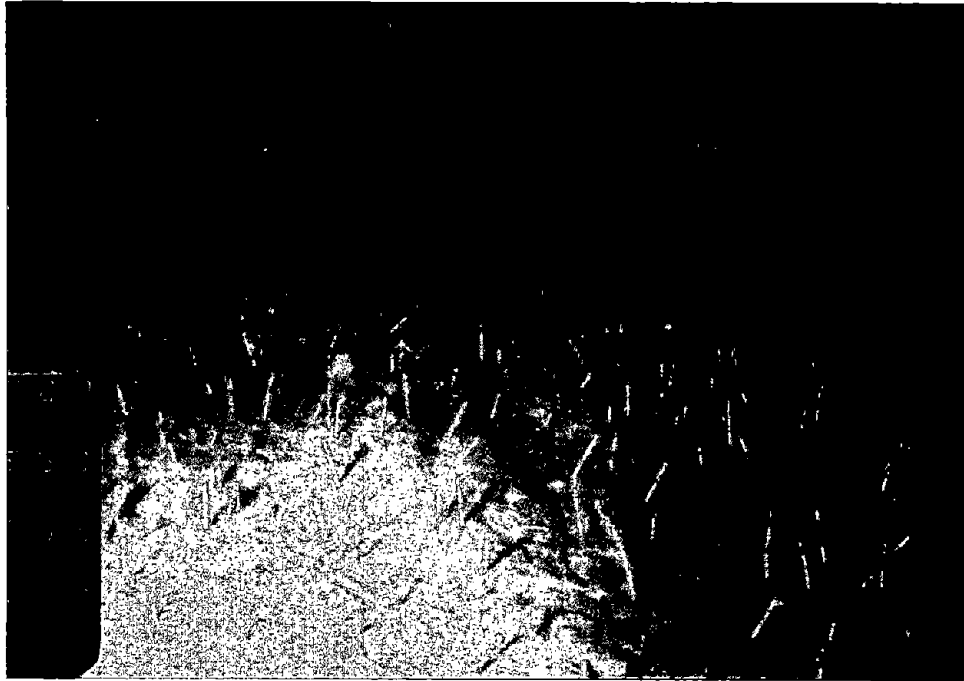


Figure 8-11. Photographs showing high and low densities of *Bathysiphon filiformis*: (a) 167 individuals m^{-2} , also three species of fish, *Aldrovandia* spp., *Dicrolene intronigra* and *Synaphobranchus* spp. (Transect A, 1,560 m); and (b) 13 individuals m^{-2} , also a *Synaphobranchus* spp. and feeding depressions (Transect B, 1,138 m).



(a)



(b)

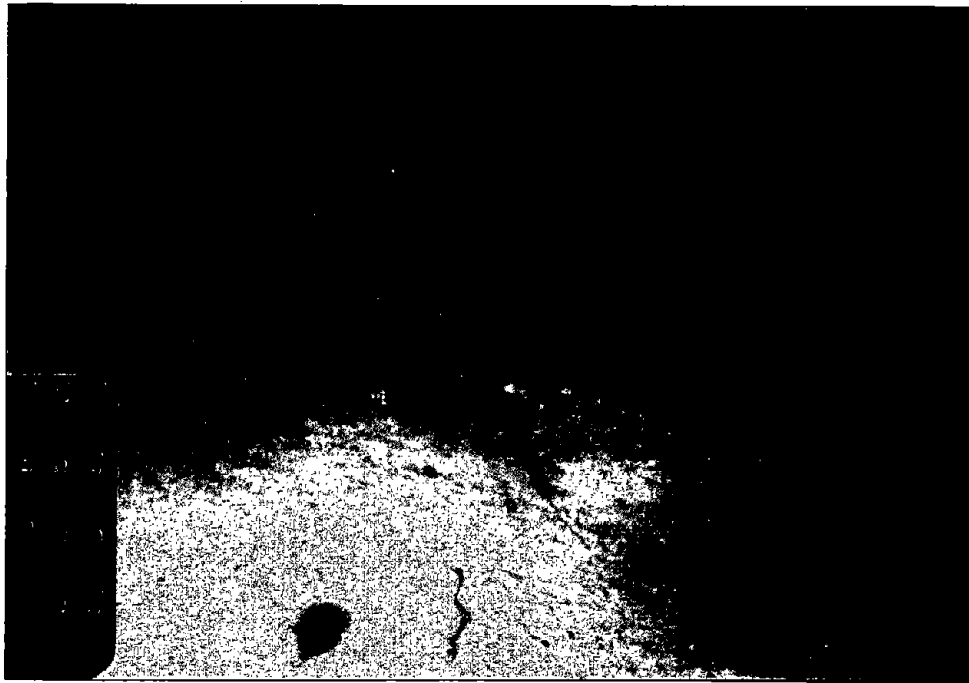


Figure 8-12. Photographs from Transect 1A (1138 m) showing the variability in the density of *Bathysiphon filiformis* over small horizontal distances (a) 75 *B. filiformis* m⁻², a contracted *Actinauge verrilli* and gastropod trails; and (b) the next photograph taken 8 meters further along the transect showing only one *B. filiformis* m⁻², *Lycenchelys verrilli*, a contracted *A. verrilli*, and the tracks of *Glyptocephalus cynoglossus*.



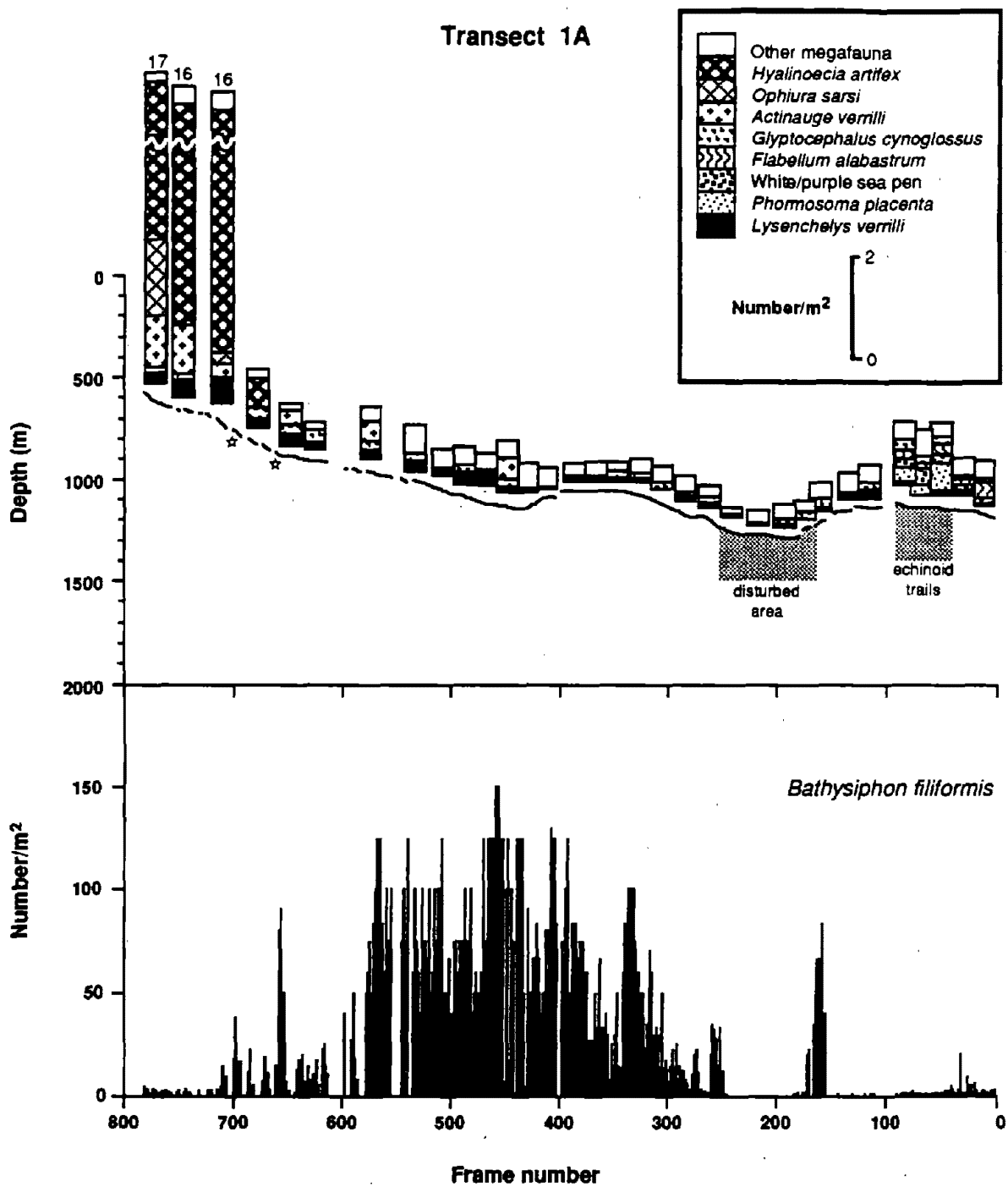
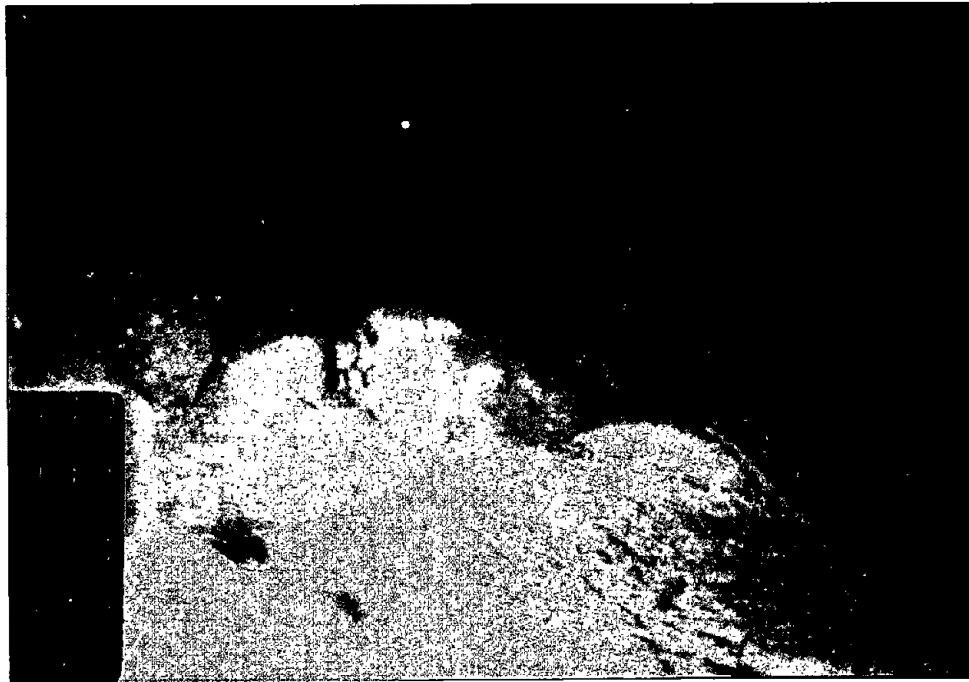


Figure 8-13. Topographic profile, sea-floor characteristics, and density of total megafauna, eight common species, and *Bathysiphon filiformis* along transect 1A. The topographic profile and *B. filiformis* densities are based on individual photographs, while the other faunal densities are based on groups of roughly 20 consecutive photographs. Stars represent subcrop.

(a)



(b)

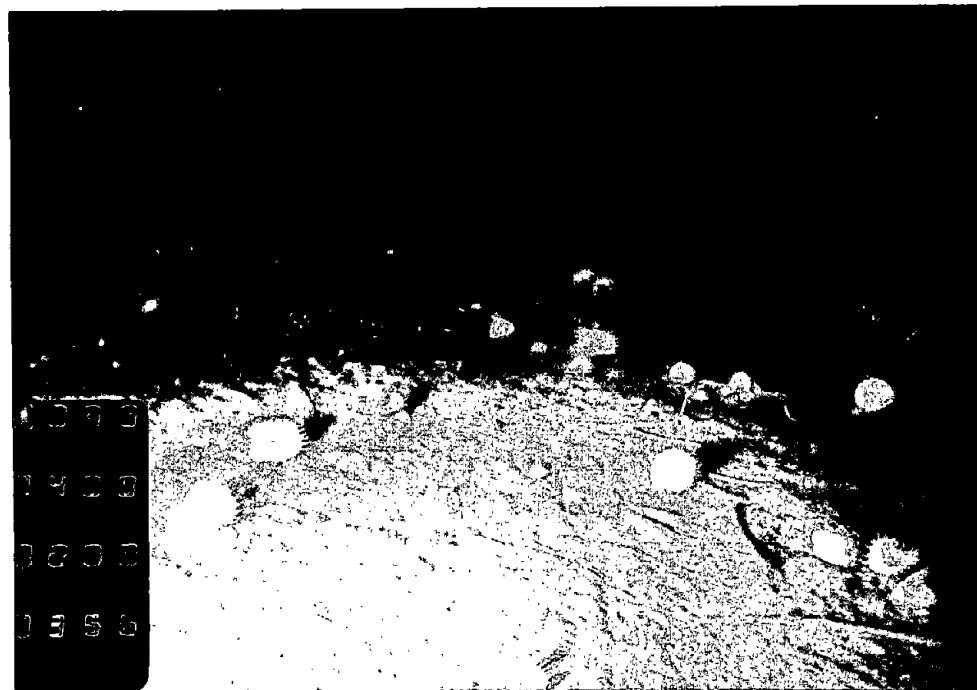


Figure 8-14.

Photographs showing two instances of sea-floor disturbance observed on the northern transects: (a) the remains of a debris flow and the scalloped tracks of *Glyptocephalus cynoglossus* in a gulley at the deeper end of Transect 1A, note the total absence of *Bathysiphon filiformis* (1,263 m); and (b) sediment-surface disturbance caused by the tubes of *Hyalinoecia artifex*, numerous juvenile *Actinauge verrilli* attached to the tubes, and only several *B. filiformis* at the shallower end of Transect 1 (756 m).



disturbed gully, and on the pock-marked ridge. Two of these instances of reduced abundances of *B. filiformis* may be related to the activity of other organisms. The reduced abundances in the shallower area may be related to disturbance of the sediment surface by the tubes of *H. artifex*. The sea floor in this region was totally covered by sinuous tracks of the large tubes of this polychaete. It is quite likely that the continual plowing of the sediment surface by echinoids at the deeper end of the transect may preclude successful settlement of the foraminiferans. The reduced abundances in the gully may reflect burial of the tubes by a debris deposit. Bent over anemones indicated the presence of strong currents at the shallower end of this transect.

Transect 1 was similar to 1A in that it consisted of a relatively flat slope with few outcrops and supported high densities of *H. artifex* at the shallower end (Figure 8-15). The tubes of this polychaete were colonized by numerous juveniles of *A. verrilli*. Several dense patches of an unidentified cerianthid anemone were found down-slope of this region. *Glyptocephalus cynoglossus* was the most abundant organism seen on the flat area in the middle of the transect. The sediment in this area was covered by the parallel scalloped lines caused by the movement of this flounder. No single species dominated the megafauna seen at the deeper end of the transect. The sea floor in part of this region was pitted by numerous feeding depressions of infaunal burrowers. The preference of *B. filiformis* for flat regions can best be seen in the deeper half of the transect. Few individuals were seen on the steep region near the middle of the transect (frames 300 to 400), but many were seen on the flat sea floor at the deep end (frames 10 to 290). The lower densities of *B. filiformis* on the flat slope at the middle of the transect may be related to disturbance of the sediment by the numerous *G. cynoglossus* that inhabit this region. Again, the reduced abundances at the shallowest end of the transect may be related to the activity of *H. artifex* (Figure 8-14b). The tubes of *B. filiformis* also were heavily fouled and appeared to be in the process of being buried on the steep slopes in this region.

The slope along Transect A was slightly steeper than at the two northern transects, and it exhibited more outcrops of consolidated clay (Figure 8-16). The sea floor at the deeper end of the transect was frequently interrupted by many biogenic mounds. The volcano-like morphology of these mounds indicates that they were probably formed by infaunal holothurians. Several regions of numerous feeding depressions (pits) were also seen in the vicinity of the middle of the transect. *A. verrilli* and *L. verrilli* dominated the fauna found on the relatively steep sediment slope at the shallower end of this transect. The sparse fauna inhabiting the sea floor down-slope of this region was frequently dominated by *Lycodes atlanticus*. *Ophiomusium lymani*, *Kophobelemnion stelliferum*, and *Distichoptilum gracile* dominated the abundant megafauna seen in the deeper end of this transect. The distribution of *B. filiformis* again appeared to be partially influenced by slope topography. A good example of this influence can be seen in the high density of this foraminiferan on a flat section near the middle of the transect (frames 1,090 to 1,140). The greatly reduced numbers of *B. filiformis* on the lower slope may be related to a combination of sediment instability caused by the formation of biogenic mounds and surface disturbance by *O. lymani* and a large holothurian (*Paelopatides gigantea*).

The slope along Transect B was moderately steep and was occasionally interrupted by outcrops and sediment-draped outcrops (Figure 8-17). Many of the outcrops on this transect appeared weathered, and the shallower ones were frequently colonized by brachiopods, polychaetes, sponges, and hydroids (Figure 8-18a). The shallower portion of the middle slope (500 to 1,100 m) was frequently disturbed by large excavations. This area supported relatively high abundances of *L. verrilli* and *A. verrilli*, and moderate abundances of *G. cynoglossus*. The sparse fauna inhabiting the lower portion of the middle slope consisted mostly of fish and was not dominated by any single species. An extensive area of numerous feeding depressions (pits) was also seen in this region. In contrast to Transect A, the lower slope of Transect B supported very few organisms. Biogenic mounds were also seen at the deeper end of this transect. The low densities of *B. filiformis* above 1,100 m may be related to a combination of steep topography and the numerous excavations seen in this area. The relatively flat lower portion of the middle slope supported moderate to high abundances of this foraminiferan. Very few tubes were seen in the region of outcrops at the deep end of the slope. The moderate to low densities of *B. filiformis* at the end of the transect appeared to be related to the mounding. In this region, the tubes frequently occurred in lines between adjacent mounds, and in many instances tubes on the sides of mounds were being buried (Figure 8-18b).

Transect D had the roughest topography encountered during this study (Figure 8-19). Most of the very steep upper and middle slope was interrupted by numerous outcrops of consolidated clay (Figure 8-20a). Most

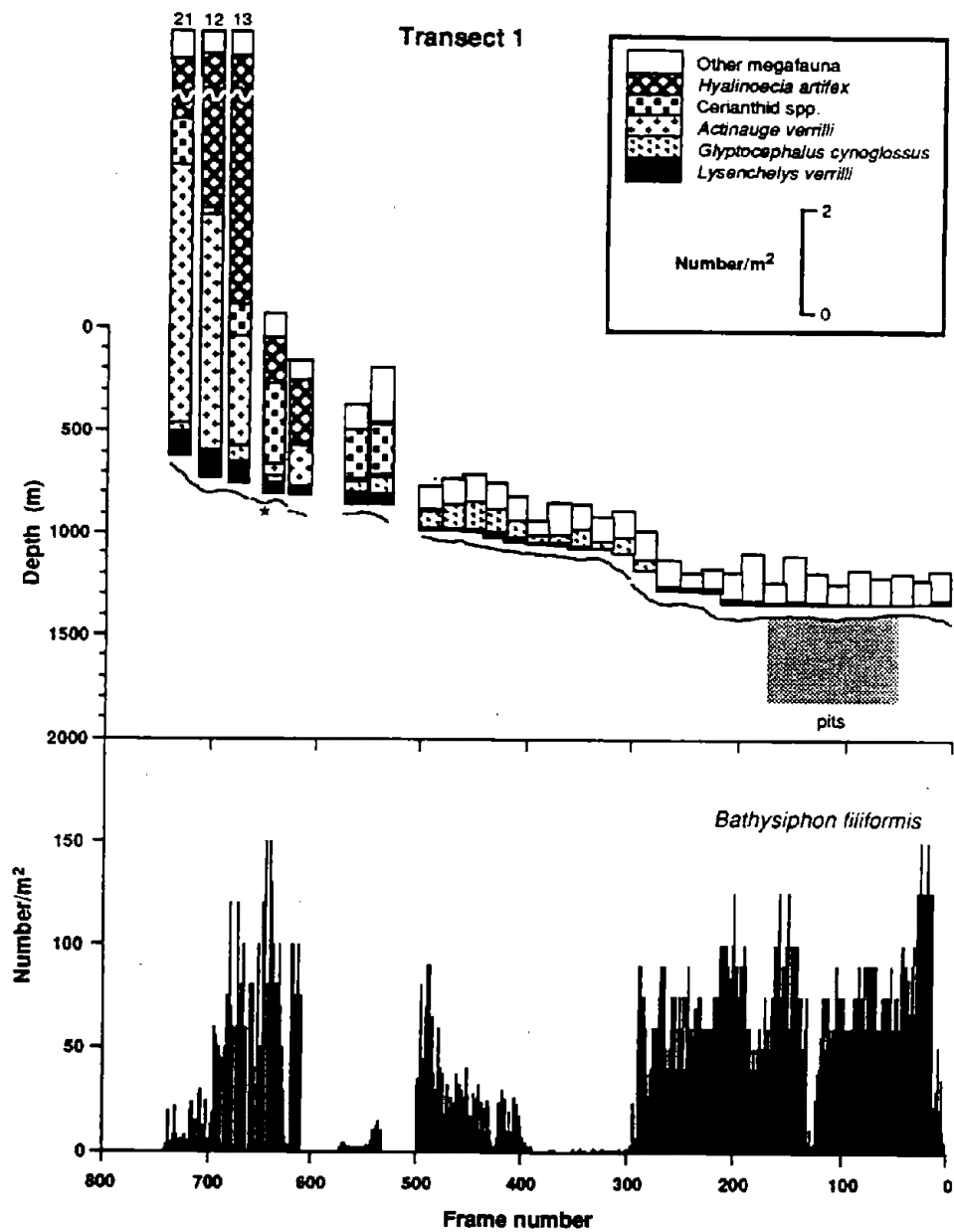


Figure 8-15. Topographic profile, sea-floor characteristics, and density of total megafauna, five common species, and *Bathysiphon filiformis* along transect 1. The topographic profile and *B. filiformis* densities are based on individual photographs, while the other faunal densities are based on groups of roughly 20 consecutive photographs. The star represents outcrop.

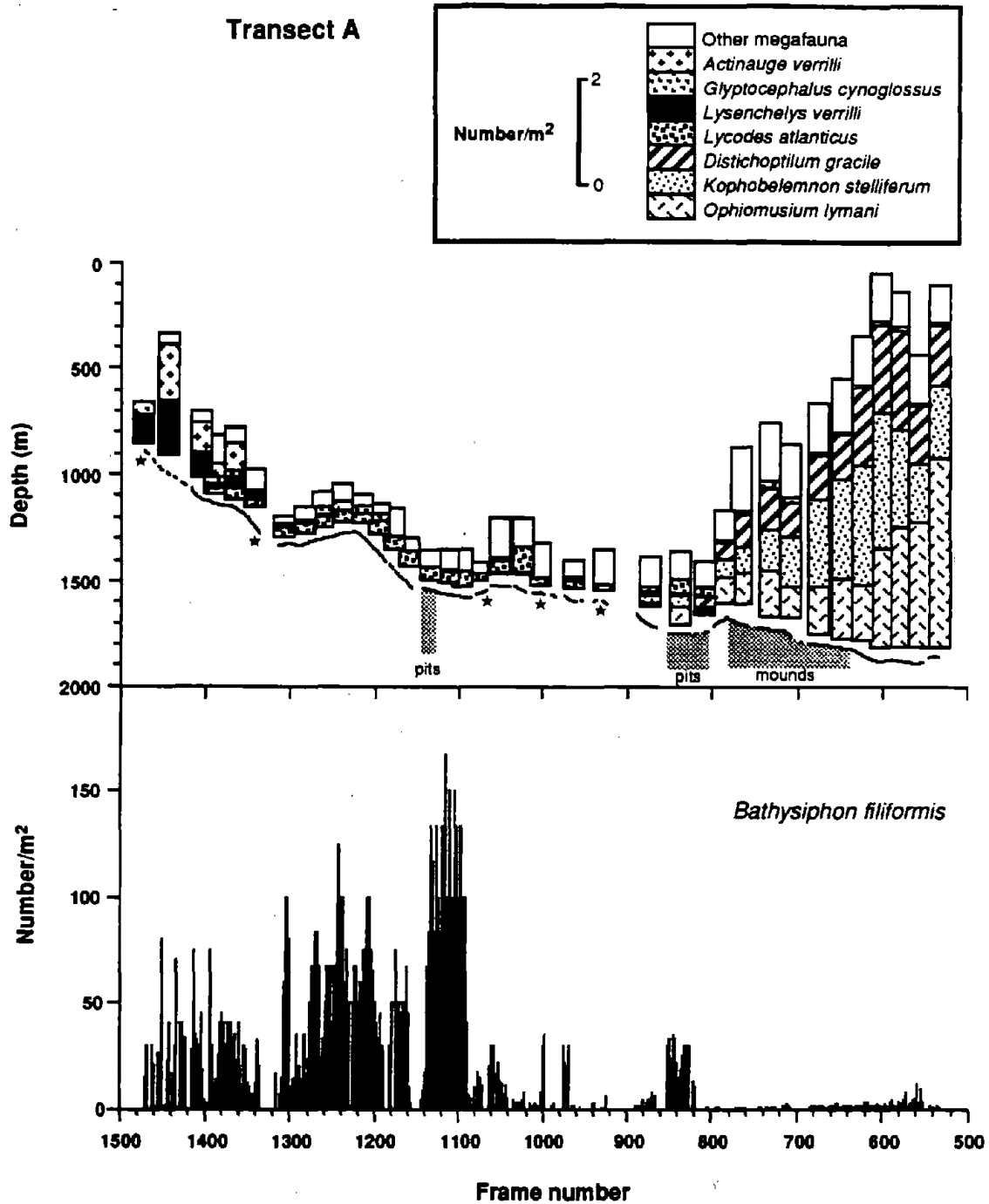


Figure 8-16. Topographic profile, sea-floor characteristics, and density of total megafauna, seven common species, and *Bathysiphon filiformis* along transect A. The topographic profile and *B. filiformis* densities are based on individual photographs, while the other faunal densities are based on groups of roughly 20 consecutive photographs. Stars represent outcrop.

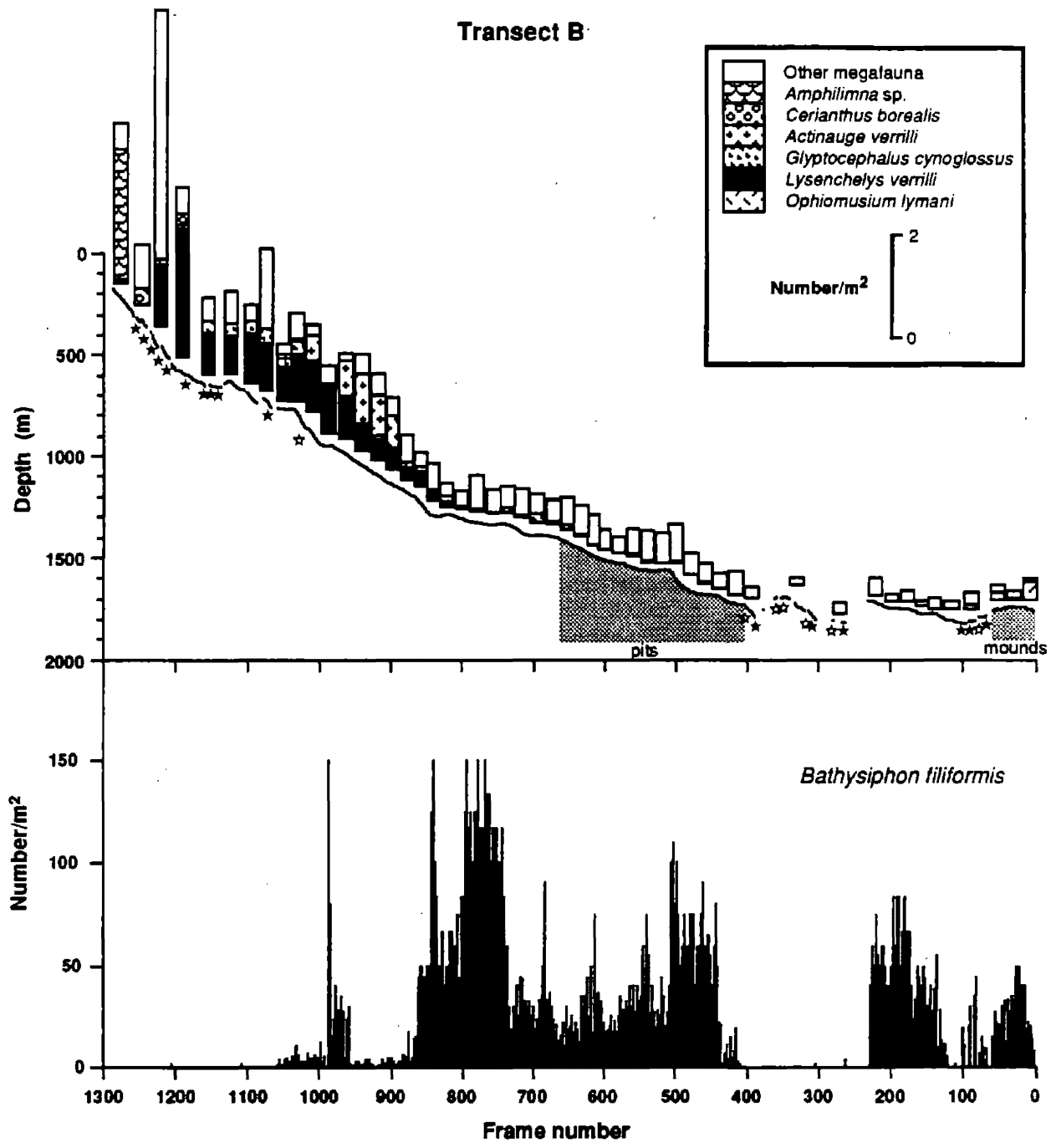
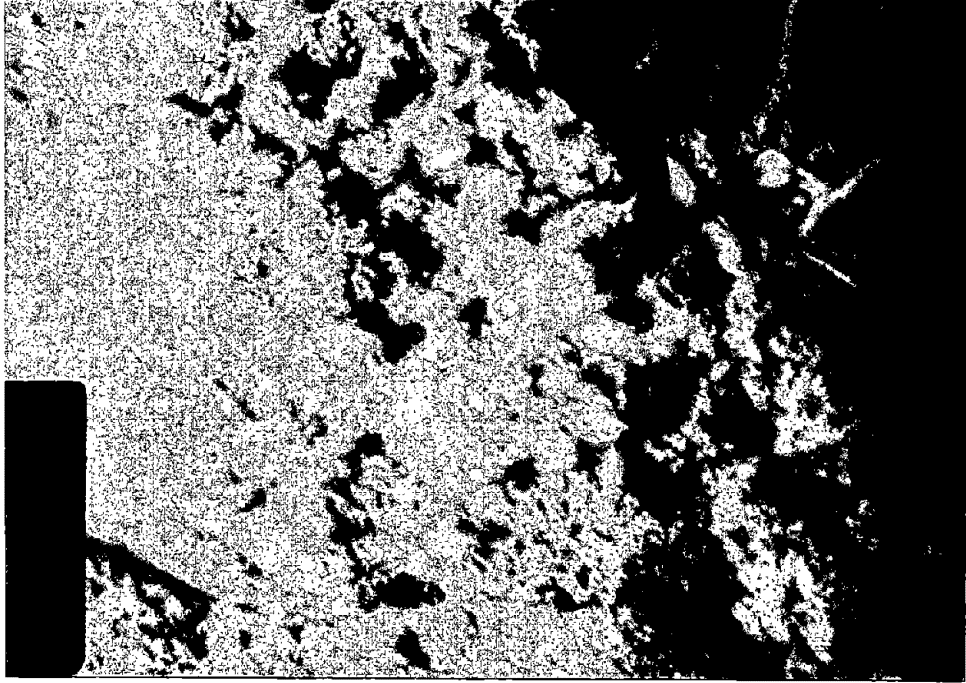


Figure 8-17. Topographic profile, sea-floor characteristics, and density of total megafauna, six common species, and *Bathysiphon filiformis* along transect B. The topographic profile and *B. filiformis* densities are based on individual photographs, while the other faunal densities are based on groups of roughly 20 consecutive photographs. Filled stars represent outcrop and open stars represent subcrop.

(a)



(b)

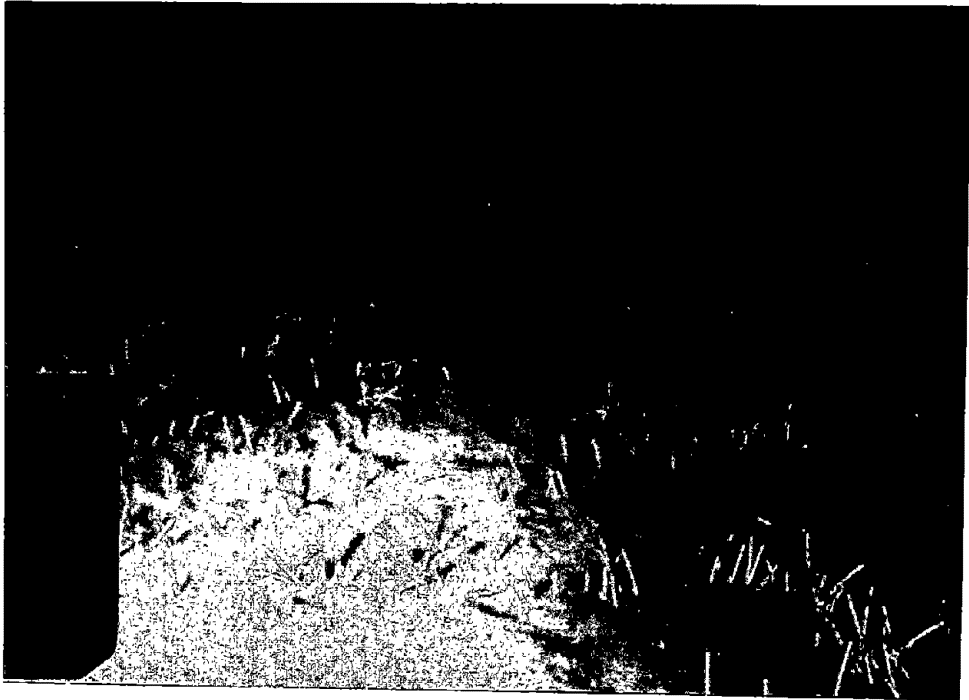


Figure 8-18. Photographs of two habitats observed on Transect B: (a) a weathered outcrop colonized by brachiopods, polychaetes, and hydroids (511 m); and (b) biogenic mounds showing the negative impact of sediment movement on *Bathysiphon filiformis*, the tubes are linearly arranged between the mounds, note the lack of megafauna (1,736 m).



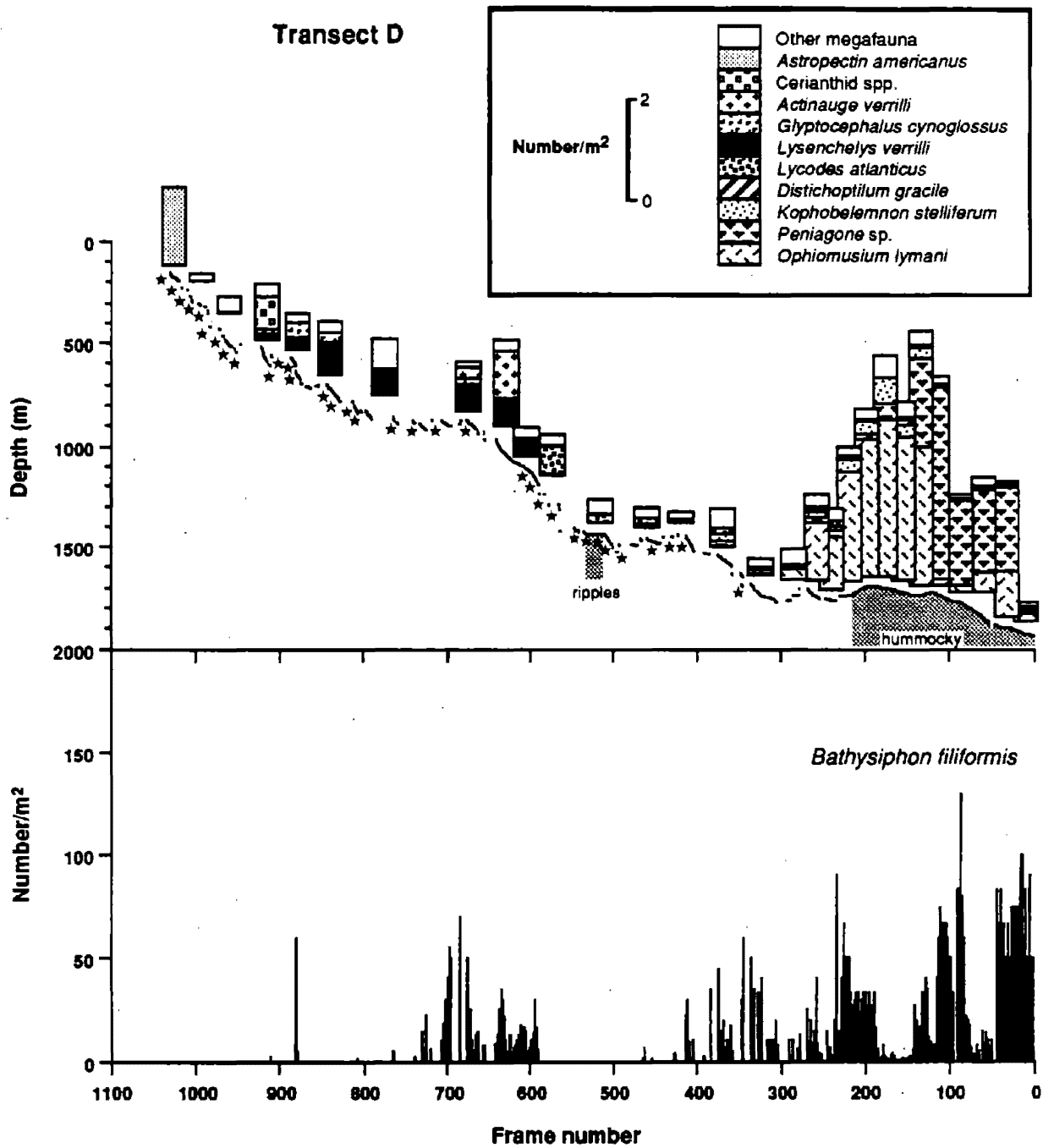
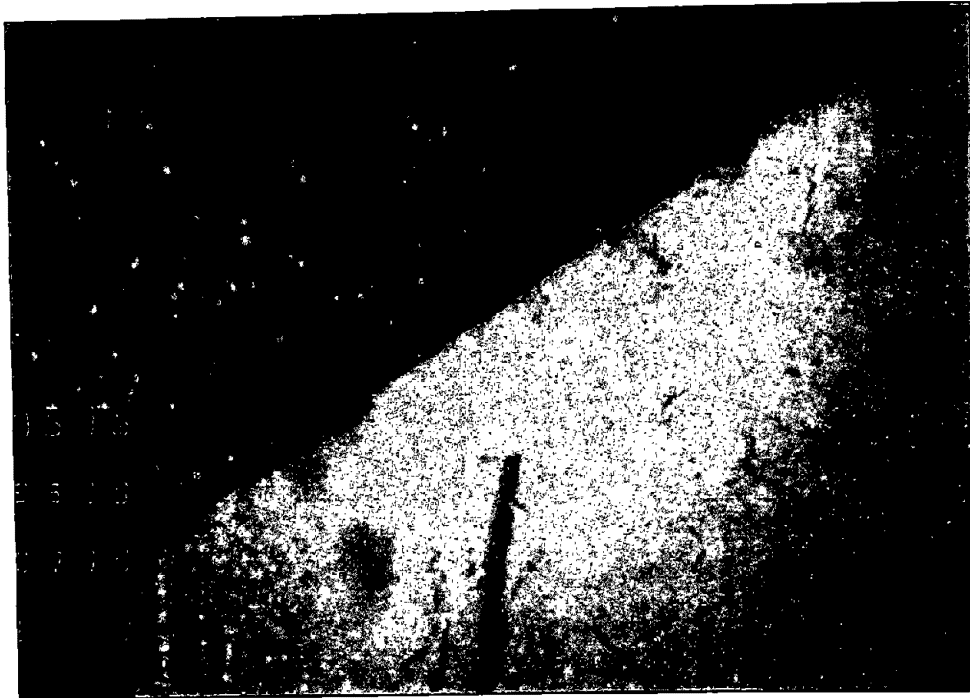


Figure 8-19. Topographic profile, sea-floor characteristics, and density of total megafauna, 10 common species, and *Bathysiphon filiformis* along transect D. The topographic profile and *B. filiformis* densities are based on individual photographs, while the other faunal densities are based on groups of roughly 20 consecutive photographs. Stars represent outcrop.

(a)



(b)

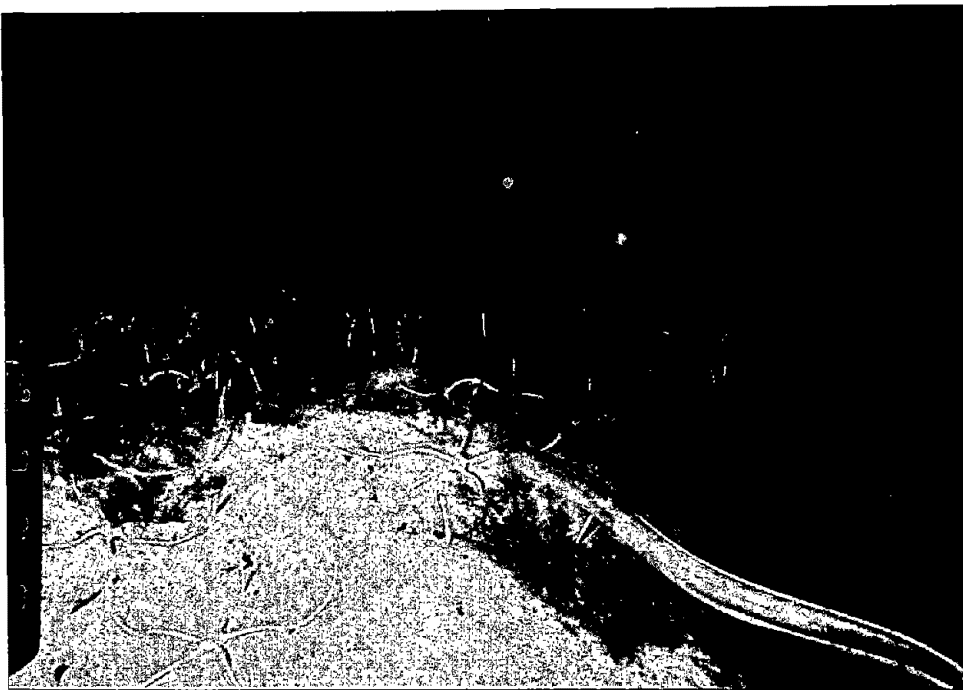


Figure 8-20. Photographs of two habitats observed on Transect D: (a) a fresh outcrop showing the scallops of recent spauling and no colonization of the surface, and a *Synaphobranchus* spp. (1435 m); and (b) biogenic mounds superimposed on a hummocky terrain, *Synaphobranchus* spp., *Ophiomusium lymani*, *Kophobelemnion stelliferum*, *Peniagone* sp. (small holothurian at lower left corner), and numerous *Bathysiphon filiformis* (1729 m).



of the middle slope was also dissected by a series of gullies and ridges (note the zigzag pattern of the depth profile). Numerous excavations were seen on the steep walls of the ridges in this region. A small area of ripple marks indicating sporadic strong current intensities was seen at the deeper end of the middle slope. The relatively flat lower slope was characterized by an undulating, hummocky terrain (on a horizontal scale of >1 m) that may be a sediment-covered debris-flow deposit. Biogenic mounds (on a horizontal scale of <1 m) were superimposed on these hummocks (Figure 8-20b). *Astropectin americanus* totally dominated the fauna seen on the few photographs taken at the extreme shallow end of this transect. The sparse fauna inhabiting outcrops immediately down-slope of this area was not dominated by any single species. A cerianthid anemone was observed on the steep slope below this region. The fauna inhabiting the ridges down-slope of this region was largely dominated by *L. verrilli*. Slightly further down-slope the fauna was dominated by a combination of *A. verrilli* and *L. verrilli*. On the deeper portion of the middle slope the fauna was dominated by *Lycodes atlanticus*. The lower slope of this transect supported high densities of *O. lymani* in the shallower end and moderate to high densities of a small holothurian, *Peniagone* sp., in the deeper end. This holothurian usually occurs in dense aggregations that actively migrate to regions of high nutrient content in the sediment and was not seen at any of the other transects. The very sparse distribution of *B. filiformis* along this transect appears to be a reflection of both the patchy coverage and steep topography. The sporadic densities of this foraminiferan on the lower slope may be related to a combination of disturbance by the mounding activity of infaunal holothurians and the surface disturbance of *O. lymani*. The numerous *Peniagone* sp. seen in this area did not appear to have a negative impact on the abundance of *B. filiformis*. This is not surprising since *Peniagone* sp. is probably not a permanent resident of this area, and it also does not visibly disturb the sediment surface.

Topography along Transect E was considerably more benign than that encountered along Transect D (Figure 8-21). The biogenic mounds found at the deeper end of this transect were asymmetric, indicating strong bottom currents. The outcrops at the shallower end of this transect were weathered and encrusted by organisms. Very high abundances of *L. verrilli* were seen down-slope of the outcrops. Further down the slope the sparse megafauna was dominated by a large red shrimp that was not seen in appreciable numbers at any of the other transects. The fauna on the lower slope was dominated by *O. lymani* and *K. stelliferum*. *B. filiformis* was found in moderate to high densities throughout most of the middle slope. Very few of these foraminiferans were seen on the lower slope, possibly as a result of surface disturbance by *O. lymani*.

The slope along Transect F was relatively steep and was occasionally interrupted by outcrops of consolidated clay (Figure 8-22). Intersecting "interference ripples" were seen on the sandy sea floor at the shallow end of the transect. The flat sea floor down-slope of this region consisted of a large expanse of lithified sand (hardground) that was overlain by cobble-sized glacial erratics at the shallower end and broken into rubble at the deeper end (Figure 8-23a). The ripples and exposed sandstone indicate the occurrence of sporadic, strong bottom currents in this region. Numerous feeding depressions (pits) were seen slightly down-slope of this region. The flat sandy sea floor at the shallowest end of this transect supported very few megafaunal organisms. Slightly deeper, relatively high densities of *A. americanus* were found in the rippled area. The hardground area supported sparse densities of fish and anemones at its shallow end and moderate densities of a small, unidentified translucent crustacean (possibly a large mysid) at its deeper end. The sediment sea floor down-slope of the hardground region supported high densities of a megafauna that was frequently dominated by anemones. *Bolocera tuidiae* dominated the fauna in the shallower area, and a cerianthid and *A. verrilli* dominated the fauna in several of the other areas. The megafauna found on two of the outcrops in this region was dominated by a small burrowing ophiuroid, *Amphilimna* sp. The steep slope further along this transect supported low densities of megafaunal organisms. The flat lower slope of this transect supported very high densities of *O. lymani* and moderate to low densities of *K. stelliferum* and *D. gracile*. The apparently patchy distribution of *B. filiformis* in the middle of this transect is largely a reflection of the sporadic coverage obtained in this region. The low density of this foraminiferan on the lower slope may be related to the numerous *O. lymani* found in this area (Figure 8-23b).

Community Analysis

Classification of 86 depth intervals and 50 species defined five major clusters (Figure 8-24). The clustering structure was largely determined by depth. Similarities of fauna within the clusters were relatively

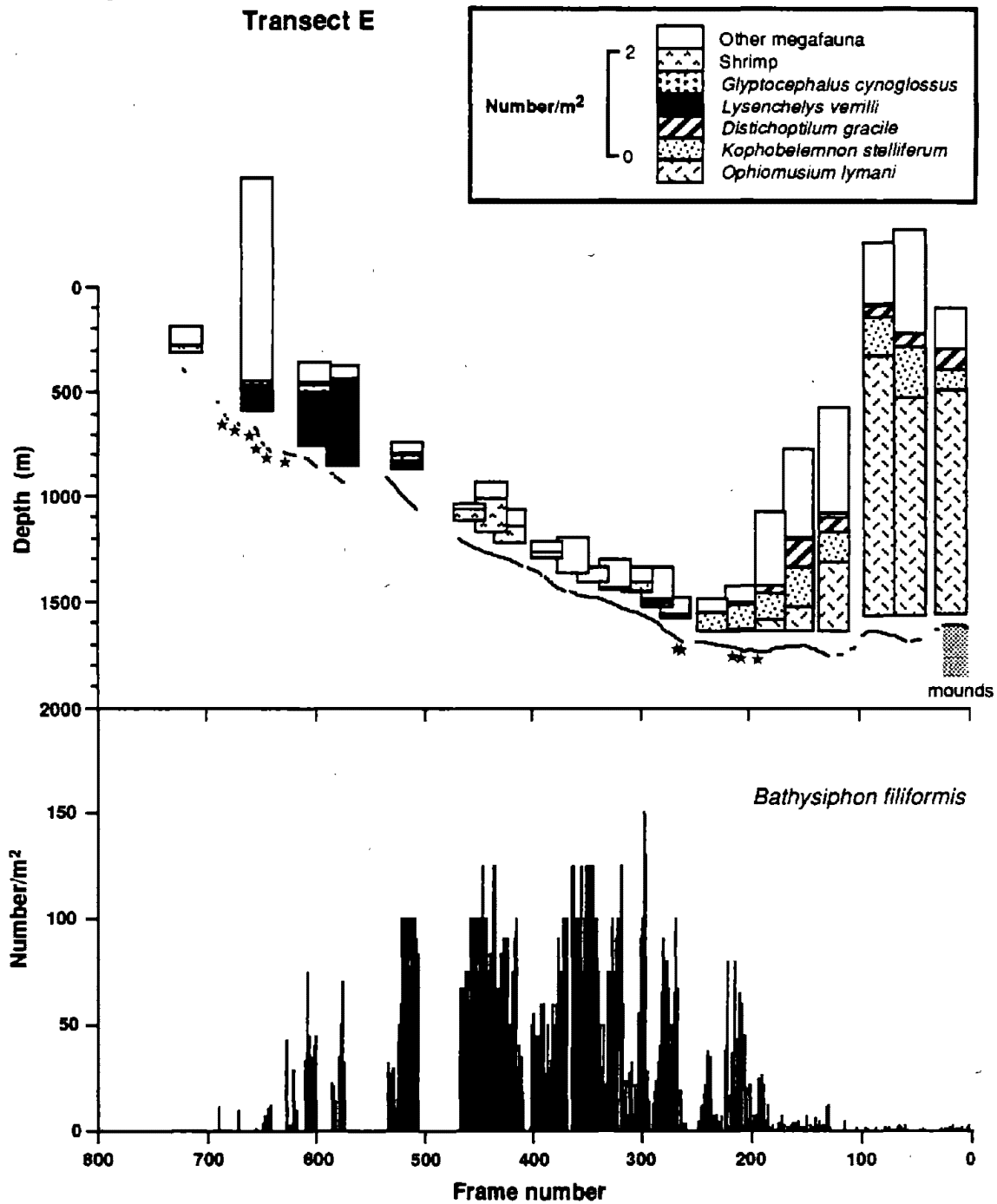


Figure 8-21. Topographic profile, sea-floor characteristics, and density of total megafauna, six common species, and *Bathysiphon filiformis* along transect E. The topographic profile and *B. filiformis* densities are based on individual photographs, while the other faunal densities are based on groups of roughly 20 consecutive photographs. Stars represent outcrop.

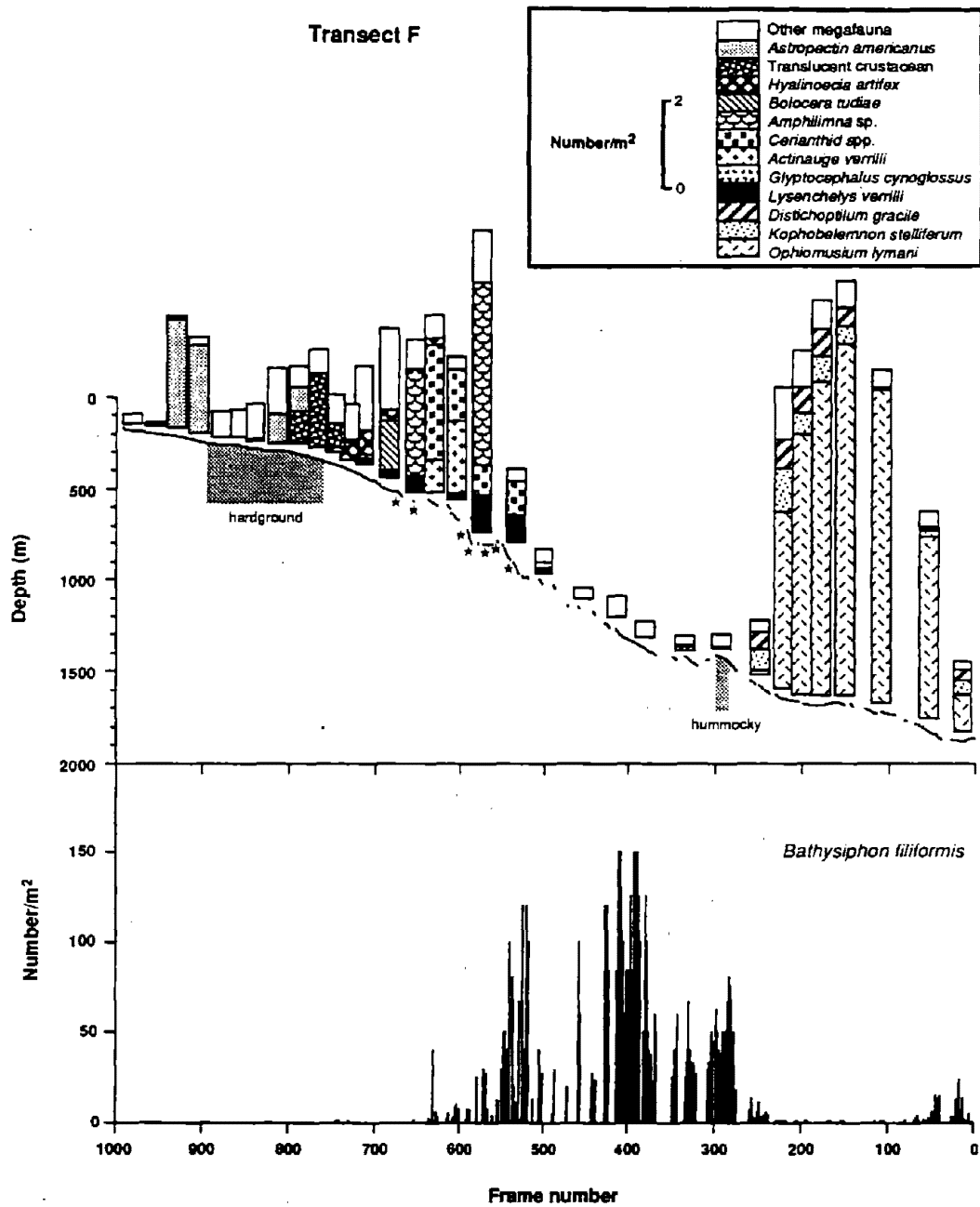


Figure 8-22. Topographic profile, sea-floor characteristics, and density of total megafauna, 12 common species, and *Bathysiphon filiformis* along transect F. The topographic profile and *B. filiformis* densities are based on individual photographs, while the other faunal densities are based on groups of roughly 20 consecutive photographs. Stars represent outcrop.

(a)



(b)



Figure 8-23. Photographs of two habitats observed on Transect F: (a) the hardground area of lithified sand rubble with the anemone *Halcurias pilatis* at 326 m; and (b) the flat lower slope showing sediment disturbance by *Ophiomusium lymani* and the holothurian *Paelopatides gigantea*, a fecal cast from *P. gigantea* (right side), and only one *Bathysiphon filiformis* (1718 m).



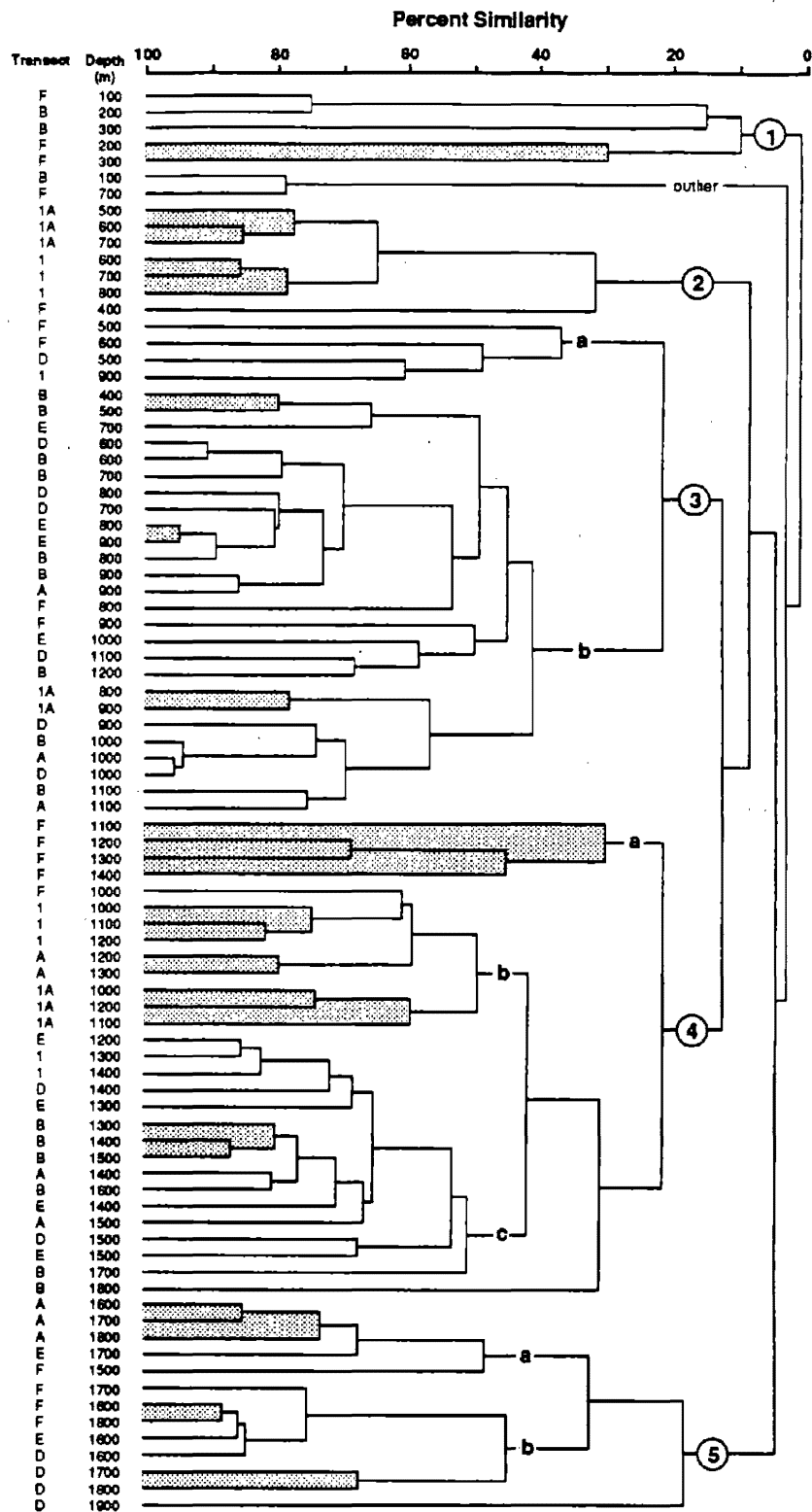


Figure 8-24. Hierarchical classification of 100-m depth intervals from the camera-sled tows. The circled numbers and letters on the dendrogram represent major clusters and groups of areas. Shaded areas highlight contiguous intervals within a transect.

low (<22%). The first cluster consisted of depth intervals from the upper slope. The next two clusters (2 and 3) consisted of depth intervals from the upper portion of the middle slope. The fourth cluster consisted of depth intervals from the lower portion of the middle slope of all transects and from the lower slope of Transect B. The last cluster consisted of depth intervals from the lower slope of the remaining transects. The three major clusters of middle and lower slope depth intervals (3, 4, 5) further separated into groups of intervals with higher levels of faunal similarity. The depth range and fauna indicative of each cluster group are presented in Table 8-3, and the cluster group designations for the depth intervals from each transect are presented in Table 8-4. Faunal breaks occurred at 800 and 1,000 m on Transect 1A, between 900 and 1,000 m on Transect 1, at 1,200 and 1,600 m on Transect A, at 400 and 1,300 m on Transect B, between 1,200 and 1,400 m and at 1,600 m along Transect D, between 1,000 and 1,200 m and at 1,600 m on Transect E, and at 400, 500, 1,000 and 1,500 m along Transect F.

The low faunal similarities among depth intervals from the upper slope (cluster 1) indicate that the faunal distributions are quite patchy in this region. The Jonah crab *Cancer* spp., and the burrowing anemone *Cerianthus borealis* were found in most regions of the upper slope. Two other species, the starfish *Astropectin americanus* and the translucent crustacean, were alternately found in some areas and not in others. Megafaunal densities were generally quite low on the upper slope. The megafauna in the shallowest interval from Transect B (100 m) also supported high abundances of a burrowing ophiuroid, *Amphilimna* sp. This area had highest faunal similarities with the 700-m interval from Transect F, which was also inhabited by this ophiuroid.

The depth intervals from the upper portion of the middle slope grouped into two clusters depending on location. The depth intervals from the shallow end of the two northern transects formed one cluster (2), and most of the remaining intervals formed another cluster (3). Most of the upper-middle slope was inhabited by *Actinauge verrilli*, a cerianthid, and *Lycenchelys verrilli*, and *Glyptocephalus cynoglossus*. The shallower end of both northern transects was also inhabited by *Hyalinoecia artifex*. The remaining areas largely separated on the basis of the relative proportions that three of these species contributed to their faunal composition. Four of the areas (group 3a) supported higher abundances of cerianthids and *A. verrilli*. The remaining areas (group 3b) generally supported higher abundances of *L. verrilli*. Most areas on the upper-middle slope supported moderately high megafaunal abundances.

Three fish, *Synaphobranchus* spp., *Lycodes atlanticus*, and *G. cynoglossus*, were found throughout most of the lower portion of the middle slope (cluster 4). The shallower areas in this region (group 4b) supported higher densities of *G. cynoglossus* and *Synaphobranchus* spp., while the deeper areas (group 4c) supported higher densities of *L. atlanticus*. Four depth intervals from Transect F (group 4a) supported lower densities of all three species, particularly *G. cynoglossus* and *L. atlanticus*. The lower-middle slope generally supported low faunal abundances. The depth intervals from the lower slope of Transect B clustered into group 4c. This was largely a reflection of the low faunal densities found in this area.

Megafauna on the lower slope was primarily dominated by *Ophiomusium lymani*. The lower slope of Transect A (group 5a) generally supported lower densities of *O. lymani* and higher densities of *Kophobelemnion stelliferum* and *Distichoptilum gracile*, while the remainder of the lower slope (group 5b) generally supported higher densities of the ophiuroid and lower densities of both sea pens. The lower slope generally supported high megafaunal abundances.

Figure 8-25a shows the ordination of the depth intervals and Figure 8-25b the ordination of species within the same ordination space (only the dominant species are shown on this figure). The upper slope depth intervals were omitted from this analysis because the patchiness of the upper slope fauna introduced too much variance. Axis 1 appears to represent the depth gradient across the middle slope, with upper-middle slope areas (clusters 2 and 3) having low values and the lower slope having high values. The second axis further separated the upper-middle slope areas, with areas from the northern transects (cluster 2, Transects 1A and 1) having low values and the areas from the other transects (cluster 3) having higher values. Areas that contained colonized outcrops (from Transect B) had the highest values on this axis. Areas characterized by extensive outcrop had low values on axis 3. The analysis indicates that the most pronounced faunal break occurs at the base of the middle slope, and a slightly less pronounced break occurs between the upper-middle slope and the lower-middle slope. The cluster designation of several of the depth intervals were modified based on the ordination analysis (Table 8-4).

Table 8-3. Density of dominant megafaunal species in the clusters (Figure 8-24) defined by classification analysis of the 100-m depth interval data. Depth ranges and location of the intervals are also listed. Densities are mean \pm standard error of the number of individuals 100-m² in the interval within the cluster group.

Cluster Group	Upper Slope	Upper-Middle Slope				Lower-Middle Slope			Lower Slope	
	1	outlier	2	3a	3b	4a	4b	4c	5a	5b
Transect	B,F	B,F	1A,1,F	F,D,1	*	F	*	*	A,E,F	F,D,E
Depth Interval	100-399	100/700	400-899	500-999	400-1299	1100-1499	1000-1399	1200-1899	1600-1899	1600-1899
<i>Cancer borealis</i>	10 \pm 5	13	2 \pm 2	-	-	-	-	-	-	-
<i>Cerianthus borealis</i>	11 \pm 7	-	12 \pm 9	6 \pm 5	1 \pm 1	-	-	-	-	-
<i>Amphilimna</i> sp.	-	618	-	3 \pm 3	1 \pm 1	-	-	-	-	-
<i>Hyalinoecia artifex</i>	2 \pm 2	-	905 \pm 250	-	-	-	-	-	-	-
<i>Actinauge verrilli</i>	-	-	163 \pm 73	48 \pm 37	21 \pm 6	-	1 \pm 0	-	-	-
<i>Cerianthid</i> sp.	-	45	42 \pm 24	82 \pm 32	4 \pm 3	-	-	-	-	-
<i>Lycenchelys verrilli</i>	-	18	35 \pm 7	10 \pm 1	64 \pm 10	-	3 \pm 1	-	-	-
<i>Glyptocephalus cynoglossus</i>	-	-	15 \pm 3	11 \pm 6	10 \pm 1	-	18 \pm 3	1 \pm 1	-	-
<i>Lycodes atlanticus</i>	-	-	2 \pm 1	2 \pm 2	3 \pm 1	-	10 \pm 2	18 \pm 2	6 \pm 2	2 \pm 1
<i>Synaphobranchus</i> spp.	-	-	1 \pm 1	1 \pm 1	1 \pm 0	5.4 \pm 2.2	11 \pm 2	8 \pm 1	10 \pm 2	2 \pm 1
<i>Ophiomusium lymani</i>	-	-	-	-	-	-	-	-	61 \pm 31	309 \pm 85
<i>Kophobelemnion stelliferum</i>	-	-	-	-	-	-	-	2 \pm 1	74 \pm 29	26 \pm 8
<i>Distichoptilum gracile</i>	-	-	-	-	-	-	-	-	52 \pm 19	14 \pm 7
Total megafauna	98 \pm 29	777	1280 \pm 303	233 \pm 67	155 \pm 24	34 \pm 4	66 \pm 7	53 \pm 4	271 \pm 83	432 \pm 82

* depth intervals from more than three tows

Table 8-4. Cluster designations defined by hierarchical classification for the 100-m depth interval data on each of the transects. Numbers in parentheses indicate changes based on ordination analysis.

Depth Interval (m)	Transect						
	1A	1	A	B	D	E	F
100-199				*			1
200-299				1			1
300-399				1			1
400-499				3b			2(3b)
500-599	2			3b	3a(3b)		3a(3b)
600-699	2	2		3b	3b		3a(3b)
700-799	2	2		3b	3b	3b	*
800-899	3b	2		3b	3b	3b	3b
900-999	3b	3a(3b)	3b	3b	3b	3b	3b
1000-1099	4b	4b	3b	3b	3b	3b(4b)	4b
1100-1199	4b	4b	3b	3b	3b		4a
1200-1299	4b	4b	4b	3b(4b)		4c	4a
1300-1399		4c	4b	4c		4c	4a
1400-1499		4c	4c	4c	4c	4c	4a
1500-1599			4c	4c	4c	4c	5a
1600-1699			5a	4c	5b	5b	5b
1700-1799			5a	4c	5b	5a	5b
1800-1899			5a	4c	5b		5b
1900-1999					5(4c)		

* outliers

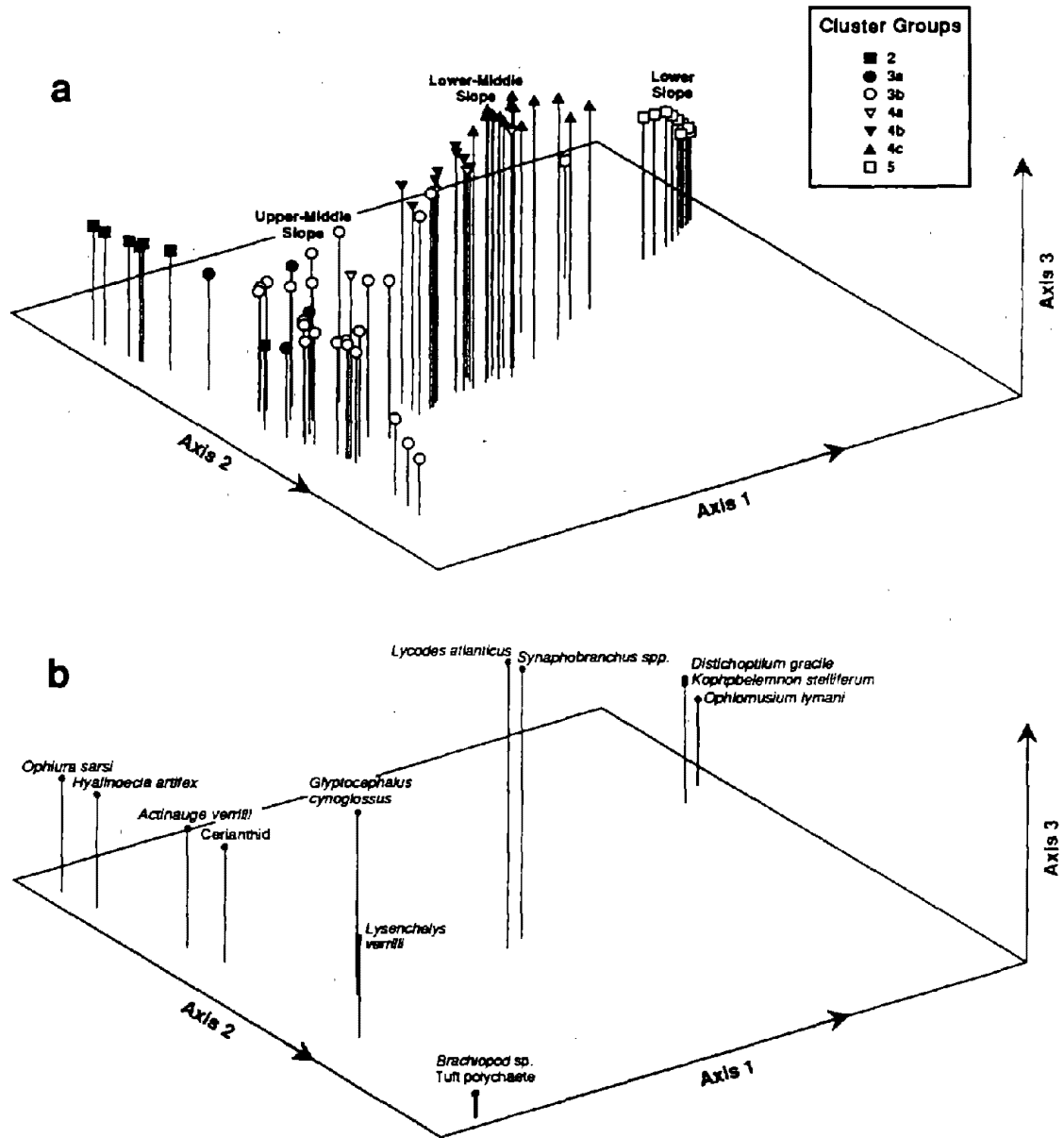


Figure 8-25. Reciprocal averaging ordination of the camera-pled data; (a) the 100-m depth intervals, and (b) the dominant species. The first three axes are plotted.

Discussion

The patterns of megafaunal density and zonation found in this study generally agree with the patterns observed on other portions of the U.S. continental slope (Hecker et al. 1983, Blake et al. 1985, 1987, Maciolek et al. 1987b, Hecker 1990a). These patterns generally reflected the distributions of several dominant species. The bimodal pattern of total megafaunal density with depth is a known phenomenon. Upper slopes generally support moderate to high abundances of anemones and fish, lower slopes generally support moderate to high abundances of echinoderms, and middle slopes generally support low abundances of fish (Hecker 1990a). The results from the present study diverge from this pattern in that higher abundances of megafauna were found on the middle slope off Cape Hatteras (Figure 8-26). At most of the other locations studied, megafaunal densities on the middle slope were below 0.50 individuals m^{-2} (Table 8-5). In contrast, densities were slightly higher off Long Bay (0.93 ± 0.20 individuals m^{-2}), much higher at the U.S./Canadian boarder (2.16 ± 0.57 individuals m^{-2}), and slightly to much higher off Cape Hatteras (0.88 ± 0.15 to 2.65 ± 0.95 individuals m^{-2} during 1985 and 1992, respectively). The high densities found in 1992 were largely attributable to very high abundances of the quill worm *Hyalinoecia artifex* on the two northern transects. This species is usually found at upper slope depths. However, densities were also higher on the middle slope of the other Cape Hatteras transects. The elevated densities of middle slope fauna found off Long Bay, the U.S./Canadian boarder, and Cape Hatteras are likely related to increased flux of organic carbon (Hecker 1990b, Blake et al. 1987, this report).

The pattern of megafaunal zonation with depth was also very similar to the pattern found on the slope off Georges Bank (Hecker 1990a) and other areas off North Carolina (Blake et al. 1985). Most of the dominant taxa found on the upper and lower slopes off Cape Hatteras, also dominated the fauna at other locations (Hecker et al. 1983, Blake et al. 1985, 1987, Maciolek et al. 1987b, Hecker 1990a). The unusual aspect of the slope off Cape Hatteras is seen in the taxa that dominate megafaunal assemblages on the middle slope, in the patchy distribution of the middle slope taxa, and in the exceptionally high densities of *Bathysiphon filiformis*. Extreme patchiness is generally the rule for the distribution of upper slope and submarine canyon species (Hecker et al. 1983, Hecker 1990a), but is rarely seen in the distributions of middle slope species. The patchiness observed on the middle slope off Cape Hatteras may well reflect the habitat heterogeneity of this exceptionally rugged slope.

The megafaunal assemblages on the continental slope off Cape Hatteras have previously been described by Blake et al. (1987). Using methods identical with the ones used in the present study, they reported that megafaunal densities off Cape Hatteras were slightly elevated and the taxonomic composition anomalous compared to other areas of the slope. In addition, the dominant species on the middle slope off Cape Hatteras were usually only a minor component of the megafauna at other locations. The most striking example of this was the high abundance of two demersal fish, the wolf eelpout *Lycenchelys verrilli* and the witch flounder *Glyptocephalus cynoglossus*. Although both species are widely distributed along the U.S. continental margin, they had not previously been found in such high abundances. Blake et al. (1987) related the high densities of these fish to the exceptionally high densities of infaunal prey in this region. Other differences that they noted included the absence of the quill worm *Hyalinoecia artifex* and the anemone *Bolocera tudiae*, lower abundance of the galatheid *Munida valida*, and higher abundance of the anemone *Actinauge verrilli*. They also noted that the megafauna found on the lower slope of this area was similar to that found at other locations. Additionally, Blake et al. (1987) mentioned finding exceedingly high densities of white tubes projecting from the sediment. These have subsequently been identified as belonging to the large foraminiferan, *Bathysiphon filiformis* (Gooday et al. 1992).

The results of the present survey support most of these earlier conclusions. The same species that were dominant in the Blake et al. (1987) study were also dominant in the present survey and high densities of *B. filiformis* tubes were observed along each of the transects. Furthermore, the present study has established the presence of these unusual assemblages over a much broader geographic area than previously observed (Blake et al. 1987, Mobil 1990, Gooday et al. 1992).

To illustrate the unusual nature of the megafaunal assemblages found on the slope off Cape Hatteras, plots of the density of *L. verrilli*, *A. verrilli*, *G. cynoglossus*, and *B. filiformis* with depth were generated for 10 locations along the eastern U.S. continental margin (Figures 8-27 and 8-28). The data for these locations were collected during a series of studies conducted between 1981 and 1986 to investigate megafaunal assemblages in

Table 8-5. Density of total megafauna (individuals m⁻²) on the middle slope at 10 locations on the eastern U.S. continental margin (Hecker et al. 1983, Blake et al. 1985, 1987, Hecker 1990a).

Location	Middle slope depths	Range	Mean \pm SE
Long Bay	600-1799	0.25-1.77	0.93 \pm 0.20
Cape Lookout	700-1599	0.15-0.87	0.49 \pm 0.08
Hatteras Canyon	800-1599	0.10-0.73	0.29 \pm 0.07
Cape Hatteras 1992	500-1599	0.48-10.19	2.65 \pm 0.95
Cape Hatteras 1985	500-1599	0.39-2.01	0.88 \pm 0.15
New Jersey 1	600-1499	0.14-1.63	0.46 \pm 0.16
New jersey 2	600-1499	0.13-0.45	0.24 \pm 0.04
Western Transect	700-1599	0.11-0.29	0.18 \pm 0.02
West Slope	500-1599	0.22-1.08	0.41 \pm 0.07
East Slope	600-1599	0.23-1.62	0.40 \pm 0.14
U.S./Canadian Boarder	500-1399	0.94-5.59	2.61 \pm 0.57

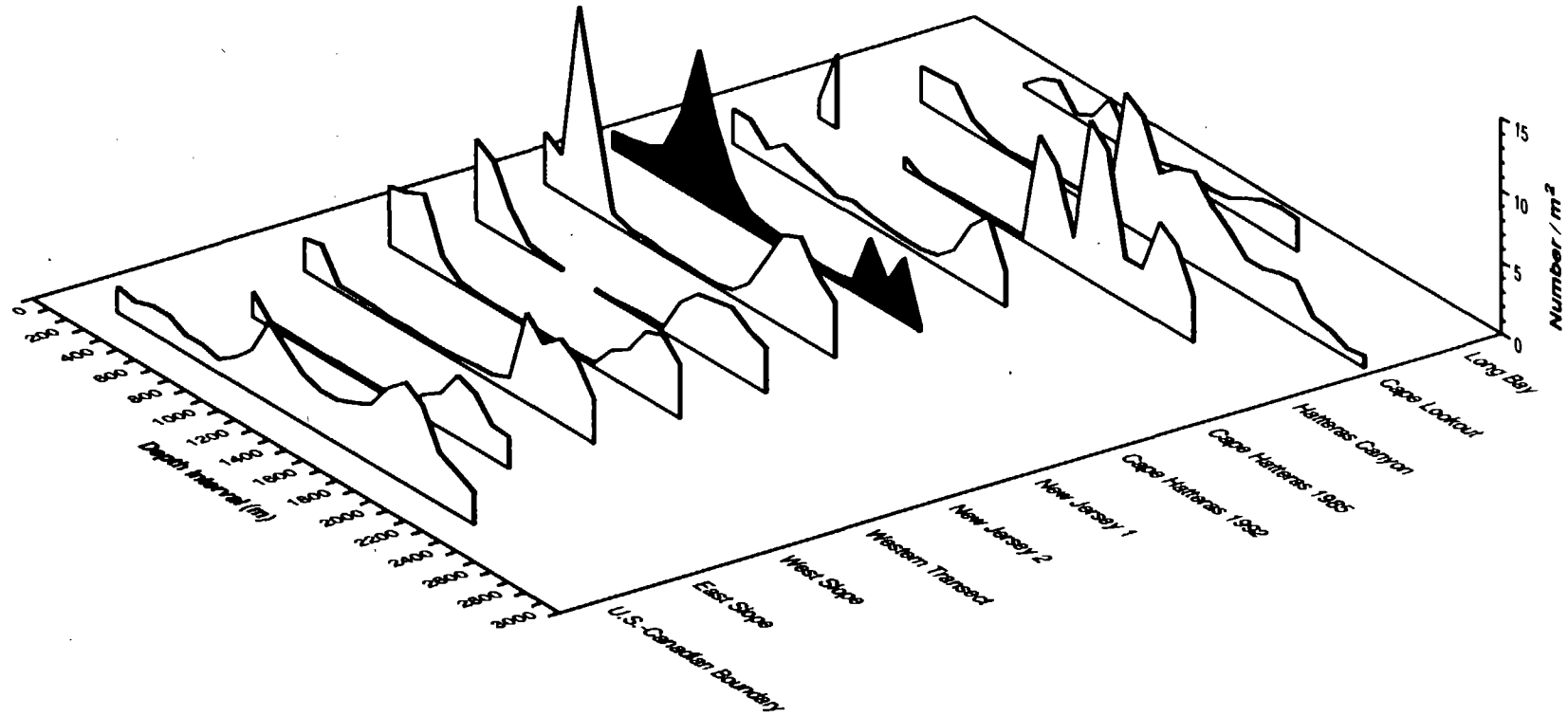


Figure 8-26. Density of total megafauna with depth at 10 locations on the eastern U.S. continental margin. Data for these locations were collected for studies described in Hecker et al. (1983), Hecker (1990a), and Blake et al. (1985, 1987). Data from the present survey are shaded (Cape Hatteras 1992).

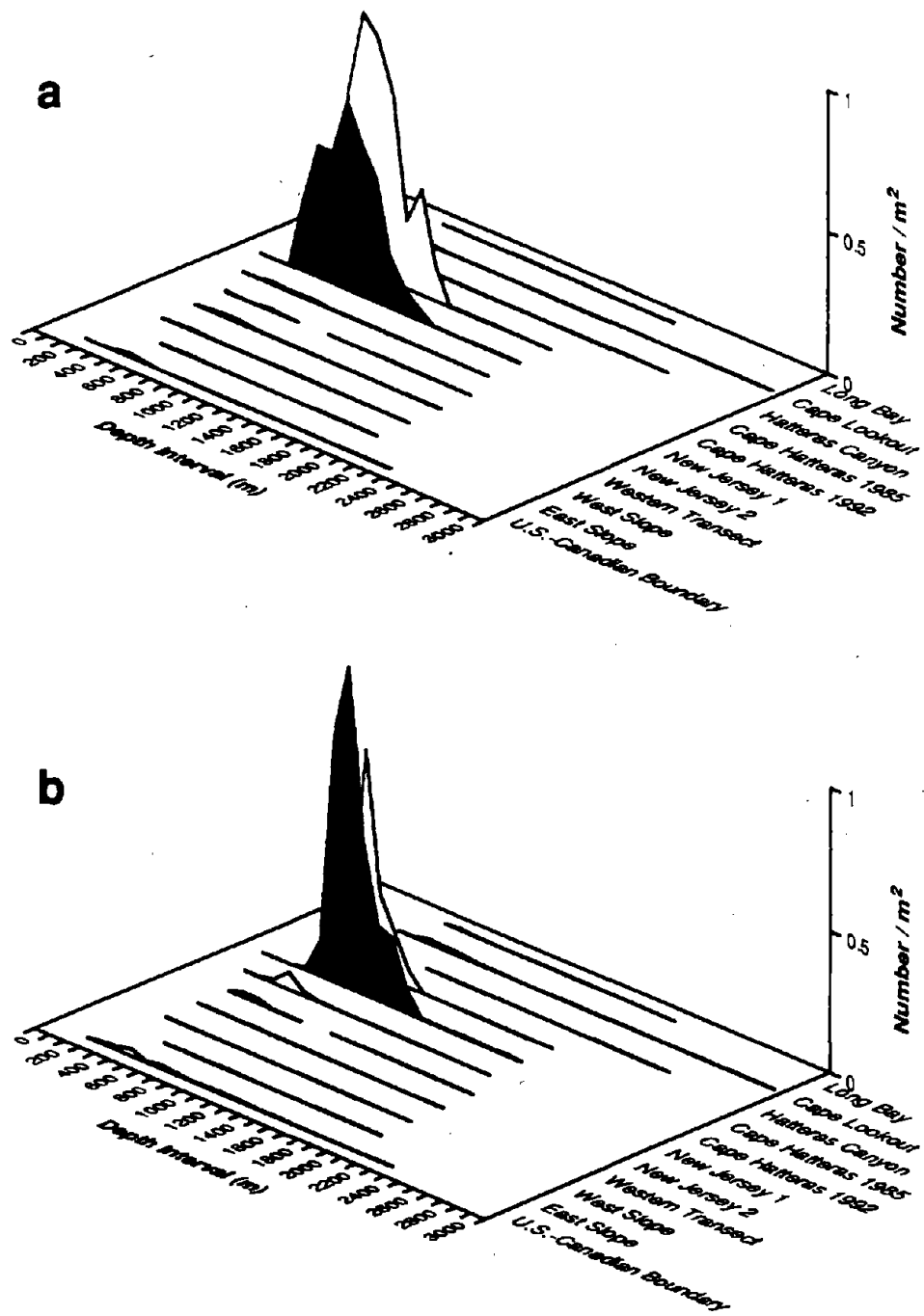


Figure 8-27. Density of (a) the wolf eelpout *Lycenchelys verrilli* and (b) the anemone *Actinauge verrilli* with depth at 10 locations on the eastern U.S. continental margin. Data for these locations were collected for studies described in Hecker et al. (1983), Hecker (1990), and Blake et al. (1985, 1987). Data from the present survey are shaded (Cape Hatteras 1992).

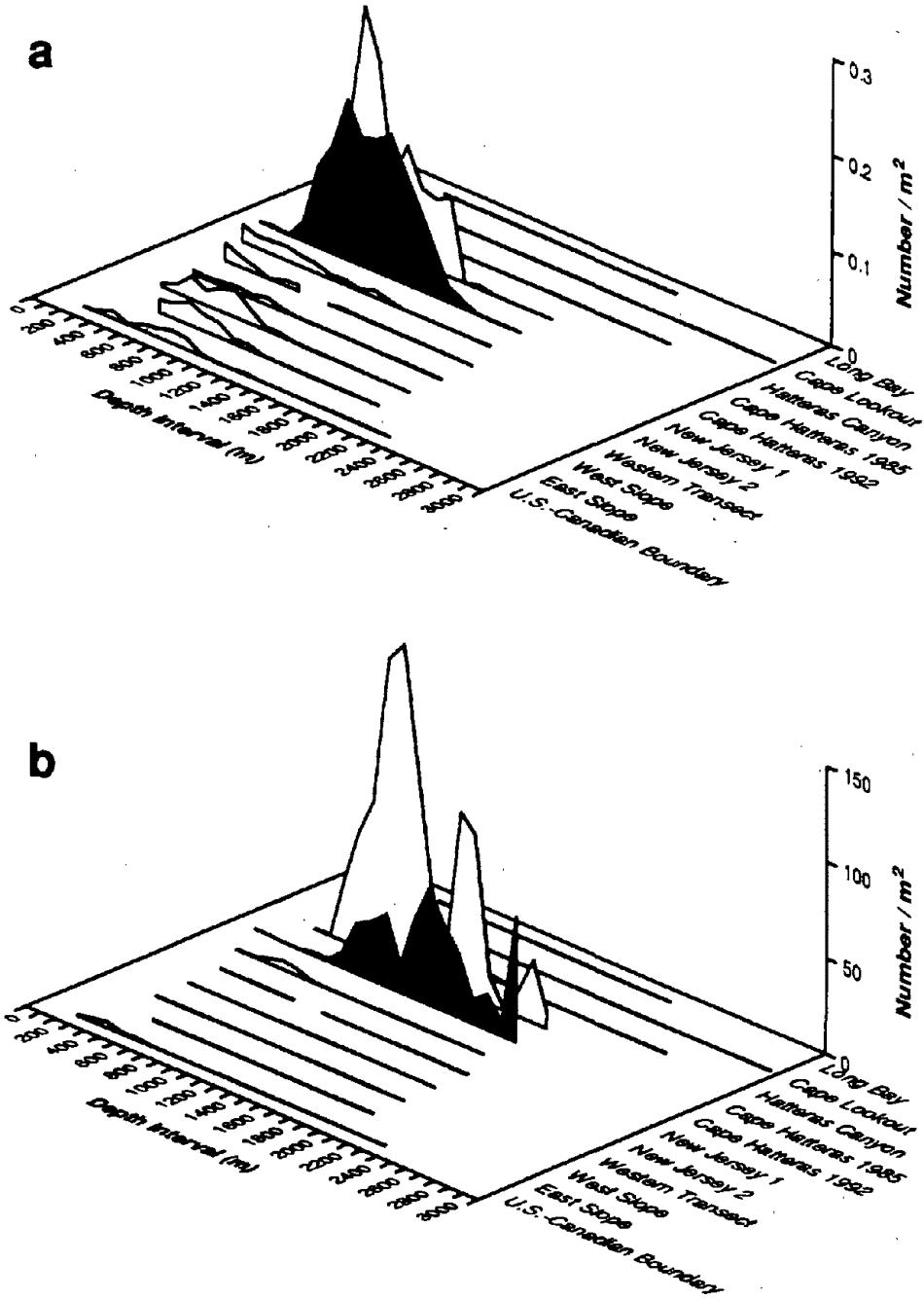


Figure 8-28. Density of (a) the witch flounder *Glyptocephalus cynoglossus* and (b) the foraminiferan *Bathysiphon filiformis* with depth at 10 locations on the eastern U.S. continental margin. Data for these locations were collected for studies described in Hecker et al. (1983), Hecker (1990), and Blake et al. (1985, 1987). Data from the present survey are shaded (Cape Hatteras 1992).

different areas of the slope. The locations ranged from the slope off Georges Bank (U.S.-Canadian Boundary) in the north to the slope off South Carolina (Long Bay) in the south. The Cape Hatteras location shows data collected during the 1985 survey along transect line D, as well as that collected over a wider geographic area during the present survey. All four species were found in much higher abundances on the slope off Cape Hatteras than at any of the other locations. It is immediately apparent that abundances of *L. verrilli* and *A. verrilli* are more than an order of magnitude higher off Cape Hatteras than at other locations along the U.S. continental slope (Figures 8-27a and 8-27b). Similarly, although *G. cynoglossus* was commonly found at the northern locations, it is also much more abundant off Cape Hatteras (Figure 8-28a). The foraminiferan *B. filiformis* is also much more abundant off Cape Hatteras (Figure 8-28b). Reasons for the lower densities of *B. filiformis* found at the shallower depths during this study are not readily apparent. This discrepancy may be related to a combination of sporadic coverage of the steep slopes in this depth range and the extreme patchiness of *B. filiformis*. It is also possible that the estimates made during the present study were more conservative than those made during the 1985 study.

The extreme patchiness of *B. filiformis* makes comparisons between data sets very difficult. A horizontal off-set of several meters could result in vastly different density estimates (Figure 8-12). The highest densities found on an individual photograph were 175 individuals m⁻² from the towed camera sled and 225 individuals m⁻² from the surface camera at the sediment profile stations (Chapter 5). Where comparable coverage in the same general area was obtained by the two methods, the range of density estimates only occasionally agreed (Table 8-5). The estimates obtained from the camera sled photographs generally tended to be lower than those obtained from the surface camera, but in several instances they were higher. Gooday et al. (1992) reported average densities of 93.8 ± 25.47 *B. filiformis* m⁻², with a range of 59 to 154 individuals m⁻² at 850 m (based on 22 photographs) and 23.4 ± 10.6 individuals m⁻² at 600 m (based on 5 photographs). The highest densities of *B. filiformis* found in this study were 60 individuals m⁻² in the 1,300-m depth interval for the entire data set pooled and 98 individuals m⁻² on an individual transect (1,200-m depth interval, Transect F). The 1985 data showed a high of 168 individuals m⁻² in the 900-m depth interval. If the estimates of the densities of *B. filiformis* made during the present study were conservative, it would not change any of the trends observed or alter the conclusions based on them. However, it would further magnify the differences between regions of low and high densities.

Some of the patchiness of *B. filiformis* appears to be related to geological and biological processes that affect sediment stability and/or surface disturbance. This foraminiferan was generally most abundant in flat regions and least abundant in steep regions. The influence of slope topography on *B. filiformis* is probably related to sediment stability, in that sediments on steep slopes are usually unstable and tend to move down-slope through slow creeping or sudden slope failure. The impact of sediment movement would be physical removal and/or burial of the tubes and interference with settlement. Examples of sediment movement down steep slopes were seen on all transects through down-slope trending, erosional furrows (rivulets), asymmetric mounds and slump scars. Partially buried tubes were occasionally seen on all seven transects. Biological activities that appeared to impact *B. filiformis* included mound formation by infaunal holothurians, excavation by fish and crustaceans, plowing of the sediment surface by large deposit feeders, and movement of many organisms causing surface disturbance. Extensive excavation of the upper portion of the middle slope by fish and crustaceans may partially be responsible for the upper limit of *B. filiformis*. Organisms that appeared to cause surface disturbance included *Hyalinoecia artifex*, *Glyptocephalus cynoglossus*, *Phormosoma placenta*, *Ophiomusium lymani*, and *Paelopatides gigantea*. However, in many instances *B. filiformis* was absent from areas that were not disturbed.

The elevated densities of two species, *A. verrilli* and *B. filiformis*, may be caused by the same factors that have been suggested to be responsible for the enhanced infaunal densities found in this region (Blake et al. 1987). Both of these species are filter feeders that would benefit from enhanced nutrient input in the form of fine particles. Sedimentation and organic carbon accumulation rates have been found to be exceptionally high in this area when compared to a typical slope environment (Chapter 3). The funnelling of sediments off the shelf and out over the slope suggested by Rhoads (Chapter 6) may provide a direct transport mechanism for organic materials to slope depths off Cape Hatteras. In addition to the high deposition rates, burrowing activities of the infauna provides a mechanism for rapid burial of organic matter in deeper sediments.

Table 8-6. Estimates of the density of *Bathysiphon filiformis* (individuals m⁻²) obtained from individual photographs taken from the towed camera sled and surface photographs at sediment profile stations.

Location	Surface camera	Towed camera sled
Transect B		
600	0-13	0-3
800	0-2	0-150
1000	113-225	0-3
Transect D		
600	74-223	4-40
800	59-196	0-23
Transect F		
600	0	0-40
800	10-80	3-100
1000	5-20	23-120
1500	0-17	0-11

The elevated densities of *L. verrilli* and *G. cynoglossus* appear to reflect the exceptionally high densities of infaunal prey found in this region. The present study has identified another species that is also more abundant in the Cape Hatteras area. Densities of the eelpout *Lycodes atlanticus* ranged from 0.02 to 0.30 individuals m⁻² on the middle slope off Cape Hatteras during both the 1985 and 1992 surveys, but never exceeded 0.01 individuals m⁻² on the slope off Hatteras Canyon or 0.002 individuals m⁻² at a number of other locations along the U.S. continental slope.

Several other observations can be added to the previous description of megafaunal assemblages on the slope off Cape Hatteras. Blake et al. (1987) noted the absence of *H. artifex* and *B. tudiae* during the 1985 survey. The broader coverage obtained during the present study shows that both species are present. *H. artifex* was found in exceptionally high numbers on the two northernmost transects and in moderate numbers on the southernmost transect. *B. tudiae* was found in moderate numbers on the southernmost transect. Both species have also been reported on the slope south and north of an area called "The Point," which is located just north of Transect D (Appendix A). *B. tudiae* was also seen in the vicinity of the proposed drill site (Mobil 1990). The ophiuroid *Ophiura sarsi*, which was found during the present survey, was not encountered in the survey conducted in 1985. Dense beds of *O. sarsi* have also been noted in the vicinity of The Point (Mobil 1990, Appendix A). It would appear that the patchy distribution of these taxa, compounded by the problem of obtaining adequate coverage in the steeper areas, makes an accurate assessment of the megafaunal assemblages in this region difficult.

The results of the present study serve to extend the geographic area over which the unusual megafaunal assemblages originally described by Blake et al. (1987) are found. Furthermore, the geographic limits of these assemblages appear to extend beyond the area surveyed for the present study. These assemblages are characterized by several species, *L. verrilli*, *G. cynoglossus*, *A. verrilli*, *L. atlanticus*, and *B. filiformis*, that are found in much higher densities on the slope off Cape Hatteras than at other locations along the eastern U.S. continental margin. Many of the species found on the slope off Cape Hatteras exhibited exceptionally patchy distributions. This finding was particularly true of *B. filiformis*. Such patchiness may well reflect the extreme heterogeneity of habitats found in this region.

CHAPTER 9. SYNTHESIS OF BIOLOGICAL DATA

James A. Blake, Brigitte Hilbig, and Robert J. Diaz

Introduction

This chapter is a synthesis of the biological data we collected to address objectives 1, 3, and 4 (Chapters 7 and 8). Where appropriate data from other studies was also included.

A conclusion from previous studies of the continental shelf off Cape Hatteras, conducted in 1984-1985 as part of the MMS ACSAR program, was that the benthic community differed from other locations off the Carolinas and elsewhere on the U.S. Atlantic coast (Blake et al. 1987). They found the benthic infaunal communities off Cape Hatteras were characterized by low species richness, low species diversity, and high density more typical of shallow continental shelf locations. Blake et al. (1987) determined that the high infaunal densities were caused by relatively few species of polychaetes and oligochaetes. Bottom photographs revealed unusually high densities of the wolf eelpout *Lycenchelys verrilli* and the witch flounder *Glyptocephalus cynoglossus*, presumably feeding on the dense infaunal. The anemone *Actinauge verrilli* was also present in unusually high densities. Both box core and photographic data yielded evidence of high densities of a large, tube-dwelling foraminiferan *Bathysiphon filiformis*.

Data collected at two stations in 1984-1985 as part of the ACSAR program (SA-9 at 600 m and SA-10 at 2,000 m, and near Transect D, Figure 2-1) were the first to recognize the unusual nature of the benthic infauna and megafauna on the slope off Cape Hatteras. However, these data could not address questions of areal extent of the unusual communities and determine potential impacts from oil and gas exploratory activity. The present study was designed to survey the areal extent of benthic assemblages over large portions of the Manteo lease area (Chapter 1).

Definition and Extent of the Biological Communities

The infaunal organisms taken from box cores included approximately 280 species of invertebrates, 45% of which were annelid worms. Molluscs (20%), crustaceans (17%), echinoderms (6%), and a variety of miscellaneous taxa comprised the rest of the fauna. The majority of individuals, however, consisted of six taxa: the oligochaetes *Limnodriloides medioporus* and *Tubificoides intermedius* and the polychaetes *Scalibregma inflatum*, *Aricidea quadrilobata*, *Cossura* spp., and *Tharyx kirkegaardi*.

Species diversity indices for Stations SA-9 (600 m) and SA-10 (2,000 m) were consistently low during the ACSAR program. Shannon-Wiener (H') indices averaged 2.89 and 4.37, respectively. The SA-9 index is especially low for a continental slope environment. During the present study, H' indices at the upper slope (600-800 m) stations ranged from 1.98 to 4.92 ($\bar{x}=2.91$). These values are consistently lower than values from upper slope communities recorded elsewhere off North Carolina and Massachusetts where H' values typically exceed 6.0 (Blake et al. 1987, Maciolek et al. 1987a,b). Hurlbert Rarefaction values are equally low for the Cape Hatteras stations. One factor which may limit the success of many species on the Cape Hatteras slope is the nature of the carbon supply. The infaunal species that are most common on the Cape Hatteras slope are typically rare in the deep sea. It is likely that these dominant species are preadapted to digesting the less labile organic material abundant in the sediments (Chapter 4).

The density of the infaunal assemblages off Cape Hatteras is very high and resembles that reported from shallower continental shelf locations such as the mud patch near Georges Bank (Neff et al. 1989). Samples previously taken at Station SA-9 (600 m) had an average density of 46,255 individuals m^{-2} (Blake et al. 1987). In the present study abundances from similar depths were also high, ranging from 15,522 to 89,566 individuals m^{-2} ($\bar{x}=37,282$ individuals m^{-2}). Densities at SA-10 (2,000 m) averaged 8,950 individuals m^{-2} in 1984-1985, which is similar to the single 1992 sample (8,522 individuals m^{-2}).

The benthic megafauna viewed from the camera-sled photographs included at least 35 species of fish, 18 species of cnidarians (alcyonarians and anemones), about 17 species of echinoderms, and a variety of crustaceans, worms, molluscs, and miscellaneous organisms. The species most characteristic of the megafaunal assemblages found throughout most of this region were the foraminiferan *Bathysiphon filiformis*, the eelpouts

Lycenchelys verrilli and *Lycodes atlanticus*, the witch flounder *Glyptocephalus cynoglossus*, and the anemone *Actinauge verrilli*. The quill worm *Hyalinoecia artifex* was locally abundant, only on the upper portion of the middle slope of the two northern transects. Cerianthid anemones were locally abundant at depths above 1,000 m. The fauna on the lower slope (> 1,600 m) was dominated by the brittlestar *Ophiomusium lymani* and the sea pens *Kophobelemnion stelliferum* and *Distichoptilum gracile*. Most of the photographs (planview and camera sled) also showed numerous instances of biological activity such as tracks and trails, burrow openings and pits caused by deep-burrowing deposit feeders, excavations caused by fish and crustaceans, and the surficial tubes of infaunal organisms.

The high densities of predators, such as the eelpouts, the witch flounder, and the quill worm are likely related to the high densities of potential infaunal prey. High abundances of filter feeding megafauna, such as *Actinauge verrilli*, *Bathysiphon filiformis*, and cerianthid anemones are probably related to the high concentrations of suspended solids seen in many of the photographs. High densities of the surface deposit feeding holothurian *Peniagone* sp., found on the lower slope of Transect D, also indicate there is a high organic flux to this area. This species is known to occur in dense aggregations that migrate toward organic rich areas. Large deep-burrowing polychaetes were found in the box cores and evidence of their activity was also noted on the photographs (as dense groups of burrow openings in the sea floor). The most abundant deposit-feeding polychaetes was *Scalibregma inflatum*. This species was often observed in the box cores deeper than 10 cm and likely exploits organic matter found in the sediments.

Geographically, the results of the 1992 surveys suggest that the area encompassed by the dense faunal assemblages extends to most of the continental slope area off Cape Hatteras. The distance between 1A in the north and Transect F in the south is approximately 50 km (Figure 2-1). The fauna is patchy, but the overall community structure extends over the entire length of the study area. We know, however, that these assemblages are not found in the vicinity of the Hatteras Canyon (Blake et al. 1985).

On a smaller scale, some interesting latitudinal differences were noted from both the camera sled photographs and the box cores. The northernmost study area (1A and 1) differed somewhat from the rest in that the infaunal species richness was higher (Table 7-2). Both camera sled transects at 1 and 1A were characterized by exceptionally high densities of the quill worm *Hyalinoecia artifex*, a species that may create microhabitats by constantly ploughing the sediment surface (Chapter 8). The infauna included some unusual organisms among the dominant species, such as priapulids, the sipunculan *Nephasoma diaphanes*, and two tanaidaceans. At the lower end of Transect A (around Station 5, 1,500 m), numerous biogenic mounds were reported. Species occurring in high numbers at only this station, such as the aplacophoran *Falcidens caudatus* and the isopod *Macrostylis* sp. 1, may have benefitted from the microhabitats created by the mounds.

There was some depth-related zonation patterns in the infaunal community. An upper slope assemblage (600 m), characterized by the dominance of oligochaetes, could be distinguished from two middle slope assemblages (800-1,400 m) that were both dominated by *Scalibregma inflatum*, but differed in the suite of less abundant species. At depths between 1,500 and 2,000 m, a lower slope assemblage was found. The megafauna showed faunal breaks at 400-500 m, between 800 and 1,200 m, and at 1,600 m. The fauna on the upper slope (< 500 m) was very patchy and consisted of a variety of shallow water species. Four fish and two anemones dominated the fauna on the middle slope, with *Lycenchelys verrilli*, *Actinauge verrilli*, and cerianthids dominating the fauna on the upper portion of the middle slope (usually between 600 and 1,200 m) and *Lycodes atlanticus* and *Synaphobranchus* spp. dominating the fauna on the lower portion of the middle slope (usually between 1,200 and 1,600 m). The witch flounder was found in moderate abundances throughout most of the middle slope. The fauna on the lower slope (> 1,600 m) was dominated by an ophiuroid and two sea pens.

In summarizing the results with reference to the objectives of this study, the definition of the benthic community on the continental slope off Cape Hatteras has been expanded to include a patchwork of different assemblages of infauna and epifauna. There appears to be a defined depth zonation. The areal extent of these assemblages has been determined to extend north-south for at least a distance of 50 km, centered on Cape Hatteras. The results of the sedimentary studies have provided evidence that sedimentation rates are higher than found in nearshore environments and that this enhanced sedimentation provides large amounts of organic carbon from the nearby shelf that fuels the dense faunal assemblages resident on the continental slope off Cape

Hatteras. The unusually low diversity of these assemblages is probably a result of the quality and quantity of the carbon source. Evidence of high and nearly continuous sedimentation to the site and extensive bioturbation by large megafaunal and infaunal organisms suggests that surface sediments, to at least 10-15 cm, are in a continuous state of flux.

The potential for any type of disturbance to affect the benthic communities of the continental slope off Cape Hatteras is related to how physical and biological factors interact to structure these communities. The high sedimentation rate, of both organic and mineral matter, and unstable slope sediment combine to form a habitat that is physically dynamic. This type of habitat would then support a community structured by species that can tolerate high sediment flux and instability, and quickly take advantage of newly arriving organic matter and colonize locally disturbed areas. We found the distribution patterns of infauna and megafauna to be consistent with this hypothesis.

Over much of the study area the sediment surface is heavily tracked by fish and other megafauna (Chapters 5, 8). Subsurface deposit-feeders that defecate at the surface, such as maldanid polychaetes and holothurians, also produce mounds on the sediment surface. This tracking and defecating adds a short-term component to the instability of surface sediments. The megafaunal and infaunal communities that populate the continental slope off Cape Hatteras appear well adapted to coping with the dynamic nature of the physical environment. These communities, in turn, provide the trophic base that supports the largest populations of demersal fish known from continental slope depth along the U.S. Atlantic Coast.

THIS PAGE LEFT BLANK INTENTIONALLY

CHAPTER 10. CONCLUSIONS

Robert J. Diaz

Physical Habitat

Data from the study area on the continental slope off Cape Hatteras all point to an unusually high input rate of sediment and organic matter (Table 10-1). The location of Cape Hatteras along the Atlantic Coast and its geomorphology combine to funnel material moving southward along the outer shelf onto the slope environment near the study site (Figure 6-1). Gulf Stream eddies which move across the shelf and impinge on the area also sweep material over the shelf edge onto the slope. Within the study area there were no depth-related gradients in grain-size distributions, sediment chemistry, or sedimentation rates. In part, this was due to topographic irregularities which tend to break-up the bottom into a diverse mosaic of patchy and discontinuous habitats of varying age and stability. Also, the size of the study area was too small to detect broad scale regional gradients.

Table 10-1. Summary of sedimentary characteristic within the study area. Estimated sediment accumulation for Station SA-10 was an outlier, possibly related to a recent sediment disturbance, so it is presented separately for parameters that use the accumulation rate.

Parameter	Mean \pm Standard Error
Fine Sand-Coarse Silt	33.0 \pm 2.0%
Sediment Accumulation Rate	0.98 \pm 0.14 cm yr ⁻¹ (0.05 SA-10)
Sediment Mixed Layer Depth	12 \pm 1 cm
Carbonate	16.6 \pm 0.7%
Carbonate Flux	1133 \pm 305 g CO ₂ m ² yr ⁻¹ (58 SA-10)
Organic Carbon	1.04 \pm 0.04%
Organic Carbon Flux	66.7 \pm 12.8 g C m ² yr ⁻¹ (4 SA-10)
Organic Nitrogen	0.13 \pm 0.01%
C:N Ratio	9.5 \pm 0.1
Chlorophyll <i>a</i>	0.75 \pm 0.15 μ g g ⁻¹ dry wt.
Total Fatty Acids	18.7 \pm 3.5 μ g g ⁻¹ dry wt. (5.6 \pm 1.0 μ g g ⁻¹ C)
Polyunsaturated Fatty Acids	1.5 \pm 0.6 μ g g ⁻¹ dry wt. (0.4 \pm 0.2 μ g g ⁻¹ C)

The organic matter found in the study site's sediments appears to be derived from both terrestrial and marine sources, and reflects the complicated interactions between sources and degradation pathways, and transport mechanisms. While there is a large supply of organic matter, only a small fraction of it is composed of easily digested and highly nutritious smaller molecules (polyunsaturated fatty acids). The majority of the organic matter was refractory which suggests that it is substantially reworked either during transport through the water column or at the sediment-water interface. Subsurface deposit feeders adapted to make use of this more refractory organic matter dominate the infauna in terms of both numbers and biomass. Their unusually high abundance is apparently directly related to the magnitude of carbon flux into the area, and the sediment grain size which, is optimal for both tube building and burrowing. The sediment fabric is almost completely reworked biologically and is a good indicator of the high level of infaunal activity. Considering the general instability of the slope and high rates of sediment accumulation, infaunal activity must be exceptionally high to obliterate most signs of physical sedimentary processes.

Over most of the study area the surface of the sediment was heavily tracked by fish and other megafauna. Subsurface deposit-feeders that defecate at the surface, such as maldanid polychaetes or holothurians, also produced mounds on the surface. These processes add a short-term component to the instability of the sediment.

The megafaunal and infaunal communities that populate the area appear well adapted to coping with a strenuous physical environment characterized by sediment instability, high sediment accumulation, and high flux of organic matter. These communities, in turn, provide the trophic base to support the largest populations of demersal fish known from continental slope depth along the U.S. Atlantic Coast.

Benthic Community Characterization and Distributional Patterns

The infaunal community was characterized by higher than average densities, and lower than average species richness and species diversity, for continental slope areas. Infaunal community structure is summarized in Table 10-2. The community was numerically dominated by six of the 280 species collected; the oligochaetes *Limnodriloides medioporus* and *Tubificoides intermedius* and the polychaetes *Scalibregma inflatum*, *Aricidea quadrilobata*, *Cossura* spp., and *Tharyx kirkegaardi*. Megafauna included at least 35 taxa of fish and 61 invertebrate taxa. Densities of total benthic megafauna were only slightly elevated for continental slope areas (Figure 8-26). However, densities of the four top dominant megafaunal species were much higher than average. These four species were the tube-building foraminiferan *Bathysiphon filiformis*, the eelpouts *Lycenchelys verrilli* and *Lycodes atlanticus*, the witch flounder *Glyptocephalus cynoglossus*, and the anemone *Actinaugea verrilli* (Figures 8-27 and 8-28).

Table 10-2. Summary of benthic community characteristics within the study area. Infaunal parameters are for 16 box core stations (Table 2-1).

Parameter	Mean \pm Standard Error
Total Infauna Density	30,968 \pm 5,152 individuals m ²
Total Species 0.09 m ²	63.3 \pm 5.0
Species/750 Individuals	45.7 \pm 5.0
H' Diversity	3.2 \pm 0.2
Top 10 Dominant Taxa of Total	64-97% (range)

Biological communities were patchy in distribution down to the smallest scales measured (meters for the megafaunal and kilometers for the infauna). Latitudinal differences were most obvious in the megafauna. The northern part of the study area (1A and 1) differed somewhat from the rest, the species richness of the infauna was higher (Table 7-2) and the megafauna was characterized by exceptionally high densities of the quill worm *Hyalinoecia artifex* (Chapter 8). The infauna included other organisms among the dominant species, such as priapulids, the sipunculan *Nephasoma diaphanes*, and two tanaidaceans (Table 7-4).

The infauna also exhibited depth-related zonation patterns. An upper slope assemblage (600 m), dominated by oligochaetes, could be distinguished from two middle slope assemblages (800-1,400 m) which were dominated by *Scalibregma inflatum*, but differed in the suite of less abundant species. In depths between 1,500 and 2,000 m, a lower slope assemblage was found. The megafauna showed faunal breaks at 400-500 m, between 800 and 1,200 m, and at 1,600 m.

While patchy, these communities were found throughout the continental slope study area off Cape Hatteras. The boundaries of these unusual communities are at least from 35° 20' to 35° 50' north latitude and from depths of 600 to 1,500 m, and possibly to 2,000 m depth. The minimum area occupied by these communities, within the study area, is estimated to be about 500 km² to the 1,500-m isobath and 900 km² to the 2,000-m isobath.

OOC Model Predictions and Aerial Distribution of Benthic Community

Our objective 4 was to determine if more than 5% of the area occupied by the unusual benthic community would be impacted by drilling muds and cuttings from the proposed well. The OOC model predicted that 0.5 km^2 of the sea floor would receive > 1 mm of drilling mud and cuttings, approximately 1 km^2 would receive >0.1 mm, and an area of approximately 12 km^2 would receive as little as 0.1 μm (the thinnest layer predicted by the model, Chapter 1). Our data indicated that the unusual infauna and megafaunal communities were distributed throughout the study area (Chapters 7, 8). Conservatively, these communities occupied a north-south distance of at least 50 km and a depth range of 600 to 1,500 m, and likely to 2,000 m. The sea floor area within this distance and depth range is approximately 500 km^2 (900 km^2 if the depth is extended to 2,000 m). Therefore, it appears that approximately 2.4% (1.3% based on 2,000 m) of the unusual benthic community within our study area could be impacted by the drilling of the proposed exploratory well in the Manteo 467 lease block. Other combinations of community area and deposition are summarized in Table 10-3.

Table 10-3. Estimated percentage of the unusual benthic community, within the study area (Figure 2-1), covered by predicted deposition of drilling muds and cuttings.

Depth Range of Community	Estimated Thickness of Drilling Muds and Cuttings			
	> 1 mm	>0.1 mm	>1.0 μm	>0.1 μm
600-1500 m	0.1	0.2	0.8	2.4
600-2000 m	0.05	0.1	0.4	1.3

More sediment is deposited by natural processes than would be deposited by the proposed well drilling. The physical and biological processes that structure bottom communities on the continental slope off Cape Hatteras result in yearly sediment deposition and reworking rates that are orders of magnitude higher than layers predicted by the OOC model, further than 154 m from the simulated well site. Sediment accumulation rates were estimated to range from 0.3 to 1.8 cm yr^{-1} at 600 to 1,500 stations (0.05 cm yr^{-1} at the 2,000 m station). The maximum deposition predicted by the OOC model, occurring within 154 m of the simulated well site, was approximately 3 cm. This is 1.7 to 10 times greater than the range in yearly natural sediment accumulation. If the natural accumulation rates are scaled to a month, the approximate time estimated for drilling the exploratory well in the Manteo 467 block, then the magnitude of predicted well deposition can be compared to the natural sediment accumulation (Table 10-4).

Table 10-4. Estimated ratio of predicted deposition, from drilling of the proposed well in the Manteo 467 lease block, relative to monthly natural sediment accumulation rates (Predicted/Measured Accumulation). Ratios are calculated for and maximum (1.5 mm mon^{-1}) and minimum (0.25 mm mon^{-1}) sedimentation rates from 600-1,500-m stations, and for the 2,000-m station (0.042 mm mon^{-1}).

Depth Range	Estimated Thickness of Drilling Muds and Cuttings			
	> 1 mm	>0.1 mm	>1.0 μm	>0.1 μm
Max 600-1500 m	0.7	0.07	0.0007	0.00007
Min 600-1500 m	4.0	0.4	0.04	0.004
2000 m	24.0	2.4	0.024	0.0024

THIS PAGE LEFT BLANK INTENTIONALLY

LITERATURE CITED

- Aller, R.A. 1982. The effects of macrobenthos on chemical properties of marine sediment and overlying water. pp. 53-102. In: P.L. McCall and M.J.S. Tevesz (eds.). Topics in Geobiology. Plenum Press, New York.
- Anderson, R.F., R.F. Bopp, K.O. Buesseler and P.E. Biscaye. 1988. Mixing of particles and organic constituents in sediments from the continental shelf and slope off Cape Cod: SEEP-I results. Cont. Shelf Res. 8:925-946.
- Barham, E.G., N.J. Ayer and R.E. Boyce. 1967. Macrobenthos of the San Diego Trough: Photographic census and observations from the bathyscaphe Trieste. Deep-Sea Res. 14:773-784.
- Beers, J.R., J.D. Trent, F.M.H. Ried and A.L. Shanks. 1986. Macroaggregates and their phytoplanktonic components in the Southern California Bight. J. Plankt. Res. 8:475-487.
- Bianchi, G., A. Pinarosa, O. Scarpa, C. Murelli, G. Audisio and A. Rossini. 1989. Composition and structure of maize epicuticular wax esters. Phytochemistry 28:165-171.
- Blake, J.A. and J.F. Grassle. Unpublished. Benthic community structure on the U.S. South Atlantic slope off the Carolinas: Spatial heterogeneity in a current dominated system.
- Blake, J.A., B. Hecker, J.F. Grassle, N. Maciolek-Blake, B. Brown, M. Curran, B. Dade, S. Freitas, and R.E. Ruff. 1985. Study of biological processes on the U.S. South Atlantic slope and rise. Phase 1. Benthic characterization study. Final report. Prepared for U.S. Department of the Interior, Minerals Management Service, Washington, DC, under Contract No. 14-12-0001-30064. 142 pp. + Appendices 1-4.
- Blake, J.A., B. Hecker, J.F. Grassle, B. Brown, M. Wade, P.D. Boehm, E. Baptiste, B. Hilbig, N. Maciolek, R. Petrecca, R.E. Ruff, V. Starczak, and L. Watling. 1987. Study of Biological Processes on the U.S. South Atlantic Slope and Rise. Phase 2. Final Report. Prepared for the U.S. Department of the Interior, Minerals Management Service, Washington, DC, under Contract No. 14-12-0001-30064. 415 pp. + Appendices A-M. NTIS No. PB87-214-359.
- Blake, J.A., J.A. Muramoto, B. Hilbig, and I.P. Williams. 1992. Biological and sedimentological investigation of the seafloor at the proposed U.S. Navy ocean disposal site. July 1991 survey (R/V *Wecoma*). Benthic biology and sediment characterization. Report prepared for PRC Environmental Management, Inc. by Science Applications International Corporation, under Navy CLEAN Contract No. N62474-88-D-5086. iii + 130 pp. + Appendices A-D.
- Blanton, J.O. 1991. Processes along ocean margins in relation to material fluxes. pp. 145-153. In: R.F.C. Mantoura, J.M. Martin and R. Wollast (eds.). Ocean Margin Processes in Global Change: Physical, Chemical, and Earth Sciences Research Reports No. 9. John Wiley and Sons, New York.
- Boesch, D.F. 1977. Application of numerical classification in ecological investigations of water pollution. U.S. Department of Commerce, EPA-60013-77-033. NTIS No. PB-269 604. 114 pp.
- Bothner, M.H., E.Y. Campbell, G.P. DeLisio, C.M. Parmenter, R.R. Rendigs and J.R. Gillson. 1987. Analysis of trace metals in bottom sediments in support of deepwater biological processes studies on the U.S. South Atlantic continental slope and rise. Final report. U.S. Department of the Interior, Minerals Management Service, Washington D.C., under Interagency Agreement No. 14-12-0001-30197, 44 pp.

- Bouma, A.H. 1969. *Methods for the study of sedimentary structures*. Wiley-Interscience, New York. 458 pp.
- Boynton, W.R., W.M. Kemp and C.W. Keefe. 1982. A comparative analysis of nutrients and other factors influencing estuarine phytoplankton production. pp. 69. In: V.S. Kennedy (ed.). *Estuarine Comparisons*, Academic Press, New York.
- Brandsma, M.G. 1990. Simulation of benthic accumulations of mud and cuttings discharged from Mobil Oil Corporation well, Manteo area, block 467, Cape Hatteras, North Carolina. Appendix N-4 In: Mobil. Exploration plan, Manteo area block 467, offshore Atlantic. Vol. III. Mobil Exploration and Producing Inc., Dallas, Texas.
- Brandsma, M.G., L.R. Davis, R.C. Ayers and T.C. Sauer. 1980. A computer model to predict the short term fate of drilling discharges in the marine environment. pp. 351-381. In: *Proceedings of a Symposium on Research on Environmental Fate and Effects of Drilling Fluids and Cuttings*, Lake Buena Vista, FL.
- Brandsma, M.G. and T.C. Sauer. 1983. The OOC model: Prediction of short term fate of drilling mud in the ocean. Part 2: Model description. pp. 58-84. In: *Proceedings of Minerals Management Service Workshop, An Evaluation of Effluent Dispersion and Fate Models for OCS Platforms*, February 1983, Santa Barbara, CA, Minerals Management Service, Los Angeles.
- Bumpus, D.F. 1973. A description of the circulation of the continental shelf of the east coast of the U.S. pp. 111-157. In: B.A. Warren (ed.). *Progress in Oceanography Volume 6*. Pergamon Press, New York.
- Burreson, E.M. and H.J. Knebel (eds.). 1979. *Middle Atlantic outer continental shelf environmental studies*. Vols. I, II, and III. Final report to U.S. Department of the Interior, Bureau of Land Management, New York.
- Cahoon, L.B. and J.E. Cooke. 1989. Depth range of productive benthic microalgae. pp. 49-58, In: M.A. Lang and W.C. Jaap, (eds.). *Diving for Science....1989*, American Academy of Underwater Sciences, Costa Mesa, CA.
- Cahoon, L.B. and J.E. Cooke. 1992. Benthic microalgal production in Onslow Bay, North Carolina, USA. *Mar. Ecol. Prog. Ser.* 84:185-196.
- Cahoon, L.B., R.A. Laws and T.W. Savidge. 1992. Characteristics of benthic microalgae from the North Carolina outer continental shelf and slope: Preliminary results. pp. 61-68, In: L.B. Cahoon (ed.). *Diving for Science....1992*, American Academy of Underwater Sciences, Costa Mesa, CA.
- Cahoon, L.B., R.S. Redman and C.R. Tronzo. 1990. Benthic microalgal biomass in sediments of Onslow Bay, North Carolina. *Estuar. Coast. Mar. Sci.* 31:805-816.
- Carney, R.S. 1989. Examining relationships between organic carbon flux and deep-sea deposit feeding. pp. 24-58. In: G. Lopez, G. Taghon, and J. Levinton (eds.). *Ecology of Marine Deposit Feeders. Lecture Notes on Coastal and Estuarine Studies No. 31*. Springer-Verlag.
- Chanton, J.P. 1985. Sulfur mass balance and isotopic fractionation in an anoxic marine sediment. Ph.D. Thesis, University of North Carolina at Chapel Hill, Chapel Hill, NC.
- Churchill, J.H., C.D. Wirick, C.N. Flagg, and L.J. Pietrafesa. 1992. Sediment resuspension over the continental shelf east of the Delmarva Peninsula. *Cont. Shelf Res.*

- Continental Shelf Associates, Inc. 1990. Technical summaries of selected Atlantic region final reports. U.S. Department of the Interior, Minerals Management Service, Washington, DC, Rpt. No. MMS 90-0036, 213 pp.
- Csanady, G.T., J.H. Churchill, and B. Butman. 1988. Near-bottom currents over the continental slope in the Mid-Atlantic Bight. *Cont. Shelf Res.* 8:653-671.
- Csanady, G.T. and P. Hamilton. 1988. Circulation of slope-water. *Cont. Shelf Res.* 8:565-624.
- Cutshall, N.H., I.L. Larsen, and C.R. Olsen. 1983. Direct Analysis of ^{210}Pb in sediment samples: Self-absorption corrections. *Nuclear Instruments and Methods* 206:309-312.
- Diaz, R.J., C. Erséus and D.F. Boesch. 1987. Distribution and ecology of Middle Atlantic Bight oligochaetes. *Hydrobiologia* 141:215-225.
- Diaz, R.J. and L.C. Schaffner. 1988. Comparison of sediment landscapes in Chesapeake Bay as seen by surface and profile imaging. pp. 222-240. In: M.P. Lynch and E.C. Krome (eds.). *Understanding the estuary: Advances in Chesapeake Bay research*. Pub. 129, CBP/TRS 24/88.
- Dobbs, F.C. and R.B. Whitlatch. 1982. Aspects of deposit-feeding by the polychaete *Chytenella torquata*. *Ophelia* 21:159-166.
- Emery, K.O. and E. Uchupi. 1972. Western North Atlantic Ocean: Topography, rocks, structure, water, life, and sediments. *Memoirs Am. Assoc. Petrol. Geol.* 17:1-532.
- Farrington, J.W., S.M. Henrichs and R. Anderson. 1977. Fatty acids and Pb-210 geochronology of a sediment core from Buzzards Bay, Massachusetts. *Geochim. Cosmochim. Acta* 41:289-296.
- Flagg, C.N. 1988. Internal waves and mixing along the New England shelf-water/slope-water front. *Cont. Shelf Res.* 8:737-756.
- Folk, R.L. 1974. *Petrology of sedimentary rocks*. Hemphill's, Austin, 170 pp.
- Fraser, A.J., J.R. Sargent, J.C. Gamble and D.D. Seaton. 1989. Formation and transfer of fatty acids in an enclosed marine food chain comprising phytoplankton, zooplankton and herring (*Clupea harengus* L.) larvae. *Mar. Chem.* 27:1-18.
- Gooday, A.J., L.A. Levin, C.L. Thomas, and B. Hecker. 1992. The distribution and ecology of *Bathysiphon filiformis* Sars and *B. major* De Folin (Protista, Foraminiferida) on the continental slope off North Carolina. *J. Foram. Res.* 22:129-146.
- Grassle, J.F. 1967. Influence of environmental variation on species diversity in benthic communities of the continental shelf and slope. Ph.D. Dissertation, Duke University, Raleigh, NC, 194 pp.
- Grassle, J.F. 1987. Benthos. pp. 186-194. In: J.D. Milliman and W.R. Wright (eds.). *Marine environment of the U.S. Atlantic continental slope and rise*. Jones & Bartlett Pub. Inc., Boston.
- Grassle, J.F. and N.J. Maciolek. 1992. Deep-sea species richness: Regional and local diversity estimates from quantitative bottom samples. *Amer. Nat.* 139:313-341.

- Grassle, J.F., H.L. Sanders, R.R. Hessler, G.T. Rowe and T. McLellan. 1975. Pattern and zonation: A study of the bathyl megafauna using the research submersible *Alvin*. *Deep-Sea Res.* 22:457-481.
- Grassle, J.F. and W.L. Smith. 1976. A similarity measure sensitive to the contribution of rare species and its use in investigation of variation in marine benthic communities. *Oecologia* 25:13-22.
- Grimalt, J.O., B.R.T. Simoneit, J.I. Gomez-Belinchon, K. Fischer and J. Dymond. 1990. Ascending and descending fluxes of lipid compounds in the North Atlantic and North Pacific abyssal waters. *Nature* 345:147-150.
- Guillard, R.R.L. and J.H. Ryther. 1962. Studies of marine planktonic diatoms. I. *Cyclotella nana* Hustedt and *Detonula confervacea* (Cleve) Gran. *Can. J. Microbiol.* 8:229-239.
- Haedrich, R.L., G.T. Rowe and P.T. Polloni. 1975. Zonation and faunal composition of epibenthic populations on the continental slope south of New England. *J. Mar. Res.* 33:191-212.
- Harvey, H.R., S.A. Bradshaw, S.C.M. O'Hara, G. Eglinton and E.D.S. Corner. 1988. Lipid composition of the marine dinoflagellate *Scrippsiella trochoidea*. *Phytochemistry* 27:1723-1729.
- Harvey H.R., G. Eglinton, S.C.M. O'Hara and E.D.S. Corner. 1987. Biotransformation and assimilation of dietary lipids by *Calanus* feeding on a dinoflagellate. *Geochem. Cosmochim. Acta* 51:3031-3040.
- Harvey, H.R., J.H. Tuttle, R. Dawson and T. Bell. 1991. Kinetics of algal carbon diagenesis in the marine water column. In: D. Manning, (ed.). *Organic Geochemistry, Advances and Application in Energy and the Natural Environment*. Manchester University Press, 237 pp.
- Hecker, B. 1982. Possible benthic fauna and slope instability relationships. pp. 335-347. In: S. Saxof and J.K. Nieuwenhuis (eds). *Marine slides and other mass movements*, Plenum Press, New York.
- Hecker, B. 1990a. Variation in megafaunal assemblages on the continental margin south of New England. *Deep-Sea Res.* 37:37-57.
- Hecker, B. 1990b. Photographic evidence for the rapid flux of particles to the sea floor and their transport down the continental slope. *Deep-Sea Res.* 37:1773-1782.
- Hecker, B., G. Blechschmidt and P. Gibson. 1980. Epifaunal zonation and community structure in three Mid- and North Atlantic canyons. Canyon assessment study. Final report. Prepared for U.S. Department of the Interior, Bureau of Land Management. BLM. 139 pp. + Appendices A-F.
- Hecker, B., D.T. Logan, F.E. Gandarilles and P.R. Gibson. 1983. Megafaunal assemblages in Lydonia Canyon, Baltimore Canyon, and selected slope areas. In: *Canyon and slope processes study*, Vol. 3, Final report. Prepared for U. S. Department of the Interior, Minerals Management Service, Washington, DC under Contract No. 14-12-001-29178. 140 pp.
- Henrichs, S.M. and J.W. Farrington. 1984. Peru upwelling region sediments near 15°S. I: Remineralization and accumulation of organic matter. *Limnol. Oceanogr.* 29:1-19.
- Hill, M.O. 1973. Reciprocal averaging: An eigenvector method of ordination. *J. Ecol.* 61:237-249.
- Hill, M.O. 1974. Correspondence analysis: A neglected multivariate method. *J. Royal Stat. Soc., Series C.* 23:340-354.

- Hurlbert, S.H. 1971. The nonconcept of species diversity: A critique and alternative parameters. *Ecology* 52:577-586.
- Jumars, P.A. and E.D. Gallagher. 1982. Deep-sea community structure: Three plays on the benthic proscenium. Chapter 10, pp. 217-255. In: W.G. Ernst, and J.G. Morin (eds.). *The environment of the deep sea*. Prentice-Hall, Englewood Cliffs, NJ.
- Kenicutt, M.C. and L.M. Jeffrey. 1981. Chemical and GC-MS characterization of marine particulate lipids. *Mar. Chem.* 10:389-407.
- Kim, B. and H.J. Bokuniewicz. 1991. Estimates of sediment fluxes in Long Island Sound. *Estuaries* 14:237-247.
- Kudenov, J.D. 1977. The functional morphology of feeding in three species of maldanid polychaetes. *Zool. J. Linn. Soc.* 60:95-109.
- Kudenov, J.D. 1978. The feeding ecology of *Axiothella rubrocincta* (Johnson) (Polychaeta: Maldanidae). *J. Exp. Biol. Mar. Ecol.* 31:209-221.
- Kukert, H. and C.R. Smith. 1992. Disturbance, colonization and succession in a deep-sea sediment community: Artificial-mound experiments. *Deep-Sea Res.* 39:1349-1371.
- Laws, R.A. and L.B. Cahoon. 1992. Benthic diatoms from the North Carolina continental shelf and slope, pp. 103-110. In: *Proceedings of the Fourth Atlantic OCS Region Information Transfer Meeting*, September, 1991. MMS 92-0001, Minerals Management Service, OCS Region, Herndon, VA.
- Lee C. and S.G. Wakeham. 1989. Organic matter in seawater: Biogeochemical processes. *Chem. Oceanogr.* 9:1-51.
- Levine, E.R. and J.M. Bergen. 1983. Temperature and current variability of a Gulf Stream meander observed off Onslow Bay, August, 1977. *J. Geophys. Res.* 88:4663-4671.
- Lyle, M. 1983. The brown-green color transition in marine sediments: A marker of the Fe(III)-Fe(II) redox boundary. *Limnol. Oceanogr.* 28:1026-1033.
- Maciolek, N., J.F. Grassle, B. Hecker, P.D. Boehm, B. Brown, W.B. Dade, W.G. Steinhauer, E. Baptiste, R.E. Ruff and R. Petrecca. 1987a. Study of biological processes on the U.S. Mid-Atlantic slope and rise. Final report. Prepared for U.S. Department of the Interior, Minerals Management Service, Washington, DC, under Contract No. 14-12-0001-30064. 310 pp. + Appendices A-M.
- Maciolek, N., J.F. Grassle, B. Hecker, B. Brown, J.A. Blake, P.D. Boehm, R. Petrecca, S. Duffy, E. Baptiste and R.E. Ruff. 1987b. Study of biological processes on the U.S. North Atlantic slope and rise. Final report for U.S. Department of the Interior, Minerals Management Service, Washington, DC, Contract 14-12-30064, 362 pp. + Appendices A-L.
- Maciolek-Blake, N., J.F. Grassle, and J.M. Neff (eds.). 1985. Georges Bank Benthic Infauna Monitoring Program. Final report for the third year of sampling. Vol. 2. Prepared for U.S. Department of the Interior, Minerals Management Service, Washington, DC, under Contract No. 14-12-0001-29192. ii + 333 pp.

- Mangum, C.P. 1964. Activity patterns in the metabolism and ecology of polychaetes. *J. Comp. Biochem. Physiol.* 11:239-256.
- Marine Experiment Station. 1973. Coastal and offshore environmental inventory, Cape Hatteras to Nantucket Shoals. Mar. Pub. Ser. No. 2, University of Rhode Island, Kingston, RI.
- Marine Geoscience Applications Inc. 1984. Environmental summary of the U.S. Atlantic continental slope and rise, 28°- 40°N. Vol. I and II. U.S. Dept. Interior, Minerals Management Service, Washington, DC, Contract No. 14-12-0001-29200.
- Marine Resources Research Institute. 1984. South Atlantic OCS area living marine resources study, Phase III. Vol. I: Final report to the U.S. Department of the Interior, Minerals Management Service, Vienna, VA, Contract No. 14-12-0001-29185. 247 pp.
- Marsh, A.G., H.R. Harvey, A. Gremare and K.R. Tenore. 1990. Dietary effects on oocyte yolk composition in *Capitella* sp. I (Annelida:Polychaeta) fatty acids and sterols. *Mar. Biol.* 106:369-374.
- Matisoff, G. 1982. Mathematical models of bioturbation. Chapter 7, pp. 289-330. In: P.L. McCall and M.J.S. Tevesz (eds.). *Animal-sediment relations. Topics in Geobiology Series 2*, Plenum Press, New York.
- Mayzaud, P., J.P. Chanut and R.G. Ackman. 1989. Seasonal changes of the biochemical composition of marine particulate matter with special reference to fatty acids and sterols. *Mar. Ecol. Prog. Ser.* 56:189-204.
- Mayzaud, P., C.A. Eaton and R.G. Ackman. 1976. The occurrence and distribution of octadecapentaenoic acid in a natural plankton population. A possible food chain index. *Lipids* 11:858-862.
- Milliman J.D. and W.R. Wright (eds.). 1987. *Marine environment of the U.S. Atlantic continental slope and rise*. Jones & Bartlett Pub. Inc., Boston, 275 pp.
- Minerals Management Service. 1990. Final environmental report on proposed exploratory drilling offshore North Carolina. Vols. I, II, and III. U.S. Department of the Interior, Minerals Management Service, Washington, DC.
- Mobil. 1990. Draft exploratory plan, Manteo area block 467, offshore Atlantic. Vols. I, II, and III. Mobil Exploration and Producing Inc., Dallas, Texas.
- Neff, J.M., M.H. Bothner, N.J. Maciolek and J.F. Grassle. 1989. Impacts of exploratory drilling for oil and gas on the benthic environment of Georges Bank. *Mar. Environ. Res.* 27:77-114.
- Nichols, P.D. and R.B. Johns. 1985. Lipids of the tropical seagrass *Thalassia hemprichii*. *J. Phytochem.* 24:81-84.
- North Carolina Environmental Sciences Review Panel. 1992. Report to the Secretary of the Interior from the North Carolina Environmental Sciences Review Panel as mandated by the Oil Pollution Act of 1990. 83 pp.
- O'Reilly, J.E., T.C. Sauer, R.C. Ayers, M.G. Brandsma and R. Meek. 1989. Field verification of the OOC mud discharge model. pp. 647-665. In: F.R. Engelhart, J.P. Ray and A.H. Gillman (eds.). *Drilling Wastes*. Elsevier Applied Science. New York.

- Parkes, R.J. and J. Taylor. 1983. The relationship between fatty acid distributions and bacterial respiratory types in contemporary marine sediments. *Estuar. Coast. Shelf Sci.* 16:173-189.
- Pearce, J.B., C.R. Berman and M.R. Rosen. 1985. Annual NEMP report on the health of the Northeast Coastal waters, 1982. NOAA Tech. Memo. NMFS-F/NEC-35, 68 pp.
- Pearson, T. and R. Rosenberg. 1978. Macrobenthic succession in relation to organic enrichment and pollution in the marine environment. *Oceanogr. Mar. Biol. Ann. Rev.* 16:229-311.
- Perry, G.J., J.K. Volkman, R.B. Johns and H.J. Bavor. 1979. Fatty acids of bacterial origin in contemporary marine sediments. *Geochim. Cosmochim. Acta* 43:1715-1725.
- Reemstma, T., B. Haake, V. Ittekkot, R.R. Nair and U.H. Brockmann. 1990. Downward flux of particulate fatty acids in the central Arabian Sea. *Mar. Chem.* 29:183-202.
- Rhoads, D.C. and S. Cande. 1971. Sediment profile camera for *in situ* study of organism-sediment relations. *Limnol. Oceanogr.* 16:110-114.
- Rhoads, D.C. and J.D. Germano. 1986. Interpreting long-term changes in benthic community structure: A new protocol. *Hydrobiologia* 142:291-308.
- Rhoads, D.C. and D.K. Young. 1970. The influence of deposit-feeding organisms on sediment stability and community trophic structure. *J. Mar. Res.* 28:150-178.
- Rhoads, D.C. and D.K. Young. 1971. Animal-sediment relationships in Cape Cod Bay, Massachusetts. II. Reworking by *Molpadia oolitica* (Holothuroidea). *Mar. Biol.* 11:255-261.
- Rodolfo, K.S., B.A. Buss and O.H. Pilkey. 1971. Suspended sediment increase due to hurricane Gerda in continental shelf waters off Cape Lookout, North Carolina. *J. Sed. Petrol.* 41:1121-1125.
- Ross, S. and K. Sulak. 1992. An unusual fish community on the middle continental slope off Cape Hatteras, North Carolina. American Society of Ichthyologists and Herpetologists (ASIH) 72nd Annual Meeting, University of Illinois, Champaign-Urbana, Illinois, Abstract No. 303.
- Sanders, H.L. 1968. Marine benthic diversity: A comparative study. *Amer. Nat.* 102:243-282.
- Schaff, T. 1991. Spatial heterogeneity of continental slope benthos off the Carolinas. M.S. Thesis, North Carolina State University, Raleigh, NC.
- Schaff, T., L. Levin, N. Blair, D. DeMaster, R. Pope and S. Boehme. 1992. Spatial heterogeneity of benthos on the Carolina continental slope: Large (100 km)-scale variation. *Mar. Ecol. Prog. Ser.* 88:143-160.
- Schaffner, L.C., R.J. Diaz and R.J. Byrne. 1987. Processes affecting recent estuarine stratigraphy. *Coastal Sediments 87*, Am. Soc. Civil Engineers, pp. 584-599.
- Science Applications International Corporation. 1990. Characterization of the currents at Manteo block 467 off Cape Hatteras, NC. Final report. Mobil Exploration and Producing Services Inc., Dallas, Texas, 152 pp.

- Science Applications International Corporation. 1992. Benthic ecology and sediment characterization ocean studies report. Detailed physical and biological oceanographic studies for an ocean site designation effort under the Marine Protection, Research and Sanctuaries Act of 1972 (MPRSA). Final report. U.S. Environmental Protection Agency Contract No. 68-CB-0062.
- Smith, D.J., G. Eglinton and R.J. Morris. 1983. The lipid chemistry of an interfacial sediment from the Peru Continental Shelf: Fatty acids, alcohols, aliphatic ketones and hydrocarbons. *Geochim. Cosmochim. Acta* 47:2225-2232.
- Sokal, R.R. and P.H.A. Sneath. 1963. Principles of numerical taxonomy. Freeman Press, San Francisco, 573 pp.
- Stehlik, L.L., C.L. MacKenzie and W.W. Morse. 1991. Distribution and abundance of four brachyuran crabs on the Northwest Atlantic shelf. *Fish. Bull.* 89:473-492.
- Sulak, K. 1992. Demersal fish fauna on the continental slope in the vicinity of "the Point." pp. 135-138. In: Proceedings Fourth Atlantic OCS Region Information Transfer Meeting, Wilmington, NC, September 1991. U.S. Dept. Interior, Minerals Management Service, Herndon, Virginia.
- Sun, M., R.C. Aller and C. Lee. 1991. Early diagenesis of chlorophyll-*a* in Long Island Sound sediments: A measure of carbon flux and particle reworking. *J. Mar. Res.* 49:379-401.
- Tucholke, B.E. 1987. Submarine geology. Chapter 4, pp. 56-113. In: J.D. Milliman and W. Redwood Wright (eds.). The marine environment of the U.S. Atlantic continental slope and rise. Jones and Bartlett Pub., Boston.
- Turekian, K.K., J.K. Cochran, L.K. Benninger and R.C. Aller. 1980. Chapter 5. The sources and sinks of nuclides in Long Island Sound. pp. 129-164. In: B. Saltzman (ed.). Estuarine physics and chemistry: Studies in Long Island Sound. Academic Press, New York, 424 pp.
- Valiela, I. 1984. Marine Ecological Processes. Springer-Verlag, New York. 546 pp.
- Van Vleet, E.S. and J.G. Quinn. 1979. Early diagnosis of fatty acids and isoprenoid alcohols in estuarine and coastal sediments. *Geochim. Cosmochim. Acta* 43:289-303.
- Venkatesan, M.I. 1988. Organic geochemistry of marine sediments in Antarctic region: Marine lipids in McMurdo Sound. *Org. Geochem.* 12:13-27.
- Volkman, J.K., G. Eglinton and E.D.S. Corner. 1980. Sterols and fatty acids of the marine diatom *Biddulphia sinensis*. *Phytochemistry* 19:1809-1813.
- Volkman, J.K., S.W. Jeffrey, P.D. Nichols, G.I. Rogers and C.D. Garland. 1989. Fatty acid and lipid composition of 10 species of microalgae used in mariculture. *J. Exp. Mar. Biol. Ecol.* 128:219-240.
- Volkman, J.K., D.J. Smith, G. Eglinton, T.E.V. Forsberg and E.D.S. Corner. 1981. Sterol and fatty acid composition of four marine haptophycean algae. *J. Mar. Biol. Ass. U.K.* 61:509-527.
- Wakeham S.G. and C. Lee. 1989. Organic geochemistry of particulate matter in the ocean: The role of particles in oceanic sedimentary cycles. *Org. Geochem.* 14:83-96.

- Walsh, J.J., E.T. Premuzic, J.S. Gaffney, G.T. Rowe, G. Harbottle, R.W. Stoenner, W.L. Balsam, P.R. Betzler and S.A. Macko. 1985. Organic storage of CO₂ on the continental slope off the Mid-Atlantic Bight, the southeastern Bering Sea, and the Peru coast. *Deep-Sea Res.* 32:853-883.
- Warwick, R.M. and J.D. Gage. 1975. Nearshore zonation of benthic fauna especially Nematoda, in Loch Etive. *J. Mar. Biol. Assoc. U.K.* 55:295-311.
- Welsh, B.L., R.B. Whitlatch and W.F. Bohlen. 1982. Relationship between carbon sources as a basis for comparing estuaries in southern New England. pp. 53-67. In: V.S. Kennedy (ed.). *Estuarine comparisons*. Academic Press, New York.
- Wenner, E.L. and D.F. Boesch. 1979. Distribution patterns of epibenthic decapod Crustacea along the shelf-slope coenocline, Middle Atlantic Bight, U.S.A. *Bull. Biol. Soc. Washington* 3:106-133.
- Weston, D.P. 1983. Distribution of macrobenthic invertebrates on the North Carolina continental shelf with consideration of sediment, hydrography and biogeography. Ph.D. Dissertation, College of William and Mary, Williamsburg, VA, 154 pp.
- Weston, D.P. 1988. Macrobenthos-sediment relationships on the continental shelf off Cape Hatteras, N.C. *Cont. Shelf Res.* 8:267-286.
- Whitney, D.E. and W.M. Darley. 1979. A method for the determination of chlorophyll *a* in samples containing degradation products. *Limnol. Oceanogr.* 24:183-186.
- Whittaker, R.H. and C.W. Fairbanks. 1958. A study of plankton copepod communities in the Columbia Basin, southeastern Washington. *Ecology* 54:46-65.
- Wiebe, P.H., E.H. Backus, R.H. Backus, D.A. Caron, P.M. Gilbert, J.F. Grassle, K. Powers and J.B. Waterbury. 1987. Chapter 6. Biological Oceanography. pp. 140-201. In: J.D. Milliman and W. Redwood Wright (eds.). *The Marine environment of the U.S. Atlantic continental slope and rise*. Jones and Bartlett Pub., Boston.
- Williams, R.G. and F.A. Godshall. 1977. Summarization and interpretation of historical physical oceanographic and meteorological information for the Mid-Atlantic Region. National Oceanographic and Atmospheric Administration, U.S. Department of Commerce. Final Report to the Bureau of Land Management, Interagency Agreement AA550-1A6-12, 295 pp.
- Yingst, J.Y. and D.C. Rhoads. 1980. The role of bioturbation in the enhancement of bacterial growth rates in marine sediment. pp. 407-421. In: K.R. Tenore and B.C. Coull (eds.). *Marine benthic dynamics*. University South Carolina Press, Columbia.

THIS PAGE LEFT BLANK INTENTIONALLY

INDEX

Subject Index

- Aerobic sediment 33, 45
Anaerobic sediment 33, 45
- BABS 11, 75
Bacterial acids 29
Benthic communities 1, 3, 55, 62, 67, 121, 126
Benthic fish 3, 75, 81, 97, 121, 123
Biogenic structure 33, 39, 46, 51, 73, 78, 81, 93, 100, 104, 123
Biomass 3
Bioturbation 46, 51, 78, 104
Box core 9, 53
Burrows 39, 45, 78
Bumpus Line 47
Buzzards Bay 28
- Camera sled 11, 75
Canadian boarder 113
Carbon flux 19, 50
Carbonate 14, 47
Carbonate flux 19
Cape Hatteras 1, 3, 4, 19, 28, 47, 49, 72, 113, 121, 125
Cape Fear 73
Cape Lookout 73
Carolina Platform 3, 47
Carolina slope 70
Chesapeake Bay 47, 49
Chlorophyll *a* 21, 22, 50, 72
C:N ratio 14
Color redox potential discontinuity 33, 45
Compaction 33
Community structure 55, 62, 67, 121
Continental margin 113
Continental rise 3, 53
Continental shelf 47, 49, 73
Continental slope 1, 3, 28, 47, 49, 50, 53, 70, 72, 73, 113
Currents 3, 5, 78
- Delaware Bay 47, 49
Deposition 5, 127
Depth zonation 62, 77, 81, 92, 113
Diatoms 21, 22, 50
Dispersion 5, 127
Diversity 55
Drilling muds 4, 5, 127
Drilling cuttings 4, 5, 127
- Fatty acids 21, 22, 28
Farallon Islands 72
Feeding voids 33, 51
Fish 4, 75, 87, 97, 109, 113, 121
Georges Bank 70, 118
Gulf Stream 3, 49, 125
Gulf of Maine 28
- Hatteras Canyon 122
Hydrocarbons 3
- Indicator species 72
Infauna 62, 67, 70, 72, 118, 121, 126
- Lipids 21
Long Island Sound 49, 50
Long Bay 113
- Manteo 467 2, 4, 5, 127
Megafauna 4, 75, 81, 97, 109, 113, 121, 123, 126
Methane 13, 19
Microalgae 21
Microbial garden 28
Microtopography 33
Mixing coefficients 19, 51
Mobile Oil 1,
- Narragansett Bay 28, 50
New York Bight 47
- Objectives 2
Offshore Operators' Committee Model 2, 5, 127
Oil Pollution Act 1990 1,
Onslow Bay 22, 49
Organic carbon 19, 22, 28, 45, 49, 121, 125
Organic Nitrogen 14
Outer continental shelf 1
- ²¹⁰Pb 13, 49
Peru 19
Physical habitat 3, 125
Phytoplankton productivity 28, 50
Polyunsaturated fatty acids 21, 28
Pore water 19, 51
- Rarefaction 55
RPD 33, 45
Rhode Island Sound 28
- Sampling design 9, 11
Saturated fatty acids 29
Sea-Floor characteristics 78
Sedimentation rate 13, 19, 49, 123
Sediment fabric 31, 39, 45, 46, 50
Sediment grain size 13, 19, 33
Sediment profile camera 11, 31
Sediment profile imaging 31

Sediment transport 47, 50
Species richness 55 -
Surface relief 33

Terrestrial input 29, 50
The Point 2, 116
Topography 3, 78, 113
Trawls 75
Turbidites 45, 51

Upwelling 19

Voids 33, 45

Well drilling 4, 127
Western Boundary Undercurrent 3, 47

X-radiography 33, 39, 45

Zonation 113

Taxonomic index

- abyssorum* (*Ceratocephale*) nr. 67
acutus (*Leitoscoloplos*) nr. 67
affinus (*Synaphobranchus*) 81
alabastrum (*Flabellum*) 87
alba (*Cylichna*) 67
americanus (*Astropectin*) 104, 109
Amphilimna sp. 104, 109
Aricidea 72
artifex (*Hyalinoecia*) 77, 81, 87, 97, 109, 113, 118, 120, 122, 126
Asterias 4
atlanticus (*Lycodes*) 81, 87, 97, 104, 109, 120, 122
aulogastressa (*Ophelina*) 67
- Barantolla* sp. 3. 67
Bathysiphon 51
biceps (*Chirimia*) 73
borealis (*Cerianthus*) 109
breviremus (*Leptognatha*) 67
brunnea (*Cossurella*) 62
- Cancer* spp. 109
capitata (*Capitella*) 67
caudatus (*Falcidens*) 67, 122
Cerianthus 4, 39
Chirimia 55
Chymenella 28
Cossura 72
Cossura sp. 121, 126
Cossurella sp. 1. 62
Cyclotella 22
cynoglossus (*Glyptocephalus*) 4, 39, 75, 81, 87, 97, 109, 113, 118, 120, 121, 122, 126
- diaphanes* (*Nephasoma*) 67, 122, 126
- equilibria* (*Caprella*) 67
Exogone sp. 4. 67
- filiformis* (*Bathysiphon*) 4, 31, 53, 55, 75, 77, 81, 87, 97, 104, 113, 118, 121, 122, 126
forcipatus (*Pseudotanais*) 67
- gigantea* (*Paelopatides*) 97, 118
glutinosa (*Myxine*) 4
gracile (*Distichoptilum*) 97, 104, 109, 122
gracilis (*Praxilla*) 67
groenlandica (*Ancistrosyllis*) nr. 67
- inflatum* (*Scalibregma*) 53, 55, 62, 67, 70, 72, 73, 121, 122, 126
intermedius (*Tubificoides*) 53, 62, 67, 70, 73, 121, 126
- jeffreysi* (*Peramphinome*) 67
- kaupi* (*Synaphobranchus*) 81
kirkegaardi (*Tharyx*) 62, 70, 73, 121, 126
- labidion* (*Ophryotrocha*) 67
longocirrata (*Cossura*) 53, 62, 67, 70, 72, 73
lymani (*Ophiomusium*) 81, 97, 104, 118, 122
lyra (*Paradoneis*) 67
- Macrostylis* sp. 2. 67, 122
medioporus (*Limnodriloides*) 53, 62, 67, 70, 73, 121, 126
Molpadia 55
Myriotrochus sp. 1. 67
- Nemertea* sp. B. 67
Nemertea sp. C. 67
Nezumia spp. 4
- obsoleta* (*Thyasira*) 62
obnusa (*Retusa*) 67
- Paraeospinosus* sp. 1. 62, 70
parvum (*Pseudoscalibregma*) 67
Peniagone sp. 104, 122
placenta (*Phormosoma*) 87, 118
Praxillella 55, 73
Praxillella sp. 1. 67
propinqua (*Harpinia*) 67
pygodactylata (*Cossura*) 62, 70
- quadrilobata* (*Aricidea*) 53, 62, 67, 70, 73, 121, 126
- sarsi* (*Ophiura*) 4, 87, 120
Scalibregma 72
Scoloura sp. 1. 67
spinicauda (*Leptognathiella*) 67
spinosissimum (*Pleurogonium*) nr. 67
stelliferum (*Kophobolemnon*) 81, 97, 104, 109, 122
Synaphobranchus spp. 4, 81, 109, 122
- Tharyx* 72
thraciaeformis (*Megayoldia*) 67
Tubificoides sp. A. 67
Tubificoides spp. 62
tudiae (*Bolocera*) 113, 120
- valida* (*Munida*) 113
verrilli (*Actinauge*) 4, 39, 75, 81, 87, 97, 104, 109, 113, 118,
verrilli (*Lycenchelys*) 4, 39, 75, 81, 87, 97, 104, 109, 113, 118, 120, 121, 122, 126